

2014

{International Journal of Computational Engineering Research(IJCER)}

{Frequency: 12 issues per year}

[International Journal of Computational Engineering Research (IJCER) is an intentional online Journal in English monthly publishing journal. This Journal publish original research work that contributes significantly to further the scientific knowledge in engineering and Technology.]

Volume 4, issue 6, June, 2014

IJCER

IJCER

www.ijceronline.com

ijceronline@gmail.com



Editorial Board

Editor-In-Chief

Prof. Chetan Sharma

Specialization: Electronics Engineering, India
Qualification: Ph.d, Nanotechnology, IIT Delhi, India

Editorial Committees

DR.Qais Faryadi

Qualification: PhD Computer Science
Affiliation: USIM(Islamic Science University of Malaysia)

Dr. Lingyan Cao

Qualification: Ph.D. Applied Mathematics in Finance
Affiliation: University of Maryland College Park,MD, US

Dr. A.V.L.N.S.H. HARIHARAN

Qualification: Phd Chemistry
Affiliation: GITAM UNIVERSITY, VISAKHAPATNAM, India

DR. MD. MUSTAFIZUR RAHMAN

Qualification: Phd Mechanical and Materials Engineering
Affiliation: University Kebangsaan Malaysia (UKM)

Dr. S. Morteza Bayareh

Qualificatio: Phd Mechanical Engineering, IUT
Affiliation: Islamic Azad University, Lamerd Branch
Daneshjoo Square, Lamerd, Fars, Iran

Dr. Zahéra Mekkioui

Qualification: Phd Electronics
Affiliation: University of Tlemcen, Algeria

Dr. Yilun Shang

Qualification: Postdoctoral Fellow Computer Science
Affiliation: University of Texas at San Antonio, TX 78249

Lugen M.Zake Sheet

Qualification: Phd, Department of Mathematics
Affiliation: University of Mosul, Iraq

Mohamed Abdellatif

Qualification: PhD Intelligence Technology
Affiliation: Graduate School of Natural Science and Technology

Meisam Mahdavi

Qualification: Phd Electrical and Computer Engineering

Affiliation: University of Tehran, North Kargar st. (across the ninth lane), Tehran, Iran

Dr. Ahmed Nabih Zaki Rashed

Qualification: Ph. D Electronic Engineering

Affiliation: Menoufia University, Egypt

Dr. José M. Merigó Lindahl

Qualification: Phd Business Administration

Affiliation: Department of Business Administration, University of Barcelona, Spain

Dr. Mohamed Shokry Nayle

Qualification: Phd, Engineering

Affiliation: faculty of engineering Tanta University Egypt

CONTENTS:

S.No.	Title Name	Page No.
Version I		
1.	The Research and Development of Measurement Robot Automatic Monitoring Systems Luo Kaitian	01-04
2.	Security Issues in Cloud Computing and Risk Assessment Darshan R , Smitha G R	05-10
3.	Cost Comparison Between Rcc & Post-Tensioned Prestressed Beams Spanning 26m. Ankit Sahuv, Prof. Anubhav Raiv, Prof. Y.K. Bajpai	11-14
4.	Applications of Modified F-Expansion Method for Nonlinear Partial Differential Equations with Variable Coefficients Priyanka M. Patel , Vikas H. Pradhan	15-26
5.	Case-Based Reasoning System for Diagnosis of Neuropsychiatric Abnormality Shabeeha Khatoon , Kavita Agarwal	27-34
6.	Cost comprisonbetween r.c.c.beam& steel composite beam structure of g+5 storeyed building the overall plan dimenssion of the building is 56.3 m x 31.94m Aniket Sijaria, Prof Anubhav Rai , Prof Y.K. Bajpai	35-37
7.	Modelling of Vapour Liquid Equilibrium by Artificial Neural Networks Dr.B.Karunanithi , Sweta Shriniwasan , Bogeshwaran.K	38-56
8.	CMOS Compound Pair Wide Band Bio-Amplifier Raj Kumar Tiwari, Gaya Prasad	57-62
9.	Macroshrinkage and mold height correlation for gery cast iron casting Nitesh Kumar, Anjani Kumar Singh, Sushil Patel, Ajit Kumar, Sachindra Kumar	63-68

Version II

1.	Latest Science Jai Prakash Goel , Ankush Goel	01-06
2.	Suitability Analysis in Determining Optimal Landfill Location Using Multi-Criteria Evaluation (MCE), GIS & Remote Sensing Olusina J. O. , D. O. Shyllon	07-20
3.	A Combined Approach for Intrusion Detection System Based on the Data Mining Techniques Pragya Diwan , Dr. R.C Jain	21-25
4.	Modelling and Prediction of Water Level for a Coastal Zone Using Artificial Neural Networks Badejo, Olusegun Temitope, Udoudo, Daniel	26-41
5.	Challenges and Design Issues in Search Engine and Web Crawler Rahul Mahajan , Dr. S.K. Gupta, Mr. Rajeev Bedi	50-55
6.	Time Frequency Based Evaluation of Surface Electromyogram Signal Using Non Invasive Technique Tanu Sharma, Deepak Agarwal	45-49
7.	Design of Wireless to Wired Audio Conversation System Digambar Patil, Prof. B. T. Salokhe	50-55
8.	Embed Watermarking in High of Image Coarseness Esraa Jaffar Baker , Sundos Abdul_ameer Hameed	56-60
9.	Block Based Discrete Wavelet Transform for Image Compression K. Bhanu Rekha , S. Ramachandran	61-67
10	Software as a Service (SaaS): Security issues and Solutions Navneet Singh Patel , Prof. Rekha B.S	68-71

11.	High Frequency Performance of Dual Gated Large Area Graphene MOSFET Md. Tawabur Rahman , Muhammad Mainul Islam , Md. Tajul Islam	72-79
12.	Automated systems for fall detection of individuals based on a network of overlapping cameras with Dempster-Shafer Theory (DST) SeyedHojjat Moghaddasi , Aliakbar Poyan	80-86

The Research And Development Of Measurement Robot Automatic Monitoring Systems

Luo Kaitian

Department of Computer Science Sichuan University for Nationalities Kangding, China

ABSTRACT:

This paper describes the hardware components and principles of measuring of the measurement robot and introduces its secondary developmental principles. For the purposes of this study serial control between the computer and the measuring robot was studied. Through the analysis and coordination of software requirements, engineering automation observations, Microsoft Visual C#2008 programming language, and Leica Geosystems GeoCOM robot programming interface, developers can achieve the engineering standards of automatic monitoring data acquisition software. Experiments show a high degree of automation software improves work efficiency in significant ways.

KEYWORDS: *Measuring robot; automatic monitoring; serial control*

I. THE BASIC COMPONENTS AND MEASURING PRINCIPLES OF THE MEASUREMENT ROBOT

The measurement robot, also known as the total station, is a comprehensive surveying system, which includes the basic functions of auto target recognition (ATR), autocollimation, auto target tracking (ATT), auto angle and distance measurement and automatic recording. It minimizes labor intensity, greatly improves work efficiency and achieves a more accurate result. The major subsystem of the measurement robot contains eight parts, namely a coordinate system, manipulator, transducer, calculator & controller, closed-circuit control sensor, decision maker, target acquisition and integrated sensor. First of all, by using a spherical coordinates system, the coordinate system can find targets in the range of 360° horizontally and 180° vertically; the manipulator is mainly used to adjust rotation; the transducer transforms electrical energy into mechanical energy that activates the stepper motor; the calculator & controller boots up and shuts down the operating system(OS) and stores data while creating conditions for other systems related to dock; the closed-circuit control sensor transmits collected data to the manipulator and controller in order to fix positions accurately and measure; the decision making is used to find targets; target acquisition, including setting thresholds, region-segmentation method and heliography, is mainly for precisely collimating targets and the integrated sensor is used to collect data. The basic measuring principles are: processing images collected by the image sensor to achieve automatic tracking and precise collimation under the control of the calculator & controller. In general, surveyors plan a measuring strategy based on information acquired from a measuring task. They obtain data using sensory recognition analyzing the surroundings and targets via the available instruments. While measuring the robot can identify, judge, analyze, automatically control, collimate and indicate. It can be connected to a computer and or softwares for data analysis and program design and has high automation, remote control, fast response and high precision features. The measurement robot has passed three stages of development. Currently, it can use image-processing to automatically recognize, match and autocollimate targets according to their counters and textures, and can realize 3D imaging.

II. THE PRINCIPLES OF MEASURING ROBOT'S DEVELOPMENT AND THE REALIZATION OF AUTOMATIC MONITORING SYSTEMS PREPARE YOUR PAPER BEFORE STYLING

The principles

Internationally famous measurement solution providers have launched their own products. The robot produced by Leica Geosystems in Switzerland has always been leader in the development of this industry because of its high precision, stability and ease of secondary development. The high-performance Leica TCRA1201 intelligent measuring robot with its high precision is widely employed for construction use. This paper studies the way its hardware device and Microsoft Visual C#2008 as the programming language are used to develop software. The secondary development can be carried out with a uniform serial interface GeoCOM instruction set. GeoCOM, a COM component in the form of DLL (Dynamic Link Library), specially developed by Leica Geosystems for secondary development, can provide users with a more personalized UI (User Interface) or allow users to develop more advanced client applications on the basis of the Leica measuring devices. It has two interface modes: the advanced function mode and ASCII. The former uses VB (Visual Basic) or C++ and can directly invoke the request, response and analytic function packaged in the COM component; the latter, constructed to demand, uses serial line to send request to the robot and immediately receiving response decoding. During each process of the latter there is a corresponding specific identification code related to given parameters. Although the advanced function mode is highly integrated and easy to invoke,

its functions are all too often called, which greatly consumes memory, drags response rate and limits the programming language. Therefore this study is based on the ASCII interface mode to realize the software's development. The ASCII command character strings format of the Leica TCRA1201 measurement robot is as follows:

Transmission serial: [] %R1Q, <RPC>, [<TrId>]: [<P0>], [<P1>, ...] <Term>, meaning of each symbol is presented in Table 1.

Table 1. Symbol Meaning of Transmission Serial

<LF>	Initialize the new line character to empty the buffer
%R1Q	First category request mark of GeoCOM
<RPC>	Remote procedure call mark, from 0 to 65535
<TrId>	Optional transaction ID, generally from 1 to 7, the same as the transaction ID of reception serial
:	Head of character string and decollator of the parameter
<P0>, <P1>...	Parameter 1, parameter 2...
<Term>	character string terminator (default: CR/LF) can be set by COM_SetTerminator

Reception serial: %R1P, <GRC>, [<TrId>]: <RC>, [<P0>, <P1>...] <Term>, meaning of each symbol is presented in Table 2.

Table 2. Symbol Meaning of Reception Serial

%R1P	First category response code of GeoCOM
<GRC>	GeoCOM return code. If it's 0, succeed; if not, fail.
<TrId>	Optional transaction ID, generally from 1 to 7
:	Head of character string and decollator of the parameter
<RC>	Remote procedure call return code. If it's 0, succeed; if not, fail.
<P0>, <P1>...	Parameter 1, parameter 2...
<Term>	Character string terminator (default: CR/LF) can be set by COM_SetTerminator

The Realization of Automatic Monitoring

Because the location and numbers of the observation spot are relatively fixed, in order to realize unattended, real-time, consecutive, effective and dynamic automatic measurement, the software used can automatically search, collimate and indicate in a certain field range to finish tasks like timing measurement, calculation, analysis and output. The objective Automation. The automatic monitoring software strictly implements auto detection and processes and analyzes data feedback according to given observation set numbers and observation intervals. Intelligence. When blocked and not meeting tolerance requirements, the software should command the robot to measure again, and if necessary, give an alarm. Mass storage. After measuring there is a large amount of data. The DLL can store and manage data effectively and provides data query and analysis. Friendly and easy user interface. For the convenience of users, the software should have an easy-to-use interface and simple operation. The main functional modules of the automatic monitoring software This software mainly consists of project management, system preferences, survey station settings, measurement learning, automatic measurement, data processing and output. Project management. Each engineering project has a corresponding database file that stores data including system preferences, original values and a range of calculated analysis.

System preferences. Set the computer's serial communication parameters to conform to the robot's baud rate, calibration stop bit, 2c mutual error, index error. Misclosure of the round will be set as well.

Survey station settings. These include settings of the name of the station, the height of the instrument and prism constants.

Measurement learning. Firstly, users supply rough information about the target spot. After auto search, precise collimating and surveying, location data is recorded.

Automatic measurement. The software will, if running over time, automatically remeasure part or all of the target according to the numbers configured.

Data processing. Based on the original data, the software will calculate and analyze.

Output. It provides enquiry and output of the original observation data, calculation and analytic results and generate forms and charts.

Friendly and easy user interface. For the convenience of users, the software should have an easy-to-use interface and simple operation.

1.3 The realization

According to the analysis and study above, the automatic monitoring software’s major structure plan of measurement robot is presented in Figure 1, and the major interface is presented in Figure 2.

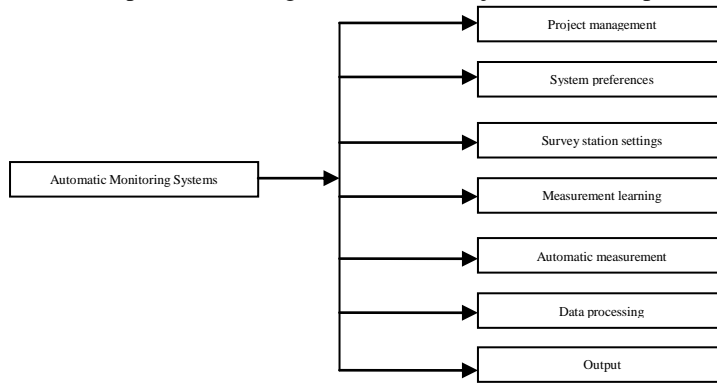


Figure 1

III. THE PRACTICAL USE OF THE AUTOMATIC MONITORING SOFTWARE

In order to analytically verify this software, a project is hence selected and its datum point & the arrangement of the observation spot is presented in Figure 3.

In Figure 3, BM1~BM4 is the datum point, J1~J2 is the observation spot.

The process of the experience is as follows:

- 1) Tolerance observation and communications parameters edition, input. Tolerance observation is presented in Table 3.

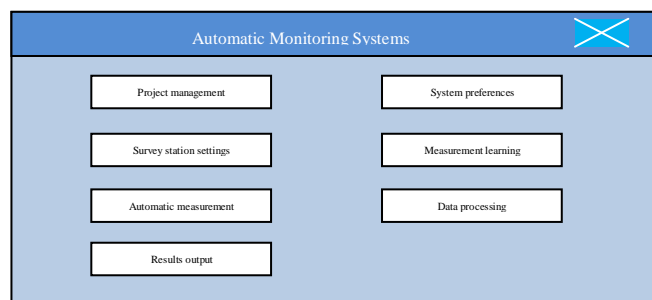


Figure 2

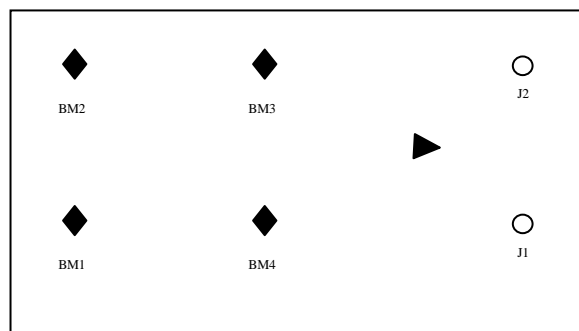


Figure 3

Table 3. Tolerance Observation

Numbers of observation set	Semiobservation of misclosure of round	Different observation set of 2c mutual error in the same direction	The same direction zero direction value is poor	2C value
3	6"	9"	6"	≤±15"

- 2) Measurement learning and storage of the Datum point BM1~BM4 and the observation spot J1~J2.
- 3) Collect data 3 times of observation set according to the parameters in Table 3. If the results do not meet the requirements in Table 3, the tester is warned and the robot will remeasure part of target or the whole.
- 4) After auto measurement, make coordinate calculations and store the results. The observation spot’s eight-period coordinate transformation is presented in Figure 4 and Figure 5. And this system based on measurement robot is proved to be capable of the surveying requirements and increasing work efficiency.

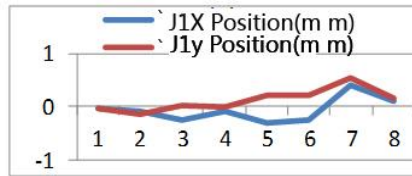


Figure 4

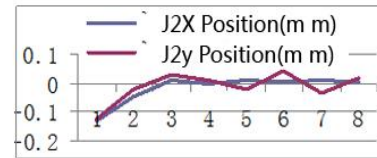


Figure 5

IV. CONCLUSION

This paper studies the development of automatic monitoring systems of the measuring robot. By connecting computer equipment and the robot, after serial steps (program delivery, command acceptance) of data collecting, the problems of huge workload and highly-required precision can be solved, which increases the efficiency and quality of the field survey.

V. ACKNOWLEDGMENT

This essay is sponsored by the projects from Sichuan Department of Education (Project No. 13ZA0136).

REFERENCES

- [1] Cai Qiangang. Study of the Multi-station Automatic Deformation Monitoring System[D]. Shandong University of Science and Technology, 2007.
- [2] Cao Titao. Automatic Measurement Method of Tunnel Cross Section and Software Development Based on Intelligent Total Station[D]. Southwest Jiaotong University, 2008.
- [3] Fan Baixing. Programming Instrument-end Application on Tps1100 with GeoBasic [J]. Surveying and Mapping of Sichuan, No.03, 2003.
- [4] GeoC++ Step by Step (V 7.00) [Z]. Leica Geosystems AG. Heerbrugg, Switzerland, 2008.
- [5] Gui Huihong, Zhang Jin. Design and Implementation of Integrated Database in Automatic Deformation Monitoring System [J]. Engineering of Surveying and Mapping, No.01, 2010.
- [6] Mei Wensheng, Zhang Zhenglu, Guo Jiming. Software of Georobot Deformation Monitoring System [J]. Journal of Wuhan University, No.02, 2002.
- [7] Tang Zhengqi, Wu Zhengming, Jiang Bo. The Application of Survey Robot Based on GeoCOM Interface Technology[J]. Journal of Hunan City University, No.04,2006.
- [8] Zhang Fengrui. The Discussion of Reflectorless Measurement Accuracy[J]. Bulletin of Surveying and Mapping, No.11, 2011
- [9] Zhang Yuanzhi, Xiao Qinggui, Miao Hongbing Positioning System of Instrument-end Application on Tps1100[J]. Surveying and Mapping of Beijing, No. 03, 1996.
- [10] Zhang Zhenglu. Measurement Robot[J]. Bulletin of Surveying and Mapping, No. 5, 2001.

Security Issues in Cloud Computing and Risk Assessment

Darshan R, Smitha G R

Department of Information Science and Engineering, RV College of Engineering, Bangalore-560059

Abstract-

Nowadays organizations use the Cloud in a variety of different service models (SaaS, PaaS, IaaS) and deployment models (Private, Public, Hybrid). In this paper we speak about the number of security issues/concerns associated with cloud computing. In most cases, the provider must ensure that their infrastructure is secure and that their clients' data and applications are protected while the customer must ensure that the provider has taken the proper security measures to protect their information. This paper also speaks about the Risks involved in cloud computing when implementing in different organisation considering three scenarios and how it affects the system and also about the risk assessment process where the level of risks are estimated on the basis of the likelihood of an incident scenario when compared against the estimated impact. Finally it concludes by discussing about some of the problems to be solved such as standardised format for the SLA (Service level agreement) and about the encryption process which is computationally expensive.

Keywords- Cloud Computing, Security issues and Risk Assessment.

I. INTRODUCTION

Cloud computing becomes more and more familiar to industry crowd, and its wide range of application areas becomes more and more wide. Building a secure computer cloud computing environments becomes one of the hot research topics. In this paper, we discuss the definition of clouding computing, its development status, and analysis part of the security problems. Along with all these some ideas about security and its effect on Cloud computing and at last we propose in this paper about the combination of reducing encryption cost and enhancing SLA strength will be a promising direction of the future cloud security researches.

II. EVOLUTION OF CLOUD COMPUTING

Cloud Computing is the result of evolution and adoption of existing technologies and paradigms. The goal of cloud computing is to give users the pleasure to take most of the advantages from all the technologies, even without much need of shear knowledge about each one of them. The cloud aims to reduce costs, and help the wide range of users to focus on the core business instead of being worried about different IT obstacles. The main enabling technology for cloud computing is virtualization. With the help of virtualization we can generalize the physical infrastructure of cloud computing, which is the most important and the most rigid component, and convert it as a soft component which will be easy to use and manage it. Doing so, virtualization provides the wide range of agility property required to speed up the IT business and operations, also reduces the cost by massively increasing infrastructure utilization. And also, autonomic computing initiates the automating the process with which the user can provision resources on-demand. In this way, by minimizing user involvement, the process of automation speeds up the process and reduces the possibility of human errors [4]. Users face difficult business problems every day. Cloud computing inherits ideas from Service-oriented Architecture (SOA) that can help the user minimize these problems into services that can be integrated to provide a solution. Cloud computing offers all of its resources as a services, and uses all the well-established rules, standards and best practices proposed in the field of SOA to allow vast global and easier access to cloud services in a standard way as shown in Fig 1.

Cloud computing also uses concepts from utility computing with the intention to provide metrics for the services used. All those metrics are at the core of the public cloud models [2]. Along with this, measured services are a necessary part of the feedback loop in autonomic computing, which allows services to measure on-demand and to initiate automatic failure recovery. Cloud computing is also a kind of grid computing, it has evolved by addressing the Quality of Service and reliability problems. It also provides all the necessary technologies and tools to build data and also to compute intensive applications with much lesser prices compared to traditional computing techniques.

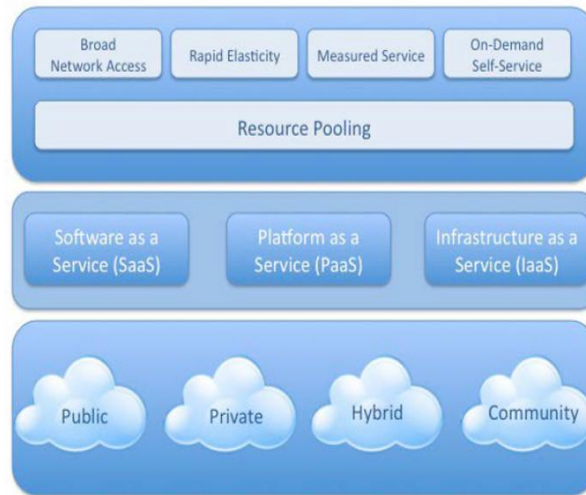


Fig 1: Visual model of Cloud Computing

Advantages

Cloud systems are very economical and useful for all kind of businesses. Cloud computing is a new technology which benefits the user in huge manner and the benefits are:

1. Flexibility.
2. Reliability and Security.
3. Portability.
4. Enhanced Collaboration.
5. Simpler devices.
6. Unlimited Storage and Speed.

III. SECURITY ISSUES

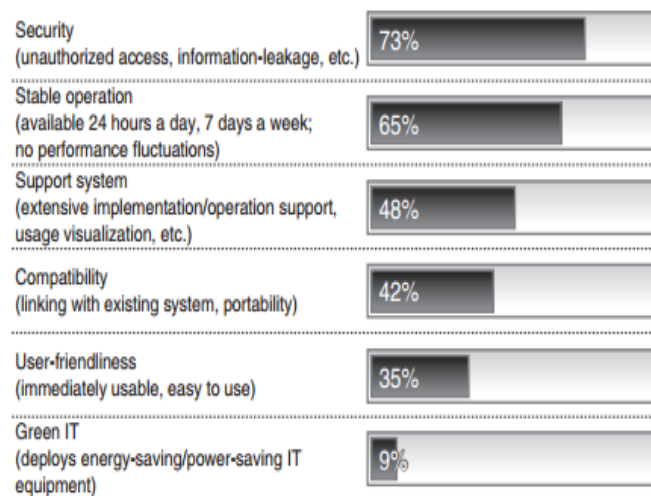


Fig 2: Concerns in Cloud Computing

As shown in the Fig 2, the security element accounts for huge mark of concern in cloud computing. The security issues affecting Cloud Computing Systems are [1]:

- Data security
- Trust
- Network traffic
- Multiple cloud tenants
- Need for access control and identity management

A. Data Security:

About using of cloud computing services, users are not aware of the hosting server location of their data and which particular server manages these data. Based on this, the cloud users and cloud service providers are very important to avoiding data loss and theft. Therefore the following will state the security of cloud computing from data privacy and data isolation [1].

- Data privacy. Data storage in the cloud are shared, that is not to open a separate storage area for the user. So the data has potentially dangerous. And compared with the traditional software, data in cloud computing are maintained by the third party, and due to the characteristics of cloud computing architecture, these data may be stored in scattered locations, and are stored in plain text form. Although the firewall can protect malicious alien attack in some degree of protection, this architecture makes some critical data might be leaked.

- Data isolation. At present in the network users share the data in data encryption ways, but in the cloud computing environment, if they can separate their own data from other user data, they can more effectively ensure data security. Because all customer data will be stored in only one instance of the software system, so it is urgent to develop additional data isolation mechanism to ensure the confidentiality of the data of every customer and provide disaster recovery plan.

B. Trust:

Trust is not easily defined, but most people agree that when it comes to cloud computing, trust can be explained better in terms of transparency. Businesses must be able to see cloud service providers are complying with agreed data security standards and practices. The standards must include controls about access to data, staff security, and the technologies and processes to segregate, backup and delete data. Vendors of cloud technologies and services are quick to claim that cloud computing is well equipped to provide the necessary controls. While Virtualization is viewed with suspicion and fear by many IT directors, suppliers like RSA, IBM and other say that the technology enables organizations to build security into the infrastructure and automate security processes, to surpass traditional data protection levels.

C. Lack of visibility into network traffic:

Many security organizations monitor network traffic to identify and block malicious traffic. The Vendors have delivered appliances that perform monitoring to ease the problems of installation and configuration. All these appliances can be installed on the network just like a normal server, also they can be up and running for longer duration. This appliance approach has simplified security practices and has been an enormous gift to hard-pressed IT and security groups.

There's one problem in the approach, virtual machines on the server communicate through the hypervisor's internal networking, where no packets crossing the physical network and also where the security appliance sits ready to stop them. Of course, if the virtual machines (VMs) are placed on different servers, traffic internal to VMs will run across the network and be available for inspection. To enhance the performance, the virtual machines associated with the same application (example, an application's database server and Web server) are always on the same physical server. Virtualization vendors have provided hooks into their hypervisors that network vendors such as Cisco and Arista have used to integrate with virtual switches that, in turn, enable traffic inspection. Hence this problem is not insurmountable, even though it requires an upgrade to the current method of network switching and the use of security products integrated with the new model. We can translate this as a need for more financial investment.

D. Need for better access control and identity management:

The cloud by nature is highly virtualized, and you need an approach to maintain control and manage identities across your cloud and other 'clouds,' says Alan Boehme, who is the senior vice president of IT strategy and architecture at financial services firm 'ING'.

E. Risk of multiple cloud tenants:

As we know cloud services make much use of virtualization technology, the amount of risks associated with multiple organizations' data located on a single hypervisor platform occurs, and that will continue to unless specific segmentation measures are enacted, says Dave Shackelford, director of security assessments and risk & compliance at Sword & Shield Enterprise Security, and a member of the faculty of research firm IANS [5].

IV. RISK ASSESSMENT**A. USE-CASE SCENARIOS**

For the purposes of this risk assessment of cloud computing, we have three use-case scenarios [3]:

- i) An SME perspective on Cloud Computing
- ii) The Impact of Cloud Computing on service resilience.
- iii) Cloud Computing and eGovernment.

For the purposes of this risk assessment of cloud computing, we analyzed three use-case scenarios:

- *An SME perspective on Cloud Computing*
- *The Impact of Cloud Computing on service resilience*
- *Cloud Computing and eGovernment (eHealth).*

Fig 3: Use case scenarios.

As shown in the Fig 3, the selection was based on the rationale that in Europe the cloud market is foreseen to have a great impact on new businesses and new start-up companies, and also on the way new business models will evolve. Since EU industry is mainly composed by SMEs (99% of companies according to EU sources- (9)) it makes sense to spotlight on SMEs. We have included several risks and recommendations which apply specifically to governments and larger enterprises. The SME scenario is based on the results of the survey: An SME perspective on Cloud Computing and it is NOT meant to be a road map for companies considering, planning or running cloud computing projects and investments. A medium-sized company was used as a use-case to guarantee to the assessment a high enough level of IT, legal and business difficulties. The main aim of this was to expose all the possible security risks. Some of those risks are specific to medium-sized businesses, others are general risks that micro or small enterprises are also likely to face when migrating to a cloud computing approach. The second scenario explores how the use of cloud computing affects the resilience of services in the face of, sudden increases in customer demand (e.g., in periods of financial crisis), denial of service attacks, localised natural disasters, misuse of the infrastructure as an attack platform, data leaks (malicious or careless insider or broken process). The third scenario explores the use of cloud computing by large government bodies which have to satisfy strict regulatory requirements and are very sensitive to negative public perception. A key consideration when using cloud services will be a public perception that there has potentially been a lack of consideration of security or privacy issues. This would be especially true should 'public' cloud services be used.

European Health represents a large government health service in Europe but does not describe any specific national health service. European Health is composed of public organisations and private suppliers providing e Health services. It is a very large organisation spread across several sites and it caters to 60 million citizens. Prior to using any kind of cloud infrastructure, it has over 20 IT service providers and more than 50 data centres.

V. RISK ASSESSMENT PROCESS

The level of risk is estimated on the basis of the likelihood of an incident scenario when compared against the estimated impact. The possibility of an incident approach is given by a threat exploiting vulnerability with a given likelihood [3]. The possibility of each incident scenario and the business impact was determined in consultation with the expert group after contributing, obtaining on their collective experience on this report. Whenever the cases where it was judged not possible to provide a well founded estimation of the possibility of an occurrence, then the value will be N/A. In most of the cases the estimate of possibility depends heavily on the cloud model or architecture under consideration. The following shows the risk level as a function of the business impact and possibility of the incident scenario, refer Fig 4. The resulting risk which is measured on a scale of 0 to 8 will be evaluated against risk acceptance criteria. And this risk scale can also be mapped to a simple overall risk rating:

- Low risk: 0-2
- Medium Risk: 3-5
- High Risk: 6-8

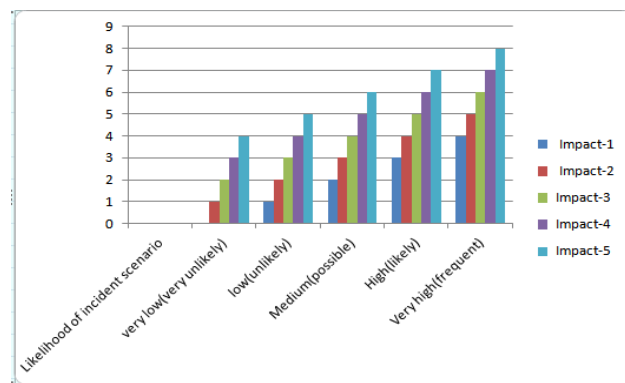


Fig 4: Risk Assessment report

VI. CONCLUSION

Cloud Computing offers some incredibly huge benefits such as unlimited storage, quick processing power and also the ability to easily share the information and process it; however, it also have several issues, and most of them are security issues. Cloud systems must overcome many difficulties before it becomes widely adopted and popular, although it can be utilized right now with some compromises and in the right conditions. Organization can enjoy all the benefits of cloud computing if we can address the very real security concerns that comes along with storing sensitive information in databases scattered around the internet. We have discussed several security issues that currently affect cloud systems; even after all that, there may be many undiscovered and unmentioned security problems. So many research work are currently being done on the different unknown issues faced by cloud systems and possible solutions for these issues, there is still a need for better solutions if cloud systems are to be widely adopted. One of the main problems that need to be addressed is coming up with a clear and standardized format for the Service Level Agreement (SLA) [5], a format that fully documents all of the services, the services and processes that would be provided by the service provider to back up its assurances. In the situations where the customers have the right amount of expectations and all the insecurities concerns are deemed manageable, cloud computing as a whole will keep ground and take firm hold as usable technology. Another major issue cloud systems face is Encryption. There are many methods like Encryption, which is the main method of ensuring security of data stored in the cloud; Encryption is computationally expensive. Encryption methods specific to Cloud Databases has been developed and more research is currently being done on Encryption mechanisms for cloud systems, more efficient methods are still needed to help accelerate the adoption of cloud systems.

VIII. ACKNOWLEDGMENT

I would like to thank my guide Mrs. Smitha G R for guiding me in all aspects in the process of preparing this paper.

REFERENCES

- [1] Liu Xiao-hui, Song Xin-fang. Analysis on cloud computing and its security. Computer science and education(ICCSE), 8th international conference on digital object identifier, 2013, pp:839-842.
- [2] O.Mirkovic. Security Evaluation in cloud. Information and communication Technology electronics and microelectronics(MIPRO), 36th International Convention.2013,pp-1088-1093.
- [3] ENISA, "Cloud computing:Benefits,risks and recommendations for information security.
- [4] Yushi Shen; Jie Yang; Keskin,T. The Evolution of IT towards Cloud computing in china and U.S.Computational Problem solving(ICCPS), International Conference on digital object identifier, 2012. Pp:224-235.
- [5] Behl,A;Behl,K; An analysis of Cloud Computing security issues. Information and communication Technologies(WICT), World congress on digital object identifier,2012,pp-109-114.
- [6] Yang Jian, Wang Haihang, Wang Jian, Yu Dingguo. Survey on Some Security Issues of Cloud Computing. Journal of Chinese Computer Systems. 2012(3):473-476
- [7] Wu Jiyi, Shen Qianli, Zhang Jianlin, Shen Zhonghua, Ping Lingdi. Cloud Computing:Cloud Security to Trusted Cloud. Journal of Computer Research and Development. 2011(48 suppl):230-231.
- [8] Tian Ming, Zhang Yongsheng. Analysis on cloud computing and its security. Information technology in medicine and education (ITME), International symposium on digital object identifier, 2012, pp:379-381.
- [9] Shaikh, F.B.Haider. Security threats in cloud computing. Internet technology and secured transactions(ICITST), International Conference, 2011, pp:214-219.

Cost Comparison Between Rcc & Post-Tensioned Prestressed Beams Spanning 26m.

Ankit Sahu, Prof. Anubhav Rai, Prof. Y.K. Bajpai.

ABSTRACT:-

I am going to work on the economic comparison between R.C.C. beam and Pre-stressed concrete beam. This work includes the design and estimate of R.C.C. Beam and post-tensioned Beam of 26m Span. The aim of this work is to design & estimate 26m span beam of R.C.C as well as pre-stressed concrete beam and then compare the results. The idea is to reach a definite conclusion regarding the superiority of the two techniques over one another.

I. INTRODUCTION

In India RCC Structures are commonly used for Residential as well as commercial Buildings. Post-tensioned Pre-stressed beams are rarely used for the same Buildings, or we can say for short Span Buildings. Two Decade ago there was a big problem of Skilled Workers for Pre-Stressing work. But now there are so many agencies for execution of the same work. In RCC Beams, depth of beam increases with increase in Span, because of deflection limitation. Depth of beam can be reduced in Pre-stressed section, for longer span pre-stressed beams are cheaper. This work is proceeding because I want to know the percentage cost difference between both techniques with respect to span.

II. SCOPE

This work includes the design and estimate of beam for Span 26 m, by R.C.C. and pre-stressed concrete techniques. And calculation of percentage cost comparison between RCC & Post-tensioned pre-stressed concrete beam.

III. METHODOLOGY

For RCC beam Design, I am taking M-30 Grade of Concrete. Initially I prepared a MS Excel Sheet for Design using IS: 456-2000. Similarly I have prepared MS Excel sheet for Design of Post-Tensioned pre-stressed beam using British code provisions. After Design comparing results. For Post-Tensioned beam M-35 Grade of Concrete is taken for Design. Design is carried out for parabolic cable profile only, which is the most popular one. Programs is also prepare for estimating & costing. Rates will be taken from Amended PWD SOR-2009 of Madhya Pradesh. In case of pre-stressed concrete, some of the rates will be obtained from a well-known private Infrastructure company . Pre-stressed concrete beams is designed for TYPE 3 only which is the practice in field. TYPE 1 & TYPE 2 structures are used only in special cases like Water Tanks, Pipes, Sleepers & Electric Poles.

Observation Table:- On the Basis of Design Results we have got Data for Estimate.

Estimate for 26 m Long RCC Beam

Support	0.5	m		
Span	26	m		
Width	0.5	m		
Depth	1.4	m		
Main Reinforcement				
Top	25	mm	5	Nos.
Main Reinforcement				
Bottom	32	mm	15	Nos.
Stirrups	10	mm	0.326	m c/c

SOR No.	Description Of Item	Nos.	Length	Width	Height	wt./m	Qty.	Unit	Rate as per MP PWD Ammended SOR-2009	Amount
5.27+5.28.2	Beam (M-30)	1	26	0.5	1.4		18.2	Cum	5603	101974.6
5.16.1	Reinforcement Top	5	29.62			3.85	570.39	Kg	48	27378.88
5.16.1	Reinforcement Bottom	15	29.62			6.31	2803.6	Kg	48	134572.7
5.16.1	Stirrups	80.8	3.75			0.61	186.611	Kg	48	8957.34
5.16.1	Skin Bars	8	26			0.88	184.572	Kg	48	8859.44
5.9.3	Shuttering Bottom	1	26	0.5			13	Sqm	229	2977
5.9.3	Shuttering sides	2	26		1.4		72.8	Sqm	229	16671.2
							Total Amount		' =	301391

Estimate for 26 m Long PT Beam

Support	0.5	m		0.5	0.25	1.2	0.15
Span	26	m					
Sectional area	355000	mm ²					
	0.355	m ²					

Main Reinforcement

Bottom	16	mm		16	Nos.
Stirrups	10	mm		0.26	m c/c
End Anchorage Reinforcement	12	mm		40	Nos.

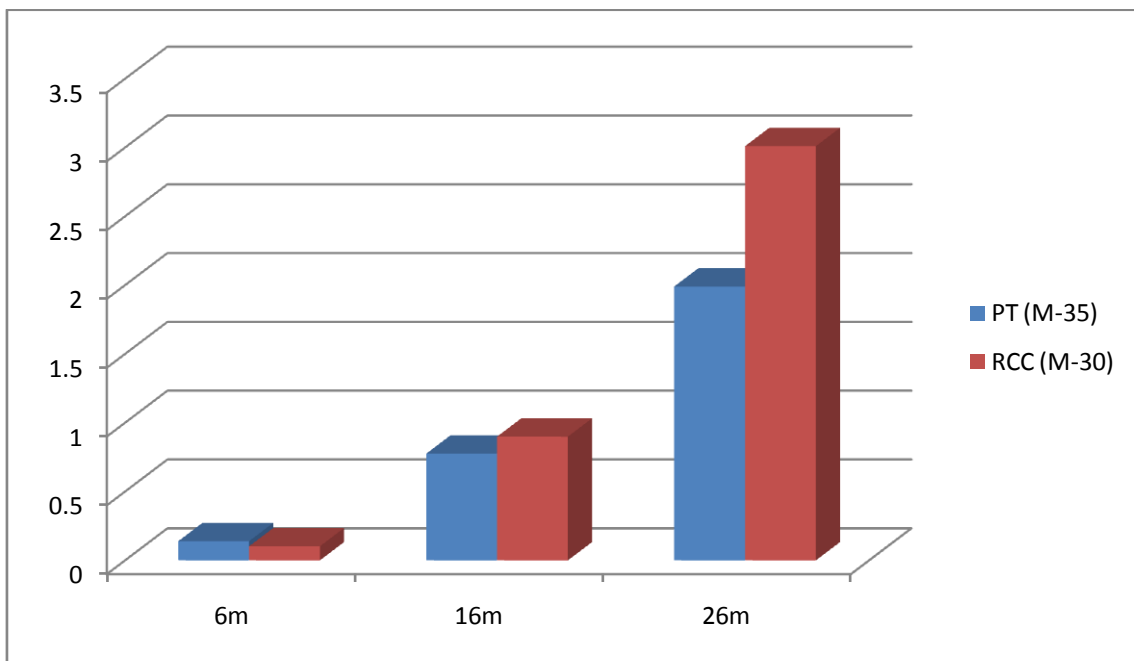
Sr. No.	Description Of Item	Nos.	Length	Width	Height	wt./m	Qty.	Unit	Rate as per MP PWD Ammended SOR-2009	Amount
5.27+5.28.3	Beam (M-35)	1	26		0.355		9.40	Cum	5658	53227.63
5.16.1	Reinforcement Bottom	16	27			1.57	681.49	Kg	48	32711.78
5.16.1	Stirrups	101	5.05			0.616	314.30	Kg	48	15086.66
5.16.1	End Anchorage Reinforcement	20	1.2			0.88	21.29	Kg	48	1022.24
5.16.1		20	0.5			0.88	8.87	Kg	48	425.93
	Anchor Plate	4	0.15	0.15	0.008	7850	5.65	Kg	52	293.90
5.9.3	Shuttering Of Bottom	1	26	0.85			22.1	Sqm	229	5060.9
5.9.3	Shuttering Of sides	2	26		1.2		62.4	Sqm	229	14289.6
NSOR	Tendons with Anchors	4	26			4.7	507.6	Kg	152.55	77434.38
							Total Amount		' =	199553

Rates as per Approved Agency for PT work in India

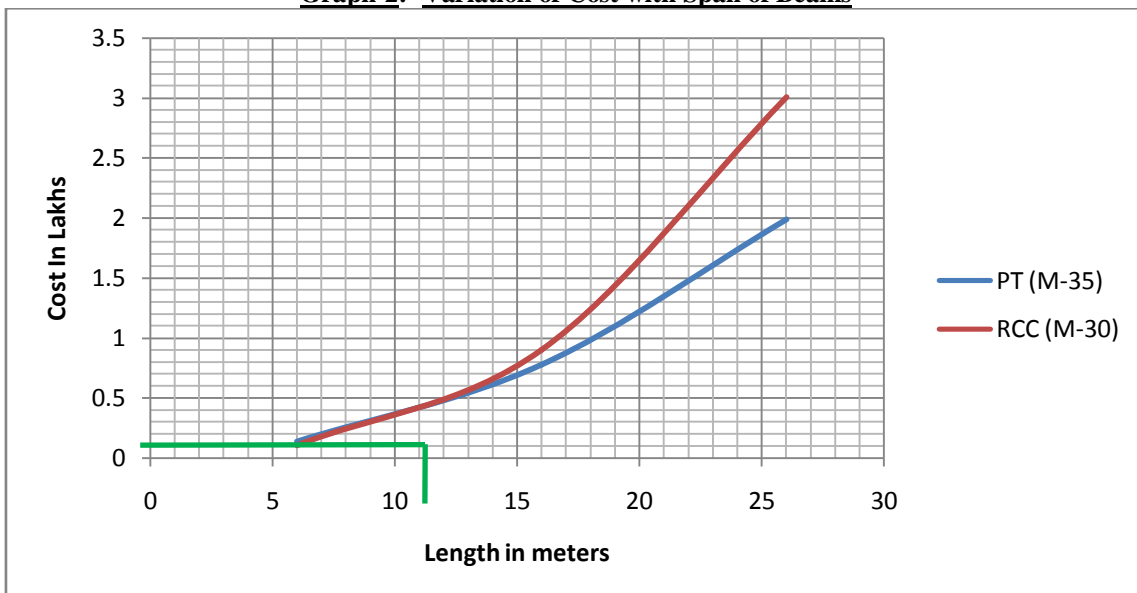
TABLE.1: "Economic comparison Between R.C.C. Beams & Post-Tensioned Pre-stressed Concrete Beams"

Sr. No.	Length of Beam in meters	Estimated Cost of RCC with M-30 grade concrete Mix in rupees (₹)	Estimated Cost of Post-tensioned with M-35 grade Concrete Mix in rupees (₹)	Percentage rate difference	Post-tensioned Beam is
1	26	301391	199553	34	cheap

Graph-1:- Variation of Cost with Span of Beams



Graph-2:- Variation of Cost with Span of Beams



IV. RESULTS & DISCUSSION

Result shows that, for span 26m Post-Tensioned Pre-stressed concrete beam is 34% cheaper than RCC beam. Table 1, & Figure-1 are showing same things, which are mentioned above. The cost of Pre-stressed concrete beam includes the cost of accessories like split cones, bearing plates, sheathing tubes, grouting etc. In our country, concrete grade higher than M: 30 are generally not used in case of RCC construction. Furthermore, simply supported T beams mostly result in under-reinforced sections. Savings resulting from using a higher grade of concrete are in a balanced or doubly reinforced section. Pre-stressing requires skilled workmanship & need for superior quality control. But we must not forget that along with these minor inconveniences pre-stressing delivers a structure that is better from limit state of serviceability & durability point of view. Bulk concreting in Large Span RCC beam creates problem during construction. It increases floor height and creates problem to design staircase.

V. CONCLUSIONS

A couple of decades back, when pre-stressing was not commonly used in India, R.C.C. beams used to be cheaper even for 25m spans. This is because the mix design for high strength concrete used to be based on 500kg/m³ (i.e. 10 bags of cement/m³) as permitted by IS: 456-1978. With modern methods of mix design based on maximum 8 bags of cement/m³ (to minimize shrinkage & creep) the cost of high grade concrete has come down. Furthermore, the price difference between HYSD bars & high tensile steel used for Pre-stressing has come down to 25-30% from more than 100%. Ditto for fixtures & accessories associated with pre-stressing. These used to be very costly then but have now become affordable because of the greater demand resulting in economics of scale for the manufacturers.

REFERENCES

- [1] IS: 456-2000. Indian Standard Code of Practice For Reinforced Concrete.
- [2] IS: 1343- 1980. Indian Standard Code of Practice For Prestressed Concrete (First Revision).
- [3] Dr. B. C. Punmia. 1990. " Reinforced Concrete Structures (Volume I)", Sixth Edition, Standard Publishers Distributors,1705-B, Nai Sarak, Delhi-6.
- [4] N. Krishna Raju, 2013. "Prestressed Concrete", Fifth Edition, McGraw- Hill Education (India) Pvt. Ltd., New Delhi.
- [5] BSEN: 1992: Eurocode-2: Design of concrete structures.
- [6] BSEN: 1992-1-1: Common Rules for Buildings and Civil Engineering Structures.
- [7] B.N Dutta, 2009 "Estimating And Costing In Civil Engineering", Twenty-Sixth Revised Edition UBS Publishers' Distributors Pvt. Ltd. New Delhi.

Applications of Modified F-Expansion Method for Nonlinear Partial Differential Equations with Variable Coefficients

¹Priyanka M. Patel , ²Vikas H. Pradhan

^{1,2}Department of Applied Mathematics & Humanities, S. V. National Institute of Technology, Surat-395007, India

ABSTRACT

The modified F-expansion method is used to obtain the new exact travelling wave solutions of Burger equation and Benjamin-Bona-Mahony (BBM) equation with variable coefficients. The obtained solutions include solitary wave solutions, trigonometric function solutions and rational solutions. In addition some figures are provided for direct viewing analysis.

KEYWORDS: modified F-expansion method, Burgers' equation and BBM equation with variable coefficients, solitary wave solutions, trigonometric function solutions, rational solutions

I. INTRODUCTION

Many phenomena arising in many fields of sciences and engineering have been modeled in modern times in terms of nonlinear partial differential equations (NLPDEs). As mathematical models of the phenomena, the study of exact solutions of NLPDEs will help us to understand the underlying mechanism that governs these phenomena or to provide better knowledge of its physical content and possible applications. Recently, the study of variable coefficients nonlinear partial differential equations (VC-NLPDEs) has become more and more attractive. This is because of the fact that a large number of important physical phenomena can be described by these equations. To find exact solutions of VC-NLPDEs, many powerful methods have been developed such as the tanh function method [3,10], exp-function method [3,6,13], F-expansion method [9,15], adomain decomposition method [1], sine-cosine [3] method, extended mapping transformation method [12], (G'/G) expansion method [4,5,11] and so on. In the present study, the modified F-expansion method is used to construct the exact solutions of VC-NLPDEs. As applications of the method, we will consider Burgers' equation [2] and BBM equation [14] with variable coefficients.

The plan of the paper is as follows: in section 2, we describe the modified F-expansion method. In section 3, we construct the exact solutions of Burgers' equation and BBM equation with variable coefficients. Some conclusions are given in the last section.

II. INTRODUCTION TO MODIFIED F-EXPANSION METHOD

Introduction of modified F-expansion method with constant coefficients is shown in [7,8]. In this study, we introduce modified F-expansion method with variable coefficients.

Consider a given nonlinear partial differential equation with variable coefficients as:

$$P(u, u_t, \alpha(t)u_x, \beta(t)u_{xx}, \gamma(t)u_{xxx}, \dots) = 0 \quad (1)$$

where $u(x, t)$ is the solution of the eq.(1).

The main points of the modified F-expansion method for solving eq.(1) are as follows:

[1]. Using the transformation,

$$u(x, t) = u(\xi) \text{ where } \xi = kx + \int v(t) dt \quad (2)$$

where $k \neq 0$ is a constant and $v(t)$ is an integrable function of t .

Substituting eq.(2) into eq.(1) yields an ordinary differential equation for $u(\xi)$

$$P(u, v(t)u', k\alpha(t)u', k^2\beta(t)u'', k^3\gamma(t)u''', \dots) = 0 \quad (3)$$

where prime denotes the derivative with respect to ξ .

[2]. Suppose that $u(\xi)$ can be expressed as

$$u(\xi) = \sum_{i=-N}^N a_i F^i(\xi) \text{ where } a_N \neq 0 \tag{4}$$

where $a_i (i = -N, \dots, -1, 0, 1, \dots, N)$ are constants, N is a positive integer which can be determined by considering the homogeneous balance between the governing nonlinear term(s) and highest order derivatives of $u(\xi)$ in eq.(3) and $F(\xi)$ is a solution of following Riccati equation,

$$F'(\xi) = A + BF(\xi) + CF^2(\xi) \tag{5}$$

where A, B, C are constants.

[3]. Substitute eq.(4) into eq.(3) and using eq.(5) then left-hand side of eq.(3) can be converted into a finite series in $F^p(\xi)$, ($p = -N, \dots, -1, 0, 1, \dots, N$). Equating each coefficient of $F^p(\xi)$ to zero yields a system of algebraic equations.

[4]. Solve the system of algebraic equations probably with the aid of Mathematica, we obtain the values of $a_i, v(t)$. Substituting these values into eq.(4), we can obtain the travelling wave solutions to eq.(3).

[5]. From the general form of travelling wave solutions listed in appendix, we can give a series of soliton-like solutions, trigonometric function solutions and rational solutions of eq.(1).

III. APPLICATIONS OF THE METHOD

3.1 Variable coefficient Burgers' equation

We consider the variable coefficient Burgers' equation in the form,

$$u_t + \alpha(t)uu_x - \beta(t)u_{xx} = 0 \tag{6}$$

where $\alpha(t)$ and $\beta(t)$ are arbitrary functions of t .

Using the transformation,

$$u(x, t) = u(\xi) \text{ where } \xi = kx + \int v(t) dt \tag{7}$$

where $k \neq 0$ is a constant and v is a function of t which is determined later.

Substituting eq.(7) into eq.(6), we get following ordinary differential equation

$$v(t)u' + k\alpha(t)uu' - k^2\beta(t)u'' = 0 \tag{8}$$

Now, balancing the orders of uu' and u'' , we get integer $N = 1$. So we can write solution of eq.(6) in the form,

$$u(x, t) = u(\xi) \text{ where } u(\xi) = a_0 + a_{-1}F^{-1}(\xi) + a_1F(\xi) \tag{9}$$

where a_0, a_{-1}, a_1 are constants and $F(\xi)$ is a solution of eq.(5).

Inserting eq.(9) together with eq.(5) into eq.(8), the left hand side of eq.(8) can be converted into a finite series in $F^p(\xi)$, ($p = -3, -2, -1, 0, 1, 2, 3$). Equating each coefficient of $F^p(\xi)$ to zero, we get system of algebraic equations for $a_0, a_{-1}, a_1, k, v(t)$.

$$\left. \begin{aligned} F^{-3}(\xi) : & -Aka_{-1}^2\alpha(t) - 2A^2k^2a_{-1}\beta(t) = 0 \\ F^{-2}(\xi) : & -Aa_{-1}v(t) - Aka_0a_{-1}\alpha(t) - Bka_{-1}^2\alpha(t) - 3ABk^2a_{-1}\beta(t) = 0 \\ F^{-1}(\xi) : & -Ba_{-1}v(t) - Bka_0a_{-1}\alpha(t) - Cka_{-1}^2\alpha(t) - B^2k^2a_{-1}\beta(t) \\ & - 2ACk^2a_{-1}\beta(t) = 0 \\ F^0(\xi) : & -Ca_{-1}v(t) + Aa_1v(t) - Cka_0a_{-1}\alpha(t) + Aka_0a_1\alpha(t) - BCK^2a_{-1}\beta(t) \\ & - ABk^2a_1\beta(t) = 0 \\ F^1(\xi) : & Ba_1v(t) + Bka_0a_1\alpha(t) + Aka_1^2\alpha(t) - B^2k^2a_1\beta(t) \\ & - 2ACk^2a_1\beta(t) = 0 \\ F^2(\xi) : & Ca_1v(t) + Cka_0a_1\alpha(t) + Bka_1^2\alpha(t) - 3BCK^2a_1\beta(t) = 0 \\ F^3(\xi) : & Cka_1^2\alpha(t) - 2C^2k^2a_1\beta(t) = 0 \end{aligned} \right\} \tag{10}$$

Solving the above algebraic equations with the help of Mathematica, we get the following results for $a_0, a_{-1}, a_1, v(t)$.

Case 1: $A = 0$, we have

$$a_0 = a_0, a_{-1} = 0, a_1 = a_1, v(t) = \frac{k^2(-2Ca_0 + Ba_1)\beta(t)}{a_1}, \alpha(t) = \frac{2Ck\beta(t)}{a_1} \quad (11)$$

Case 2: $B = 0$, we have

$$a_0 = a_0, a_{-1} = 0, a_1 = a_1, v(t) = -\frac{2Ck^2a_0\beta(t)}{a_1}, \alpha(t) = \frac{2Ck\beta(t)}{a_1} \quad (12)$$

$$a_0 = a_0, a_{-1} = -\frac{Aa_1}{C}, a_1 = a_1, v(t) = -\frac{2Ck^2a_0\beta(t)}{a_1}, \alpha(t) = \frac{2Ck\beta(t)}{a_1} \quad (13)$$

Case 3: $A = B = 0$, we have

$$a_0 = a_0, a_{-1} = 0, a_1 = a_1, v = -\frac{2Ck^2a_0\beta(t)}{a_1}, \alpha(t) = \frac{2Ck\beta(t)}{a_1} \quad (14)$$

Substituting these results into eq.(9) and using appendix, we obtain the following travelling wave solutions of eq.(6).

(1) Select $A = 0, B = 1, C = -1$ and $F(\xi) = \frac{1}{2} + \frac{1}{2} \tanh\left(\frac{\xi}{2}\right)$ from appendix and using eq.(11), we get

$$u_1(x, t) = a_0 + a_1 \left(\frac{1}{2} + \frac{1}{2} \tanh \left[\frac{1}{2} \left(kx + \frac{k^2(2a_0 + a_1) \int \beta(t) dt}{a_1} \right) \right] \right) \quad (15)$$

(2) Select $A = 0, B = -1, C = 1$ and $F(\xi) = \frac{1}{2} - \frac{1}{2} \coth\left(\frac{\xi}{2}\right)$ from appendix and using eq.(11), we get

$$u_2(x, t) = a_0 + a_1 \left(\frac{1}{2} - \frac{1}{2} \coth \left[\frac{1}{2} \left(kx + \frac{k^2(-2a_0 - a_1) \int \beta(t) dt}{a_1} \right) \right] \right) \quad (16)$$

(3) Select $A = \frac{1}{2}, B = 0, C = -\frac{1}{2}$ and $F(\xi) = \coth(\xi) \pm \operatorname{csc} h(\xi)$,

$\tanh(\xi) \pm i \operatorname{sec} h(\xi)$ from appendix and using eq.(12) and eq.(13) respectively, we get

$$u_3(x, t) = a_0 + a_1 \left(\coth \left[kx + \frac{k^2 a_0 \int \beta(t) dt}{a_1} \right] \pm \operatorname{csc} h \left[kx + \frac{k^2 a_0 \int \beta(t) dt}{a_1} \right] \right) \quad (17)$$

$$u_4(x, t) = a_0 + a_1 \left(\coth \left[kx + \frac{k^2 a_0 \int \beta(t) dt}{a_1} \right] \pm \operatorname{csc} h \left[kx + \frac{k^2 a_0 \int \beta(t) dt}{a_1} \right] \right)^{-1} + a_1 \left(\coth \left[kx + \frac{k^2 a_0 \int \beta(t) dt}{a_1} \right] \pm \operatorname{csc} h \left[kx + \frac{k^2 a_0 \int \beta(t) dt}{a_1} \right] \right) \quad (18)$$

$$u_5(x, t) = a_0 + a_1 \left(\tanh \left[kx + \frac{k^2 a_0 \int \beta(t) dt}{a_1} \right] \pm i \operatorname{sec} h \left[kx + \frac{k^2 a_0 \int \beta(t) dt}{a_1} \right] \right)$$

$$u_6(x, t) = a_0 + a_1 \left(\tanh \left[kx + \frac{k^2 a_0 \int \beta(t) dt}{a_1} \right] \pm i \operatorname{sec} h \left[kx + \frac{k^2 a_0 \int \beta(t) dt}{a_1} \right] \right)^{-1} + a_1 \left(\tanh \left[kx + \frac{k^2 a_0 \int \beta(t) dt}{a_1} \right] \pm i \operatorname{sec} h \left[kx + \frac{k^2 a_0 \int \beta(t) dt}{a_1} \right] \right) \quad (19)$$

$$(20)$$

(4) Select $A = 1, B = 0, C = -1$ and $F(\xi) = \tanh(\xi), \coth(\xi)$ from appendix and using eq.(12), eq.(13) respectively, we get

$$u_7(x, t) = a_0 + a_1 \left(\tanh \left[kx + \frac{2k^2 a_0 \int \beta(t) dt}{a_1} \right] \right) \quad (21)$$

$$u_8(x, t) = a_0 + a_1 \left(\tanh \left[kx + \frac{2k^2 a_0 \int \beta(t) dt}{a_1} \right] \right)^{-1} + a_1 \left(\tanh \left[kx + \frac{2k^2 a_0 \int \beta(t) dt}{a_1} \right] \right) \quad (22)$$

$$u_9(x, t) = a_0 + a_1 \left(\coth \left[kx + \frac{2k^2 a_0 \int \beta(t) dt}{a_1} \right] \right) \quad (23)$$

$$u_{10}(x, t) = a_0 + a_1 \left(\coth \left[kx + \frac{2k^2 a_0 \int \beta(t) dt}{a_1} \right] \right)^{-1} + a_1 \left(\coth \left[kx + \frac{2k^2 a_0 \int \beta(t) dt}{a_1} \right] \right) \quad (24)$$

(5) Select $A = \frac{1}{2}, B = 0, C = \frac{1}{2}$ and $F(\xi) = \sec(\xi) + \tan(\xi), \csc(\xi) - \cot(\xi)$ from appendix and using eq.(12), eq.(13) respectively, we get

$$u_{11}(x, t) = a_0 + a_1 \left(\sec \left[kx - \frac{k^2 a_0 \int \beta(t) dt}{a_1} \right] + \tan \left[kx - \frac{k^2 a_0 \int \beta(t) dt}{a_1} \right] \right) \quad (25)$$

$$u_{12}(x, t) = a_0 - a_1 \left(\sec \left[kx - \frac{k^2 a_0 \int \beta(t) dt}{a_1} \right] + \tan \left[kx - \frac{k^2 a_0 \int \beta(t) dt}{a_1} \right] \right)^{-1} + a_1 \left(\sec \left[kx - \frac{k^2 a_0 \int \beta(t) dt}{a_1} \right] + \tan \left[kx - \frac{k^2 a_0 \int \beta(t) dt}{a_1} \right] \right) \quad (26)$$

$$u_{13}(x, t) = a_0 + a_1 \left(\csc \left[kx - \frac{k^2 a_0 \int \beta(t) dt}{a_1} \right] - \cot \left[kx - \frac{k^2 a_0 \int \beta(t) dt}{a_1} \right] \right) \quad (27)$$

$$u_{14}(x, t) = a_0 - a_1 \left(\csc \left[kx - \frac{k^2 a_0 \int \beta(t) dt}{a_1} \right] - \cot \left[kx - \frac{k^2 a_0 \int \beta(t) dt}{a_1} \right] \right)^{-1} + a_1 \left(\csc \left[kx - \frac{k^2 a_0 \int \beta(t) dt}{a_1} \right] - \cot \left[kx - \frac{k^2 a_0 \int \beta(t) dt}{a_1} \right] \right) \quad (28)$$

(6) Select $A = -\frac{1}{2}, B = 0, C = -\frac{1}{2}$ and $F(\xi) = \sec(\xi) - \tan(\xi), \csc(\xi) + \cot(\xi)$ from appendix and using eq.(12), eq.(13) respectively, we get

$$u_{15}(x, t) = a_0 + a_1 \left(\sec \left[kx + \frac{k^2 a_0 \int \beta(t) dt}{a_1} \right] - \tan \left[kx + \frac{k^2 a_0 \int \beta(t) dt}{a_1} \right] \right) \quad (29)$$

$$u_{16}(x,t) = a_0 - a_1 \left(\sec \left[kx + \frac{k^2 a_0 \int \beta(t) dt}{a_1} \right] - \tan \left[kx + \frac{k^2 a_0 \int \beta(t) dt}{a_1} \right] \right)^{-1} + a_1 \left(\sec \left[kx + \frac{k^2 a_0 \int \beta(t) dt}{a_1} \right] - \tan \left[kx + \frac{k^2 a_0 \int \beta(t) dt}{a_1} \right] \right) \quad (30)$$

$$u_{17}(x,t) = a_0 + a_1 \left(\csc \left[kx + \frac{k^2 a_0 \int \beta(t) dt}{a_1} \right] + \cot \left[kx + \frac{k^2 a_0 \int \beta(t) dt}{a_1} \right] \right) \quad (31)$$

$$u_{18}(x,t) = a_0 - a_1 \left(\csc \left[kx + \frac{k^2 a_0 \int \beta(t) dt}{a_1} \right] + \cot \left[kx + \frac{k^2 a_0 \int \beta(t) dt}{a_1} \right] \right)^{-1} + a_1 \left(\csc \left[kx + \frac{k^2 a_0 \int \beta(t) dt}{a_1} \right] + \cot \left[kx + \frac{k^2 a_0 \int \beta(t) dt}{a_1} \right] \right) \quad (32)$$

(7) Select $A = 1, B = 0, C = 1$ and $F(\xi) = \tan(\xi)$ from appendix and using eq.(12), eq.(13) respectively, we get

$$u_{19}(x,t) = a_0 + a_1 \tan \left[kx - \frac{2k^2 a_0 \int \beta(t) dt}{a_1} \right] \quad (33)$$

$$u_{20}(x,t) = a_0 - a_1 \left(\tan \left[kx - \frac{2k^2 a_0 \int \beta(t) dt}{a_1} \right] \right)^{-1} + a_1 \tan \left[kx - \frac{2k^2 a_0 \int \beta(t) dt}{a_1} \right] \quad (34)$$

(8) Select $A = -1, B = 0, C = -1$ and $F(\xi) = \cot(\xi)$ from appendix and using eq.(12), eq.(13) respectively, we get

$$u_{21}(x,t) = a_0 + a_1 \cot \left[kx + \frac{2k^2 a_0 \int \beta(t) dt}{a_1} \right] \quad (35)$$

$$u_{22}(x,t) = a_0 - a_1 \left(\cot \left[kx + \frac{2k^2 a_0 \int \beta(t) dt}{a_1} \right] \right)^{-1} + a_1 \cot \left[kx + \frac{2k^2 a_0 \int \beta(t) dt}{a_1} \right] \quad (36)$$

(9) Select $A = 0, B = 0, C \neq 0$ and $F(\xi) = -\frac{1}{C\xi + m}$ from appendix and using eq.(14), we get

$$u_{23}(x,t) = a_0 - \frac{a_1^2}{C k a_1 x - 2C^2 k^2 a_0 \int \beta(t) dt + a_1 m} \quad (37)$$

where m is an arbitrary constant.

Graphical presentation:

For the graphical presentation, we taking solution $u_1(x,t)$ given by eq.(15) as an example. For simplicity we set

$a_0 = 1, a_1 = -1$ and $k = \frac{1}{2}$. Here we plot solution $u_1(x,t)$ for different values of $\beta(t) = (a)e^t, (b)\sin(t), (c)\tanh(t)$.

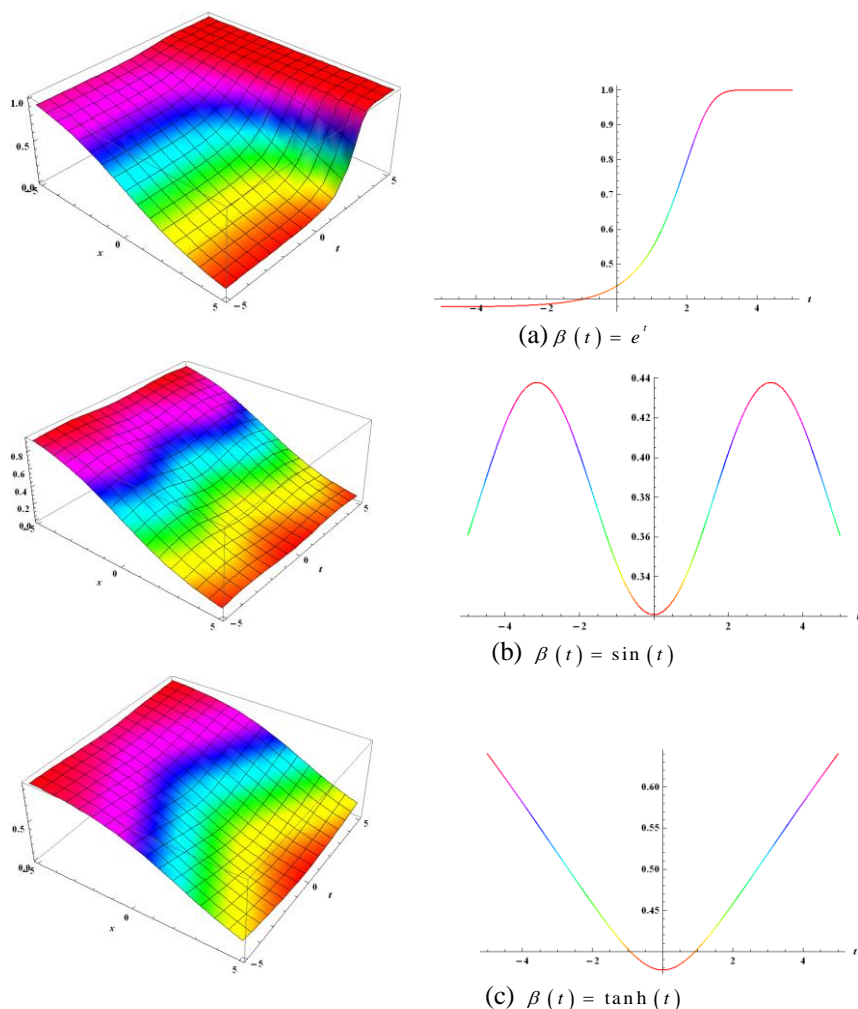


Figure 1. Solution of Burgers' equation with variable coefficients in different form

3.2 Variable coefficient BBM equation

We consider following variable coefficient BBM equation

$$u_t + a(t)u_x + b(t)u^p u_x - u_{xxt} = 0 \tag{38}$$

where $p > 0$ and $a(t), b(t)$ are arbitrary functions of t .

For simplicity here we consider $p = 1$

$$u_t + a(t)u_x + b(t)uu_x - u_{xxt} = 0 \tag{39}$$

Taking the transformation,

$$u(x, t) = u(\xi) \text{ where } \xi = kx + \int v(t) dt \tag{40}$$

where $k \neq 0$ and v is a function of t which is determined later.

Substituting eq.(40) into eq.(39), we get ordinary differential equation

$$v(t)u' + k a(t)u' + k b(t)uu' - k^2 v(t)u'' = 0 \tag{41}$$

Balancing the orders of $u u'$ and u'' , we get integer $N = 2$. So we can write solution of eq.(39) in the form,

$$u(\xi) = a_0 + a_{-2}F^{-2}(\xi) + a_{-1}F^{-1}(\xi) + a_1F(\xi) + a_2F^2(\xi) \tag{42}$$

Substituting eq.(42) together with eq.(5) into eq.(41), the left hand side of eq.(41) can be converted into a finite series in $F^p(\xi)$, ($p = -5, -4, -3, -2, -1, 0, 1, 2, 3, 4, 5$). Equating each coefficient of $F^p(\xi)$ to zero, we get system of algebraic equations for $a_0, a_{-2}, a_{-1}, a_1, a_2, k, v(t)$.

$$\begin{aligned}
 F^{-5}(\xi) &: -2Ab(t)ka_{-2}^2 + 24A^3k^2a_{-2}v = 0 \\
 F^{-4}(\xi) &: -2b(t)Bka_{-2}^2 - 3Ab(t)ka_{-2}a_{-1} + 54A^2Bk^2a_{-2}v(t) + 6A^3k^2a_{-1}v(t) = 0 \\
 F^{-3}(\xi) &: -2a(t)Aka_{-2} - 2Ab(t)ka_0a_{-2} - 2b(t)Cka_{-2}^2 - 3b(t)Bka_{-2}a_{-1} \\
 &\quad - Ab(t)ka_{-1}^2 - 2Aa_{-2}v(t) + 38AB^2k^2a_{-2}v(t) + 40A^2Ck^2a_{-2}v(t) \\
 &\quad + 12A^2Bk^2a_{-1}v(t) = 0 \\
 F^{-2}(\xi) &: -2a(t)Bka_{-2} - 2b(t)Bka_0a_{-2} - a(t)Aka_{-1} - Ab(t)ka_0a_{-1} - 3b(t)Cka_{-2}a_{-1} \\
 &\quad - b(t)Bka_{-1}^2 - Ab(t)ka_{-2}a_{-1} - 2Ba_{-2}v(t) + 8B^3k^2a_{-2}v(t) + 52ABCK^2a_{-2}v(t) \\
 &\quad - Aa_{-1}v(t) + 7AB^2k^2a_{-1}v(t) + 8A^2Ck^2a_{-1}v(t) = 0 \\
 F^{-1}(\xi) &: -2a(t)Cka_{-2} - 2b(t)Cka_0a_{-2} - a(t)Bka_{-1} - Bb(t)ka_0a_{-1} - b(t)Cka_{-1}^2 \\
 &\quad - b(t)Bka_{-2}a_{-1} - 2Ca_{-2}v(t) + 14B^2Ck^2a_{-2}v(t) + 16AC^2k^2a_{-2}v(t) - Ba_{-1}v(t) \\
 &\quad + B^3k^2a_{-1}v(t) + 8ABCK^2a_{-1}v(t) = 0 \\
 F^0(\xi) &: -a(t)Cka_{-1} - b(t)Cka_0a_{-1} + a(t)Aka_1 + Ab(t)ka_0a_1 - b(t)Cka_{-2}a_1 + 6BC^2k^2a_{-2}v(t) \\
 &\quad - Ca_{-1}v(t) + B^2Ck^2a_{-1}v(t) + 2AC^2k^2a_{-1}v(t) + Aa_1v(t) - AB^2k^2a_1v(t) - 2A^2Ck^2a_1v(t) \\
 &\quad + Ab(t)ka_{-1}a_2 - 6A^2Bk^2v(t)a_2 = 0 \\
 F^1(\xi) &: a(t)Bka_1 + Bb(t)ka_0a_1 + Ab(t)ka_1^2 + Ba_1v(t) - B^3k^2a_1v(t) - 8ABCK^2a_1v(t) + 2a(t)Aka_2 \\
 &\quad + 2Ab(t)ka_0a_2 + b(t)Bka_{-1}a_2 + 2Av(t)a_2 - 14AB^2k^2a_2v(t) - 16A^2Ck^2a_2v(t) = 0 \\
 F^2(\xi) &: a(t)Cka_1 + Cb(t)ka_0a_1 + Bb(t)ka_1^2 + Ca_1v(t) - 7B^2Ck^2a_1v(t) - 8AC^2k^2a_1v(t) \\
 &\quad + 2a(t)Bka_2 + 2b(t)Bka_0a_2 + b(t)Cka_{-1}a_2 + 3Ab(t)ka_1a_2 + 2Bv(t)a_2 - 8B^3k^2v(t)a_2 \\
 &\quad - 52ABCK^2v(t)a_2 = 0 \\
 F^3(\xi) &: b(t)Cka_1^2 - 12BC^2k^2a_1v(t) + 2a(t)Cka_2 + 2b(t)Cka_0a_2 + 3b(t)Bka_1a_2 + 2Cv(t)a_2 \\
 &\quad - 38B^2Ck^2v(t)a_2 - 40AC^2k^2v(t)a_2 + 2Ab(t)ka_2^2 = 0 \\
 F^4(\xi) &: -6C^3k^2a_1v(t) + 3b(t)Cka_1a_2 - 54BC^2k^2a_2v(t) + 2b(t)Bka_2^2 = 0 \\
 F^5(\xi) &: -24C^3k^2a_2v(t) + 2b(t)Cka_2^2 = 0
 \end{aligned}$$

(43)

Solving above algebraic equations with the help of Mathematica, we obtain following results:

Case 1: $A = 0$, we have

$$\begin{aligned}
 a_0 = a_0, a_{-2} = 0, a_{-1} = 0, a_1 = a_1, a_2 = \frac{Ca_1}{B}, v(t) = \frac{b(t)a_1}{12BCK} \\
 a(t) = \frac{-12b(t)BCK^2a_0 - b(t)a_1 + b(t)B^2k^2a_1}{12BCK^2}
 \end{aligned}
 \tag{44}$$

Case 2: $B = 0$, we have

$$\begin{aligned}
 a_0 = a_0, a_{-2} = 0, a_{-1} = 0, a_1 = 0, a_2 = a_2, v(t) = \frac{b(t)a_2}{12C^2k} \\
 a(t) = \frac{-12b(t)C^2k^2a_0 - b(t)a_2 + 8b(t)ACK^2a_2}{12C^2k^2}
 \end{aligned}
 \tag{45}$$

$$\begin{aligned}
 a_0 = a_0, a_{-2} = \frac{A^2a_2}{C^2}, a_{-1} = 0, a_1 = 0, a_2 = a_2, v(t) = \frac{b(t)a_2}{12C^2k} \\
 a(t) = \frac{-12b(t)C^2k^2a_0 - b(t)a_2 + 8b(t)ACK^2a_2}{12C^2k^2}
 \end{aligned}
 \tag{46}$$

Case 3: $A = B = 0$, we have

$$a_0 = a_0, a_{-2} = 0, a_{-1} = 0, a_1 = 0, a_2 = a_2, v(t) = \frac{b(t)a_2}{12C^2k}, \tag{47}$$

$$a(t) = \frac{-12b(t)C^2k^2a_0 - b(t)a_2}{12C^2k^2}$$

Substituting these results into eq.(42) and using appendix, we obtain the travelling wave solutions of eq.(39) as follows:

(1) Select $A = 0, B = 1, C = -1$ and $F(\xi) = \frac{1}{2} + \frac{1}{2} \tanh\left(\frac{\xi}{2}\right)$ from appendix and using eq.(44), we get

$$u_1(x,t) = a_0 + \frac{a_1}{4} \operatorname{sech} \left[\frac{kx}{2} - \frac{a_1 \int b(t) dt}{24k} \right]^2 \tag{48}$$

(2) Select $A = 0, B = -1, C = 1$ and $F(\xi) = \frac{1}{2} - \frac{1}{2} \coth\left(\frac{\xi}{2}\right)$ from appendix and using eq.(44), we get

$$u_2(x,t) = a_0 - \frac{a_1}{4} \operatorname{csc h} \left[\frac{kx}{2} - \frac{a_1 \int b(t) dt}{24k} \right]^2 \tag{49}$$

(3) Select $A = \frac{1}{2}, B = 0, C = -\frac{1}{2}$ and $F(\xi) = \coth(\xi) \pm \operatorname{csc h}(\xi)$,

$\tanh(\xi) \pm i \operatorname{sech}(\xi)$ from appendix and using eq.(45) and eq.(46) respectively, we get

$$u_3(x,t) = a_0 + a_2 \left(\operatorname{csc h} \left[kx + \int \frac{b(t)a_2}{3k} dt \right] \pm \coth \left[kx + \int \frac{b(t)a_2}{3k} dt \right] \right)^2 \tag{50}$$

$$u_4(x,t) = a_0 + a_2 \left(\operatorname{csc h} \left[kx + \int \frac{b(t)a_2}{3k} dt \right] \pm \coth \left[kx + \int \frac{b(t)a_2}{3k} dt \right] \right)^{-2} + a_2 \left(\operatorname{csc h} \left[kx + \int \frac{b(t)a_2}{3k} dt \right] \pm \coth \left[kx + \int \frac{b(t)a_2}{3k} dt \right] \right)^2 \tag{51}$$

$$u_5(x,t) = a_0 + a_2 \left(\tanh h \left[kx + \int \frac{b(t)a_2}{3k} dt \right] \pm i \operatorname{sech} \left[kx + \int \frac{b(t)a_2}{3k} dt \right] \right)^2 \tag{52}$$

$$u_6(x,t) = a_0 + a_2 \left(\tanh h \left[kx + \int \frac{b(t)a_2}{3k} dt \right] \pm i \operatorname{sech} \left[kx + \int \frac{b(t)a_2}{3k} dt \right] \right)^{-2} + a_2 \left(\tanh h \left[kx + \int \frac{b(t)a_2}{3k} dt \right] \pm i \operatorname{sech} \left[kx + \int \frac{b(t)a_2}{3k} dt \right] \right)^2 \tag{53}$$

(4) Select $A = 1, B = 0, C = -1$ and $F(\xi) = \tanh(\xi), \coth(\xi)$ from appendix and using eq.(45) and eq.(46) respectively, we get

$$u_7(x,t) = a_0 + a_2 \left(\tanh \left[kx + \int \frac{b(t)a_2}{12k} dt \right] \right)^2 \tag{54}$$

$$u_8(x,t) = a_0 + a_2 \left(\tanh \left[kx + \int \frac{b(t)a_2}{12k} dt \right] \right)^{-2} + a_2 \left(\tanh \left[kx + \int \frac{b(t)a_2}{12k} dt \right] \right)^2$$

$$(55) u_9(x,t) = a_0 + a_2 \left(\coth \left[kx + \int \frac{b(t)a_2}{12k} dt \right] \right)^2 \tag{56}$$

$$u_{10}(x,t) = a_0 + a_2 \left(\coth \left[kx + \int \frac{b(t)a_2}{12k} dt \right] \right)^{-2} + a_2 \left(\coth \left[kx + \int \frac{b(t)a_2}{12k} dt \right] \right)^2 \tag{57}$$

(5) Select $A = \frac{1}{2}, B = 0, C = \frac{1}{2}$ and $F(\xi) = \sec(\xi) + \tan(\xi), \csc(\xi) - \cot(\xi)$ from appendix and using eq.(45) and eq.(46) respectively, we get

$$u_{11}(x,t) = a_0 + a_2 \left(\sec \left[kx + \int \frac{b(t)a_2}{3k} dt \right] + \tan \left[kx + \int \frac{b(t)a_2}{3k} dt \right] \right)^2 \tag{58}$$

$$u_{12}(x,t) = a_0 + a_2 \left(\sec \left[kx + \int \frac{b(t)a_2}{3k} dt \right] + \tan \left[kx + \int \frac{b(t)a_2}{3k} dt \right] \right)^{-2} + a_2 \left(\sec \left[kx + \int \frac{b(t)a_2}{3k} dt \right] + \tan \left[kx + \int \frac{b(t)a_2}{3k} dt \right] \right)^2 \tag{59}$$

$$u_{13}(x,t) = a_0 + a_2 \left(\csc \left[kx + \int \frac{b(t)a_2}{3k} dt \right] - \cot \left[kx + \int \frac{b(t)a_2}{3k} dt \right] \right)^2 \tag{60}$$

$$u_{14}(x,t) = a_0 + a_2 \left(\csc \left[kx + \int \frac{b(t)a_2}{3k} dt \right] - \cot \left[kx + \int \frac{b(t)a_2}{3k} dt \right] \right)^{-2} + a_2 \left(\csc \left[kx + \int \frac{b(t)a_2}{3k} dt \right] - \cot \left[kx + \int \frac{b(t)a_2}{3k} dt \right] \right)^2 \tag{61}$$

(6) Select $A = -\frac{1}{2}, B = 0, C = -\frac{1}{2}$ and $F(\xi) = \sec(\xi) - \tan(\xi), \csc(\xi) + \cot(\xi)$ from appendix and using eq.(45) and eq.(46) respectively, we get

$$u_{15}(x,t) = a_0 + a_2 \left(\sec \left[kx + \int \frac{b(t)a_2}{3k} dt \right] - \tan \left[kx + \int \frac{b(t)a_2}{3k} dt \right] \right)^2 \tag{62}$$

$$u_{16}(x,t) = a_0 + a_2 \left(\sec \left[kx + \int \frac{b(t)a_2}{3k} dt \right] - \tan \left[kx + \int \frac{b(t)a_2}{3k} dt \right] \right)^{-2} + a_2 \left(\sec \left[kx + \int \frac{b(t)a_2}{3k} dt \right] - \tan \left[kx + \int \frac{b(t)a_2}{3k} dt \right] \right)^2 \tag{63}$$

$$u_{17}(x,t) = a_0 + a_2 \left(\csc \left[kx + \int \frac{b(t)a_2}{3k} dt \right] + \cot \left[kx + \int \frac{b(t)a_2}{3k} dt \right] \right)^2 \tag{64}$$

$$u_{18}(x,t) = a_0 + a_2 \left(\csc \left[kx + \int \frac{b(t)a_2}{3k} dt \right] + \cot \left[kx + \int \frac{b(t)a_2}{3k} dt \right] \right)^{-2} + a_2 \left(\csc \left[kx + \int \frac{b(t)a_2}{3k} dt \right] + \cot \left[kx + \int \frac{b(t)a_2}{3k} dt \right] \right)^2 \tag{65}$$

(6) Select $A = 1(-1), B = 0, C = 1(-1)$ and $F(\xi) = \tan(\xi), \cot(\xi)$ from appendix and using eq.(45) and eq.(46) respectively, we get

$$u_{19}(x,t) = a_0 + a_2 \left(\tan \left[kx + \frac{b(t)a_2}{12k} \right] \right)^2 \tag{66}$$

$$u_{20}(x,t) = a_0 + a_2 \left(\tan \left[kx + \frac{b(t)a_2}{12k} \right] \right)^{-2} + a_2 \left(\tan \left[kx + \frac{b(t)a_2}{12k} \right] \right)^2 \tag{67}$$

$$u_{21}(x, t) = a_0 + a_2 \left(\cot \left[kx + \frac{b(t)a_2}{12k} \right] \right)^2 \quad (68)$$

$$u_{22}(x, t) = a_0 + a_2 \left(\cot \left[kx + \frac{b(t)a_2}{12k} \right] \right)^{-2} + a_2 \left(\cot \left[kx + \frac{b(t)a_2}{12k} \right] \right)^2 \quad (69)$$

(7) Select $A = B = 0, C \neq 0$ and $F(\xi) = \left(-\frac{1}{C\xi + m} \right)$ from appendix and using eq.(47), we get

$$u_{23}(x, t) = a_0 + a_2 \left(-\frac{1}{C \left(kx + \int \frac{b(t)a_2}{12C^2k} dt \right) + m} \right)^2 \quad (70)$$

where m is an arbitrary constant.

Graphical presentation:

Here we taking solution $u_1(x, t)$ given by eq.(48) for the graphical presentation. Fixing $a_0 = k = 1, a_2 = 4$ in eq.(48). When $b(t) = e^t, \sin(t)$ and $\sec h(t)$, the structures of eq.(48) are illustrated in figures 2(a), 2(b) and 2(c).

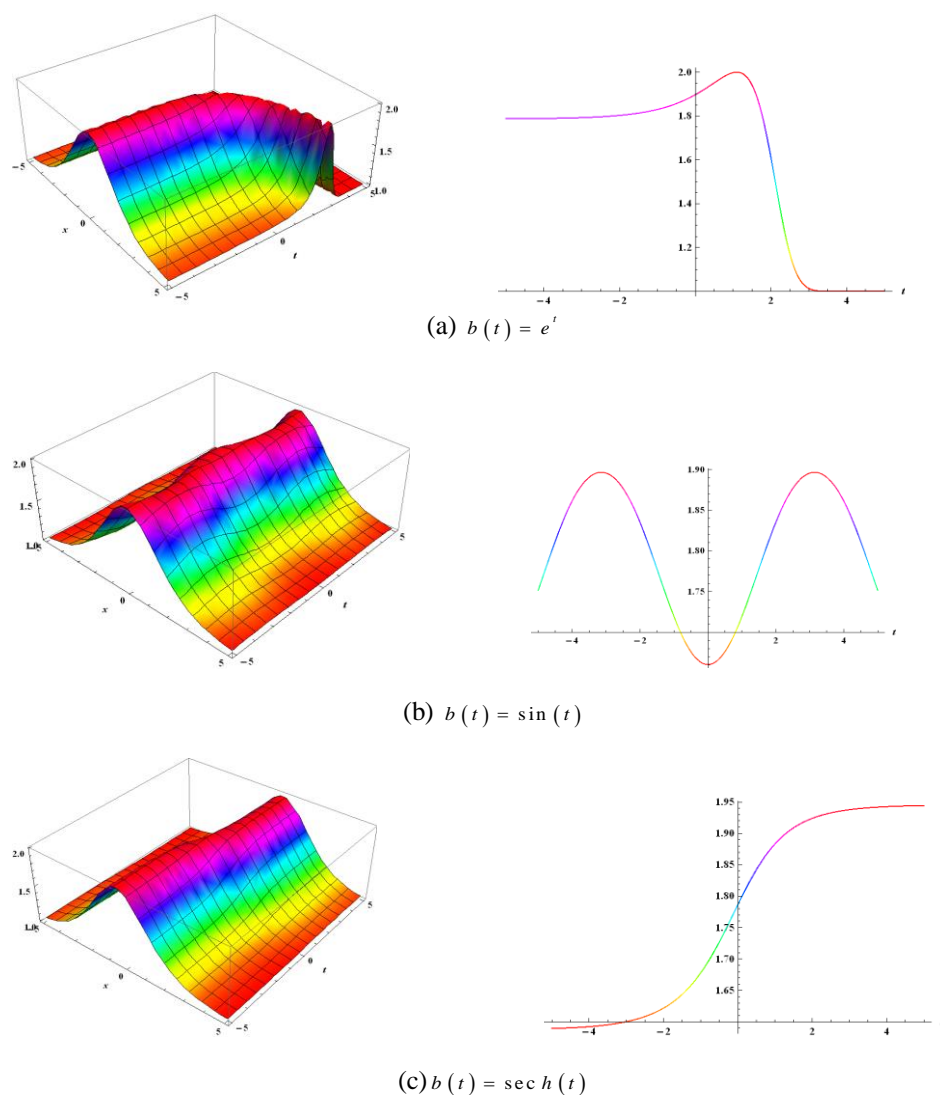


Figure 2. Solution of BBM equation with variable coefficients in different form

IV. CONCLUSION

In this paper, exact travelling wave solutions of the Burgers' equation and BBM equation with variable coefficients have been obtained using the modified F-expansion method. These solutions are expressed in terms of hyperbolic, trigonometric and rational functions with arbitrary parameters. The obtained solutions may be useful to further understand the variable coefficients Burger equation and BBM equation and mechanism of the physical phenomena. The modified F-expansion method is promising and powerful method for handling other nonlinear partial differential equations with variable coefficients arising in mathematical physics.

Appendix: Relations between values of (A , B , C) and corresponding F (ξ) in Riccati equation

$$F'(\xi) = A + B F(\xi) + C F^2(\xi)$$

A	B	C	F (ξ)
0	1	-1	$\frac{1}{2} + \frac{1}{2} \tanh\left(\frac{\xi}{2}\right)$
0	-1	1	$\frac{1}{2} - \frac{1}{2} \coth\left(\frac{\xi}{2}\right)$
$\frac{1}{2}$	0	$-\frac{1}{2}$	$\coth(\xi) \pm \csc h(\xi), \tanh(\xi) \pm i \sec h(\xi)$
1	0	-1	$\tanh(\xi), \coth(\xi)$
$\frac{1}{2}$	0	$\frac{1}{2}$	$\sec(\xi) + \tan(\xi), \csc(\xi) - \cot(\xi)$
$-\frac{1}{2}$	0	$-\frac{1}{2}$	$\sec(\xi) - \tan(\xi), \csc(\xi) + \cot(\xi)$
1(-1)	0	1(-1)	$\tan(\xi), \cot(\xi)$
0	0	≠ 0	$-\frac{1}{C\xi + m}$ (m is an arbitrary constant)

REFERENCES

- [1] A-M. Wawaz, A. Gorguis, "Exact solutions for heat-like and wave-like equations with variable coefficients", Applied mathematics and computation, 149(1), pp.15-29, 2004
- [2] B. A. Malomed, V. I. Shrira, "Soliton caustics", Physica D: nonlinear phenomena, 53(1), pp.1-12, 1991
- [3] E. M. E. Zayed and M. A. M. Abdelaziz, "Exact solutions for the nonlinear Schrödinger equation with variable coefficients using the generalized extended tanh-function, the sine-cosine and the exp-function methods", Applied mathematics and computation, 218, pp. 2259-2268, 2011
- [4] E. M. E. Zayed and M. A. M. Abdelaziz, "Exact travelling wave solutions of nonlinear variable-coefficients evolution equations with forced terms using the generalized (G'/G) expansion method", Computational mathematics and modeling, 24(1), pp. 103-113, 2013
- [5] E. M. E. Zayed, "Exact travelling wave solutions for a variable-coefficient generalized dispersive water-wave system using the generalized (G'/G)-expansion method", Mathematical science letters-an international journal, 3(1), pp. 9-15, 2014
- [6] F. Khani, S. Hamed-Nezhad, "Some new exact solutions of the (2+1)-dimensional variable coefficient Broer-Kaup system using the exp-function method", Computers and mathematics with applications, 58, pp.2325-2329, 2009
- [7] G. Cai and Q. Wang, " A modified F-expansion method for solving nonlinear pdes", Journal of information and computing science, 2(1), pp. 3-16, 2007
- [8] G. Cai et al., "A modified F-expansion method for solving breaking soliton equation", international Journal of nonlinear science, 2(2), pp. 122-128, 2006
- [9] J-F Zhang et al., "Variable coefficient F-expansion method and its application to nonlinear Schrödinger equation", Optics communications, 252(4-6), pp. 408-421, 2005

- [10] L. Wei, "New exact solutions to some variable coefficients problems", *Applied mathematics and computation*, 217(4), pp.1632-1638, 2010
- [11] M. A. Abdou et al., "New exact travelling wave solutions of nonlinear evolution equations with variable coefficients", *Studies in nonlinear sciences*, 1(4), pp. 133-139, 2010
- [12] M. S. Abdel Latif, "Some exact solutions of kdv equation with variable coefficients", *Communications in nonlinear science and numerical simulation*, 16(4), pp. 1783-1786, 2011
- [13] S. Zhang, "Application of exp-function method to a kdv equation with variable coefficients", *physics letters A*, 365(5-6), pp.448-453, 2007
- [14] V. Bisognin, G. Perla Menzala, "Asymptotic behaviour of nonlinear dispersive models with variable coefficients", *Annali di matematica pure ed applicata*, 168(1), pp. 219-235, 1995
- [15] Y. Zhou et al., "Periodic wave solutions to a coupled kdv equations with variable coefficients", *Physics letters A*, 308(1), pp. 31-36, 2003

Case-Based Reasoning System for Diagnosis of Neuropsychiatric Abnormality

¹, Shabeeha Khatoon, ², Kavita Agarwal

¹, Student, Deptt of CSE, Integral University, Lucknow

², Professor, Deptt of CSE, Integral University, Lucknow

ABSTRACT

At the present time in medical field, neuropsychiatry abnormality diagnosis is limited and discussed partially in research papers, books and journals. It was very difficult to diagnose neuropsychiatric abnormality, by doctors, research groups and related agencies. There are many similar syndromes availability had caused difficulties to diagnose neuropsychiatric abnormality. Therefore, it was necessary to implement the algorithm, computerized method or software tool to diagnose the neuropsychiatric abnormality. In this paper for the diagnosis Case Based Reasoning (CBR) is used. CBR system includes four phases such as retrieve, reuse, revise, and retain. The first phase of the CBR (retrieve) makes cases from the previous knowledge. This method has been developed conceptually by using similarity factor. This method is used for basis of further programming development. By using this method, diagnosis of similar cases that occurred normally in neuropsychiatric abnormality is easily diagnose and will be given the appropriate solution.

KEYWORDS: Neuropsychiatry, CBR, similarity factor

I. INTRODUCTION

Neuropsychiatric is the branch of medical science which is dealing with psychological, cognitive, and physical parameters [1]. In this for the diagnosis of neuropsychiatric disease EEG and FMRI parameters is also included. Neuropsychiatric is the branch of mental disorder which consider both type of disorder that are associated with dis- functioning of brain due structure as well as due to behavioral changes. We can create table for syndromes abnormality description (Table-1) of neuropsychiatric abnormality on the basis of their three important syndromes: Psychophysical syndromes, EEG parameters and brain image (FMRI) analysis [2]. Psychophysical parameter is again divided into three sub parameters: Psychological parameters containing of 11 syndromes such as: Hyper Activity (HA), Anxiety (AX), Abnormal Behavior (AB), Delusion (DE), Anger (AN), Need of Perfection (NP), Agitation (AG), Distraction of Work (DW), Hallucination (HL), Fear (FR), Stress (ST), ; and Cognitive parameters containing of 8 syndromes such as: Speech (SH), Confusion in Decision Making (CD), Forgetting Memory (FM), Learning (LR), Reasoning (RS), Judgment (JG), Hearing (HR), Speech (SH) and Vision (VS); and Physical symptoms consisting of 8 syndromes such as: Vision (VS), Climbing (CL), Over Sleeping (OS), Walking (WL), Hearing (HR), Speech (SH), Locomotion (LO), and Hygiene (HG). The EEG signal characteristics are ACC (AC),

Temporal (TL), CG (CG), Frontal (FL), Parietal (PL) and Occipital (OL). The Image (FMRI) characteristics are ACC (AC), Frontal (FL), CG (CG), Parietal (PL), Temporal (TL), BG (BG) and Occipital (OL). In Table-1 first Column contains ten different cases of five different diseases. The second column contains different syndromes of the diseases. The respective columns contain "1" if the corresponding syndrome is present in the disease in that row. For example, Mood Disorder has Psychological syndrome such as: Agitation (AG), Anger (AN), Abnormal Behavior (AB), Stress (ST), Anxiety (AX), Distraction of Work (DW), Therefore, the columns contain "1" as in Table-1. The third and fourth columns of the Table-1 consist EEG and FMRI parameters such that respective row contain "1" or "0" depending upon whether the particular parameter present or not.

Computers as a evidence of the development of science, technology and telecommunication have been well-known by community. Computer technology had developed to utilize the computer act as human being. Development of computer science both hardware and software that simulate human intelligence and behavior is called Artificial Intelligence. According to [7], Artificial Intelligence consider: NLP, Computer Vision, Pattern

recognition, Robotics, Speech Recognition, ANS, Expert System, RBR and the upcoming latest development of Artificial Intelligence is CBR. However, the application of CBR is rarely used for the diagnosis of diseases.

The main goal of this research is to build and design a system that can provide information about the neuropsychiatric abnormality accurately and quickly, perform design engineering systems that can provide information on how to diagnose neuropsychiatric abnormality quickly and effectively, and design an interactive computerized system using the method CBR system. The advantage deliver from this study is as a input to develop science and technology, especially computers and neuropsychiatry field to be developed and exploited to a wider domain in future, for the doctors/patient as users can utilize this system to help solve the problems of neuropsychiatric abnormality accurately, quickly and efficiently. Furthermore, users are expected to evaluate, reasons behind the emergence of a abnormality.

II. RESEARCH METHOD

This paper is the developing system/method, which is used with computer software [20]. According to Pressman process of software engineering measures must be initiating from requirement gathering and analysis, design, implementation (programming) and testing.

Case based reasoning system design that has been worked as follows (Fig-1). When a new problem is comes, the CBR system *retrieves* most similar cases. By using retrieved solutions, after that *reuse* stage denotes a suggest solution, then *revision* stage corroborate the solution, and then *retain* stage can store the new case into the previous case base.

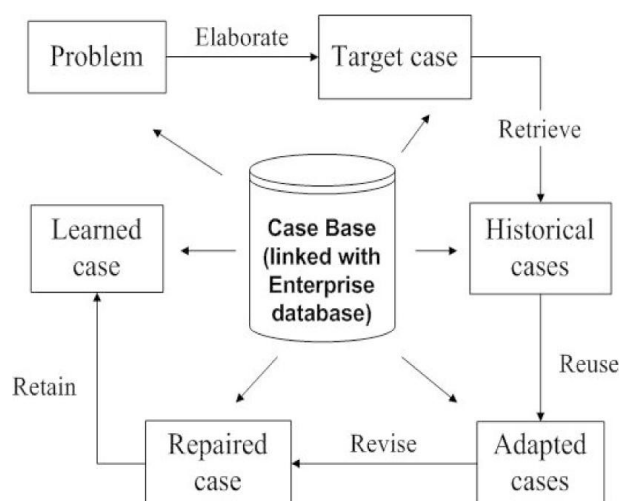


Fig. 1 CBR system for Neuropsychiatric abnormality
Fig 1 CBR system for fish disease Case

III. RESULTS AND DISCUSSION

Basic requirement in the development of Computer-Based Reasoning System for diagnosis of neuropsychiatric abnormality cases are:

A. Acquisition Database of Cases

This requirement is gathered from DSM-4, experts or Doctors having authority various reference sources about various cases of neuropsychiatric abnormality [1], [2], [3], [4], [5], [6], [11], [13], [14], [15], [21], [22], [23], [24], [25].

B. New Case Search

The design of this method is to help users to identifying neuropsychiatric abnormality by giving the value to the different syndromes. After given value, the system will search for cases which is similar to the new cases or similar cases in the database.

CBR techniques to diagnose the neuropsychiatric abnormality including: the representation of the different cases, introduce cases, the new problem identification phase, and selection stage.

C. Representation of different cases

Representation form in the case of computer-based reasoning system for the identification of fish disease cases are as follows (Fig. 2):

The first data from database:

<p>Neuropsychiatric Abnormality Parameters:</p> <ol style="list-style-type: none"> 1. Psychological <ol style="list-style-type: none"> a. AN : 1 b. AB : 1 c. AX : 1 d. AG : 1 e. DW : 1 f. HA : 1 2. Cognitive <ol style="list-style-type: none"> a. HR : 1 g. JG : 1 h. LR : 1 i. VS : 1 3. Physical <ol style="list-style-type: none"> j. CL : 1 k. HR : 1 l. VS : 1 m. HG : 1 4. EEG <ol style="list-style-type: none"> n. FL : 1 5. Image <ol style="list-style-type: none"> o. CG : 1 p. FL : 1 q. PL : 1 r. TL : 1 <p>Disease Diagnose: ADHD</p>
--

Fig. 2 Representation form case for ADHD disease
Fig.-2 The second data from the Data Base

D. Retrieve

Retrieve stage search cases by using CBR system for diagnosis of neuropsychiatric abnormality cases using the nearest neighbor technique. Nearest neighbor is a technique for search that supplies a measure of similarity of new case cases with original case. In the nearest neighbor method, to find a suitable case, the case should be matched with the saved case within a case base. Similarity is calculated for each index. Similarity calculation is done for selecting the most suitable cases or the most relevant. Different stages in the retrieve process are:

- Problem Identification phase
 - Matching phase
 - Selecting
- 1) *Problem Identification phase:* Problem identification phase includes the following steps: the user selects different syndromes from table-1.
 - 2) *Match Stage:* At this stage in the process includes the following steps: computer CBR system will perform a search process in the different cases as well as syndromes that are determined, then the search process result data associated with particular disease as well as the corresponding syndromes. After that, data from table-1 diseases previously obtained, find its value, and then process of calculation is done for each data similarity for different neuropsychiatric diseases.

3) Selecting:
 EXAMPLE of similarity calculation

a. Data from the user (Fig. 3):

```

Neuropsychiatry
Parameters
  1. Psychological
    a. AN      : 1
    b. AB      : 1
    c. AX      : 1
    d. AG      : 1
    e. FR      : 1
    f. NP      : 1
  2. Cognitive
    g. CD      : 1
    h. JG      : 1
    i. LR      : 1
    j. RS      : 1
  3. Physical
    k. WL      : 1
    l. VS      : 1
  4. EEG
    m. AC      : 1
    n. CG      : 1
    o. FL      : 1
    p. PL      : 1
    q. OL      : 1
    r. TL      : 1
  5. Image
    s. AC      : 1
    t. CG      : 1
    u. FL      : 1
Disease : ?
    
```

Fig. 3 Data input from users

b. Data from database of different neuropsychiatric abnormality. Search results from data types and syndromes of different diseases is (Fig. 4 and Fig. 5):

The second data from database:

```

Neuropsychiatry
Parameters
  1. Psychological
    a. AN      : 1
    b. AB      : 1
    c. AX      : 1
    d. AG      : 1
    e. HA      : 1
    f. SW      : 1
  2. Cognitive
    g. CD      : 1
    h. HR      : 1
    i. JG      : 1
    j. RS      : 1
  3. Physical
    k. WL      : 1
    l. HR      : 1
    m. VS      : 1
  4. EEG
    n. AC      : 1
    o. FL      : 1
    p. PL      : 1
    q. TL      : 1
  5. Image
    r. AC      : 1
    s. CG      : 1
    t. PL      : 1
Disease : OCD
    
```

Fig. 4 The second data from the Data Base

- c. Then count the value of each syndromes against each disease data derived from search results
- d. Comparison of results and similarity values of input data is by the user (Fig. 3) with the first data of the search results in Fig. 4 can be seen in Table-2.

TABLE -2 LOCAL SIMILARITY TABLE OF THE FIRST DATA ON DATABASE

Neuropsychiatry	
Syndromes	Weight
Psychological	0.8
Cognitive	1
Physical	0.6
EEG	0.2
Image	0.4

Similarity₁ = 1/41 [1*0.8+1*0.8+1*0.8+1*0.8+1*1+1*1+1*1+1*0.6+1*0.2+1*0.4+1*0.4]
=0.1463

TABLE 2 SIMILARITY TABLE OF THE SECOND DATA ON DATABASE

Neuropsychiatry	
Syndromes	Weight
Psychological	0.8
Cognitive	1
Physical	0.6
EEG	0.2
Image	0.4

Similarity₂ = 1/41 [1*0.8+1*0.8+1*0.8+1*0.8+1*1+1*1+1*1+1*0.6+1*0.6+1*0.2+1*0.2+1*0.2+1*0.2+1*0.4+1*0.4]
=0.2194

From the calculation similarity₁ and similarity₂, the calculation of the greatest is 0.4285. This result diagnose that patient is suffer from OCD.

E. Reuse

In case based reasoning system for diagnosis of neuropsychiatric abnormality using the reuse of the result from the search solution that are resemble (using the calculation of similarity) with new cases. Once previous known cases which are similar to the new case, then the solution of most similar cases will be replaced to be propose to the user as an result from the system. This method reuse a case like this is.

F. Revise

There are two main tasks of this phase: evaluation of result and correction of errors. Evaluation of result is how the results obtained after analyze the solutions with the actual situation. Betterments include the introduction of a new case made an error free result and take or make an explanation of the error. Revise process on this case based reasoning system for diagnosis of neuropsychiatric disease can only be done by experts in that field.

G. Retain

In this process of retaining, using result of similar cases are treated as the new cases. This New cases will be recorded as new cases until any expert has said the new cases as a valid new cases. Then the case is updated into the base case.

H. Adaptation

During the process of adaptation in this Case based reasoning system for diagnosis of neuropsychiatric disease is the null adaptation technique. Null adaptation techniques do not take any adaptation. This null adaptation technique is simply to take whatever result given from the search results equal to the case of a any new case. None of this adaptation is very useful for problems that include complex reasoning but with a simple solution.

IV. CONCLUSION

This paper has produced a system of Case based reasoning system to diagnose neuropsychiatry abnormality conceptually Retrieve phase (search cases) by using CBR system for diagnosis of neuropsychiatric abnormality cases using the nearest neighbor technique. Nearest neighbor is a technique for search that supplies a measure of similarity of new case cases with original case. In the nearest neighbor method, to find a suitable case, the case should be matched with the saved case within a case base. Similarity is calculated for each index. Similarity calculation is done for selecting the most suitable cases or the most relevant The basic thought used is that similar cases will have similar solutions as well as. reuse method is abnormality using the reuse of the result from the search solution that are resemble (using the calculation of similarity) with new cases. Once known case which are same as to the new case, then the solution of same cases will be recommended to the user as a result from the system. Result is referred to diagnosis of neuropsychiatric disease. Evaluation of result and correction of errors. This process can only be c by completed experts. In the process of In this process of retaining, using result of similar cases are treated as the new cases. This New cases will be recorded as new cases until any expert has said the new cases as a valid new cases. Then the case is updated into the base case .In adaptation process null adaptation process is used. Null adaptation techniques do not take any adaptation. This null adaptation technique is simply to take whatever result given from the search results equal to the case of a any new case.

REFERENCES

- [1] Mohit Gangwar ,International Journal of Computer Applications (0975 – 8887) Volume 55– No.17, October 2012
- [2] Afrianto, E. and E. Liviawaty, *Pengendalian Hama dan Penyakit Ikan*, Yogyakarta: Kanisius, 1992.
- [3] Yudofsky, S.C.; Hales, E.H. (2002). "Neuropsychiatry and the Future of Psychiatry and Neurology". *American Journal of Psychiatry* 159 (8): 1261–1264.
- [4] Alifuddin, M, "Studi Inaktivasi Fisik Monodon Baculovirus (MBV), Virus Patogen Udang Windu (*Penaeus monodon* Fab.)", *J. Akuakultur Indonesia*, vol. I (1), pp. 55 – 69, 2002.
- [5] Amlacher, E., *Textbook of Fish Diseases*, Delhi: Narendra Publishing House, 2005.
- [6] Dana, D. and S. L. Angka, "Masalah Penyakit Parasit dan Bakteri pada Ikan Air Tawar Serta Cara Penanggulangannya," in *Seminar Nasional II Penyakit Ikan dan Udang Tanggal 16 – 18 Januari 1990*. paper Balai Penelitian Perikanan Air Tawar Bogor, p. 10 – 23.
- [7] Mustafidah, H. dan Suwarsito, "Pengembangan Sistem Pakar untuk Mendiagnosa dan Memberikan Nasehat Cara Pengobatan Penyakit Ikan", Laporan Penelitian UMP, Tech. Rep., 2007.
- [8] Fikrivet and Tagged. (2009). Gejala-Motile-Aeromonas-Septicaemia on Fibiblog homepage on Fibiblog. [Online]. Available: <http://fikrivet.fipiblog.com/2009/03/29/gejala-motile-aeromonas-septicaemia/>.
- [7] Firebaugh, M. W., *Artificial Intelligence : A Knowledge-Based Approach*. Boston: PWS-KENT Publishing Company, 1988.
- [8] (2008) The CEE website [Online]. Available: <http://www/cee.hw.ac.uk/~alison/ai3notes/all.html>.
- [9] (2005) The OCW website [Online]. Available: <http://ocw.mit.edu/OcwWeb/Electrical-Engineering-and-Computer-Science/6-871Spring-2005/DownloadthisCourse/index.htm>
- [10] (2005) The OCW website [Online]. Available: <http://ocw.mit.edu/OcwWeb/Electrical-Engineering-and-Computer-Science/6-871Spring-2005/LectureNotes/index.htm>
- [11] (2009) The Breederkoi website [Online]. Available: http://breederkoi.com/article/article_detail.asp?cat=1&id=6.
- [12] (2009) The Openair website [Online]. Available: <https://openair.rgu.ac.uk/bitstream/10059/54/1/ker05-mantarasetal.pdf>
- [13] Kamiso, H.N., "Status Penyakit Ikan dan Pengendaliannya di Indonesia", in *Proc. Pengendalian Penyakit pada Ikan dan Udang Berbasis Imunisasi dan Biosecurity* 2004, paper Unsoed Purwokerto, p.13 – 21.
- [14] Lesmana, D.S., *Mencegah dan Menanggulangi Penyakit Ikan Hias*, Jakarta: Penebar Swadaya, 2002.
- [15] Mangunwiryo, H., "Pengenalan Penyakit Virus pada Ikan dan Udang serta Kemungkinan Pengendaliannya", in *Seminar Nasional II Penyakit Ikan dan Udang Tanggal 16 – 18 Januari 1990*, paper Balai Penelitian Perikanan Air Tawar Bogor, p. 1 – 9.

Neuropsychiatry		
Parameters		
1.	Psychological	
a.	AN	: 1
b.	AB	: 1
c.	AX	: 1
d.	AG	: 1
e.	HA	: 1
2.	Cognitive	
f.	CD	: 1
g.	HR	: 1
h.	JG	: 1
i.	LR	: 1
j.	SH	: 1
3.	Physical	
k.	WL	: 1
l.	LO	: 1
m.	SH	: 1
4.	EEG	
n.	CG	: 1
o.	PL	: 1
p.	OL	: 1
5.	Image	
q.	AC	: 1
r.	CG	: 1
s.	FL	: 1
t.	OL	: 1
Disease : SI		

Case Representation table

Cost comprisonbetween r.c.c.beam& steel composite beam structure of g+5 storeyed building the overall plan dimenssion of the building is 56.3 m x 31.94m

Aniket Sijaria, Prof Anubhav Rai , Prof Y.K. Bajpai

ABSTRACT

The Project involves Planning, Analysis, Design & Cost Comparison of an Institutional Building with steel-concrete composite construction. The proposal structure is a G+5 building, with 3.658m as the height of each floor. The overall plan dimension of the building is 56.3 m x 31.94m.

I. METHODOLOGY

The Analysis and design involves the structure planning, load calculation, analysis it by 2D modeling using STAAD-Pro 2003, design of composite floors and columns, design of steel beams and design of foundation. Analysis has been done for various load combinations including seismic load, wind load, etc. as per the Indian standard Code of Practice.

The project also involves analysis and design of an equivalent R.C.C. structure so that a cost comparison can be made between a steel-concrete composite structure and an equivalent R.C.C. structure.

II. NEED OF STEEL IN CONSTRUCTION

In building construction, role of steel is same as that of bones is a living being. Steel is very advantages because it:-

- Officer considerable flexibility in design and is easy for fabrication
- Facilities faster construction scheduling of projects.
- Enables easy construction scheduling even in congested sites.
- Permits large span construction repair/modification.
- In an ideal material in earthquake prone locations due to high strength stiffness, ductility.
- Is environment friendly and fully recyclable on replacement.

III. ADVANTAGES OF COMPOSITE CONSTRUCTION

IN conventional composite construction, concrete slabs rest over steel beams and are supported by them. Under load, these two components act independently and a relative slip occurs at the interface if there is no connection between them. With the help of deliberate and appropriate connection provided between the beam and the concrete slab, the slip between them can be eliminated. In this case, the steel beam and the slab act as a “Composite beam” and their action is similar to that of a monolithic Tee beam. Since concrete is stronger in compression than in tension, and steel is acceptable to book ling in compression, by the composite action between the two, we can utilize their respective advantages to the fullest extent. There are many advantages associated with steel-concrete composite construction. Some of these are listed below:-

- The most effective utilization of steel and concrete is achieved.
- Keeping the span and loading unaltered, a more economical steel section (in terms of depth and weight) is achievable in composite construction compared with conventional non-composite construction.
- As the depth of beam reduces, the construction depth reduces, resulting in enhanced headroom.
- Because of its larger stiffness, composite beams have less deflection than steel beams.
- Composite construction is amenable to “fast-track” construction because of using rolled steel and pre-fabricated components, rather than case-in situ concrete.
- Encased steel beam sections have improved fire resistance and corrosion.
- Considerable flexibility in design, pre-fabrication and construction schedule in congested areas.

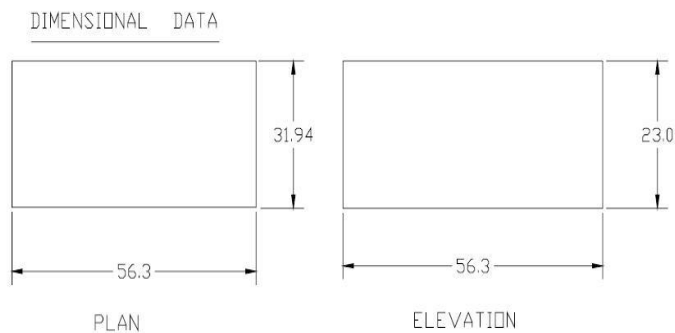
IV. DESIGN CONSIDERATIONS

Composite floors are developed based on limit state design philosophy. Since IS 456:2000 is also based on limit state methods, the same has been followed wherever it is applicable.

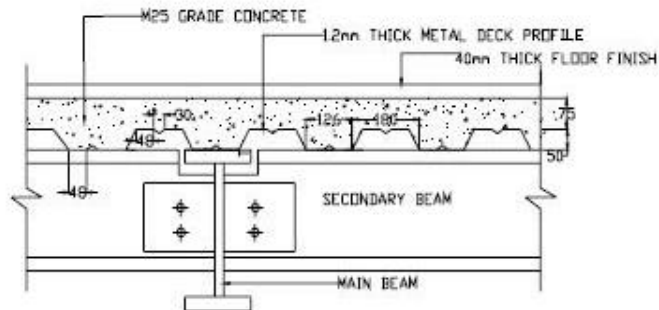
The design should ensure an adequate degree of safety and serviceability of structure. The structure should therefore be checked for ultimate and serviceability limit states.

The main economy in using profiled deck is achieved due to speed in construction. Normally 2.5 to 4.0m spans can be handled without propping and spans in excess 4m will require propping. The yield strength of decking steel is in the range of 220 to 460 N/mm²- Though light – weight concrete is preferable both from reducing the effect of ponding deflection as well as increasing the fire resistance, the normal practice in India is to use concrete of grade M20 to M30.

The analysis of composite section is made using Limit state of collapse method. IS:11384-1985 Code deals with the design and constructions of only simply supported composite beams. Therefore, the method of design suggested in EC 4 is also referred along with IS: 11384.



PLAN & ELEVATION



CROSS SECTION OF PROFILED DECK SLAB

COSTCOMPARISIONCHART

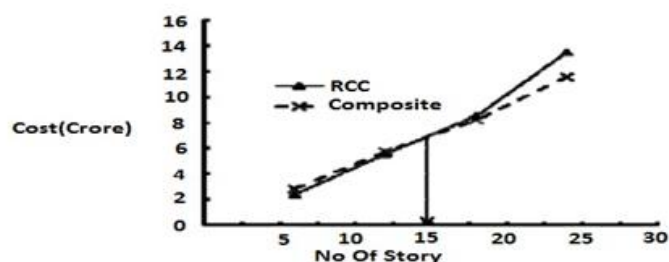
BEAMS

a. Considering shorter span beams,

Material	Rate	Composite Design	Amount	R.C.C. Design	Amount
Steel	Rs. 45/Kg.	1839 Kg.	Rs. 82755	650 Kg.	Rs. 29250
Concrete	Rs. 4390/m ³	--	--	2.46 m ³	Rs. 10800
Form work	Rs. 219/sq.m	--	--	19.194Sq.m/m	Rs. 4202
		Total	Rs. 82755	Total	Rs. 44252

b. Considering longer span beams.

Material	Rate	Composite Design	Amount	R.C.C. Design	Amount
Steel	Rs. 45/Kg.	277.2 Kg.	Rs. 12474	131.5 kg	Rs. 5917
Concrete	Rs. 4390/m ³	--	--	0.675 m ³	Rs. 2963
Form work	Rs. 219/sq.m	--	--	6.525 Sq.m./m	Rs. 1429
		Total	Rs. 12474	Total	Rs. 10309



Cost Versus number of storey curve for composite and RCC building

SUMMARY AND CONCLUSION

- 1) A G + 5 structure of plan dimensions 56.3m x 31.94m has been analyzed, designed and cost per unit quantities worked out.
- 2) An equivalent R.C.C. structure has also been analyzed, designed and cost per unit quantities worked out.
- 3) (A) A comparative study of the quantity of material and cost has been worked out both for composite and concrete construction.
- (B) Though, the cost comparison reveals that Steel-Concrete composite design structure is more costly, reduction in direct costs of steel composite structure resulting from speedy erection will make Steel Composite structure economically viable. Further, under earthquake considerations because of the inherent ductility characteristics, Steel Concrete structure will perform better than a conventional R.C.C. structure.
- 4) For analysis, STAAD Pro-2003 software has been used.
- 5) Manual design has been carried out both for Steel-Concrete composite and R.C.C. structure.
- 6) Sufficient insight into the analysis and design of Steel-Concrete composite structure which is an emerging area has been gained
- 7) Immense confidence has been gained in the analysis and design of a multi-storeyed structure using STAAD Pro 2003 software.

REFERENCES

- [1]. Handbook on Code of Practice for Design Loads (Other than Earthquake) for Buildings and Structures (IS : 875(Part 1) – 1987), Bureau of Indian Standards, New Delhi, 1989.
- [2]. Handbook on Code of Practice for Design Loads (Other than Earthquake) for Buildings and Structures (IS : 875(Part 2) – 1987), Bureau of Indian Standards, New Delhi, 1989.
- [3]. Handbook on Code of Practice for Design Loads (Other than Earthquake) for Buildings and Structures (IS : 875(Part 3) – 1987), Bureau of Indian Standards, New Delhi, 1989.
- [4]. Handbook on Criteria for Earthquake Resistant Design of Structures (IS : 1893(Part 1) – 2002), Bureau of Indian Standards, New Delhi, 1989...
- [5]. IS-456:2000 Indian Standards Code.
- [6]. BS 5950 (Part 3), Design of Simple and Continuous Beams, British Standards Institution, London
- [7]. Eurocode 4: Design of Composite steel and Concrete Structures, British Standards Institution, London, 1994
- [8]. M.P. SOR -2009.

Modelling of Vapour Liquid Equilibrium by Artificial Neural Networks

¹, Dr.B.Karunanithi, ², Sweta Shrinivasan, ³, Bogeshwaran.K,

¹, Department of Chemical Engineering, SRM University, Kattankulathur, 603 203. India.

², Department of Chemical Engineering, SRM University, Kattankulathur, 603 203. India

³, Department of Chemical Engineering, VeltechHightechDr.RangarajanDr.Sakunthala Engineering College, Avadi.600 062.

ABSTRACT:

Vapour liquid equilibrium is condition wherein the liquid and vapour state of the components of a system are in equilibrium with each other. Conventionally, the vapour liquid equilibrium data is evaluated using the thermodynamic models, namely the equation of state (EOS), and the activity co-efficient models. The models falling under these categories are Peng-Robinson model, Margules model, vanLaar model, Wilson's model, NRTL, UNIQUAC and UNIFAC model. VLE data is required in designing distillation columns and any doubt or inaccuracy in the prediction of the VLE data results in variation in design parameters which leads to variations in purity of the distillate, number of theoretical plates, reflux ratio and energy consumption which consequently leads to variation in cost. The VLE data predicted by the existing thermodynamic models show deviations from the experimental data. Hence, an Artificial Neural Network (ANN) model has been developed to predict the VLE so as to minimize the deviations from the experimental values. Several binary systems (1 simple and 6 azeotropic systems) have been considered and VLE data has been predicted using the ANN, Margules and the van Laar models. The Root Squared Mean Deviation (RSMD) of predicted values has been calculated with respect to the experimental values. It has been observed that the data predicted by the ANN model is more accurate as compared to the Margules and van Laar models.

KEYWORDS: vapour liquid equilibrium, ANN, RSMD, binary systems, model.

I. INTRODUCTION

Vapour liquid equilibrium is condition wherein the liquid and vapour state of the components of a system are in equilibrium with each other. In other words, it is the state of the system at which rate of condensation is equal to the rate of evaporation. Vapour liquid equilibrium data is required for the design, analysis and control of distillation columns. Conventionally, the vapour liquid equilibrium data is evaluated using the thermodynamic models, namely the equation of state (EOS), and the activity co-efficient models. The models falling under these categories are Peng-Robinson model, Margules model, vanLaar model, Wilson's model, NRTL, UNIQUAC and UNIFAC model.

The thermodynamic methods mentioned above use linear and nonlinear regression techniques to represent the relations among the variables of a given system. The relationship between the physical and thermodynamic properties is highly non-linear, and consequently an artificial neural network (ANN) can be a suitable alternative to model and develop a non-linear relation between the input and the output parameters. ANN is an efficient methodology to approximate any function with finite number of discontinuities by learning the relationships between input and output vectors.

VLE data is required in designing distillation columns and any doubt or inaccuracy in the prediction of the VLE data leads to design of distillation columns with variation in various parameters. The VLE data predicted by the existing thermodynamic models show deviations from the experimental data, though they are adequate for most engineering applications.

Moreover, with the increase in the use of software packages for data evaluations, the use of artificial neural networks can be integrated along with the existing software packages. Artificial neural network (ANN) is an evolutionary computation or optimization technique. The accuracy of the computed values is said to be better than many other mathematical models. In this thesis, it is intended to develop an artificial neural network model to predict the vapour liquid equilibrium values for 7 binary systems and compare these predicted values to that predicted by the existing mathematical models like the Margules and the van Laar models.

Existing models

Several empirical models have been developed to estimate the vapour liquid equilibrium data and the activity coefficients of various systems. The Margules and the van Laar are two of the empirical models that have been developed to estimate the activity coefficient. Modern activity coefficient models are based on the local-composition concept, which was introduced by Wilson (1964). Due to molecular size and intermolecular forces, local compositions are assumed to take into account the short range orders and non-random molecular orientations inside a liquid solution. Two of the most widely used models are the Non-Random-Two-Liquid (NRTL) developed by Renon and Prausnitz (1968) and the Universal QUASI-Chemical (UNIQUAC) developed by Abrams and Prausnitz (1975). These models are capable of correlating experimental activity coefficients for a species in a liquid solution over a wide composition and temperature range. They are also capable of interpolating and/or extrapolating the experimental activity coefficients for a wide range of temperatures and compositions based on a few experimental points.

In the absence of experimental data, group contribution methods have been devised to predict the activity coefficients of a system. In these methods, atoms in a chemical compound are grouped to form functional groups that are assumed to have their own physical and chemical identity (Fredenslund *et al.*, 1975). Wilson and Deal (1962) introduced the Analytical Solutions of Groups (ASOG) method. Fredenslund *et al.* (1975) developed the Universal Functional-group Activity Coefficients (UNIFAC) method to predict activity coefficients based on molecular functional groups contribution. UNIFAC is one of the most prominent methods that uses a combinatorial and a residual part with functional groups parameters such as: group volume, group surface area, and binary group interactions to predict the activity coefficients.

The group-contribution methods mentioned above use linear and non-linear regression techniques to represent the relations among the variables of a given system. The relationship between the physical and thermodynamic properties in a system is highly non-linear. Hence, an artificial neural network(ANN) can be a suitable alternative to model or to predict the vapour liquid equilibrium data.

Research so far

Maria Iliuta *et al* (1999), proposed artificial neural network correlations for the prediction of vapour-liquid equilibrium for mixed dual-solvent single electrolyte systems, and validated over an extensive VLE database (2900 data points, 16 binary solvents, 24 salts, 11 cations, 6 anions)^[7]. Performance of these correlations to predict the vapour phase mole fraction, equilibrium temperature and total pressures was compared with the experimental data and the data generated by the UNIFAC model. The mean absolute deviations in the predicted data were found to be minimized.

Bilgin *et.al* (2003), employed a neural network model to predict VLE data for six different binary systems having different chemical structures and solution types in various conditions^[1]. The VLE data was also predicted by the UNIFAC model. It was observed that the values predicted by the ANN model show close agreement with the experimental values.

Mehmet Bilgin (2004), employed a neural network model to calculate the isobaric vapour-liquid equilibrium of binary systems composed of different chemical structures, which do not show azeotropic behaviour^[2]. Results generated by the ANN model were compared to those generated by the UNIFAC and the Margules model. In all cases, the deviations between the experimental activity co-efficients and those calculated by the neural network were less than those obtained by those obtained by the Margules and the UNIFAC models.

Govindarajan and Sabarathinam (2006), used the radial basis neural networks, a type of artificial neural networks to predict the VLE data for 4 binary systems and 1 ternary system^[8]. A neural network based on the equation of state was used to predict the liquid phase composition and vapour phase compositions at the given conditions of temperature and pressure. The performance of the network was evaluated on the basis of an overall absolute error and root mean square error specified by the difference in the desired and the actual outputs. It was concluded that this technique to predict VLE data is efficient, reliable and robust. In 2006, Rajesh *et.al*, used ANN for the prediction of the prediction of equilibrium solubility of CO₂ in aqueous alkanolamines. An ANN model was employed to predict the VLE data of two systems, viz:- CO₂ – N-methyldiethanolamine(MDEA) – H₂O system and CO₂ – 2-amino-2-methyl-1-propanol(AMP)-H₂O system. The predictions made by the ANN model were found to be in the accuracy of $\pm 5\%$ for 95% of the data^[11].

Ghaemiet *et.al* (2008), developed an ANN model for the prediction of VLE data in aqueous solutions of electrolytes^[5]. VLE data for ternary system of NH₃- CO₂ – H₂O were predicted using the ANN model which was compared with the predictions of some thermodynamic models.

Moghadassiet.al (2009), developed an ANN model to predict the VLE data of high pressure systems^[3]. Moghadassiet.al (2011), developed a model for predicting the VLE data for binary systems containing propane^[4]. Four binary refrigerant systems containing propane were considered. Results generated by the ANN model were compared with those generated by Margules and vanLaar models. The ANN model showed superiority over the other thermodynamic models.

Pandharipandeet.al (2012) developed a model for the evaluation of VLE data for ten binary systems, results obtained indicated minimum error is obtained in the case of ANN models^[9]. Pandharipandeet.al (2012), modeled combined VLE of four quaternary mixtures using artificial neural network. It was observed that in the ANN model, the error difference between the predefined value and output calculated is minimized^[6]. Nasri et al (2012) developed an ANN model to predict the VLE of a carbon dioxide methanol system at high pressure. Predicted values using ANN are satisfactory.

Inference from literature review

A general overview of the literature shows that the experimental data or a set data points (experimental) available in literature are fed to the neural network for pattern recognition. Pattern recognition or the relation between the input and output is generated by the ANN. Thus, in other words, the ANN generates a mathematical model. Once this model is generated, it is tested for its accuracy with a set of new data points which have not been fed earlier to the ANN for pattern recognition. By entering a new set of data points for testing, the efficiency of prediction of the developed ANN model can be known.

As per the literary review, it was inferred that only a few azeotropic systems have been considered, hence in this report, six azeotropic systems have been considered to show the versatility of ANN in predicting VLE data. Systems considered in this report have not been considered so far. If ANN model is proved to be better than the existing thermodynamics models then, it can be easily integrated with the design and simulation softwares which are generally used for the VLE data estimation.

II. THEORETICAL BACKGROUND

Thermodynamic models

Basically two kinds of thermodynamic models are used to evaluate the VLE data.

They are:

1. Activity co-efficient models (Excess Gibbs Free Energy Models)
2. Equation of state models

Activity co-efficient models have been widely used for the evaluation of VLE data. In this thesis also, the values predicted by the ANN model will be compared with the values computed using the activity co-efficient models, viz: Margules and the van Laar models.

Basic equation for Vapour-liquid Equilibrium

Consider a closed system consisting of co-existing vapour and liquid phases, each phase containing 'c' each components in a state of equilibrium at constant temperature (T) and pressure (P). The criterion for equilibrium between the two phases is given by

$$f_i^l = f_i^v \quad i = [1, 2, 3, \dots, c] \quad (1)$$

where, f_i^l, f_i^v are the fugacities of the pure components of the liquid and vapour.

Equation (1) can be rewritten as

$$\gamma_i x_i f_i^* = \Phi_i^v y_i P \quad (2)$$

The standard state fugacity is given by

$$f_i^* = P_i^s \Phi_i^s \exp\left\{\frac{v_i^l (P - P_i^s)}{RT}\right\} \quad (3)$$

where, P_i^s = saturation pressure of component i at temperature T

v_i^l = molar volume of liquid for component i

Φ_i^s = fugacity coefficient of component i at saturation pressure

Substituting (3) in (2)

$$\gamma_i x_i P_i^s = \frac{\Phi_i^v}{\Phi_i^s} y_i P \exp\left\{-\frac{v_i^l (P - P_i^s)}{RT}\right\} \quad (4)$$

The above equation is the basic equation for vapour liquid equilibrium. It provides a relation between among the variables T, P, x_i 's and y_i 's.

At low pressures (upto atleast 1 bar), the vapour phase can be assumed to behave like an ideal gas and hence $\Phi_i^v = 1$, and $\Phi_i^s = 1$. At low pressures the Poynting correction factor $\exp\left\{\frac{v_i^l (P - P_i^s)}{RT}\right\}$ is negligibly small and it is approximately equal to unity. At low to moderate pressures (upto 10 bar), Φ_i^v and Φ_i^s are equal to each other and hence it is reasonable to assume $\Phi_i^v / \Phi_i^s = 1$.

Thus at low to moderate pressures

$$\gamma_i x_i P_i^s = y_i P \quad (5)$$

or
$$\gamma_i = \frac{y_i P}{x_i P_i^s} (i = 1, 2, 3, \dots, c)$$

The value of γ_i is evaluated by the thermodynamic models like Margules, van Laar, etc.

For a binary system, the activity coefficients can be evaluated as

Margules equation

$$\ln \gamma_1 = x_2^2 \{ A_{12} + 2 * (A_{21} - A_{12}) * x_1 \} \quad (6)$$

$$\ln \gamma_2 = x_1^2 \{ A_{21} + 2 * (A_{12} - A_{21}) * x_2 \} \quad (7)$$

where, A_{12}, A_{21} are the Margules interaction parameters for the binary system consisting of components 1 and 2.

vanLaar equation

$$\ln \gamma_1 = \frac{A}{(1 + \frac{Ax_1}{Bx_2})^2} \quad (8)$$

$$\ln \gamma_2 = \frac{B}{(1 + \frac{Bx_2}{Ax_1})^2} \quad (9)$$

where, A and B are van Laar constants and subscripts 1 and 2 stand for components 1 and 2 respectively in the binary system.

Artificial neural networks (ANN): General Overview

Artificial neural networks (ANN) are non-linear information processing paradigm, which are built from interconnected elementary processing devices called neurons. They are inspired by the way the human brain processes information. ANNs like people, learn by an example. ANN is configured for a specific application, such as pattern recognition or data classification, through a learning process. Learning in biological systems involves adjustments to the synaptic connections/weights that exist between the neurons, which is applied to ANNs as well. ANNs can also be defined as parameterized computational nonlinear algorithms for data/signal/image processing. These algorithms are either implemented on a general purpose computer or built on a dedicated hardware.

An efficient way of solving a complex problem is to divide or decompose it into simpler elements in order to be able to understand it. Also, simple elements may be gathered to produce a complex system. Use of networks is one of the approaches to achieve this. There are a large number of networks of different types. They are all characterized by the following components: a set of nodes, and connections between the nodes.

The nodes, which are analogous to the neurons in the biological nervous system are computational units. They receive inputs and process them to obtain an output. This processing may be simple (summing of input) or complex (a node contains another network). The connections determine the flow of information between the nodes. The interactions of the nodes through the connections lead to a global behaviour of the network which cannot be observed in the elements of the network. In other words, abilities of the network supercede the ones of its elements.

Elements called neurons (nodes), process the information. The signals are transmitted by means of connection links. The links possess an associated weight, which is multiplied along with the input signal (net input) for any typical neural net. The output signal is obtained by applying activations to the net input.

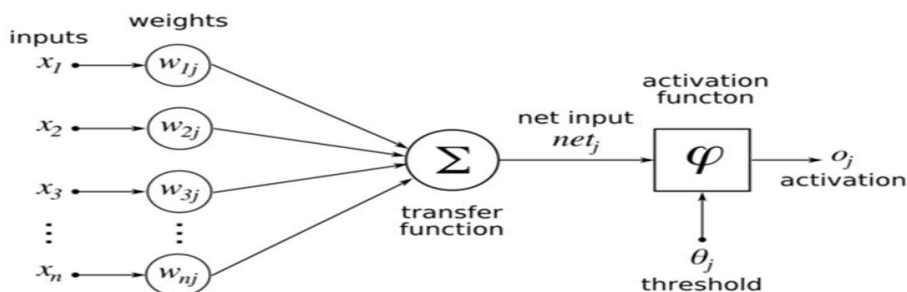


Figure 3.1 – General representation of an artificial neural network [iv]

The figure above represents a simple structure of an artificial neural network. It has ‘n’ input neurons (x_1, x_2, \dots, x_n), w stands for the interconnected weights. The suffix ‘ij’ is added to the weights where, i stands for the corresponding input neuron number, j stands for the number corresponding to the weighted connections. In the above figure, there is only a single layer, there can be as many layers as the user defines. When there are more than one layers, the neural network is called a multilayer net. The value o_j stands for the output which is processed by the net.

The transfer function is the summation of the weighted inputs or also called as the net input. It can be represented mathematically as

$$\text{net}_j = \sum_{i=0}^n W_{ij}X_i + \text{bias};$$

The output is obtained by the activation of the net input. It is given by,

$$o_j = f(\text{net}_j);$$

The activation functions are of several types. In this case, two activation functions have been used namely the log-sigmoid and the linear activation functions. The mathematical representations of these functions are,

Log-sigmoid function:

$$f(x) = \frac{1}{1 + \exp(-x)}, \text{ where } x \text{ is any variable.}$$

Linear function:

$$f(x) = x, \text{ where } x \text{ is any variable.}$$

The arrangement of neurons into the layers and the pattern of connection within and in-between layer are generally called as the architecture of the net. The neurons within a layer are found to be fully interconnected or not interconnected. The number of layers in the net can be defined to be the number of layers of weighted interconnected links between particular slabs of neurons. If two layers of interconnected weights are present, then it is found to have hidden layers. The various types of network architecture are feed-forward, feedback, fully interconnected net, competitive net etc. The feed-forward network architecture has been used to evaluate the network. It can be represented as:

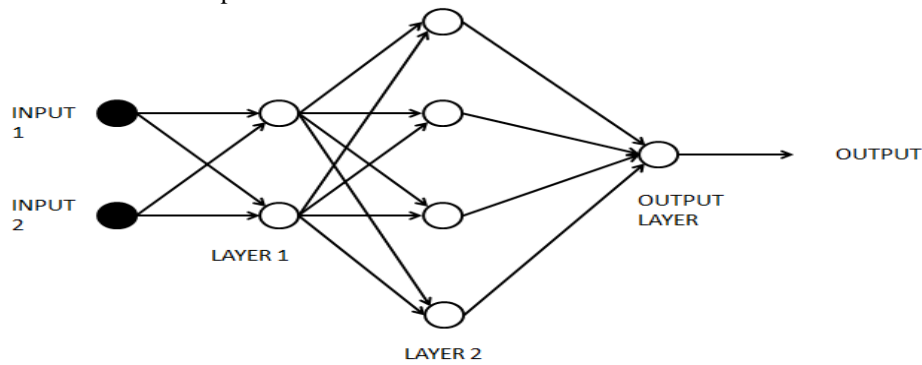


Figure 3.2 – General representation of a feed forward neural network architecture

Feed forward networks may have a single layer of weights where the inputs are directly connected to the outputs or it may consist of multiple layers with intervening sets of hidden unit units. Neural networks use hidden units to create internal representations of the input patterns. The figure 3.2, represents a multi-layer feed-forward network consisting of an input layer, two hidden layers and an output layer. In multilayer nets, signal flow from input units to output units in a forward direction. It can be used to solve complex problems.

The neural net learns or recognises a pattern by the process of learning or training. In the learning/training process, the network is presented with a set of values of the input and its corresponding output. In this process, the network learns or establishes a relation between the input and the output by setting weights and biases accordingly. This process is also called as supervised learning as for each input value, the value of the desired input is provided by the user and the network establishes a non-linear relation between the input and the output.

A training algorithm and function is employed for the training of the values. The back-propagation training algorithm and the resilient back-propagation training function is used. Input vectors and the corresponding target vectors are used to train a network until it can approximate a function, associate input vectors with specific output vectors, or classify input vectors in an appropriate way as defined by the user. Networks with biases, a sigmoid layer, and a linear output layer are capable of approximating any function with a finite number of discontinuities.

Properly trained back-propagation networks tend to give reasonable answers when presented with inputs that they have never seen. Typically, a new input leads to an output similar to the correct output for input vectors used in training that are similar to the new input being presented. This generalization property makes it possible to train a network on a representative set of input/target pairs and get good results without training the network on all possible input/output pairs.

There are four steps in the process of predicting the VLE data using neural networks:

1. Assemble the training data.
2. Create the network object.
3. Train the network.
4. Simulate the network response to new inputs

In this learning pattern, the back-propagation of errors takes place. Initially the random values of weights are assumed. The evaluation of the network takes place which is compared with the predefined mean squared error (MSE) value or error difference between the output and the target. MSE is given by the equation:

$$MSE = \frac{1}{N} \sum_0^N (y_c - y_t)^2$$

i.e. Error (E) = F(weighted inputs, target output)

If the desired value of MSE is reached then the evaluation of the network is stopped, else the weights are updated to new values to evaluate the network and check the value of MSE. If MSE is reached the evaluation stops or else the weights are updated and the cycle continues till the predefined MSE is reached or till the maximum limit of predefined iterations (epochs) are reached.

The updation of weights takes place by the method of resilient propagation^{[16][17]}. Resilient propagation is an effective learning scheme. It performs a direct adaption of weight step based on local gradient information. For each weight an individual update value Δ_{ij} is used which determines the size of the weight update. An adaptive update-value evolves during the training process based on local sight of the error function.

Every time the partial derivative of the corresponding weight w_{ij} changes its sign, which indicates that the last update was too big and the algorithm has jumped over a local minimum, the update-value Δ_{ij} is decreased by the factor η . If the derivative retains its sign, the update-value is slightly increased in order to accelerate convergence in shallow regions. Given as:

$$\Delta_{ij}^{(t)} = \begin{cases} \eta^+ * \Delta_{ij}^{(t-1)}, & \text{if } \frac{\partial E^{(t-1)}}{\partial w_{ij}} * \frac{\partial E^{(t)}}{\partial w_{ij}} > 0 \\ \eta^- * \Delta_{ij}^{(t-1)}, & \text{if } \frac{\partial E^{(t-1)}}{\partial w_{ij}} * \frac{\partial E^{(t)}}{\partial w_{ij}} < 0 \\ \Delta_{ij}^{(t-1)}, & \text{else.} \end{cases}$$

Once the update-value for each weight is adapted, the weight-update itself follows a very simple rule:

- if the derivative is positive (increasing error), the weight is decreased by its update-value
- if the derivative is negative, the update-value is added

$$\Delta w_{ij} = \begin{cases} -\Delta_{ij}^{(t)} & \text{, if } \frac{\partial E^{(t)}}{\partial w_{ij}} > 0 \\ +\Delta_{ij}^{(t)} & \text{, if } \frac{\partial E^{(t)}}{\partial w_{ij}} < 0 \\ 0 & \text{, else} \end{cases}$$

Updation is carried out by the formula,

$$w_{ij}^{(t+1)} = w_{ij}^{(t)} + \Delta w_{ij}^{(t)}$$

There is one exception: If the partial derivative changes sign, i.e. the previous step was too large and the minimum was missed, the previous weight-update is reverted.

$$w_{ij}^{(t+1)} = -\Delta w_{ij}^{(t-1)}, \text{ if } \frac{\partial E^{(t-1)}}{\partial w_{ij}} * \frac{\partial E^{(t)}}{\partial w_{ij}} < 0$$

Due to that 'backtracking' weight-step, the derivative is supposed to change its sign once again in the following step. In order to avoid a double punishment of the update value, there should be no adaptation of the update-value in the succeeding step. In practice this can be done by setting the differential of the error w.r.t the weights to zero in the Δ_{ij} adaptation rule. The update-values and the weights are changed every time the whole pattern set has been presented once to the network (learning by epoch/iteration). In other words, the update values and weights are changed after every epoch/iteration till the maximum number of iterations or till the error between the computed and the target output reach the predefined MSE value.

III. METHODOLOGY

The main aim of this project was to predict the VLE data based on the non-linear correlation generated by the artificial neural network. The artificial neural network model was developed with the help of a code using Matlab 7.0. Firstly, a basic code was executed and it was tested for a binary system of Methanol(1) – Acetone(2) at 101.325 kPa. There were modifications made in the basic code to obtain a suitable code which has been used to evaluate VLE data of all the systems considered in this report.

As mentioned in the previous chapter, the neural network learns the patterns for a set of values and it applies it for a new set values. Hence, an input data is provided with its corresponding target or desired target value. The neural network studies the set of input and its corresponding output and it generates a non-linear model relating the input to the output.

Steps in developing the model

The development of the ANN model consists of the following steps which have been written as a Matlab code

1. Identification of the number of inputs and outputs
2. Designing an architecture for the neural network
3. Training the neural network with a set of data points
4. Simulating the trained neural network with a new set of data points which have not been used in the training stage.

The data simulated by the neural network for the new set of data points is compared with the data obtained by solving this set using the Margules and the van Laar models. The comparison of the data is reported in the form of a graph.

1. Identifying the number of inputs and outputs

In this step, the number of inputs and outputs are decided. For eg: in this work, binary systems have been considered and according to the phase rule, the number of degrees of freedom is given as :

$$F = C - \pi + 2$$

Where, F = number of degrees of freedom, C = number of components, π = number of phases. For a binary system in vapour liquid equilibrium conditions, C = 2, π = 2, so number of degrees of freedom is F = 2.

Thus two known parameters are taken as the input to the neural networks. There can be one or two outputs considered. Thus, the input to the ANN can be either T, x1 data or P, x1 data and y1 data is the desired output.

2. Designing an architecture for the neural network

Optimum network architecture has to be designed such that the convergence of the values or the training of the network is fast and the output obtained does not show much deviations from the experimental values. The number of layers, the number of neurons in each layer and the activation function for each layer is to be set to form a neural network.

3. Training of the neural networks for a set of data points

The set of data points used for training the neural network serves as the input to the system. The data points are trained using the following steps

- a) Input data – the input set and the corresponding target output set is fed to the ANN.
- b) Initialize training – the network structure is defined and the training function is defined. The parameter associated with the training function like the maximum number of epochs, minimum gradient, mean squared errors (MSE) limit is defined.
- c) Epoch is set as 1 and the training is started.
- d) Weights and bias of the network are initialized to random values
- e) With the entered input value and the value of weights and bias the output values are calculated.
- f) Deviation of the calculated output and the desired target output is calculated using MSE.
- g) If $MSE \leq MSE_{\text{minimum}}$ evaluation is stopped else do step (h).
- f) If number epochs \leq epochs_{maximum} go to step (i), else stop.
- g) Weights are updated on the basis of the training function and the number of epoch is increased by 1 and the steps are repeated from step (e).

Once, the training is stopped, a model is generated with fixed values of weights and biases forming a numerical non-linear model (relation) between the input and output.

1. Simulating the trained neural network with a new set of data points which have not been used in the training stage.

A new set of data input is provided to the trained network to evaluate the output value or the value of the mole fraction of the components in the vapour phase. This simulated data has been compared with the experimental values and the values of the mole fraction of the vapour phase computed by the Margules and the van Laar's model.

The VLE data required for training and testing has been taken from the explorer edition of the Dortmund Data Bank (DDBST) online. For each system, considered, a number of data points have been used for training and a different set has been used for simulation and testing.

Systems considered:

The systems considered and number of data sets used for training and testing are as given below

- i. Chloroform(1) – Ethanol(2) system (308.15 K) (Data sets: Training – 23, Testing – 5)
 - ii. Methanol(1) – Acetone(2) system (101.325 kPa)(Data sets: Training – 18, Testing – 6)
 - iii. Methanol(1) – Hexane(2) system (333.15 K)(Data sets: Training – 25, Testing – 5)
 - iv. Methanol(1) – Benzene (2) system (101.33 kPa)Data sets: Training – 36, Testing – 6)
 - v. Benzene(1) – Acetonitrile(2) system (293.15 K)(Data sets: Training – 38, Testing – 7)
 - vi. Water(1) – m-Xylene(2) system (101.3 kPa) (Data sets: Training – 15, Testing – 5)
 - vii. Hexane(1) – Cyclohexane(2) system (101.33 kPa)(Data sets: Training – 28, Testing – 6)
- All the data sets considered have been mentioned in the appendices

Example

Considering the Methanol (1) – Acetone (2) system (101.325 kPa). The neural network is trained by the input and target data. The Matlab code given in appendix (A1) is executed, the neural network architecture is a feed-forward architecture consisting of input T-x₁ data and output y₁ data. The neural net architecture is as given in figure (4.1). The net consists of 1 input layer, 2 hidden layers with 2 and 4 neurons respectively and the output layer with one neuron. The activation function in the hidden layers is logsig and in the output layer is purelin. MSE set is 1e-6. Minimum gradient set is 1e-6, maximum weight change is set as 100. The maximum number of epochs is set as 100000. After the training the relational bias and weights obtained can be represented in the net as given below.

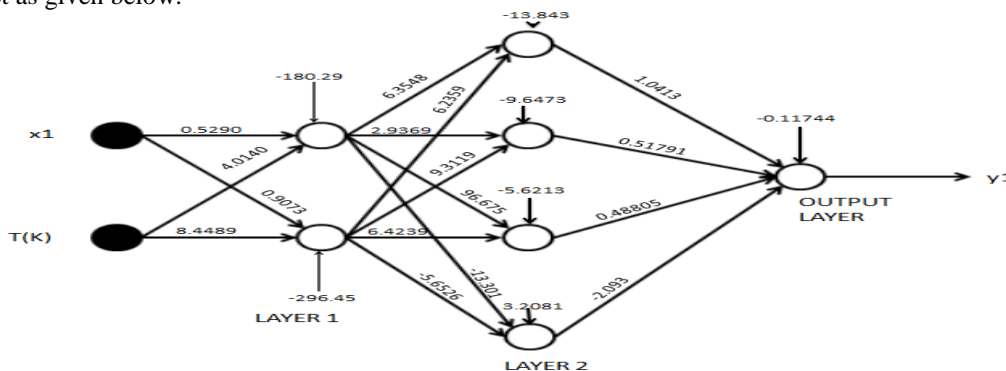


Figure 4.1 – Basic model developed by ANN for Methanol(1) – Acetone (2) system

With a new set of input values, the output is simulated and it is compared with the values given in literature and those calculated using a thermodynamic model. It is represented in the form of a graph as shown in appendix.

The training of the data takes 41656 epochs or iterations. But since the number of epochs taken is more, a neural network has to be designed in such a way that it predicts data with better accuracy and the epochs taken are less.

After designing and testing many neural network models, a neural network model was optimized to give accurate and faster convergence of results. The code written in Matlab 7.0 is as given in Appendix(A.2). For all the 7 systems considered, the neural network has been trained and the values are simulated using the trained network in each of the cases. The values have been calculated by the neural network, Margules and the van Laar models and a graph has been plotted to represent the result. The graphical representation of the calculated parameters has been presented in Appendix(B). For each system, the deviation between the calculated and the experimental values has been evaluated by the Root Mean Squared Deviation(RSMD) formula which is given by the expression.

$$RSMD = \sqrt{MSE}$$

$$RSMD = \sqrt{\frac{\sum_{i=1}^N (y_c - y_t)^2}{N}}$$

For all the systems, the model has been developed as per the Matlab code given in Appendix (A.2) (Optimized model). The model consists of four layers viz : an input layer with two inputs, two hidden layer with 30 neurons each and an output layer with one neurons. The activation function used in all the layers is the log-sigmoid (logsig) and the Resilient Propagation (trainrp) training algorithm is used. The parameters set for this training this network are:

- 1) Maximum number of epochs/ iterations = 100000

- 2) Minimum gradient = $1e-10$
- 3) Mean squared error = $1e-9$
- 4) Maximum weight change = 100

Using these parameters the systems have been trained to recognise the input patterns and to develop a non-relation between the input and output values. This relation developed is used to simulate the test data sets.

NAME OF THE SYSTEM	ROOT SQUARED MEAN DEVIATION (RSMD)		
	MARGULES	VAN LAAR	ANN
Chloroform(1) – Ethanol(2) system (308.15 K)	0.00790	0.02862	0.00500
Methanol(1) – Acetone(2) system (101.325 kPa)	0.00847	0.00885	0.00099
Methanol(1) – Hexane(2) system (333.15 K)	0.06728	0.05852	0.00569
Methanol(1) – Benzene (2) system (101.33 kPa)	0.06879	0.05889	0.00699
Benzene(1) – Acetonitrile(2) system (293.15 K)	0.01811	0.01981	0.00607
Water(1) – m-Xylene(2) system (101.3 kPa)	0.17764	0.19103	0.01671
Hexane(1) – Cyclohexane(2) system (101.33 kPa)	0.00563	0.00865	0.00201

IV. RESULTS AND DISCUSSIONS

In this study, 7 binary systems have been considered. Out of these 7 systems, 6 systems are azeotropes and 1 is a binary mixture. The values of the output (y_1) data has been calculated using the different models (ANN, Margules, van Laar). The values of Root Mean Squared Deviation (RSMD) have been calculated for various systems. It is obtained as shown in the table given below.

Table 5.1. Root Squared Mean Deviation from experimental values

The Root Squared Mean Deviation (RSMD) calculated for all the systems considered have been represented in the table above. The comparison of the RSMD values of all the models, shows that the deviations shown by the ANN model is lesser as compared to the Margules and van Laar models. In other words, for all the systems considered, the values of mole fraction of the vapour phase predicted by the ANN model show lesser deviations from the experimental values as compared to the thermodynamic models. The graphical representation (Appendix) of the mole fractions in the liquid phase versus the mole fractions in the vapour phase shows the closer proximity of ANN values to the experimental values as compared to those of thermodynamic models considered.

In the Methanol (1) – Acetone (2) system, the RSMD value obtained for the mole fractions of vapour phase calculated by the ANN model is the least. Also in the Chloroform(1) – Ethanol(2) system, Methanol(1) – Hexane(2) system, Methanol(1) – Benzene (2) system, Benzene(1) – Acetonitrile(2) system, Water(1) – m-Xylene(2) system, the values of the RSMD obtained for ANN values is considerably lesser than the van Laar and the Margules model values. Hence, the VLE data prediction by ANN for these systems is much accurate as compared to the thermodynamic models considered. While, for Hexane(1) – Cyclohexane(2) system the accuracy of prediction of ANN model is as much as the thermodynamic models.

V. CONCLUSIONS

An artificial neural network (ANN) model has been developed and used for the prediction of Vapour Liquid Equilibrium (VLE) data. This model developed is a non-linear, non-thermodynamic model. The results of VLE data prediction using this model for various systems show satisfactory results. For all the systems considered the data predicted by the ANN shows closer agreement with the experimental literature as compared to the Margules and vanLaar models, especially for the azeotropic systems considered, the VLE data prediction by the ANN model is better than that predicted by the Margules and van Laar models.

APPENDICES

APPENDIX A: MATLAB CODE

D) BASIC MATLAB CODE FOR METHANOL (1) – ACETONE (2) SYSTEM

```

clc, clear;
% asking the user the Excel file name containing the data
R=input('training set file name:','s');
T=input('target file name: ','s');
S=input('input set file name: ','s');
    
```

```
%Reading the Excel file
RR=xlsread(R);
TT=xlsread(T);
SS=xlsread(S);
% Taking transpose of the input matrix
RR1 = RR';
TT1 = TT';
SS1 =SS';
% Defining function and parameters for the creation of the ANN
net = newff(minmax(RR1),[2 4 1], {'logsig' 'logsig' 'purelin'}, 'trainrp'); net.trainParam.epochs =100000;
net.trainParam.show=5000;
net.trainParam.lr=0.1;
net.trainParam.lr_inc = 1.05;
net.trainParam.deltamax=100.0;
net.trainParam.goal = 1e-6;
%training the network
net = train(net,RR1,TT1);
%saving the net
save(['m1.mat'],'net');
% Simulation of new sets of data
y=sim(net,SS1)
```

II) MATLAB CODE USED FOR ALL THE SYSTEMS

```
clc,
clear;
R=input('training set file name:','s');
T=input('target file name: ','s');
S=input('input set file name: ','s');
RR=xlsread(R);
TT=xlsread(T);
SS=xlsread(S);
RR1=RR';
TT1=TT';
SS1=SS';
% new network with 1 input layer, 2 hidden layer with 30 neurons each
% output layer with one neuron
% training function 'trainrp' Resilient Propagation
% activation function in each layer Log-sigmoid (logsig)
net = newff(minmax(RR1),[30 30 1], {'logsig' 'logsig' 'logsig'}, 'trainrp');
net.trainParam.epochs =100000; % maximum epochs/iterations
net.trainParam.show=5000; %parameters shown on matlab screen
net.trainParam.lr=0.1;% learning rate
net.trainParam.min_grad = 1e-10; %minimum gradient
net.trainParam.lr_inc = 1.05; %learning rate increment
net.trainParam.deltamax=100.0; %maximum weight increase
net.trainParam.goal = 1e-9; % goal to be achieved (MSE)
net = train(net,RR1,TT1); %network training command
save(['NETNAME.mat'],'net'); % saving the neural network developed
y=sim(net,SS1) % simulating values using the developed network
```

APPENDIX B: TRAINING DATA FOR ALL THE SYSTEMS

These sets of data points have been obtained from the Explorer edition of the Dortmund Data Bank (DDBST). The y1 data is the target output for network. And P, x1 or T, x1data is the input.

TABLE B.1 CHLOROFORM(1) - ETHANOL (2) SYSTEM (308.15 K) – TRAINING DATA		
P [kPa]	x1	y1
13.703	0	0
13.982	0.0062	0.0254
14.84	0.0241	0.0991
15.147	0.0297	0.121
16.775	0.0594	0.2343
19.766	0.1109	0.3885
23.678	0.173	0.5304
27.422	0.2361	0.6207
30.563	0.3014	0.687
31.531	0.3227	0.7009
33.783	0.3845	0.737
34.035	0.3922	0.7412
35.684	0.4384	0.7646
38.923	0.6185	0.8181
39.587	0.6783	0.8327
40.403	0.7746	0.8554
40.715	0.8265	0.8698
40.83	0.8483	0.8783
40.803	0.9315	0.9161
40.646	0.956	0.9363
40.553	0.9586	0.9385
40.489	0.96	0.9403
39.345	1	1

TABLE B.2 METHANOL (1) – ACETONE (2) SYSTEM (101.325kPa) – TRAINING DATA		
T(K)	x1	y1
328.82	0.07	0.082
328.46	0.181	0.188
328.39	0.217	0.218
328.45	0.265	0.255
328.54	0.34	0.311
328.89	0.406	0.356
329.3	0.481	0.406
330.05	0.593	0.486
330.2	0.606	0.496
330.44	0.631	0.515
331.47	0.719	0.59
331.64	0.737	0.608
332.12	0.771	0.643
332.72	0.805	0.681
334.68	0.9	0.809
335.36	0.926	0.852
335.94	0.947	0.89
336.84	0.976	0.947

TABLE B.3 METHANOL (1) – HEXANE (2) SYSTEM (333.15 K) – TRAINING DATA		
P [kPa]	x1	y1
76.047	0	0
107.484	0.005	0.285
130.869	0.016	0.407
138.002	0.033	0.438
141.868	0.06	0.463
145.108	0.098	0.482
147.148	0.145	0.488
148.308	0.175	0.496
148.988	0.218	0.499
149.348	0.399	0.512
149.641	0.522	0.517
149.494	0.57	0.52
149.388	0.613	0.521
149.308	0.657	0.522
148.961	0.79	0.524
147.761	0.828	0.533
145.028	0.877	0.54
144.241	0.883	0.543
138.495	0.919	0.574
131.603	0.938	0.616
126.47	0.951	0.645
121.59	0.962	0.681
111.484	0.979	0.752
110.471	0.98	0.763
83.9	1	1

TABLE B.4 METHANOL(1) – BENZENE(2) SYSTEM (101.33 kPa) – TRAINING DATA		
T [K]	x1	y1
351.76	0.002	0.041
350.8	0.0028	0.066
350.67	0.003	0.0684
350.43	0.003	0.0812
350.37	0.0041	0.082
348.45	0.0058	0.1386
346.92	0.0134	0.1924
346.21	0.019	0.206
344.11	0.0276	0.2658
341.1	0.046	0.3392
340.9	0.048	0.344
334.23	0.1437	0.4998
334.19	0.17	0.518
333.07	0.1858	0.5212
332.55	0.276	0.5442
331.58	0.364	0.5736
331.3	0.4558	0.587
331.19	0.524	0.5981
331.12	0.637	0.62
331.13	0.6739	0.629
331.14	0.68	0.6322
331.2	0.7024	0.6408
331.21	0.7071	0.6416
331.37	0.744	0.6531
331.6	0.7768	0.6691
331.8	0.8031	0.6838
332.14	0.838	0.709
332.75	0.8754	0.748
333.75	0.9178	0.8002
334.05	0.925	0.8118
334.79	0.9424	0.851
335.75	0.9652	0.8998
336.72	0.9849	0.9492
336.87	0.988	0.9572
337.1	0.9918	0.9684
337.36	0.9949	0.9799

TABLE B.5
 BENZENE(1) –
 ACETONITRILE(2)
 SYSTEM (293.15 K) –
 TRAINING DATA

P [kPa]	x1	y1
9.799	0.018	0.054
10.106	0.033	0.096
10.599	0.063	0.161
11.106	0.098	0.221
11.386	0.128	0.256
11.719	0.168	0.3
11.852	0.187	0.321
11.932	0.198	0.33
12.226	0.256	0.376
12.359	0.284	0.395
12.439	0.31	0.412
12.466	0.32	0.417
12.612	0.368	0.442
12.666	0.424	0.473
12.679	0.446	0.484
12.692	0.446	0.486
12.719	0.47	0.498
12.692	0.481	0.501
12.746	0.511	0.518
12.746	0.535	0.532
12.719	0.572	0.551
12.719	0.607	0.571
12.666	0.648	0.593
12.639	0.657	0.597
12.612	0.679	0.612
12.519	0.71	0.632
12.186	0.793	0.695
12.119	0.815	0.709
12.012	0.841	0.734
11.866	0.857	0.757
11.706	0.874	0.767
11.252	0.92	0.829
11.106	0.933	0.849
11.026	0.939	0.86
10.879	0.953	0.883
10.506	0.975	0.93
10.319	0.983	0.95
10.186	0.991	0.972

TABLE B.6
 WATER(1) - m-
 XYLENE(2) SYSTEM
 (101.3 kPa) –
 TRAINING DATA

T [K]	x1	y1
408.15	0.0022	0.1216
407.59	0.0029	0.1396
399.85	0.0082	0.3082
395.63	0.0122	0.4013
391.15	0.0163	0.4807
382.35	0.0231	0.6023
377.35	0.0349	0.6704
374.89	0.0864	0.6921
372.65	0.1294	0.7126
369.87	0.2435	0.7378
367.16	0.9992	0.7924
367.46	0.9994	0.8138
368.06	0.9996	0.8313
369.32	0.9998	0.8723
372.84	1	0.9897

TABLE B.7
 HEXANE (1) –
 CYCLOHEXANE(2)
 SYSTEM (101.33 kPa)
 –TRAINING DATA

T [K]	x1	y1
353.95	0	0
353.75	0.008	0.018
353.5	0.019	0.032
352.9	0.063	0.0975
352.45	0.094	0.135
351.8	0.133	0.187
350.3	0.239	0.316
349.65	0.287	0.373
349.2	0.318	0.4
348.5	0.369	0.4575
347.65	0.443	0.5335
347.4	0.462	0.553
346.9	0.498	0.5835
346.55	0.536	0.6175
346.4	0.549	0.63
345.9	0.596	0.673
345.25	0.655	0.724
344.85	0.693	0.7575
344.1	0.757	0.808
344.05	0.769	0.818
343.95	0.777	0.8295
343.7	0.807	0.852
343.5	0.831	0.8715
343.3	0.85	0.883
343.1	0.874	0.902
342.5	0.935	0.95
342.2	0.969	0.976
341.95	1	1

APPENDIX B: GRAPHS (x1 v/s y1)

GRAPHICAL REPRESENTATION OF OUTPUT

The calculated vapour mole fraction obtained from the various models is plotted against the liquid mole fractions to compare between the values calculated by the different models.

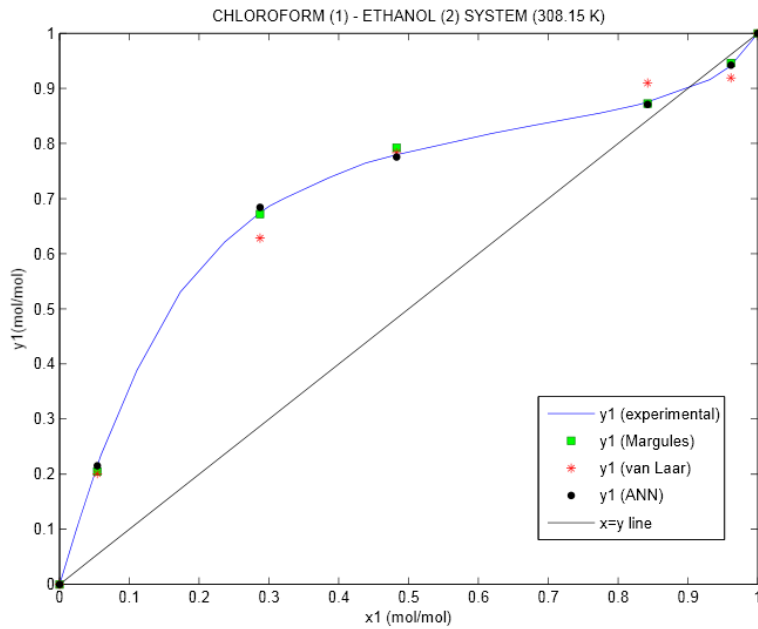


FIGURE B.1: Chloroform (1) -Ethanol (2) System (308.15 K) – (x-y Graph)

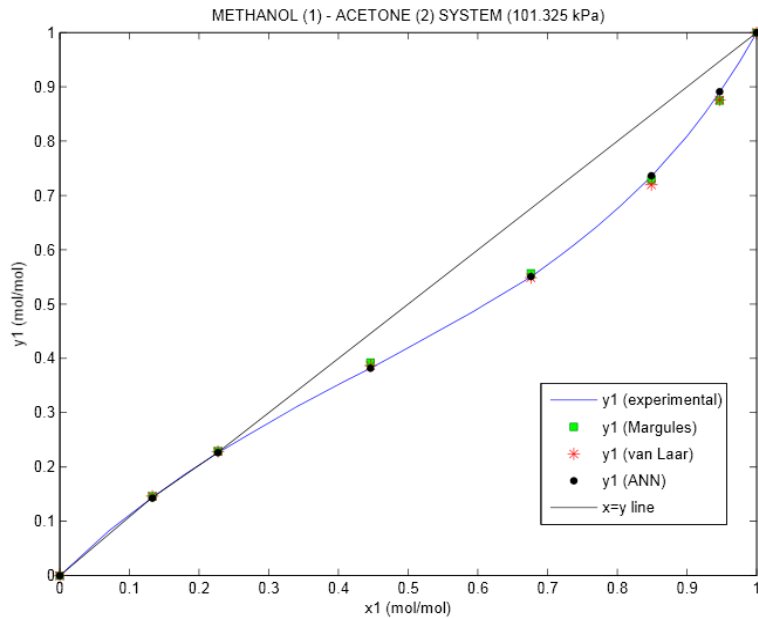


FIGURE B.2 : Methanol (1) – Acetone (2) System (101.325 kPa) – (x-y Graph)

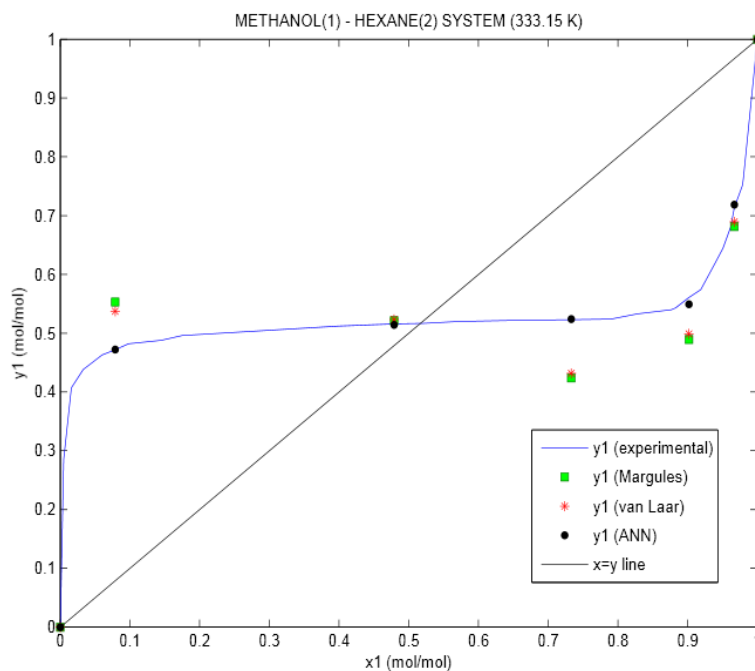


FIGURE B.3: Methanol (1) – Hexane (2) System (333.15 K) – (x-y Graph)

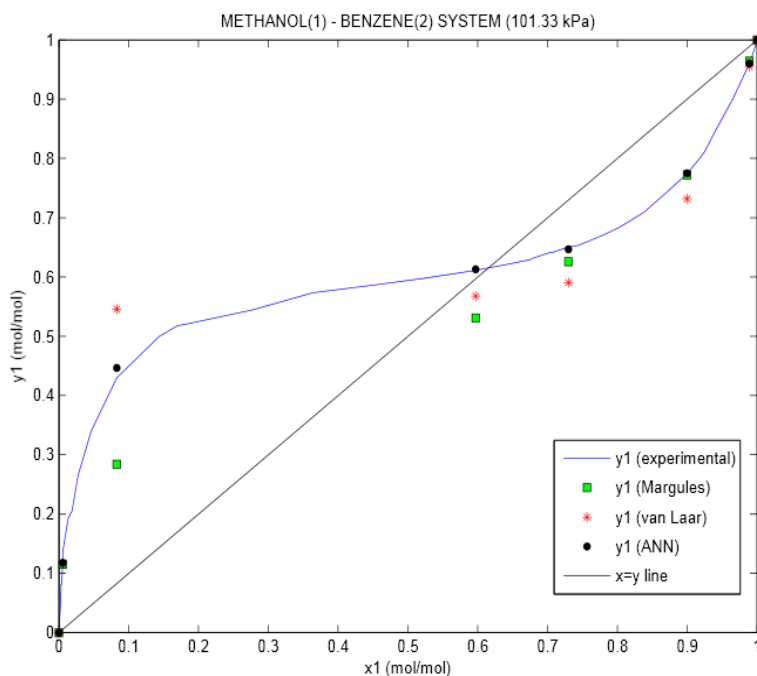


FIGURE B.4: Methanol (1) –Benzene (2) System (333.15 K) – (x-y Graph)

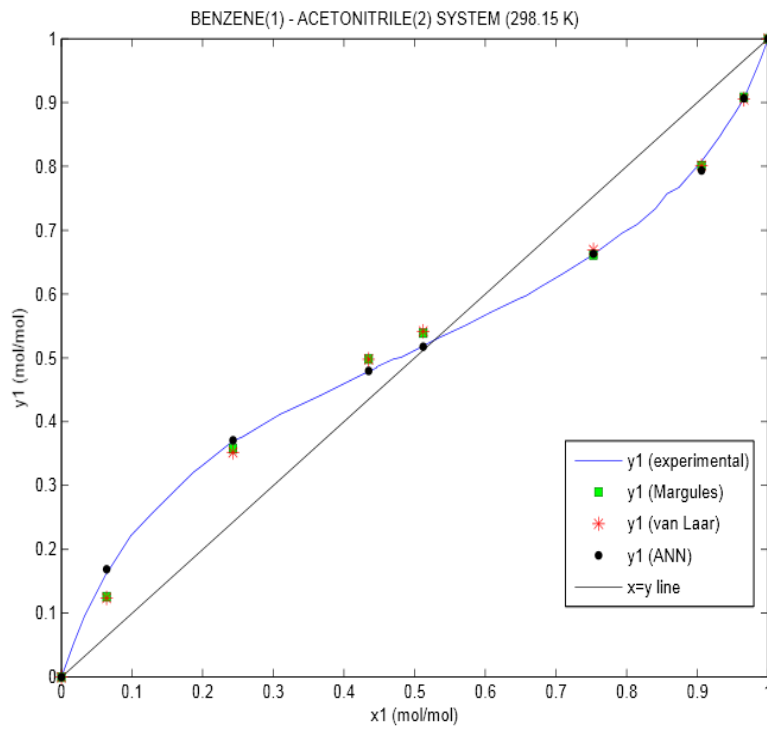


FIGURE B.5: Benzene (1) – Acetonitrile (2) System (293.15 K) – (x-y Graph)

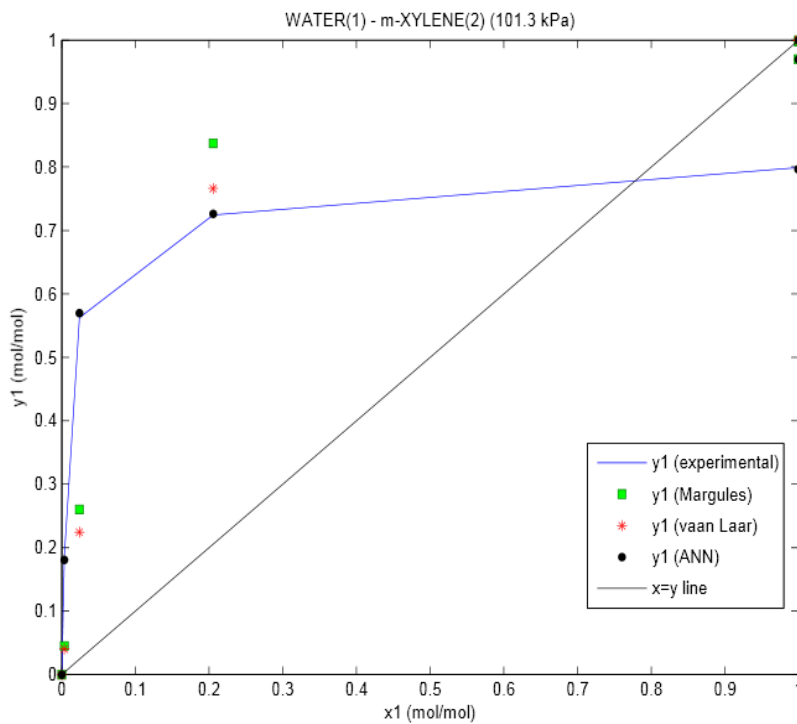


FIGURE B.6: Water (1) – m-Xylene (2) System (101.3 kPa) – (x-y Graph)

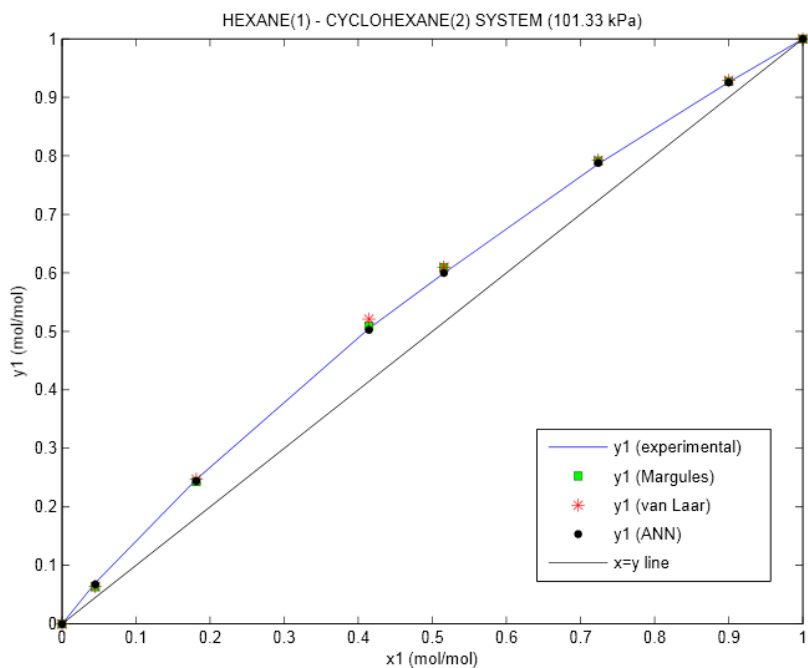


FIGURE B.7:Hexane (1) – Cyclohexane (2) System (101.33 kPa) – (x-y Graph)

TABLE C.1 CHLOROFORM(1) – ETHANOL(2) SYSTEM (308.15 K) – OUTPUT DATA					
		EXPERIMENTAL	MARGULES	VAN LAAR	ANN
P [kPa]	x1	y1	y1	y1	y1
16.471	0.0542	0.2154	0.2047	0.201	0.2151
30.006	0.2873	0.6747	0.672	0.6282	0.6842
36.536	0.4827	0.7797	0.7924	0.7831	0.7755
40.679	0.8423	0.8752	0.8722	0.91	0.871
40.518	0.9616	0.9414	0.9459	0.9189	0.9424
		RSMD	0.0079	0.0286	0.005

TABLE C.2 METHANOL(1) – ACETONE(2) SYSTEM (101.325 kPa) – OUTPUT DATA					
		EXPERIMENTAL	MARGULES	VAN LAAR	ANN
T(K)	x1	y1	y1	y1	y1
328.58	0.133	0.144	0.1461	0.1463	0.1427
328.4	0.227	0.226	0.2293	0.2284	0.2265
329.11	0.446	0.382	0.3924	0.3868	0.3818
330.84	0.676	0.55	0.5566	0.5486	0.5505
333.56	0.849	0.735	0.7295	0.7197	0.7365
335.94	0.947	0.89	0.8747	0.8759	0.8912
		RSMD	0.0085	0.0089	0.000993

TABLE C.3 METHANOL(1) – HEXANE(2) SYSTEM (333.15 K) – OUTPUT DATA					
		EXPERIMENTAL	MARGULES	VAN LAAR	ANN
P [kPa]	x1	y1	y1	y1	y1
143.468	0.079	0.472	0.553	0.5373	0.4724
149.561	0.479	0.516	0.5212	0.5234	0.5141
149.254	0.733	0.523	0.4238	0.4318	0.5241
141.762	0.902	0.561	0.4893	0.4987	0.5494
116.67	0.967	0.714	0.6815	0.6895	0.7186
		RSMD	0.0673	0.0585	0.0057

TABLE C.4 METHANOL(1) – BENZENE(2) SYSTEM (101.33 kPa) – OUTPUT DATA					
		EXPERIMENTAL	MARGULES	VAN LAAR	ANN
T [K]	x1	y1	y1	y1	y1
349.2	0.0055	0.1172	0.1153	0.1176	0.11776
337.17	0.083	0.43	0.2842	0.5458	0.44651
331.12	0.597	0.6114	0.5309	0.5677	0.61283
331.28	0.7298	0.6509	0.6257	0.5903	0.64674
333.33	0.8998	0.7742	0.7723	0.7319	0.77495
336.93	0.989	0.961	0.9642	0.955	0.96013
		RSMD	0.0688	0.0589	0.006995

TABLE C.5
BENZENE(1) – ACETONITRILE(2) SYSTEM (293.15 K) – OUTPUT DATA

		EXPERIMENTAL	MARGULES	VAN LAAR	ANN
P	x1	y1	y1	y1	y1
10.639	0.064	0.162	0.1257	0.1239	0.169
12.186	0.243	0.37	0.3577	0.352	0.3709
12.679	0.435	0.479	0.4981	0.4976	0.4798
12.732	0.512	0.519	0.5391	0.5418	0.5177
12.359	0.753	0.662	0.6615	0.6693	0.6631
11.386	0.906	0.808	0.801	0.801	0.7937
10.692	0.966	0.906	0.908	0.905	0.9068
		RMSD	0.0181	0.0198	0.0061

TABLE C.6
WATER(1) – m-XYLENE(1) SYSTEM (101.3 kPa) – OUTPUT DATA

		EXPERIMENTAL	MARGULES	VAN LAAR	ANN
T [K]	x1	y1	y1	y1	y1
405.01	0.0035	0.1875	0.0451	0.0404	0.18079
385.91	0.0242	0.5627	0.2601	0.2246	0.56964
370.25	0.2057	0.7243	0.8373	0.7659	0.72621
367.2	0.9993	0.7992	0.9698	1	0.79638
371.21	0.9999	0.9334	0.997	1	0.96934
		RSMD	0.1776	0.191	0.016712

TABLE C.7
HEXANE(1) – CYCLOHEXANE(2) SYSTEM (101.33 kPa) – OUTPUT DATA

		EXPERIMENTAL	MARGULES	VAN LAAR	ANN
T [K]	x1	y1	y1	y1	y1
353.15	0.045	0.07	0.0632	0.0639	0.0676
351.15	0.1815	0.247	0.2433	0.2473	0.2442
347.95	0.4145	0.505	0.509	0.5209	0.5024
346.75	0.5155	0.5995	0.6088	0.6098	0.5996
344.55	0.724	0.786	0.7912	0.7926	0.7879
342.9	0.9	0.926	0.9272	0.9291	0.9254
		RMSD	0.0056	0.0086	0.002

APPENDIX C: TRAINING OF DATA AND TRAINING GRAPH

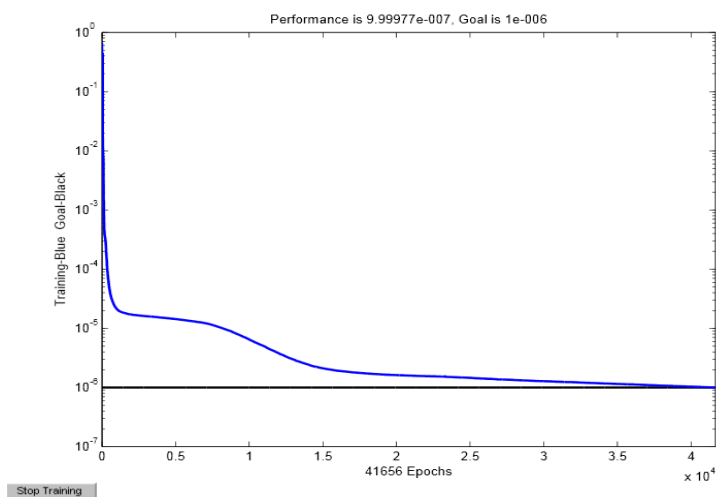
The Methanol (1) – Acetone(1) system was trained with the training data given in appendix (B.2) by implementing the Matlab code given in appendix (A.1)

The training output obtained is training set file name: maa-input target file name: maa-target input set file name: maa-test

TRAINRP, Epoch 0/100000, MSE 0.660786/1e-006, Gradient 36.7999/1e-006

TRAINRP, Epoch 5000/100000, MSE 1.43502e-005/1e-006, Gradient 0.00193372/1e-006
 TRAINRP, Epoch 10000/100000, MSE 6.49147e-006/1e-006, Gradient 0.0037737/1e-006
 TRAINRP, Epoch 15000/100000, MSE 2.11517e-006/1e-006, Gradient 0.000254585/1e-006
 TRAINRP, Epoch 20000/100000, MSE 1.62195e-006/1e-006, Gradient 0.000552213/1e-006
 TRAINRP, Epoch 25000/100000, MSE 1.45938e-006/1e-006, Gradient 0.000329364/1e-006
 TRAINRP, Epoch 30000/100000, MSE 1.27897e-006/1e-006, Gradient 0.000208013/1e-006
 TRAINRP, Epoch 35000/100000, MSE 1.15176e-006/1e-006, Gradient 0.000179174/1e-006
 TRAINRP, Epoch 40000/100000, MSE 1.03867e-006/1e-006, Gradient 0.00016271/1e-006
 TRAINRP, Epoch 41656/100000, MSE 9.99977e-007/1e-006, Gradient 0.000333166/1e-006
 TRAINRP, Performance goal met.

The training graph obtained is



C.1. Training graph for Methanol (1) – Acetone (2) system 101.325kPa

REFERENCES

- [1]. Mehmet Bilgin, I.MetinHasdemir and OguzhanOztas, "The use of neural networks on VLE data prediction", Journal of Scientific and Industrial Research, April 2004, Volume: 63, Pages: 336-343.
- [2]. Mehmet Bilgin, "Isobaric vapour-liquid equilibrium calculations of binary systems using a neural network", Journal Of The Serbian Chemical Society, 2004, Volume: 69, Number:8-9, Pages: 669 – 674.
- [3]. AbdolrezaMoghadassi, FahimeParvzian, SayedMohsenHosseini, "A New Approach Based on Artificial Neural Networks for Prediction of High Pressure Vapor-liquid Equilibrium", Australian Journal of Basic and Applied Sciences, 2009, Volume: 3 Number: 3, Pages: 1851-1862.
- [4]. A. R. Moghadassi, M. R. Nikkholgh, S. M. Hosseini, F. Parvzian and A. Sanaeirad, "Vapour Liquid Equilibrium Data Prediction For Binary Systems Containing Propane", ARPN Journal of Engineering and Applied Sciences, September 2011, Volume: 6, Number: 9, Pages: 94 - 103.
- [5]. A.Ghaemi, Sh.Shahhoseini, M.GhannadiMarageh, M.Farrokhi, "Prediction of Vapour Liquid Equilibrium for Aqueous Solution of Electrolytes Using Artificial Neural Networks", Journal of Applied Sciences, 2008, 8(4):615-621.
- [6]. ShekharPandharipandee *et. al.*, "Modeling Combined VLE Of Four Quaternary Mixtures Using Artificial Neural Network", International Journal of Advances in Engineering, Science and Technology (IAEST), May-July 2012, Vol. 2 No. 2.
- [7]. Maria C. Iliuta, Ion Iliut, FaicalLarachi, "Vapour liquid equilibrium data analysis for mixed solvent electrolyte systems using neural network models", Chemical Engineering Science, 2000, Volume:55, Pages: 2813-2825.
- [8]. L. Govindarajan and PL. Sabarathinam, "Prediction of Vapor-liquid Equilibrium Data by Using Radial Basis Neural Networks", Chemical Biochemical Engineering Journal, 2006, Volume: 20, Number: 6, Pages: 319-323.
- [9]. S.L.Pandharipandee *et. al.*, "Modeling Combined VLE of Ten Binary Mixtures using Artificial Neural Networks", International Conference on Intuitive Systems & Solutions(ICISS) 2012, Proceedings published by International Journal of Computer Applications (IJCA).
- [10]. FariborzNasri, HiuaDaraei, TahmasbHatami And AfshinMaleki, "Phase Equilibrium of Binary System Carbon Dioxide - Methanol at High Pressure Using Artificial Neural Network", April 2012.
- [11]. R. Rajesh, S. Chattopadhyay, M. Kundu, "Prediction Of Equilibrium Solubility Of CO2 in Aqueous Alkanolamines Through Artificial Neural Network", Paper presented at CHEMECA'06, Auckland, New Zealand from 17-20 September 2006.
- [12]. ManishVashishtha, "Application of Artificial Neural Networks in the Prediction of Vapour Liquid Equilibrium Data", Proceedings 25th European Conference on Modeling and Simulation (ECMS), 2011.
- [13]. J.M.Smith, H.C.Van Ness, Introduction to Chemical Engineering Thermodynamics, Seventh Edition, Tata McGraw Hill Publications.
- [14]. S.N.Sivanandam, Introduction to Neural Networks using Matlab 6.0, Tata McGraw Hill Publications.
- [15]. Y.V.C. Rao, Chemical Engineering Thermodynamics, University Press.
- [16]. MartienRiedmiller, "A Direct Adaptive Method for Faster BackpropagationLearning : The RPROP Algorithm".
- [17]. MartienRiedmiller, "RPROP – Description and Implementation details".
- [18]. Frauke Gunther and Stefan Fritsch, 'Neuralnet: Training of Neural Networks', The R Journal, June 2010, Pages: 30-38.

CMOS Compound Pair Wide Band Bio-Amplifier

Raj Kumar Tiwari¹, Gaya Prasad²

1,2 Department of Physics and Electronics, Dr. R.M.L. Avadh University, Faizabad, U.P., India

ABSTRACT:

In the present paper we study about CMOS compound pair (RKTG Pair) circuit with proper choice of inductor as additional circuit element. The proposed circuit work for very low input voltage signal like pulse rate of heart beat with higher gain wide band frequency response. The proposed circuit shows excellent temperature stability in the temperature range -50, 27 and 100 °C. We have also study about input voltage gain, output voltage gain, Fast Fourier Transform, current gain, input admittance, input impedance, output impedance and voltage gain at various frequencies for inductor range 10H to 10nH and it is found that proposed circuit works as Bio amplifier with the help of Bio-medical sensor for suitable value of inductor.

KEYWORDS: CMOS compound Pair, Frequency response, Input Impedance, Output Impedance, temperature stability, voltage gain, current gain.

I. INTRODUCTION

In the present time cardiac arrhythmia, disorder of cardiac rhythm, may cause serious heart diseases or the person can be dying. Early diagnosis of cardiac arrhythmia and choose appropriate medical treatment in daily life prevent from disorder of cardiac rhythm. Therefore, there is a maximum demand of a portable Electrocardiogram (ECG) monitoring system. In general, an ECG acquisition system consists of Bio-medical sensor, transducer, amplifier, filter, ADC and DSP. Fig.1 shows a block diagram of analog front-end Bio-medical Instrument. The analog front-end circuit is the interface between physical signal and digital processor and several methods for arrhythmia detection have been developed. In order to accurately process the ECG data for exact arrhythmia detection, required high quality signal. In the portable devices, it is most important for the analog front-end Bio-medical instrument to operate with small-size implementation while providing proper signal conditioning and low-power dissipation [1, 2].

Biosensor investigated by Arnold & Mayerhoff in 1998. The Biosensor is self contained analytical devices that incorporate a Biological recognition element combined with an artificial transducer [3]. Biosensor senses the heartbeat in the form of mechanical energy. Transducer converts it in electrical energy or electrical signal. Then amplifier amplify signal and filter is use for filtrate the signal then signal precede to ADC and DSP.

The amplifiers find wide applications, particularly in a system that require a low power supply voltage in biomedical system, communication system and instrumentation system. Complementary metal–oxide–semiconductor (CMOS) uses complementary and symmetrical pairs of p-type and n-type metal oxide semiconductor field effect transistors (MOSFETs) for logic functions. Literature survey [4-11] shows that CMOS devices have high noise immunity and low static power consumption because CMOS devices do not produce as much waste heat as other forms of logic families, like transistor–transistor logic (TTL) or NMOS logic. So in present investigation we use CMOS compound pair (also known as RKTG Pair) model that works for low voltage and high speed application having high current gain with good temperature stability as compare to reference devices [12]. All the simulation result has been obtained by PSPICE OrCAD 9.2 student version [13].

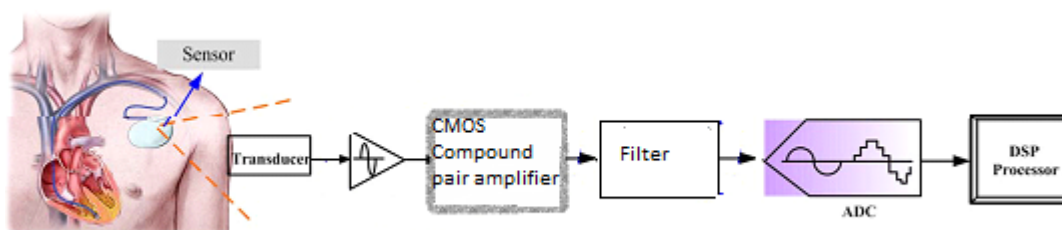


Fig.1 Block diagram of analog front-end Bio-medical Instrument.

II. EXPERIMENTAL CIRCUITS

The reference CMOS compound pair amplifier circuit shown in the Fig.2 have been simulated having an a.c. input signal $V1=1nVac$ and $0Vdc$, $Ci=1\mu f$, $Ri=500\Omega$, $R1=47k\Omega$, $R2=5k\Omega$, $Rd=10k\Omega$, $Rs=2k\Omega$, $Rl=10k\Omega$, $Vd=5Vdc$, $Cs=10\mu f$, $Co=10\mu f$ and the CMOS as combination of $M1=M2=MbreakP$ and $M3=M4=MbreakN$ is used as an active component to design the circuit.

Proposed CMOS compound pair bio-amplifier circuit shown in the Fig.3, an inductor (DI) is connected in series drain resistance and remaining all components are same as in Fig.2.

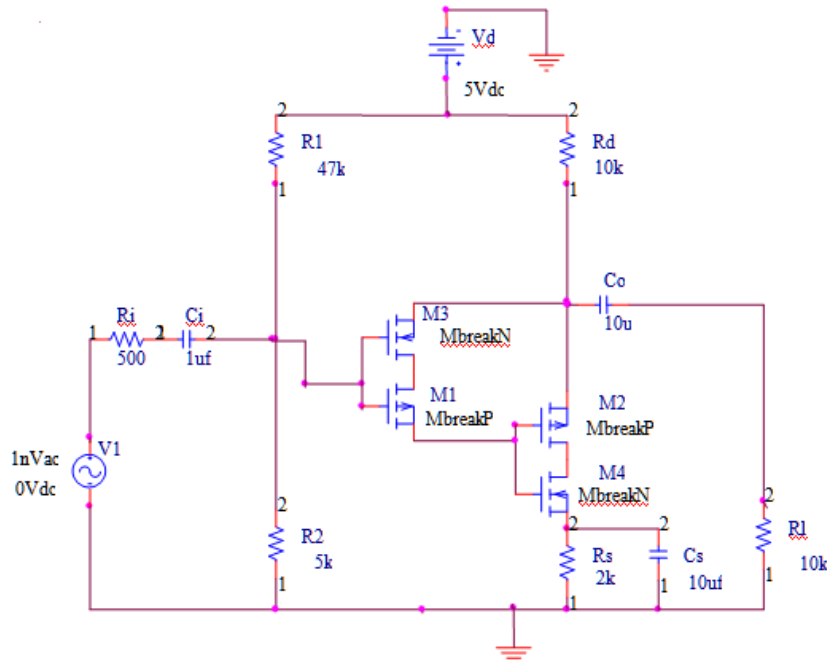


Fig.2 CMOS compound Pair (RKTG Pair) reference circuit.

Fig.2 CMOS compound Pair (RKTG Pair) reference circuit.

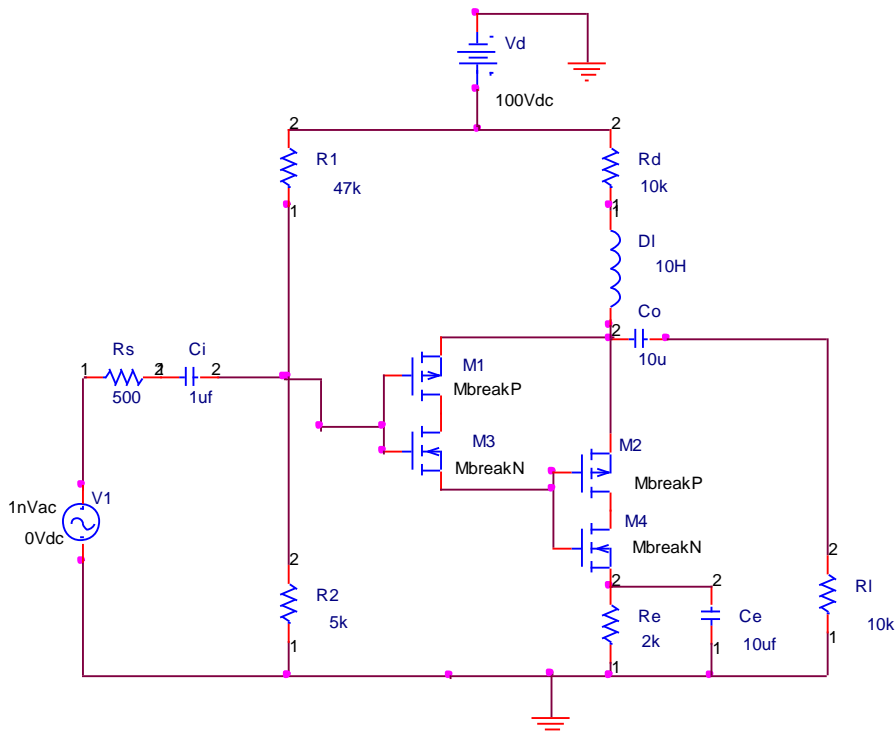


Fig. 3 CMOS compound pair (RKTG Pair) with inductor (Proposed circuit).

III. RESULTS AND DISCUSSIONS

Proposed CMOS compound pair Bio-amplifier circuit provides high voltage gain as compared to reference circuit as shown in fig.4. The Fast Fourier Transform of fig.4 is shown in fig.5. The Fast Fourier Transform curve is instantly varied at 0s then straight line which shows the circuit is stable. Fig.6 shows excellent temperature stability curve between -50 to 100 °C. Fig.7 shows that the current gain of reference and proposed circuits. The current gain of CMOS compound Pair amplifier circuit is shown by symbol (\square) and green line, the current gain of CMOS compound pair Bio-amplifier circuit shown by symbol (\diamond) and red line in fig.7. Current gain of proposed circuit initially high after 1 KHz frequency becomes low while current gain of reference circuit is constant. Fig. 8 shows input Admittance of reference and proposed circuit. The input Admittance of proposed circuit is higher than reference circuit. Fig. 9 shows input impedance, input impedance of the proposed CMOS compound pair Bio-amplifier circuit is lower as compare to reference CMOS compound pair amplifier circuit. Fig.10 shows output impedance of CMOS compound pair Bio-amplifier circuit and CMOS compound pair amplifier. The output impedance of both circuits is initially low after 1THz increase the output impedance of the proposed circuit. Fig.11 shows variation of voltage gain with frequency for the value of inductance from 10nH to 10H. It is found that the value of voltage gain shifted from high frequency range to low frequency range with the value of inductance 10nH to 10H respectively. The important outcome of the present study is that one can use proposed new CMOS compound pair Bio-amplifier circuit for very high (Terahertz reason) frequency as well as for very low frequency with proper choice of inductance. Table1 shows voltage gain of proposed CMOS compound pair Bio-amplifier at various values of Inductor at output capacitor 10 μ f.

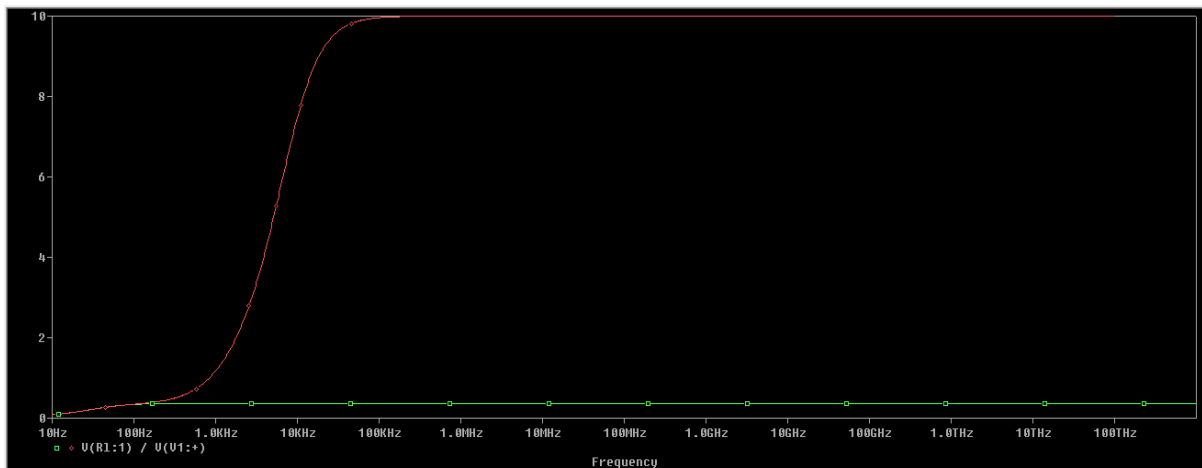


Fig.4 Frequency response of CMOS compound pair (RKTG Pair) and CMOS compound pair (RKTG Pair) with inductor.

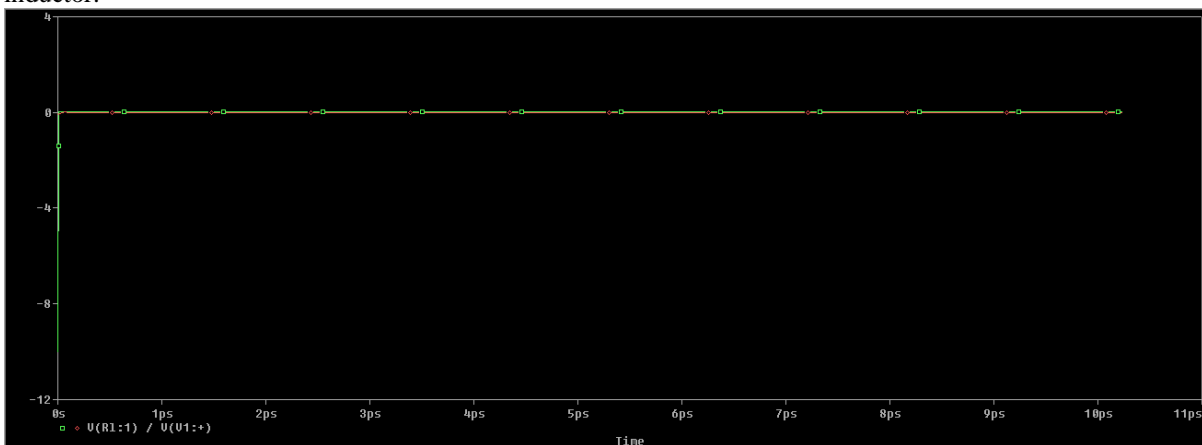


Fig.5 Fast Fourier Transform of CMOS compound pair (RKTG Pair) and CMOS compound pair (RKTG Pair) with inductor.

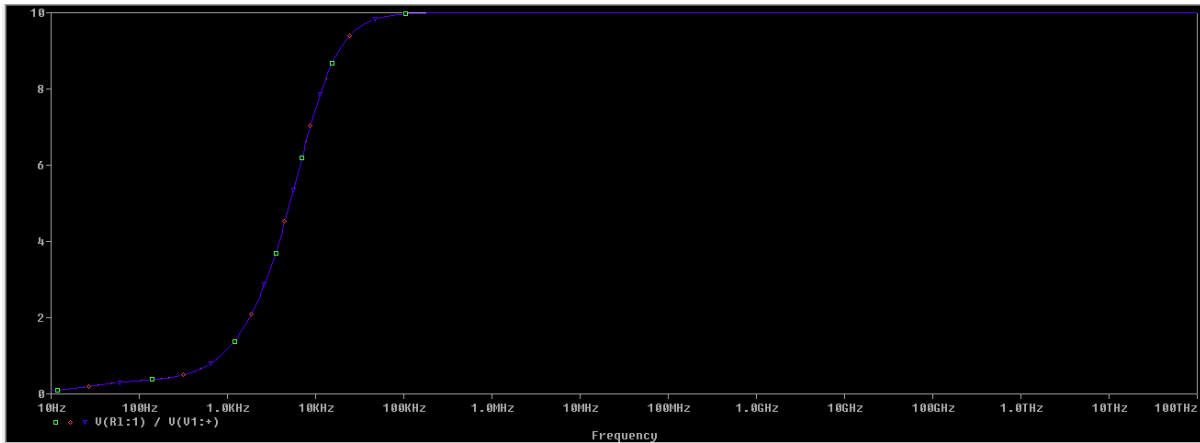


Fig.6 Frequency response of CMOS compound pair (RKTG Pair) with inductor at -50, 27 and 100 °C.

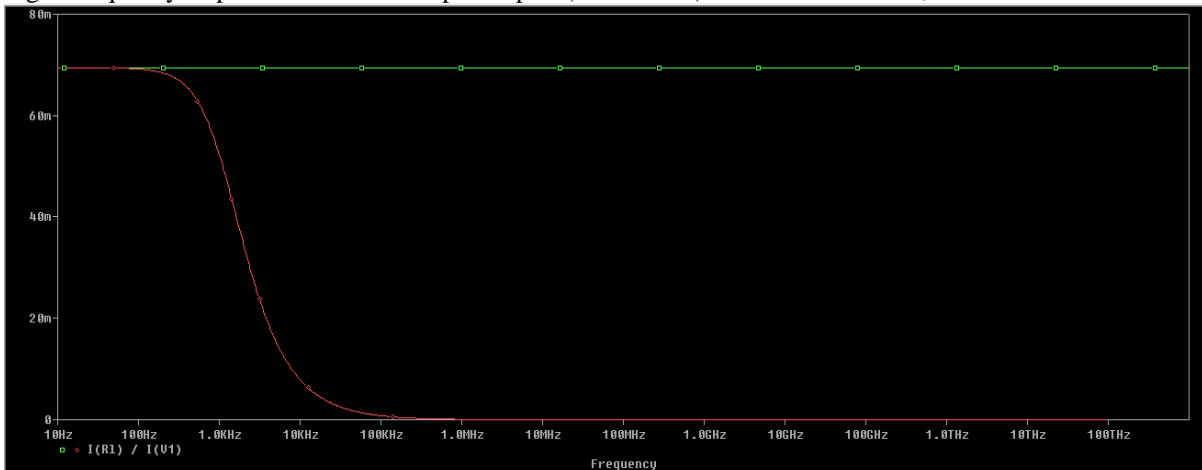


Fig.7 Current gain of CMOS compound pair (RKTG Pair) and CMOS compound pair (RKTG Pair) with inductor.

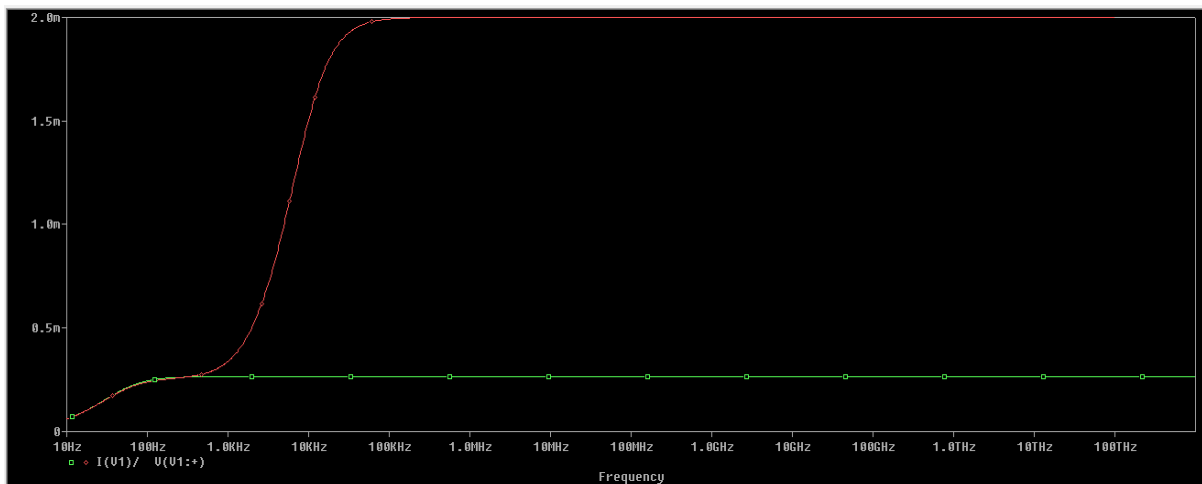


Fig.8 Input admittance of CMOS compound pair (RKTG Pair) and CMOS compound pair (RKTG Pair) with inductor.

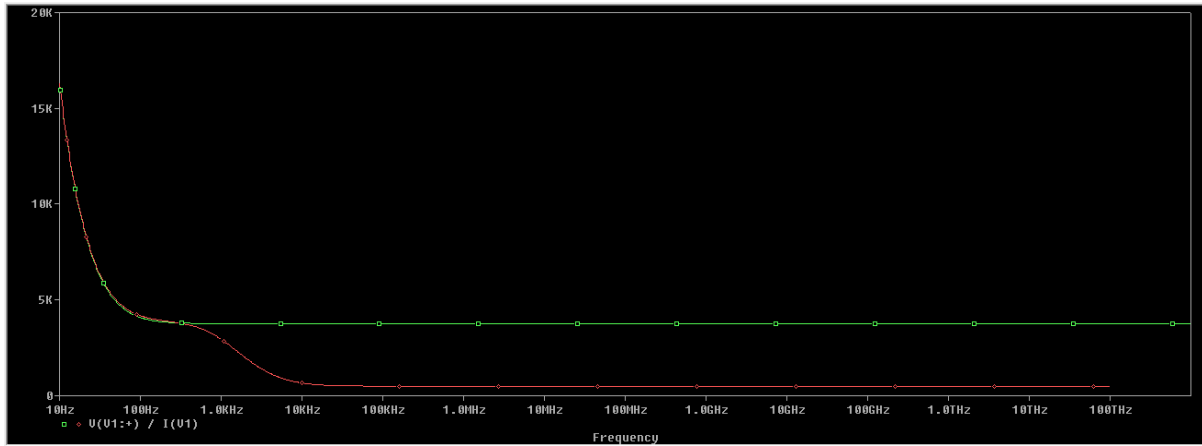


Fig.9 Input impedance of CMOS compound pair(RKTG Pair) and CMOS compound pair (RKTG Pair) with inductor.

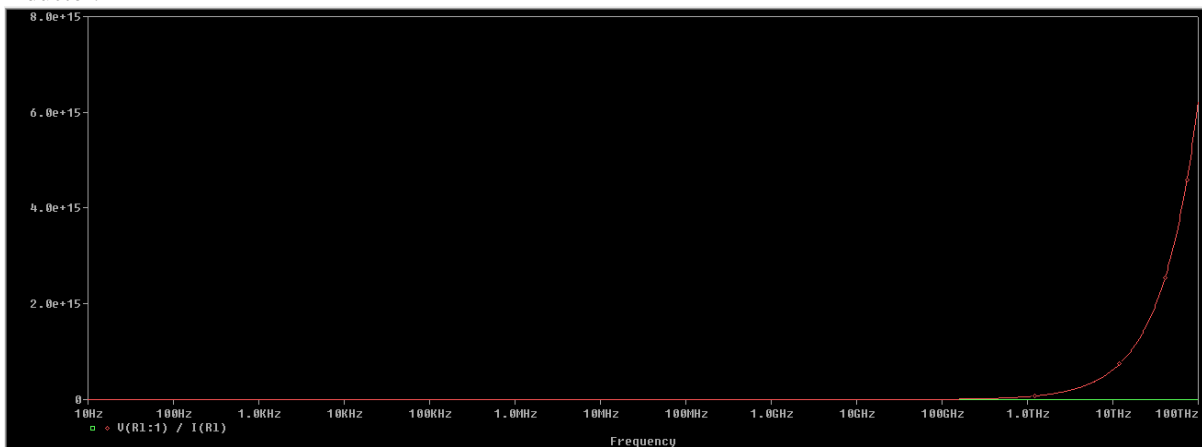


Fig.10 Output impedance of CMOS compound pair (RKTG Pair) and CMOS compound pair(RKTG Pair) with inductor.

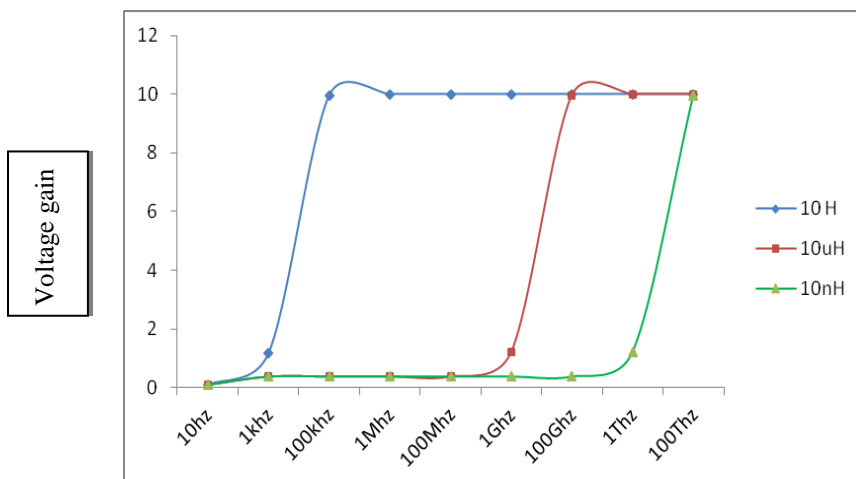


Fig.11 voltage gain of proposed circuit with various value of inductor at Co=10μf.

4. Tables

L	10hz	1khz	100khz	1Mhz	100Mhz	1Ghz	100Ghz	1Thz	100Thz
10 H	0.085	1.17	9.961	10	10	10	10	10	10
10uH	0.085	0.368	0.368	0.369	0.369	1.206	9.96	10	10
10nH	0.085	0.368	0.368	0.368	0.368	0.368	0.368	1.208	9.96

Table1 Voltage gain at various values of Inductor.

IV. CONCLUSION

From above discussion it is concluded that the proper choice of the circuit element play an important role to make CMOS compound pair(RKTG Pair) Bio-amplifier with inductor more flexible and versatile. Due to high voltage gain proposed circuit can be used as voltage amplifier for low voltage and high frequency applications. As the proposed CMOS compound pair (RKTG Pair) Bio-amplifier circuit is working at $1nV$, so together with Bio-medical sensor at the input terminal it can be use to design new portable Bio-medical instruments like ECG etc. That is capable of sensing extremely low level heart pulses. Present proposed CMOS Compound pair (RKTG Pair) amplifier can be also used to design low voltage high speed reversible logic devices. Due to its property of low power dissipation, such devices are capable to design reversible quantum computing electronic devices. This is demand of coming future reversible technology.

REFERENCES

- [1] Tsung-Heng Tsai and Yen-Cheng Chen, "Low-power systematic integration of the instrumentation amplifier and the OTA-C filter for ECG Acquisition Systems", IEEE.
- [2] Tsung-Heng Tsai, Member, IEEE, Jia-Hua Hong, Liang-Hung Wang, and Shuenn-Yuh Lee, Member, IEEE "Low-Power Analog Integrated Circuits for Wireless ECG Acquisition Systems" IEEE Transaction on Information Technology in Biomedicine, Vol.16, No.6, September 2012.
- [3] J. Negandhi, A. Ray, and P. Vadgama, " Biomedical sensor"Interdisciplinary Research Centre in Biomedical Materials Queen Mary, University of London, London, UK, pp.385-386, 2010
- [4] Nail H.E. Weste and Kamran Eshraghian, "Principles of CMOS VLSI Design A systems Perspective" Addison-Wesley Publishing Company, pp63-94, Reprint june1988.
- [5] G. Palmisano, G. Palumbo, S. Pennisi, "CMOS Current Amplifiers", Kluwer Academic Publishers, 1999.
- [6] Y.K. Seng, "New current conveyor for high-speed low-power current sensing", IEEE Procc. Circuits Devices Syst., Vol. 145, No.2. April 1998, pp.85-89.
- [7] E. L. Douglas, D.F. Lovely and D.M. Luke, "A Low-Voltage Current-mode Instrumentation Amplifier Designed in a0.18-Micron CMOS Technology", in Proc. IEEE CCECE, pp. 1777-1780, 2004.
- [8] D.Jackuline Moni, and N.Gopalakrishnan, "A Low Power CMOS Electrocardiogram Amplifier Using 0.18 μ M Technology". International Journal of Advancements in Research & Technology, Volume 2, Issue2, February-2013
- [9] Yazicioglu,R.F.; Merken,P and Van Hoof, C., "Integrated low-power 24-channel EEG front-end," Electronics Letters , vol.41, no.8, pp. 457- 458, 14 April 2005
- [10] Raj Kumar Tiwari and Anil Kumar Shukla, "Gain Enhancement in Folded Cascode Op-Amp with Class AB Output Buffer", International Journal of Electronics, Electrical and Communication Engineering, Vol.3, No.2, 2011, pp. 163-167.
- [11] Raj Kumar Tiwari, Gaya Prasad and Monika Tiwari, "Low Input Voltage High Gain Wideband CMOS Push-Pull Amplifier for Tuned High Pass Filter" Published in International Journal of Research in Electronics & Communication Technology, Volume-2, Issue-3, May-June, 2014, pp. 27-31, © IASTER 2014, ISSN Online: 2347-6109, Print: 2348-0017
- [12] Raj Kumar Tiwari and Gaya Prasad, "A New Circuit Model Of Low Voltage High Current Gain CMOS Compound Pair Amplifier" Published in International Journal of Electronics and Communication Engineering & Technology (IJECET), ISSN 0976 – 6464(Print), ISSN 0976 – 6472(Online), Volume 5, Issue 4, April (2014), pp. 65-71 © IAEME, Journal Impact Factor (2014): 7.2836 (Calculated by GISI)
- [13] Muhammad H. Rashid, Introduction to Pspice using OrCAD for circuits and electronics, Pearson Education, 3rd Edition p.p. 150-153 (2004).

Macroshrinkage and mold height correlation for grey cast iron casting

¹Nitesh Kumar, ²Anjani Kumar Singh, ³Sushil Patel, ⁴Ajit Kumar,
⁵Sachindra Kumar

^{1,4} M.Tech, Materials Science and Engineering, National Institute of Foundry and Forge Technology, Hatia, Ranchi, Jharkhand, India.

² Ph.D Scholar, Materials and metallurgical Engineering National Institute of Foundry and Forge Technology, Hatia, Ranchi, Jharkhand, India.

³ M.Tech, Foundry and Forge Technology, National Institute of Foundry and Forge Technology, Hatia, Ranchi, Jharkhand, India

⁵ Asst. Prof. Cambridge Institute of Technology, Tatisilway, Ranchi, Jharkhand, India.

ABSTRACT:

Macro shrinkage results, due to the interaction of several complex influences in iron. The grating, risering, and the iron chemistry needs to be revised, when the shrinkage is constantly present in cast products on a regular basis. It has been observed that the problem of macro shrinkage is within the control and timing of the graphitizing process, when it occurs irregularly and the iron chemistry is consistent during the episodes of shrinkage.

It is necessary to maximize the formation of late graphite, without having to reduce the actual amount of graphite, in an effort to minimize the problem of macro shrinkage in cast products.

KEY WORDS – S.G. Iron, grey cast iron, wooden cylindrical pattern

I. INTRODUCTION

Grey and ductile irons have very different solidification characteristics with gray iron having minimum shrinkage issues and ductile iron constantly having shrinkage issues. This month we will examine what makes the difference and what you can do to about it.

Gray Iron typically runs 3.2 to 3.4 percent carbons while ductile are more typically 3.6 to 3.8 percent carbons. The end results are also a little different. Gray iron typically is pearlitic while ductile can be ferritic, 40-50% pearlitic, 80% pearlitic or even 100% pearlitic. So since 100% pearlite requires 0.8% carbon, there is that much less graphite to counteract shrinkage. Let me explain.

Graphite density ranges from 2.09 to 2.23 and iron density is 7.874 so 1 gram of graphite has the same volume as 3.53 grams of iron for high density graphite to 3.77 grams of iron for low density graphite.

A 100 gram casting of iron will shrink 10% or 10 grams volume on cooling to room temperature. That volume loss could be replaced by 2.65 to 2.83 grams of graphite or 2.65% C to 2.83% C depending on the density of the graphite. Assuming high density graphite, 2.83% carbon as graphite + 0.8% carbon as pearlite gives us a total of 3.83% C. Low density graphite gives 2.65% carbon as graphite + 0.8% carbon as pearlite = 3.45% carbon to produce shrink free gray iron.

Assuming an average gray iron value of 3.3% carbon leaves us with a shortage of 0.15% C to 0.53% C which then equates to a volume loss of 0.57% to 1.87% actual shrinkage. This shrinkage occurs in three stages: liquid cooling, liquid to solid transformation, and solid cooling. The liquid cooling is generally made up by risers or a well-designed gating system and the solid state cooling shrinks the entire casting the same amount so there is no concentration of shrinkage to form internal porosity. It is the Liquid to solid transformation that we generally have to worry about.

One of the key points of gray iron is that the graphite forms during the liquid to solid transformation with some graphite flakes actually growing from the solid metal out into the liquid. The shrinkage can then go into four different places: smaller dimensions, actual micro-porosity, less dense graphite, and grain boundary disorder (stress). Since gray iron is hypoeutectic, strong walls quickly form so only in slow cooling areas (sharp fillets and hot spots) is there an actual chance of dimensional change or suck-in. These can usually be resolved by chills or redesign of the casting [1, 2].

The energy to form less dense graphite, or even disordered grain boundaries is considerably less than the energy required to form an interior surface or a shrinkage void. So the casting tries to hide its lost volume into these features first before actually forming shrinkage. Thus we generally find stubborn gray iron shrinkage only in unfed heavy sections. Ductile iron is different in that the graphite grows later. Whereas in Grey iron, the graphite growth is faster than the phase diagram suggests (level rule), in ductile iron, it is slower than the phase diagram suggests. Magnesium inhibits the formation of graphite, so it generally doesn't form in the liquid below 4.6 C.E. And even at the end of solidification (solidus), much of the graphite to be is still in the austenitic iron matrix. By my estimates, at solidus, only 50 to 60% of the total final graphite has formed. This causes a problem in the casting. Without the volume growth of graphite, the casting has a volume deficit that can push the casting over into actual shrinkage dimensional change or suck-in. These can usually be resolved by chills or redesign of the casting [3, 4].

The energy to form less dense graphite, or even disordered grain boundaries is considerably less than the energy required to form an interior surface or a shrinkage void. So the casting tries to hide its lost volume into these features first before actually forming shrinkage. Thus we generally find stubborn gray iron shrinkage only in unfed heavy sections. Ductile iron is different in that the graphite grows later. Whereas in Grey iron, the graphite growth is faster than the phase diagram suggests (level rule), in ductile iron, it is slower than the phase diagram suggests. Magnesium inhibits the formation of graphite, so it generally doesn't form in the liquid below 4.6 C.E. And even at the end of solidification (solidus), much of the graphite to be is still in the austenitic iron matrix. By my estimates, at solidus, only 50 to 60% of the total final graphite has formed. This causes a problem in the casting. Without the volume growth of graphite, the casting has a volume deficit that can push the casting over into actual shrinkage.

Macro shrinkage: - Macro shrinkage is a phenomenon associated with metal casting process. Macro shrinkage occurs, when the liquid metal is surrounded by significant amount of solid material, which is strong enough to resist the depression of the contracting liquid. The phenomenon of macro shrinkage occurs as a concentrated zone of shrinkage holes or single shrinkage cavity in cast products that can be detected through non-destructive tests, such as radiography, ultrasound, and magnetic particle method. The non-destructive tests and techniques help in eliminating the problem of macro shrinkage in cast products and improve their quality [5].

II. SHRINKAGE

A 100 gram casting of ductile iron will shrink 10% or 10 grams volume on cooling to room temperature. That volume loss could be replaced by 2.65 to 2.83 grams of graphite or 2.65% C to 2.83% C depending on the density of the graphite. Assuming high density graphite (worst possible case), 2.83% carbon as graphite + 0.8% carbon as pearlite gives us a total of 3.83% C. A ferritic casting would only require 2.83% carbon, well below the typical 3.6 to 3.8% typical carbon levels. So this logic would lead one to think that all of our ductile castings should be solid. Well obviously there is a problem: only about 60% of that graphite is present when the casting is finally solid. The rest grows as the casting cools down to the eutectoid temperature of about 1400 F (745 C – varies with chemistry composition). That means that our useable graphite is only 2.16 to 2.28% at solidus leaving us with a deficit of about ½ % volume. A 5 pound casting could have a shrinkage hole of about ¾ inch (1.9 cm) diameter if that volume deficit were to result in shrinkage.

There are three things that can happen to that volume loss: it can be expressed as stress, suck-in or shrinkage. The idea casting will have it expressed as grain boundary stress because this stress will be eliminated by the later graphite growth. The suck-in and shrinkage voids don't get eliminated by the late graphite growth, but the casting may swell slightly. The trick then is to get the casting wall strength high enough to resist suck-in by eliminating hot spots, and then, somehow to avoid the concentration of stress in one area that would lead to the formation of an interior surface (a void). Higher stress is better, lower stress suggests that the stress has somehow been relieved through shrinkage or suck-in [6]. The following is a general discussion of the chemistry and gating of ductile iron and how it affects solidification.

Smaller size ductile iron is generally made close to eutectic composition of 4.3% C.E. This leads to a slow thickening of the walls, and the casting is slow to take on the strength necessary to resist shrinkage forces. But this also keeps the gating open as the gates are very slow to freeze off so good gating and risering can compensate and feed the casting through the first part of solidification whereas in gray and heavy section ductile, the hypoeutectic composition causes dendrites to quickly block off the gates. [1]

There is sometimes a problem with the chemistry of smaller ductile iron where increasing carbon starts causing more problems than it solves. Many foundries have found that C.E. can be increased beyond 4.3% and give beneficial results. They typically run 4.4 to 4.6% C.E. and get the added benefit of more graphite and better fluidity for thin section. The problem happens when the higher carbon starts forming graphite in the liquid. As of right now, I do not know if there is an inverse relationship between graphite formation and magnesium content. But I have seen liquidus graphite arrests in irons exceeding 4.6% C.E. This also shows up in micros as a strong bimodal distribution of nodules. The nodules growing in the graphite show up as the larger nodules. These early nodules are growing during the time the gates are still open, so their volume change pushes iron out of the casting cavity and back into the runner/riser system producing sound risers. Then, of course, when the casting freezes off, there is insufficient graphite forming during solidification and cooling and so the shrink that should have happened in the risers is transferred into the casting [2].

Mechanical Properties of Gray Cast Iron

1. Graphite morphology and matrixfig- 1, 2, Characteristics affect the physical and mechanical properties of gray cast iron. Large graphite flakes produce good dampening capacity, dimensional stability, resistance to thermal shock and ease of machining. While on the other hand, small flakes result in higher tensile strength, high modulus of elasticity, and resistance to crazing and smooth machined surfaces.

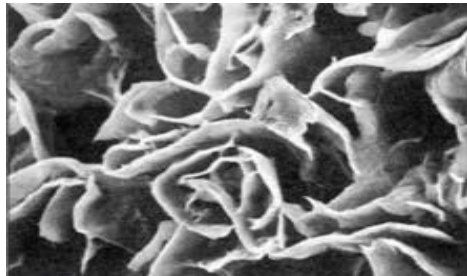


Fig-1 SEM image of grey iron with flake graphite Fig. 2: Well-polished graphite flakes

2. Mechanical Properties can also be controlled through heat treatment of the gray cast iron. For example as quenched gray cast iron is brittle [7]. If tempering is accomplished after quenching, the strength and toughness can be improved, but hardness decreases. The tensile strength after tempering can be from 35-45% greater than the as-cast strength and the toughness can approach the as-cast level.

III. MATERIALS AND EXPERIMENTAL PROCEDURE

Material: - 5kg of gray cast iron, 10kg of S.G. Iron, green, sand moulding box, wooden cylindrical pattern of height 17cm, 23cm, 25 cm.

Procedures:-

1. Make a wooden cylindrical pattern of diameter 3cm and heights of 17cm, 23cm, and 25cm.
2. Pattern is rammed in a mould box with green sand and pattern is removed
3. Gray cast iron, S.G. iron is melted in induction furnace to temperature 1200c.
4. Melted iron is poured in different mould boxes, cooled to room temperature, finally castings is removed out.
5. Cylindrical castings are cutted vertically downward symmetrically in machine shop. As shown in figures.
6. Sample taken for hardness testing and microstructure

IV. METALLOGRAPHIC PREPARATION

Cutting: White cast iron is very hard and therefore difficult to cut.

Grinding and polishing: Graphite is soft and retaining it in its true shape and size can be difficult. The matrix of ferritic and/or austenitic cast irons is prone to deformation and scratching. Gray iron, or grey iron, is a type of cast iron that has a graphitic microstructure. It is named after the gray color of the fracture it forms, which is due to the presence of graphite. It is the most common cast iron and the most widely used cast material based on weight [8].

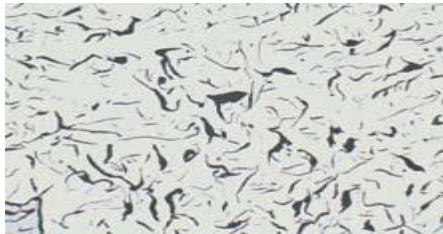


Fig.1: grey iron with flake graphite, 200 x insufficient polish



Fig. 2: showing correct polish 200x

It is used for housings where tensile strength is non-critical, such as internal combustion engine cylinder blocks, pump housings, valve bodies, electrical boxes, and decorative castings. Grey cast iron's high thermal conductivity and specific heat capacity are often exploited to make cast iron cookware and disc brake rotors [9].

Gray Cast Irons contain silicon, in addition to carbon, as a primary alloy. Amounts of manganese are also added to yield the desired microstructure. Generally the graphite exists in the form of flakes, which are surrounded by a ferrite or Pearlite matrix. Most Gray Irons are hypoeutectic, meaning they have carbon equivalence (C.E.) of less than 4.3.

Fig 1. Gray cast irons are comparatively weak and brittle in tension due to its microstructure; the graphite flakes have tips which serve as points of stress concentration. Strength and ductility are much higher under compression loads.



Fig.3. Microstructure of Gray iron under a 100x microscope



Fig 3a. Gray surface after fracture



Fig. 3b Grey iron with flake graphite in 200x

V. RESULT AND DISCUSSION

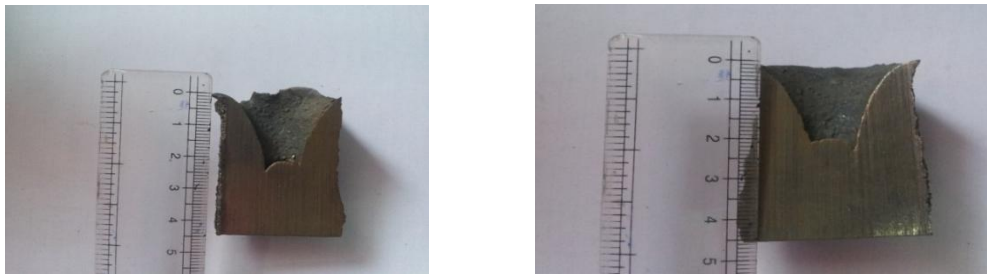


Fig. photographs of Macro shrinkage of gray cast iron cylindrical height 23 cm & 17cm



S.G cast iron height 18cm S.G cast iron 27cm mould height

Mould height(h) of S.G iron	Shrinkage height(hs)	Mould height of gray cast iron	Shrinkage height (hs1)
17	4.2	17.2	4
22.5	3.7	18	2.4
23	5	20	0.5
23.5	3.6		
25	4.7		
27	3.3		

Measurements in cm, diameter is constant 3cm

Table 1- Hardness testing result for : - diameter of indenter 10mm Gray cast iron, Load 3000 kg

S.No	INDENTATION DIAMETER (cm)			B.H.N		
	Point A	Point B	Point C	Point A	Point B	Point C
1	4.65	4.60	4.4	167	170	187
2	4.2	4.35	4.41	207	192	187

Table 2- Hardness result for S.G. Iron:- diameter of indenter 10mm, Load 3000kg

S.No.	Indentation diameter (cm)			B.H.N		
	Point A	Point B	Point C	Point A	Point B	Point C
1	4.4	4.45	4.5	187	183	179

Castings unfortunately can contain defects which may render them unsuitable for service, resulting in higher costs and/or lower profits for the production foundry and delivery delays to the customer. Some defects may not always be found prior to service - in fact, some *cannot* be found using normal non-destructive techniques - and there is always a danger that service stressing may cause a pre-existing defect to propagate, leading to premature failure.

VI. CONCLUSION

This lecture has provided an introduction to the nature and origin of major solidification defects in castings. Emphasis has been placed on how such defects can be diagnosed correctly and, more importantly, eliminated from the outset by using correct foundry techniques. Quality-conscious foundries are increasingly recognising that all parts of the production process must be properly controlled if the industry is to maintain its position of being a leading supplier of metallic components.

REFERENCES

- [1] C.F. Walton, *Gray and Ductile Iron Castings Handbook*, Iron Founder's Society, 1971, p 193.
- [2] C.F. Walton and T.J. Opar, *Iron Castings Handbook*, Iron Casting Society, 1981, p 235 & p 297-321
- [3] Donald B. Wagner (1993) *Iron and Steel in Ancient China*. BRILL. pp. 335
- [4] Keith Krause (August 1995). *Arms and the State: Patterns of Military Production and Trade*. Cambridge University Press. p. 40.
- [5] Smith & Hashemi 2006, p. 432.
- [6] Modern Casting, Inc Cuttino, J. F., Andrews, J., Piwonka, Developments in Thin-Wall Iron Casting Technology," *AFS Transactions*, vol 189, pp 363-372 (1999)
- [7] M. J. Beffel, J. O. Wilkes, and R. D. Pehlke, "Finite Element Simulation of Casting Processes," *AFS Trans.*, 94 (1986), pp. 757-764.
- [8] Samuel, A.M., Samuel, F.H., "Metallographic study of porosity and fracture behavior in relation to the tensile properties in 319.2 end chill," *Metallurgical and Materials Transactions A.*, vol. 26A, pp 2359-2372 (1995)
- [9] Showman, R.E., Aufderheide, R.C., "A Process for Thin-Wall Sand Castings," B., Iveland, T., and Harkegard, G., "Fatigue Life Assessment of Aluminum Alloys with Casting Defects," *Engineering Fracture Mechanics*, " vol 44, pp 857-874 (1993).

Latest Science

¹Jai Prakash Goel , ²Ankush Goel

¹BComRohtak University

²Be-Techin Electronics Inderprastha University India M S in Computer Science Columbia University USA

ABSTRACT

There is a network of many layers of waves, made of electric current, in our brain. That is called mind. Our mind circulates electric current to our each and every cell. There is a bone of the shape of our full body image, from head to toe, nearby our heart. This bone is surrounded by electric current, circulated by our mind. Laymen call this bone as Soul bone. We can contact Aliens through this process. Earthquake is a scientific natural happening. There is molten lava in the crust of our earth. This liquid movement is managed by electric current, one force of Nature. When there is movement in this liquid, the upper solid layer of our earth feels violent movements. We can make earthquake safe homes. In Alien world, there is no loss of life and goods during earthquakes or other natural happenings.

KEYWORDS : Mind, Electric Current, Nature, Computer, Earthquakes, Four Forces, Brain, Other Planets, Space Junk, Asteroids

I. INTRODUCTION

As a Nature Scientist, I have been doing research work on Aliens for last forty years. Both the British Library and the American Library have helped me immensely with my research. National News Service, New Delhi and All India Freelance Journalists Association, Chennai and Computer Society of India, Mumbai have also helped me during my extensive research work. My son, a post graduate in Electronics and Computer Science, also deserves to be credited for having unstintingly assisting me in my research work. Following my research, I have concluded that it is possible to link up with other existent worlds or aliens by simply activating our mind waves.

BRAIN AND MIND

Nature created man and gifted it several powers like the power to think, the power to imagine, the power to observe, explore, experiment, invent and so on. We have made advancements and inventions because Nature intended us to do so. But Nature did not bestow man with any power to know how his own mind works, how it is connected to other worlds and how the mind controls the brain. This is a hidden code of Nature which no one has been able to unearth till date. Brain is just a fleshy organ. Heart is also a fleshy organ. Mind is separate from the brain. Mind makes brain, function. Brain makes heart, function. Mind is made of waves, in weight 21 grams. This has been proved by an experiment where a dying dog was air sealed in a glass container. As it died the strong glass container just cracked and the dead body weighed 21 grams less. Hence it was concluded that something has left the body which had weight equal to 21 grams. That something has many names in the civilized human society, some call it soul, some call it consciousness, some call it mind or intelligence and so forth. All these are one and the same thing. Man is so programmed that it always seeks information and that is the very reason for our constant development as a thinking race. Today we know much about our body, heart, lungs, liver, stomach and kidneys but we don't know anything about our own mind. Medical science today has reached great heights of sophistication but the concept of mind waves is alien to them. They can't even define what is mind and what is brain and how the two work together or the difference between them. Hidden powers of our mind have largely been unexplored.

How To Contact Aliens

Mind waves is a powerful concept that is scientifically true. There is a network of many layers of waves made of electric current in our brain. That is called mind. There is a bone of the shape of our full image from head to toe nearby our heart. This bone is surrounded by electric current circulated by our mind. Laymen call this bone as Soul bone. We can contact Aliens through this process. Considerable advancements in science and technology have also unearthed various laws of Nature. We know that this world is made up of five elements namely air, water, earth, sky and fire.

We also know that these are the very elements we all are made up of. We can see and feel these elements but we are not able to see or feel the force that controls them. That is what we call Nature. Nature created earth, the solar system, the universe and every corner of it. It also follows that if Nature created life in one corner of the universe there ought to be other corners of the universe where life exists. This idea however far fetched can not be fully written off. Think of an ant cave in a jungle. And suppose you are an ant living in your well organized colony comprising of millions of ants. To you the possibility of life is limited to your immediate surroundings. But is it really true? The ant is limited in thinking because neither it has wandered far beyond its cave nor it has any means to explore and understand the vast expanse of space beyond its cave due to its miniscule size. The jungle to an ant is what is universe to a man. This simile is a classic example of the reality of our being. We know all about the earth and the solar system which represents the ant cave, but what information do we have of lands beyond the solar system which represents the huge jungle?

II. NATURE AND MIND WORKING

My research has unearthed some interesting findings which I want to share with you. Nature is kind enough... She/He looks at all worlds with one eye. In our universe, there are many galaxies. In each galaxy, there are many solar systems. In each solar system, one world, like ours, is living. Whatever we see, think, do, read or write, all this is controlled by mind waves. There is a space constraint in the brain. So, our actions, instructions, data and pictures travel in the universe.

Nature Vs. Computer

The computer also works in the similar style. All the functions in the computer are a complete electronic circuit. All the natural activities in the universe also make a complete electronic circuit. The earthquakes, cyclones, hurricane and tsunami occur just for balancing other mankind. Nature is kind enough. It control the mind-waves of a single person, makes him move to a lonely place and then punish him. In case a person is driving and Nature wants to punish, then his mind is controlled by Nature and he meets his fate. Nature makes him go to on roof and he meets his fate. He may become target of sky lighting. The complete map of a world is geographically intact with Nature. Nature strives for the least loss of man-kind at all times.

The network of mind waves has plus (+) intensity as well as minus (-) intensity in points. The plus (+) points may be more or equal than the minus (-) points but the minus (-) points can never be more than the plus (+) points. In layman's language negativity will never be more than positivity.

This universe started with a big bang and since then it is expanding. This expansion will continue. Mankind will never come to an end.

III. COMPUTER WORKING

The information technology is governed by hardware and software. In a similar fashion we humans are also governed by body and soul. A computer hardware requires an appropriate operating system on which various utility programs can run. Similarly our soul comes with a unique operating system (our Nature) on which various utility programs run (our deeds) As in a computer program our actions are triggered at appropriate times until and unless we go beyond our mind and reprogram ourselves the way we want. This could also be part of the pre-program. Preprogramming means whatever is written in destiny of a person, he gets or loses appropriately. As all computers are controlled by algorithms we humans also have an algorithm. We can access any information from the past and the future once we access the universal grid. Universal grid means international linkage and universal linkage. International linkage means our minds are linked with each other on this earth and universal linkage means our minds are linked with life forms beyond our earth or Aliens.

Natural Happenings

After years of quiet, the sun is coming alive with solar storms in a big way. It will not harm our world. Nature sees all the worlds with equality. Solar storms may charge particles that may knock out satellites, power grids and even garage door openers. Nature is kind enough towards all the worlds. Massive solar eruptions will never hit earth. They could affect airlines routes, power grids and satellites. They may affect GPS systems and other communications when it reaches the earth's magnetic field. Whenever there is a worldly thing in the way of solar flares, the solar storm takes a convenient turn.

NATURE AND CHILD: Have you ever observed the pure joy on a child's face! The innocence, the earlessness, the uninhibited joy; it reflects his limitless imagination, the free will of his curiosity and the sheer pleasure of living. If we open our minds, we too can learn big lessons from the small acts of children. Only a child can think the unthinkable, see the unseen and know the unknown without even knowing it.

Our brain has billions of interconnected neurons. They are stimulated and our brain starts functioning. What stimulates them is called the mind or soul. Our mind is a network of interconnected waves. These waves travel through the universe. We should not scoff space exploration and a future beyond earth. We can certainly contact other worlds by activating our mind waves. There is God in our mind. We call it Nature. The working style of God (or Nature) is based on logic and justification.

Our mind (or soul) has two parts. The first part (the conscious mind), can heal our **physical and mental diseases. The second part (the unconscious mind) travels in the universe and is the part which has all the secrets of past present and future stored in it. By activating the** second part of our mind we can activate mind waves. The first part of mind can get energy from the second part.

IV. CONTACT WITHALIENS

We can contact aliens by activating second part of mind. When I came in contact with aliens on 28.11.2011, I was told that Aliens are happier than us. In other worlds, a solar flare sparked a spectacular light show. Whenever there is a worldly thing in it's way, the solar storm takes a convenient turn. It has happened many times in their world. It has also happened in our world. It has been proved by our scientists.

Encounters With Aliens

I was told that as one ocean flows into another ocean in our world same is the case in other worlds. This improves climatic predictions. We are lagging behind in prediction of climate and weather changes than other worlds.

I was told that the other worlds know the source of the highest energy particles in the universe. The rivers flow into the oceans and meet the energy needs of the people without emitting Carbon Dioxide (CO₂).

The other worlds do space exploration. They find natural resources with mining asteroids.

Other worlds also observe meteors and shooting stars showers. It happens in every world. Sometimes, this process is on high level or peak.

Deploying self-replicating robots or exobots in space explorations is the only way to clean up space junk. There are rocks having precious metals in the space of our world and other worlds. Aliens have started transporting rocks from the space to their earth and then started mining them. They do this work with help of robots. Robots and exobots are the same thing.

People of other worlds use robotic space crafts to squeeze chemical components of fuel and minerals such as platinum and gold out of space junk.

V. BERMUDA TRIANGLE

In other worlds, there is an area in the sea where it is said that any ship/plane passing through that sector vanishes, never to be seen again. The gravitational force there, is so great that it sucks any thing passing through it into the ocean....it is the reason for the Bermuda triangle.

INDENATIONS AND EQUATIONS

Universal Happening in Nature-Part One

I have come to know that all the countries of our world are coming closer to each other geographically. After some years, some countries will get merged with other countries. It will occur after five years and all the countries will be affected. It will be a great event by Nature. It will be beneficial for our world. We all will be able to enjoy this great event. Our current world map will be changed after this event. This is currently happening at a very slow speed but it may get faster in the future. This event has taken place in other worlds of other solar systems. I was told by Aliens on 28.11.2011 that we are in contact with other worlds also in addition to your world in our Galaxy. This happening is beneficial. It brings the countries close to each other. This event has taken place in some worlds. It will take place in some other worlds including our world.

Universal Happening by Nature-Part Two

All the countries of our world will collide with each other. At that time we will need to activate our mind waves to ensure our survival during this Universal Happening by Nature. Nature is liable for all our acts whether good or bad. Our complete world map is intact with Nature. Nature can destroy a single building due to electric short circuit or sky lighting or earthquake or some other natural happenings. All the natural

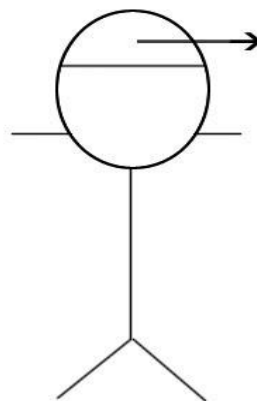
happenings like cyclones, hurricanes and tsunamis are caused by Nature just to balance all worlds. Nature is kind enough and always tries to make least loss to a world.

Logics of Contacting Aliens

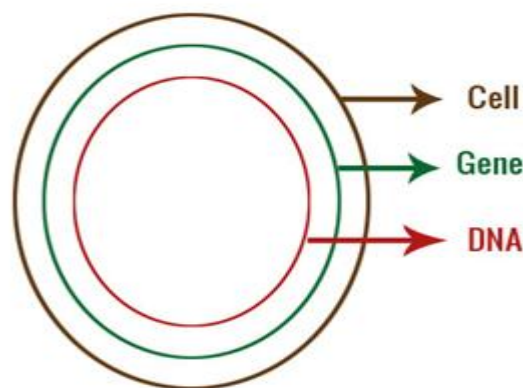
The first part of mind (conscious mind) can heal our physical and mental diseases. The second part (unconscious mind) travels in the universe. First part of mind can get energy from the second part of mind. We can contact Aliens by activating second part of mind. We should learn to activate the second part of mind. Our minds are linked at international level (human level) called international linkage and at universal level (intergalaxies) called universal linkage. Universal linkage means our minds are linked with aliens. Natural activities are based on completion of electronic circuit. Nature maintains ratio of fifty percent in every world. Good persons are equal or more than fifty percent in every world. More the good happier the community. There is Nature or God in our mind. The working style of Nature is based on logic and justification. Sometimes, we get our own electric current. It is not harmful for health. This is called electric force of Nature on which our mind is working. Whatever we see, do, write, think or read... it is an act of Nature. Our data, pictures and information is saved in first part of mind. We may transfer our saved data, pictures and information from first part of mind into second part of mind. Thus, our data, etc. are kept in the safe custody of Nature. Aliens are happier than us.

FIGURES AND TABLES

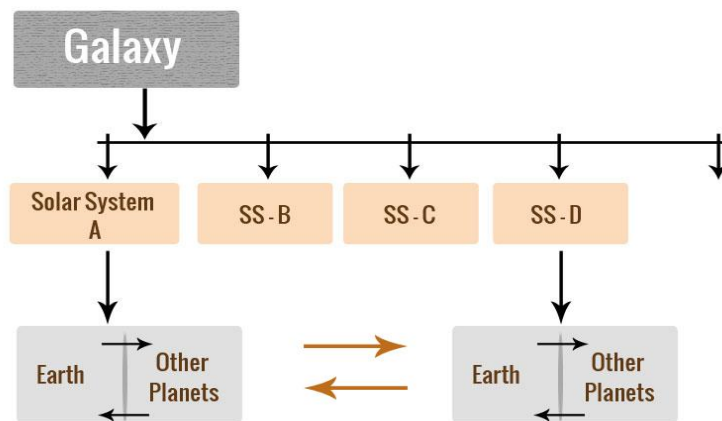
21 Gms Weight mind / Soul / Conscious / Intelligency



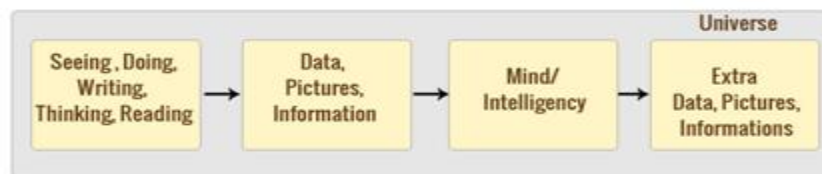
There is 21 gms. Weight mind/soul/conscious/intelligency in human body



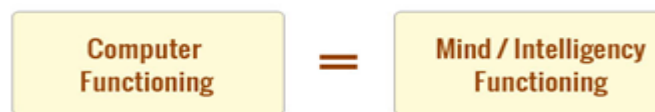
This 21 gms. Weight matter isn't made of cells. The smallest part of this matter isn't the DNA.



Other mankind are also living in other Solar-systems in our Galaxy. Other mankind have started life on other planets, than earth, of their solar-system. They can also contact other mankind, living in other solar-systems of our galaxy.



Whatever we see, think, do, read, write once that's in our brain but due to less space in the brain, those extra informations, data and pictures move in the Universe has a part and parcel of our 21 gms. Weight matter.

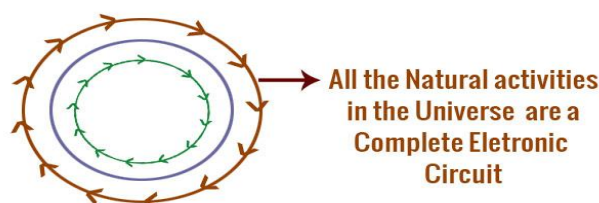


The Computer also works in the same style.



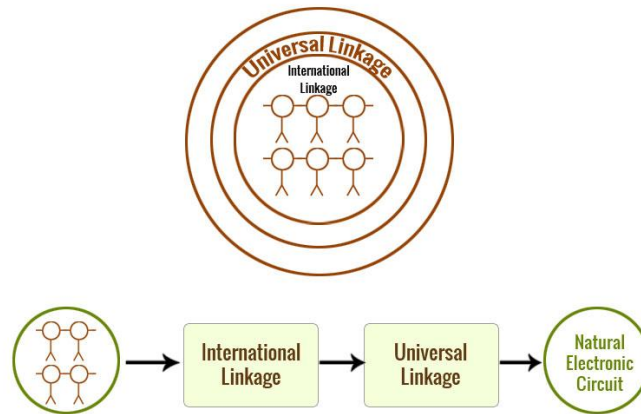
This matter has plus (+) intensity as well as minus (-) intensity in points. The plus (+) points may be more than of (-) points, but (-) points can never be more than of plus (+) points. Our mankind will never come to an end, in the same way, as the expansion of the Universe is going-on.

7.



All the natural activities in the Universe are a complete electronic circuit. That's why we get earth-quake and cyclones. It happens just to balance other mankind's.

Natural Electronic Circuit



The 21 gms weight mind/intelligence of all human-beings in a mankind are inter-linked. This linkage is called international-linkage. All international-linkages are also linked with each other. This linkage is called universal-linkages. The universal-linkages is a part of natural electronic circuit."

VI. CONCLUSION

Earthquake is a natural phenomenon. Earth has molten lava in its crust. When there is disturbance in this liquid the solid upper layer of the earth experiences violent movements sometimes resulting in widespread death and destruction. Japan is a classic example where earthquakes are frequently experienced in certain parts of their country. They have started building earthquake proof houses. We can also make earthquake safe homes. In Alien world, there is no loss of mankind or goods during earthquakes or other natural happenings like these because they know nature much better than us and so are better prepared for such happenings. There was a meteorite strike over Russian sea. That was a scientific combination of electric current with space junk or asteroids. We should start mining of space junk at the earliest without any further delay. Aliens are not harmful for us. Aliens space crafts have started visiting our solar system. We can not contact Aliens at a physical level as Nature's four forces will not allow us to do so. Nature wants to remain supreme power in this universe. That is why Nature made four forces, invisible. SHE was aware that man will try to overtake HER. It is golden rule of Nature that first we will start life on other planets of our solar system. Then, we will start mining of space junk or asteroids. Then, we will contact Aliens.

Suitability Analysis in Determining Optimal Landfill Location Using Multi-Criteria Evaluation (MCE), GIS & Remote Sensing

¹Olusina J. O. , ²D. O. Shyllon

¹Department of Surveying & Geoinformatics, Faculty of Engineering University of Lagos, Nigeria

²c/o Department of Surveying & Geoinformatics, Faculty of Engineering University of Lagos, Nigeria

ABSTRACT

Most of human activities often result in numerous wastes as their by-products. Rapid and uncontrolled urban expansion, poor planning, lack of adequate financial support just to mention a few often lead to poor management of municipal solid waste (MSW) in most cities, especially in developing countries like Nigeria. Similarly, changes in consumption patterns worldwide have resulted in a sporadic increase in commercial, industrial and household wastes thereby causing serious environmental and health hazards. However, with various waste management techniques in developed economy which is being adopted by developing nations, waste dump sites still manifest physically in developing countries as the primary means of waste disposal. In Lagos Metropolis, there are challenges in handling the various legal and illegal waste dump sites and in adopting holistic approach to the management of wastes by the state agency in-charge of waste disposal. This paper examines the locations of the existing dump sites, and adopts Geographic Information Systems (GIS), Remote Sensing technology and Multi-Criteria Evaluation (MCE) technique to carry out suitability mapping of optimal locations for Landfills within Lagos Metropolis. For the optimal site selection, fourteen different criteria were identified and each criterion was weighted using MCE. Finally, based on transportation and minimum area criteria requirements using overlaying and buffering analysis, the suitability map was generated. The map revealed four classifications as: “unsuitable (96.0%)”, “least suitable (0.4%)”, “moderately suitable (1.0%)”, and “most suitable (2.6%)”.

KEYWORDS: Solid Waste, Landfill, Geographic Information Systems (GIS), Remote Sensing, Multi-Criteria Evaluation (MCE).

I. INTRODUCTION

In Nigeria like other developing countries, proper solid waste management is one of the undaunted monster that is confronting various municipal authorities as it has posed threats to lives and the environmental. Indiscriminate disposal of effluent and toxic waste have endangered healthy living. Diseases transmission, fire hazards, odour nuisance, atmospheric and water pollution, aesthetic nuisance and economic losses are some of the problems associated with improper management of solid waste (Nwambuonwo and Mughele, 2012). **Solid** waste means any garbage, refuse, sludge from a wastewater treatment plant, water supply treatment plant or air pollution control facility and other discarded materials including solid, liquid, semi-solid, or contained gaseous material, resulting from industrial, commercial, mining and agricultural operations and from community activities but does not include solid or dissolved materials in domestic sewage, solid or dissolved materials in irrigation return flows or industrial discharges that are point sources. Some of these wastes can be recycled while others are discarded and disposed of properly (New York State Department of Environmental Conservation, 2010). A suitable disposal site must have environmental safety criteria and attributes that will enable the wastes to be isolated so that there is no unacceptable risk to people or the environment. Criteria for site selection include physical, socioeconomic, ecological and land-use factors. Different tools and techniques are being developed for solid waste disposal site selection in developed countries. Out of these, landfilling is the most common method used in many countries (Yesilnacar and Cetin 2005). In modern times, finding a site to locate undesirable facilities is becoming a significant problem in the planning sector (Erkut and Moran, 1991). In particular, the siting of landfills is an issue due to prevalent “not in my backyard (NIMBY)” and “not in anyone’s backyard (NIABY)” concerns from the public. Siting of landfills is important because of the imperative nature of landfills due to the expanding population and the corresponding volume of garbage (Kao and Lin, 1996). Despite the existence of solid waste dumpsites, the problem of waste management has continued

to be a menace in developing countries such as Nigeria. Lagos being the commercial nerve centre of Nigeria with a fast population growth, the problem of waste management is still a huge monster that is plaguing the city. The concerted efforts of State Agency in charge of waste management (Lagos Waste Management Authority, LAWMA) in tackling this menace are yet to achieve the desired result. There is still need to ensure effective and efficient disposal of both residential and industrial wastes in Lagos. To assist in achieving effective and efficient waste management, this research is aimed at the determination of: (i) suitable optimal site for landfills in Lagos State, and (ii) waste optimal planned collection route using Geographic Information Systems (GIS), Remote Sensing technology and Multi-Criteria Evaluation (MCE) technique. Existing dump sites were considered, fourteen non-exclusionary and exclusionary criteria (geomorphology, underground water depth, wetland, mangroves, land-use, surface waters, drainage, forest and vegetation, rivers, slope, roads, settlements and airport) were examined, Analytical Hierarchy Process (AHP) was used to assign weights, maps were overlaid and buffering technique was used to carry out suitability evaluation. Transportation needs for effective waste management were discussed and a typical *shortest-path* route from waste collection site to the landfill site was created in a GIS environment for efficient transferring and transporting of solid wastes.

Study Area

Lagos Metropolitan Area (3,345Km¹) spreads over much of Lagos State. Lagos is the most populous conurbation in Nigeria with 7,937,932 inhabitants at the 2006 census as a result of heavy migration from all parts of the country as well as from outside the country. It is currently the second most populous city in Africa (*after Cairo*), and currently estimated to be the second fastest growing city in Africa (7th fastest in the world), immediately following Bamako. Formerly the capital of Nigeria, Lagos is a huge metropolis which originated on islands separated by creeks, such as Lagos Island. The city is the economic and financial capital of Nigeria. The multi-ethnic nature of the place made it hard to get a good grip on the place. The city of Lagos lies in south-western Nigeria, on the Atlantic coast in the Gulf of Guinea, west of the Niger River delta, located on longitude 3° 24' E and latitude 6° 27' N. There are two major urban islands of Lagos in Lagos Lagoon, Lagos Island and Victoria Island (Lagos Travel Guide, 2014).The lagoons provides places of abode and recreation, means of livelihood and transport, dumpsite for residential and industrial discharges and a natural shock absorber to balance forces within the natural ecological system. The Lagos Lagoon consists of three main segments: Lagos Harbour, the Metropolitan end and Epe Division (Oyenekan, 1988).

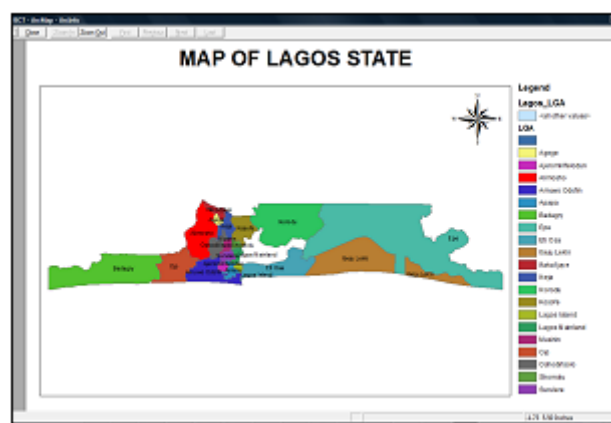


Fig. 1. Showing the map of Local Government Areas in Lagos State.

II. SOLID WASTES GENERATION AND MANAGEMENT

2.1 Solid Wastes Generation

Generally, municipal solid waste is defined as waste arising from human activities in household, commercial and institutional areas that are useless or unwanted. The knowledge of the sources and types of solid wastes, along with data on composition and rates of generation, is basic to the design and operation of the functional elements associated with the management of solid wastes. Sources of solid wastes in a community are, in general, related to the land use and zoning. Tchobanoglous et al (1993) gave a description of sources and types of solid wastes within a community (Table 1).

Table 1. Sources and types of solid wastes within a community (Tcholobanogous et al, 1993).

Source	Typical facilities, activities, or locations where solid waste is generated	Types of Solid Wastes
Residential	Single family and multifamily, detached dwellings, low, medium, and high-rise apartments, etc	Food wastes, paper, cardboard ,plastics ,textiles, leather, yard wastes, wood, glass, tin cans, aluminium, other metals, ashes, street leaves, special wastes (including bulky items, consumer electronics, white goods, yards wastes collected separately, batteries, oil, and tires), household hazardous wastes.
Commercial	Stores, restaurants, markets, office buildings, hotels, motels, print shops, service stations, auto repair shops, etc	Paper, cardboard, plastics, wood, food waste ,glass, metals, special wastes, hazardous wastes, etc.
Institutional	School, hospitals, prisons, governmental centres.	As above in commercial
Industrial	Construction, fabrication, light and heavy manufacturing, chemical plants, power plants, demolition, etc.	Industrial process wastes, scrap material, etc. Non-industrial wastes including food wastes, rubbish, ashes, demolition and construction wastes, special wastes, hazard wastes.
Agricultural	Field and farms	Spoiled food wastes, agricultural wastes, rubbish, hazardous wastes.
Public Areas	Streets, parks, recreation areas.etc	Special wastes, rubbish.

Like in most developing countries, scientific data are scare and very scanty. The data on waste generation in Lagos till date is still scanty. However, the estimated wastes generated/tonnes in Lagos are shown in Table 2:

Table 2. Development of Waste Generation and Management in Lagos (LAWMA, 2008).

Year	Area	Population	Generation Rate per Day	Ton/Day	Trucks
1945	>200km ²	40000	0.1(E)	4+	1
1967	1200km ²	1,500,000	0.12 (E)	180	6(2 trucks)
1976	10000km ²	3,200,000	0.2	640	100(35 trucks)
1990	35000km ²	5,000,000	0.25	1,250	210(70trucks)
2006	<40000km ²	18,000,000	0.4	7,200	1200(400-500 trucks)
2008	<40000km ²	18,000,000	0.5	9,000	1500(550-600 trucks)
2015	<60000km ²	23,000,000	0.7	16,100	2500(800 trucks)
2020	<60000km ²	30,200,000	0.7	21,140	(1,057 trucks)

2.2 Solid Waste Management

Solid waste management may be defined as the discipline associated with the control of generation, storage, collection, transfer and transport, processing and disposal of solid wastes. Integrated solid waste management includes the selection and application of suitable techniques, technologies and management programmes to achieve specific waste management objectives and goals Tchobanoglous and Kreith, 2002). Solid waste management technologies entails: 1) Source reduction, 2) Recycling, 3) Waste transformation and 4) Landfilling. For most industrialized nations today, solid waste management is a multibillion dollar business which is also crucial to survival, unlike in developing countries where solid wastes create losses. The conditions, issues and problems of urban waste management in the industrialized and developing worlds are different. Though the developed countries generate larger amounts of wastes, they have developed adequate facilities, competent government institutions and bureaucracies to manage their wastes. Developing countries are still in the transition towards better waste management but they currently have insufficient collection and improper disposal of wastes. Disposal of wastes is commonly done by dumping (on land or into water bodies), incineration or long term storage in a secured facility. All these methods have varying degrees of negative environmental impacts with adverse environmental and health risks if wastes are improperly disposed or stored. (Longe and Balogun, 2010).

For Nigerian cities, including Lagos Metropolis, waste removal is one of the most pressing issues and not a new problem. Most Nigerian cities consist of heaps of refuse in street corners, side-walks to mention but a few. As at 1977, Lagos was described as the dirtiest capital city in the World to host FESTAC 77. Several government agencies emerged to manage waste until the transformation of Waste Disposal Board to Lagos State Waste Management Authority (LAWMA) in 1991 with the mandate of collection and disposal of municipal and industrial waste in the State and improved commercial services to the State and Local Governments. From 1994, LAWMA started the private sector participation (formal / informal) in waste management in the State (Rugiramanzi, 2013). However, illegal dumping of waste into water and land environment by cart pushers and individuals alike has necessitated the review of waste management and disposal system in the State. In readiness for the Lagos Metropolitan Development Governance project supported by the World Bank, Lagos State restructured the Lagos State Waste Management Authority in 2005.

2.3 Existing Landfill Operations in Lagos State

There are three (3) major landfills (Fig. 2) and three (3) temporary sites serving Lagos State. The major landfills fall within the case study. The major landfills and their capacities are shown in Table 3.

Table 3. Major Landfill Sites in Lagos Metropolis (LAWMA, 2008).

Name	Location	Coordinates		Average daily tonnage	Approximate Waste Received (%)	Size (Hectares)	Residual Life Span (Years)
		Latitude (N)	Longitude (E)				
Olushosun	Ikeja Local Government (L.G.). Situated at Ojota / Oregun	6.5911	3.3814	211,667.33	35	42	20
Abule-Egba	Alimosho L.G. Located within Agbado Oke-Odo LCDA	6.6411	3.3027	97,611.67	80	10.5	8
Soluos	Soluo II Along Lagos State University – IBA Road	6.5703	3.2537	53,178.33	Over 70	7.8	5
	Soluo III Along Lagos State University – IBA Road	6.5703	3.2537	53,178.33	Over 70	5	5

Their pictorial view are shown below.



Olushosun



Abule-Egba



Soluos

Fig. 2. Major Landfills in Lagos.

Other Satellite (minor) Landfill Sites comprise of Owutu (Ikorodu L.G.), Sangotedo (Eti-Osa L.G.) and Temu (Epe L.G.) dumpsites. These sites serve as back-ups for the three major landfill sites, and also have an advantage of proximity. They are temporary sites and fall outside the scope of this study area,

2.4 General Criteria for Selecting Potential Sites for a Solid Waste Landfill

International practices always account for environmental, economic, social, and technical factors in the construction of landfills. Landfill designers are primarily concerned with the viability of a site. To be commercially and environmentally viable, a landfill must be constructed in accordance with specific rules, regulations, factors and constraints which vary from place to place or from country to country. These specific rules, regulations, factors, and constraints must cover: geomorphology, land value, slope and proximity to recreational areas (Dorhofer and Siebert, 1996; Erkut and Moran, 1991; Lin and Kao, 1999). In summary, Chang et al, 2007 gave the following criteria for specifying the best site for a landfill:

- (i) Distance from historical sites, ancient areas and including international museums should not be less than 1 Km;
- (ii) Keep the distance from well-water or water supply for manufacturing g not less than 1 Km away,
- (iii) Keep the distance from the road not less than 750 m away,
- (iv) Keep the distance away from rivers of not less than 1 Km,
- (v) In addition, the landfill should be situated at a significant distance away from urban residential areas due to public concerns, such as aesthetics, odour, noise, and decrease in property value. Urban buffers may range from 150 m to 5 Km, and
- (vi) Moreover the selected area shouldn't often flood.

III. METHODOLOGY

Siting a sanitary landfill requires a substantial evaluation process in order to identify the best available disposal location, that is, a location which meets the requirements of government regulations and minimizes economic, environmental, health, and social cost (Siddiqui et al. 1996). In this research, the following steps were taken to determine the best locations for siting landfills in Lagos Metropolis.

3.1 Data Acquisition and Image Processing

In GIS, availability of data is crucial. In this work, a comprehensive body of secondary information related to environmental (streams network and wetlands), socio-cultural (municipal development area, historic and important conserved sites and land use), and economic factors (road network, land slope, soil cover, and geology) were collected and produced in a digital format.

Sources of data include primary and secondary sources:

Primary Data- Spatial and Aspatial data of the existing dumpsites were obtained from the field.

Secondary Data- these include: Average daily waste generated per tonnage dumped at the existing dump sites obtained from Lagos Waste Management Agency (LAWMA); Lagos State Land Use map from Land Use Department of the Lagos State Ministry of Environment; LandSat imagery for Lagos Metropolis from GLCF; and Height data of the study area from SRTM (shuttle radar topography mission); Lagos State Local Government Administrative Map from LASPPDA; and Lagos road network map from the Department of Surveying & Geoinformatics.

3.2 Data Compilation and Processing

The acquired data (both primary and secondary) were processed, and plotted in a GIS environment with their attributes attached:

1. Features Extraction- Acquired Landsat imagery was processed using ENVI 4.5 (Fig. 3) and transformed in WGS 1984 UTM Zone 31N.

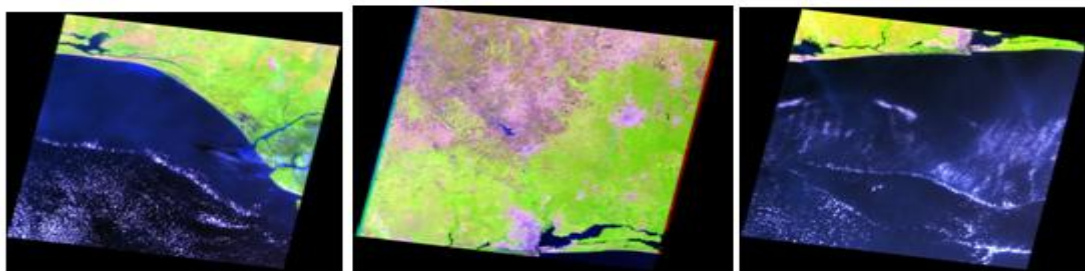


Fig. 3. The Three (3) Landsat Images covering the entire Lagos State.

For better land use classification of the study area, the acquired Land Use Map of Lagos State was overlaid on the processed Landsat imageries and five (5) distinct feature classes were identified out: (i) Built up areas, (ii) Water bodies, (iii) Forests and other vegetation, (iv) Wetlands, and (v) Mangroves. The Land Use Map of Lagos State and Lagos State mosaicked aerial photography were used to assist feature location and identification. Region of Interest (ROI) was specified for each feature class during the supervised classification. Feature extractions were carried out based on the five (5) identified classes (Figs. 4a and 4b).

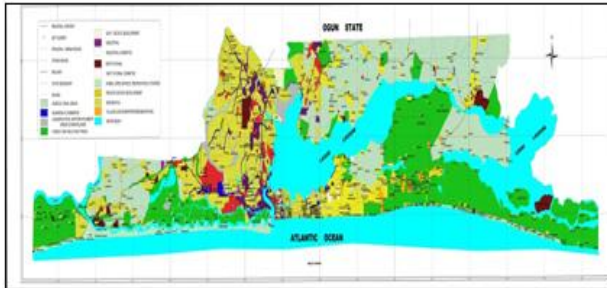


Fig. 4a Land Use map of Lagos State (Lagos State Land Use Department, 2002)

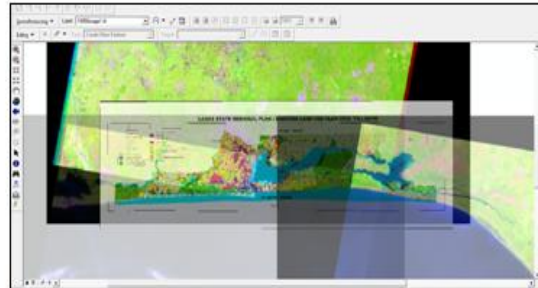


Fig. 4b. Overlaying of the Landsat imageries and the existing land use map.

Post-classification was carried out to vectorize classified areas and the vectorized features were exported as shape files to ArcMap. Feature trimming was carried out. The three Landsat imageries (Fig. 3) were merged using similar feature edge-matching technique and overlaid on a boundary map of Lagos Metropolis. Water bodies were extracted (Fig. 5).

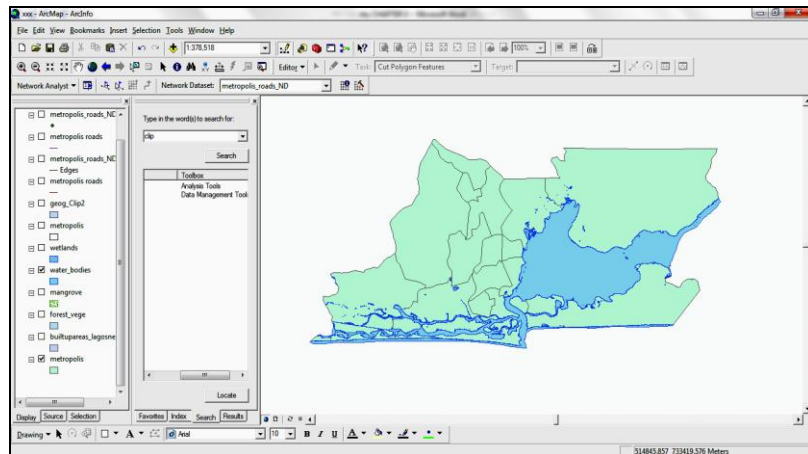


Fig. 5. Water Bodies classification within Lagos Metropolis.

2. Spot Heights Extraction- Spot heights were acquired from SRTM (Shuttle Radar Topography Mission) data (*GeoTIFF* and *HGT*, Fig. 6) and processed.

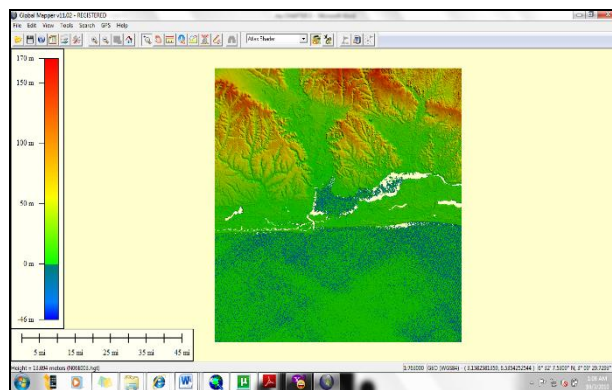


Fig. 6. *hgt* SRTM data covering Lagos State and some part of the Atlantic Ocean.

The XYZ grid data were later converted to a .dbf (database file), plotted as points on ArcMap and clipped to fit in the boundaries of Lagos Metropolis.

3.3 Criteria and Restriction Parameters for Landfill siting in Lagos State

According to Lagos Waste Management Authority (LAWMA), the simple preliminary guidelines used for landfill site selection includes: (1) Size of area/capacity, (2) Distance to populated areas, (3) Distance to sensitive water resources, and (4) Hydrology and Hydrogeology. Since an optimal landfill location must comply with all Federal and State Governments’ regulations, therefore, location restriction criterion, which varies depending on environmental and climatic regional factors must be considered. With a little modifications in this work, the Land Use Department of Lagos State Ministry of Environment agreed with the criteria used in Dhaka City [Table 4].

Table 4. Criteria and Restriction Parameters for Landfill siting (Mohammad, Kidokoro and Syed, 2009)

Criterion	Parameter	Criterion	Parameter
Distance from water bodies	300 – 500m	Distance from urban area	500 – 2000m
Distance from forest, park, etc.	50 – 500m	Distance from roads	50 – 100m
Distance from well	500 – 1000m	Haul distance	30 – 45m
Soil permeability	< 10 - 6cm/sec.	Slopes	< 15 – 20%

In this work, fourteen non-exclusionary and exclusionary criteria were considered. Non-exclusionary criteria (Factors) were classified into two groups: (i) Biophysical factors (i.e. biological and physical environmental related factors) and (ii) Socio-economic factors (human related activities). The Biophysical factors include: geomorphology, underground water depth, wetland, mangroves, land-use, surface waters, drainage, forest and vegetation and rivers; while the socio-economic factors include: slope, roads, settlements (i.e. residential area) and airport. Constraints for the Biophysical factors are: (i) the waste disposal site cannot be built on landslides which are active or may become active in the future, (ii) the waste disposal site can only be constructed in areas which do not have an important economic or ecological value, (iii) areas should have sufficient size/capacity to be used as a waste disposal site for a prolonged time, and (iv) the waste disposal site must be close as possible to existing roads for saving road development, transportation, and collection costs. Details on the exclusionary criteria with respective buffer distances are discussed in Section 4.2. Three decision criteria, using buffering (proximity) techniques, were considered for suitability evaluation: (i) Stream proximity, (ii) Urban proximity, and (iii) Road proximity. The decision criteria were analysed for sensitivity of land suitability (Effat and Hegazy, 2012; Rugiramanzi, 2013).

3.3 Multi-Criteria Evaluation (MCE)

According to Mohammad, Kidokoro and Syed (2009), Multi-Criteria Evaluation is a process that combines and transforms geographical data (the input) into a decision (the output). This process consists of procedures that involve the utilization of geographical data, the decision maker's preferences and the manipulation of the data and preferences according to specified decision rules. In this process, multidimensional geographical data and information were aggregated into one-dimensional values for the alternatives. Landfill site selection by GIS is a multi-criteria evaluation (MCE) process and generally has four steps: (i) Criterion establishment, (ii) Standardization of factors, (iii) Establishment of factors weight, and (iv) Weighted linear combination. With a weighted linear combination, factors were combined by applying a weight to each followed by a summation of results to yield a suitability map i.e.

$$S = \sum w_i x_i \dots\dots\dots (1)$$

where, S = suitability, w_i = weight of factor i, x_i = criterion score of factor i. The procedure can be modified by multiplying the suitability calculated from the factors by the product of the constraints, i.e.

$$S_{i,j} = \left(\sum_{x=1}^p f_x w_x \prod_{y=1}^q r_y \right)_{i,j} \dots\dots\dots (2)$$

where $S_{i,j}$ = land suitability of cell i for the land use type j , f_x = attribute of factor x at cell i , w_x = weight of the factor x , p = number of factors f , r_y = attribute of constraint y at cell i , q = number of constraints r .

Using a weighted linear combination in MCE, the weights summed to 1. AHP being a multi-objective, multicriteria decision-making technique was used to assigning weights to all the factors and to control the level of risk and trade-off for the alternatives. In the AHP, weight was derived by taking the principal eigenvector of a square reciprocal matrix of pair-wise comparisons between the criteria. The AHP hierarchical structure is shown in Figure 7. The AHP results were thereafter integrated into GIS for better analysis to determine optimal landfill site suitability (Mendoza, 1997). Flowchart for the MCE optimal suitable site selection is shown in Figure 8 (Saaty, 1980).

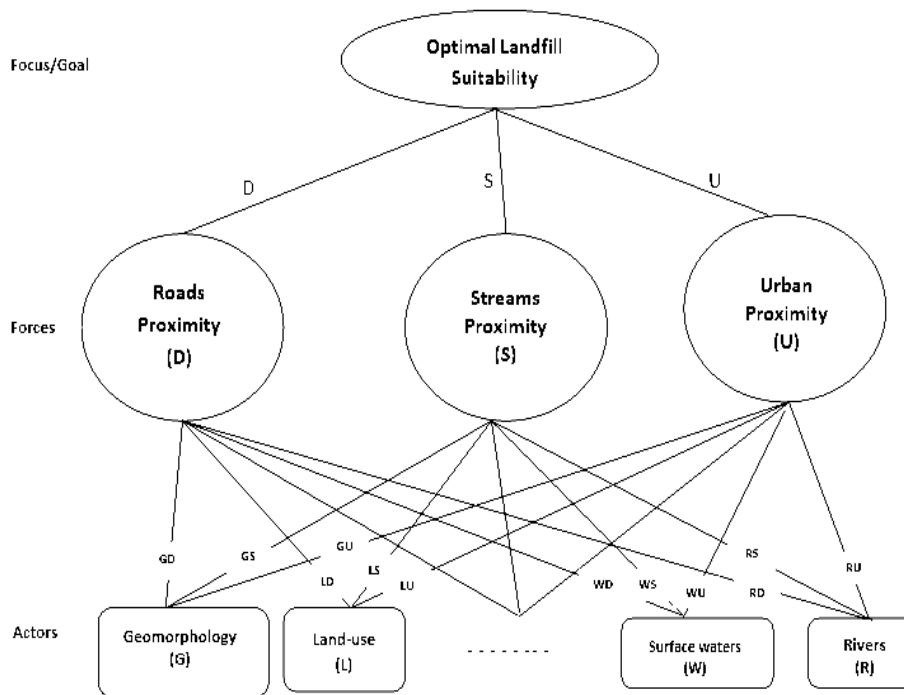


Fig. 7. AHP Hierarchical Structure of Ranking of all Factors (Saaty, 1980).

Factor Maps

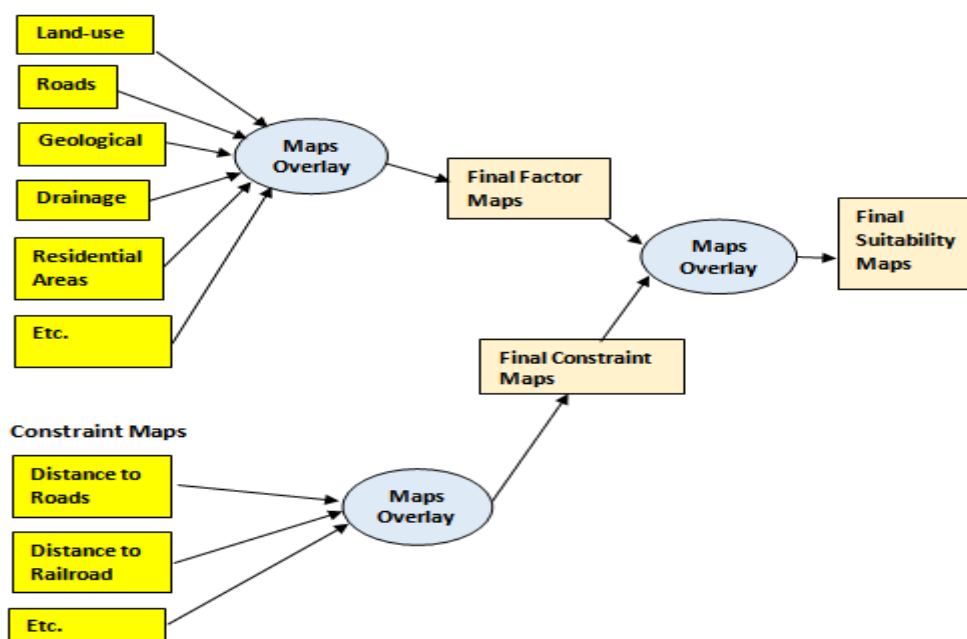


Fig. 8. Multi-criteria Evaluation (MCE) Model Flowchart.

IV. RESULTS GENERATION AND ANALYSIS

Results on creation of factor maps, eliminating unsuitable areas and selecting most suitable site are shown below:

4.1 Creation of Factor Maps

The AHP Pairwise Comparisons for the Biophysical factors' Scores for Geomorphology = 0.595; Depth of the underground water = 0.246; Wetland = 0.099 and Mangrove = 0.059. The Eigen Value (λ max.) i.e. Average = 4.192; CI = 0.064 and while Consistency Ratio = 0.071.

Similarly, the AHP Pairwise comparison for the Proximity Criteria Scores revealed that Stream Proximity (S) = 0.724; Urban Proximity (U) = 0.193; and Road Proximity (D) = 0.083. The Eigen Value (λ max.) i.e. Average = 3.066; CI = 0.033 and while Consistency Ratio = 0.057.

All the factors (geology, residential areas, forest and other vegetation, etc.) were used to create the factor maps:

- ☐ **Geological Criteria-** Geological map derived for the study area is shown in Figure 9a (Alluvium [Light Blue], Benin Formation [Yellow] and Ilaro Formation [Pink]).
 - ☐ **Wetlands-** Wetlands map of the study area is shown Figure 9b.
 - ☐ **Mangroves-** The areas classified as mangroves in the study area are shown Figure 9c.
 - ☐ **Drainage-** The drainage system of the study area is shown in Figure 9d.
 - ☐ **Surface Water-** Figure 9e shows the rivers network in the study area.
 - ☐ **Forests and other Vegetation-** The areas classified as forests and vegetation in the area are shown in Figure 9f.
 - ☐ **Slope-** Slope map shown in Figure 9g.
 - ☐ **Road Network Map-** Lagos road network map is shown in Figure 9h.
 - ☐ **Residential Areas-** The map of residential areas was derived from the land use map as shown in Figure 9i.
 - ☐ **Airports-** The location of the airport is shown in Figure 9j.
 - ☐ **Railroad Map-** Lagos railroad map (Fig. 9k) as obtained from the Dept. of Surveying & Geoinformatics.
- Some of these factor maps are shown in Figures 9a - 9k.

Some of the Biophysical factors:

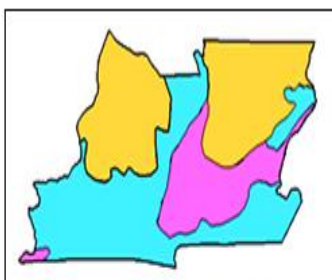


Fig. 9a. Geological map.

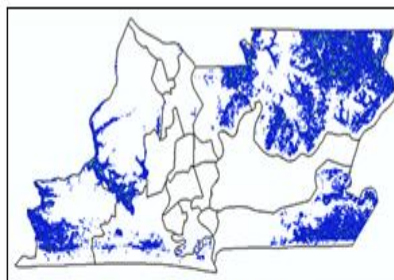


Fig. 9b. Wetlands.

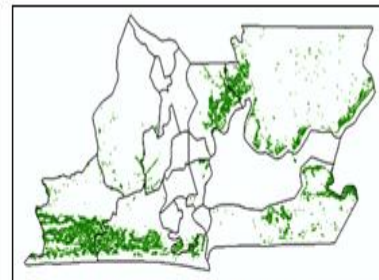


Fig. 9c. "Mangrooves".

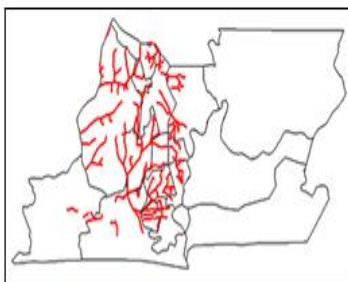


Fig. 9d. Drainage map.



Fig. 9e. Rivers.

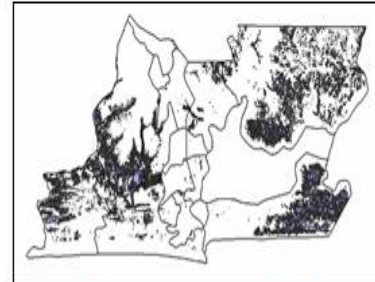


Fig. 9f. Forests and other Vegetation.

Some of the socio-economic factors:

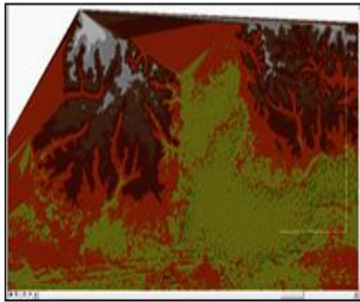


Fig. 9g. "Slope" Map

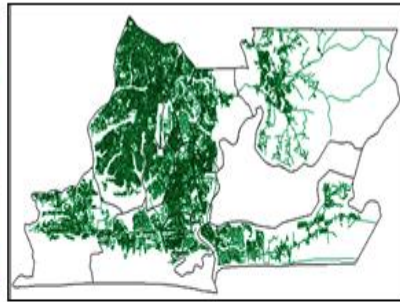


Fig. 9h. Road network

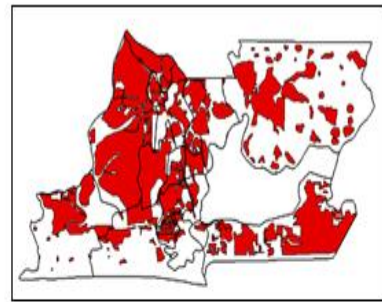


Fig. 9i. "Residential Areas".

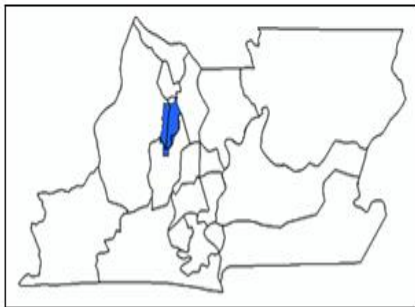


Fig. 9j. Airport.

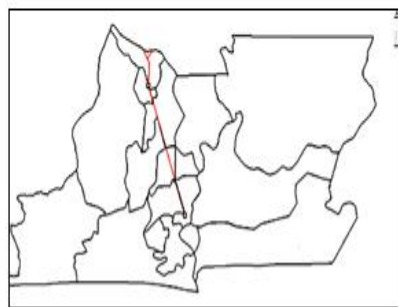


Fig. 9k. Railroad.

4.2 Analysis and Buffering

In the AHP Pairwise Comparisons for the Biophysical factors, Geomorphology was given highest priority (0.595), while Mangrove got the least rating of 0.059. Similarly, AHP Pairwise Comparisons for the Proximity Criteria; Stream Proximity (S) got the highest priority (0.724), while Road Proximity had the least 0.083. Analysing the Factor Maps, unsuitable areas were screened out by imposing exclusionary buffer criteria within the GIS environment thus leading to the creation of Buffer Maps. The analysis and the buffer maps are discussed below:

- ☒ **Wetlands and Mangroves-** Are not ideal for landfill locations since hazardous solutes from the landfill can easily endanger (i.e. pollute) nearby rivers and other water bodies, hence they are just factored out (Figure 10a).
- ☒ **Drainage-** Landfill must avoid areas with leachate flow contaminations. There is need to avoid the impact of drainage system failure. Therefore, a buffer distance of 100m from the drainage network was considered safe in this study (Fig. 10b).
- ☒ **Surface Water-** Surface water (rivers) is very important because of its ecological balance to all the human activities and as a natural resource. Rivers can be endangered by the landfill because of leachate thus bringing a great pollution to the river. A buffer distance of 100m from the river was considered for landfill location (Figure 10c).
- ☒ **Forests and other Vegetation-** Forests and other Vegetation areas are not suitable as landfill sites; hence they are just factored out.
- ☒ **Slope-** A low slope is required to minimize erosion and water runoff. A low slope also facilitates the construction of the site to be much easier and with lower costs. Furthermore, the slope map of Lagos Metropolis area was not utilized because based on the Lagos State Contour Map, almost all parts of the study area comprise low gradient that ranges from 9% to 15%.
- ☒ **Road Network Map-** Road network generally comprised of four main roads with the highest hierarchy being expressways and the lowest is local roads. This region has a good network system and access to landfills anywhere in this area is possible (Fig. 10d). For landfill siting, the suitable distance from road network is within 100m buffer in order to meet environmental requirement, property protection and pollution reduction). (Cointreau, 1996).
- ☒ **Residential Areas-** Locating a landfill away from urban land areas is noted for several reasons, including aesthetics, odor, noise, decrease in property value and health concerns. To define a limit around urban areas that would protect the population from landfill hazards (such as scavenging animals and strong odour) and using the NIMBY ("Not in my backyard") approach, a buffer of 500m is established (Fig. 10e). (Chang et al, 2007 and Dikshit et al., 2000).

☐ **Airports-** A landfill should not be situated around the regulatory zone of an airport authority. The site shall not be 3km nearer to the airport area. Therefore, a 3km buffer was used as a criterion for selecting suitable landfill site (Fig. 10f).

☐ **Railroad Map-** Since railroads and roads have similar transportation characteristics, therefore, to avoid any conflict with transportation along the rail system buffer distance of 100m was employed (Fig. 10g).

☐ **Geological Criteria-** Leachate migration from the landfill could be a potential source of surface and groundwater contaminations (Rugiramanzi, 2013). In Figure 9a, only 3 major soil types were identified (Alluvium [Light Blue], Benin Formation [Yellow] and Ilaro Formation [Pink]). The Ilaro formation is basically sedimentary formation found mostly under and around water bodies hence was classified as unfit. The remaining Alluvium and Benin formation consist mainly of clay, and clay can serve as a very good support due to its low permeability. The unsuitable geological area was factored out (Fig.11a).

Some are graphically shown in Figures 10a – 10g and 11a.

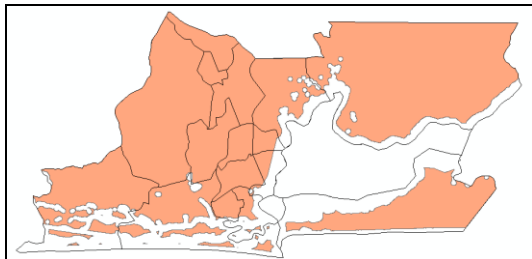


Fig. 10a. Unsuitable areas due to “Wetlands”.

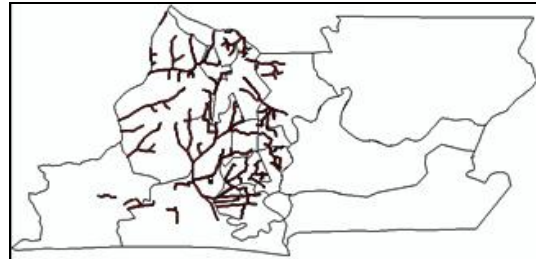


Fig. 10b. 100m buffer from the Drainage.

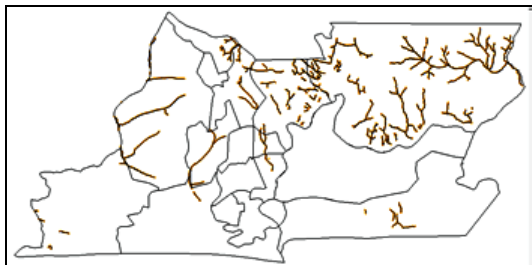


Fig. 10c. 100m buffer from the Rivers.

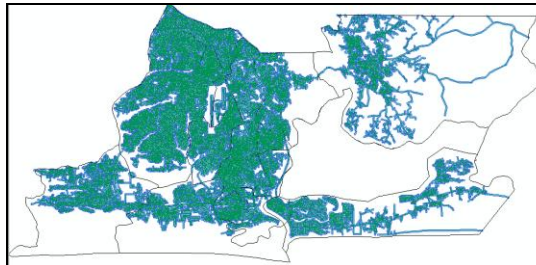


Fig. 10d. 100m buffers from the Roads.

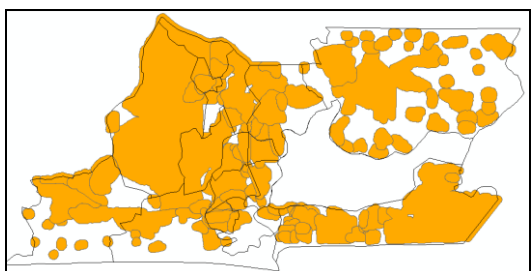


Fig. 10e. 500m buffers from the Residential Areas.

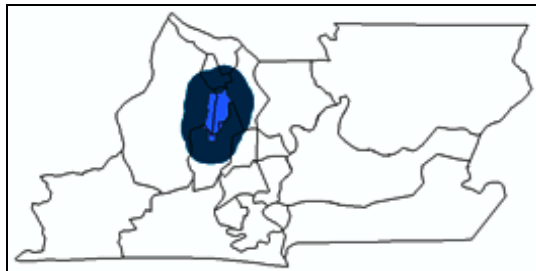


Fig. 10f. 3km buffer from the Airport.

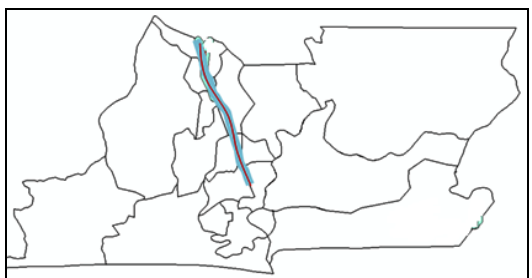


Fig. 10g. 100m buffer from the Railroad.

After applying the exclusionary criteria, decision factors, standardization of factors, and weighting of factors, using multi-criteria evaluation (MCE) for land suitability analysis, weighted linear combination (WLC) method, as discussed in Section 3.4, was adopted to obtain the final suitability map.

4.3 Optimal Landfill Location Determination through Objectivity

The factors, the buffers and the constraint maps were used in form of negative mapping. This was carried out by factoring out the constraints from the map of the study area until areas suitable and optimal for locating landfills are left (Mohammad, Kidokoro and Syed, 2009):

- [1] The map of the study area was subtracted from the map of the unsuitable Geology (Fig. 11a).
- [2] The resulting map (Fig. 11a) of suitable geology was overlaid on the map showing the water bodies with buffer distance, and negative mapping was also carried out to obtain a map showing areas not within the Water Bodies criteria and with suitable "Geology" (Fig. 11b).
- [1] The wetlands map is then overlaid on the resulting map (Fig. 11b) to obtain the areas suitable under the Wetlands criteria (Fig. 11c).
- [2] The mangrove map is overlaid on the resulting map (Fig. 11c) to obtain the areas suitable under the Mangroves criteria (Fig. 11d).
- [3] The rivers map is overlaid on the resulting map (Fig. 11d) to obtain the areas suitable under the Rivers criteria (Fig. 11e).
- [4] This procedure was repeated for other criteria to select areas suitable under the Vegetation, Residential Areas and Airports criteria (Fig. 11f).



Fig. 11a. Excluding unsuitable Geology



Fig. 11b. Excluding "Water bodies" but with suitable "Geology"

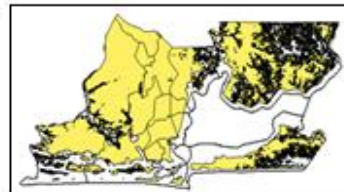


Fig. 11c. Excluding "Water bodies" and "Wetlands" but with suitable "Geology",

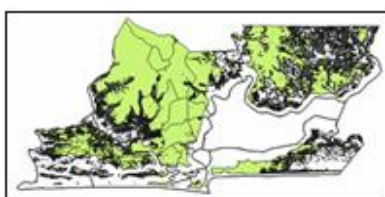


Fig. 11d. Excluding "Water Bodies", "Wetlands" and "Mangroves" but with suitable "Geology",

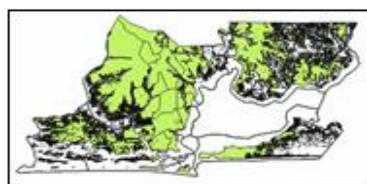


Fig. 11e. Excluding "Water Bodies", "Wetlands", "Mangroves", "Forests", and "Rivers" but with suitable "Geology",

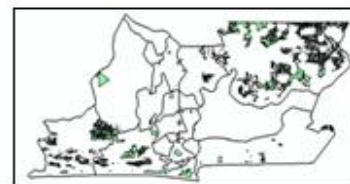


Fig. 11f. Excluding "Water bodies", "Wetlands", "Mangroves", "Forests", "Rivers", "Vegetation", "Residential Areas" and "Airports" but with suitable "Geology"

Finding the best suitable areas depends upon the objectives or goals of the land suitability analysis. In this study, transportation of wastes and potential sites' space availability (≥ 10 Hect.) were considered during land suitability analysis:

4.3.1 Transportation Scheduling and Routing Principle in Waste Management

No matter the methods of eliminating unsuitable areas, ranking suitable sites and selecting the most suitable landfill site, as mentioned in Section 3.3 a major determinant is the transportation costs. Therefore, the landfill site should be placed as close as possible to existing roads for saving road development, transportation, and collection costs. A "Planned Collection Route [PCR]", (Fig. 12), will ensure a productive and economical service. It will: (i) serve as map-based detailed route configurations and collection schedules for the selected collection system, and (ii) make citizens to be aware of the collection schedule (e.g. regular weekly schedule). Efficient routing and rerouting of solid waste collection vehicles will decrease labour, equipment and fuel costs, and increase customer satisfaction by making pick-up predictable. The size of each route must therefore depend on: all service points, all one-way streets, any culs-de-sac and areas that do not require a service. Since the amount of waste collected per stop depends on: distance between stops, loading time, traffic conditions and method of collection, therefore, the following rules for routing must be followed: (1) routes should not be

fragmented or overlapping; (2) the collection route should start as close to the garage or motor pool as possible taking into account heavily travelled and one-way streets; (4) collection from heavily travelled streets should not be carried out during rush hours; (5) collection routes should be planned to maximize vehicle capacities; and (6) for the convenience of householders it is preferable to maintain a regular routine, to ensure their waste is ready for collection (CSIR, 2014 and TALG, 2008). For the present waste disposal in Lagos; (1) there is no strictly designed collection schedule; (2) sometimes for two (2) weeks the collectors may not collect waste in some areas whereas the local cart pushers have been sent away from the roads by the State Government; (3) in the course of discharging their duties, the waste collectors always stay (block) the roads even during rush hours hindering other commuters rushing to work, claiming that nobody can arrest them because they are on “essential duty”; (4) sometimes when wastes are not collected bills are brought for payment; and (5) the collectors do litter the roads at the point of collection and the routes to the dumpsite. In this research, since the shortcomings mentioned above are still prevalent, to minimize transportation costs, a typical optimal route from the collection centre to the landfill site was created using “Shortest-Path” Algorithm (Fig. 13).

After all the factors have being erased from the base map of the area by negative mapping, criterion on proximity of the land fill site to roads was carried out. A 100m buffered road network map of Lagos Metropolis was overlaid on Figure 11f to determine which of the areas to be chosen as potential sites (Fig. 14).

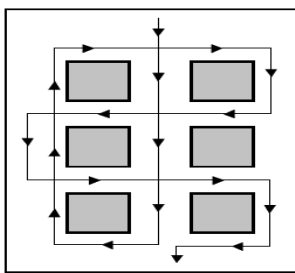


Fig. 12. PCR Collection Route from Two Sides of of the road (CSIR, saved 2014).

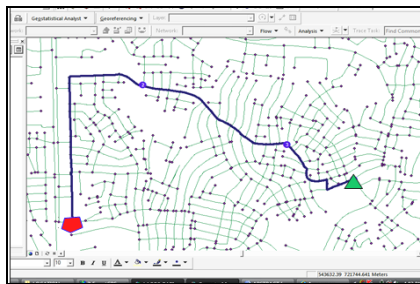


Fig. 13. A typical Waste Optimal Planned Collection Route (WOPCR).

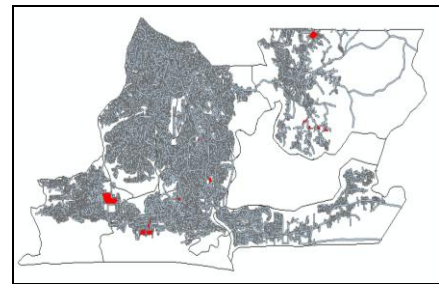


Fig. 14. Final Potential Sites meeting the 100m proximity to Roads criteria

4.3.2 Size of Land Space

The final suitability map was produced based on potential sites of which suitability ranges between 10–25hectares, in terms of land space. Three major locations were finally selected (Fig. 15).

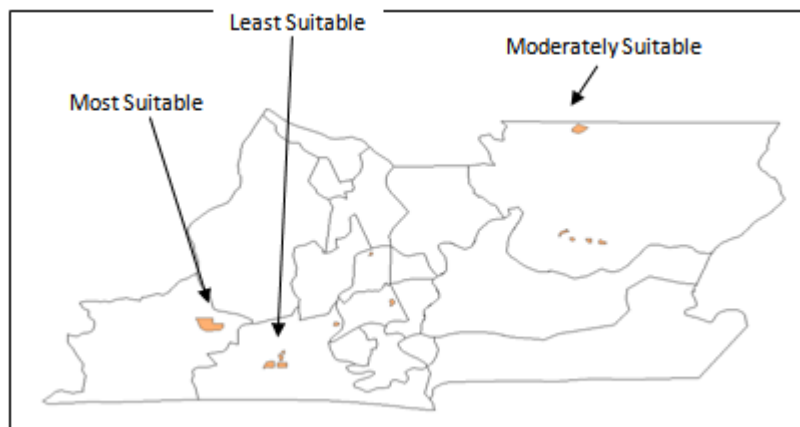


Fig. 15. Result of query showing potential areas meeting the 10-25 Hectares minimum area criteria. All other locations are “unsuitable”.

The final suitability map revealed four classifications: “unsuitable (96.0%)”, “least suitable (0.4%)”, “moderately suitable (1.0%)”, and “most suitable (2.6%)”.

V. CONCLUSION

Solid waste management is an obligatory function of the urban and local government authorities. However, a poorly sited landfill will result in health hazard and socio-economic and environmental degradations (Nwambuonwo and Mughele, 2012). In this study, the utilization of GIS, Remote Sensing and MCE in identifying suitable and optimal landfill locations in Lagos Metropolis was carried out. Highly suitable locations were determined based on predefined parameters, most especially space availability and transportation planned collection routes (PCR). The selected locations will minimize social conflict, environmental and economic impacts. With the fourteen factors considered, the final suitability map revealed four classifications with most part of the study area “unsuitable” for landfilling. Therefore, with increasing annual growth in urban population and the rapid pace of urbanization in Lagos Metropolis, the existing deficiencies related to solid waste management (SWM); such as use of inefficient tools by contractors, non-punctuality of contractors, creating congestion during peak traffic periods and inadequate transportation of wastes; need to be quickly addressed. Rules governing transportation scheduling and routing in waste management must facilitate safety, ease and speed of collection. Clear government policies and competent bureaucracies for management of solid wastes are needed urgently to resolve these deficiencies.

REFERENCES

- [1] Chang, N.B.; Parvathinathan, G. and Breeden, J.B. (2007). Combining GIS with fuzzy multicriteria decision-making for landfill siting in a fast-growing urban region. *J. Environ. Manage.* <http://dx.doi.org/10.1016/j.jenvman.2007.01.011>
- [2] Cointreau, S (2004) Sanitary Landfill Design and Siting Criteria, Guidance Published in May 1996 by the World Bank as an Urban Infrastructure Note.
- [3] Dikshit, A. K., Padmavathi, T., & Das, R. K. (2000). Locating Potential Landfill Sites Using Geographic Information Systems. *Journal of Environmental Systems*, 28(1), 43-54.
- [4] Dorhofer, G., & Siebert, H. (1996). The search for landfill sites--Requirements and implementation in Lower Saxony, Germany. *Environmental Geology*, 35(1), 55-65.
- [5] Erkut, E., & Moran, S. R. (1991). Locating obnoxious facilities in the public sector: An application of the hierarchy process to municipal landfill siting decisions. *Socio-Economic Planning Sciences*, 25(2), 89-102.
- [6] Hala A. Effat & Mohamed N. Hegazy. Mapping potential landfill sites for North Sinai cities using spatial multicriteria evaluation. *The Egyptian Journal of Remote Sensing and Space Sciences* (2012) 15, 125–133.
- [7] Kao, J. J., & Lin, H. (1996). Multifactor spatial analysis for landfill siting. *Journal of Environmental Engineering*, 122(10), 902-908.
- [8] Lagos State Waste Management Authority` (LAWMA), 1998. An official Report on tonnage of different type of waste collected and disposed between 1988-1999 by LAWMA, Lagos State, Nigeria.
- [9] Lagos Travel Guide, 2014. Available at: <http://www.world66.com/africa/nigeria/lagos> (Downloaded on 29/05/2014).
- [10] Longe E.O. and Balogun M.R. (2010) Groundwater Quality Assessment near a Municipal Landfill, Lagos, Nigeria. *Research Journal of Applied Sciences, Engineering and Technology* 2(1): 39-44, 2010. ISSN: 2040- 7467. © Maxwell Scientific Organization, 2009.
- [11] Mendoza, G.A. 1997. Introduction to Analytic Hierarchy Process, Theory and Applications to Natural Resource Management, 1997 ACSM / ASPRS Annual Convention & Exposition Technical papers, Seattle. Washington, pp. 130-139.
- [12] Mohammad R. H., Kidokoro, T. and Syed A. I. (2009). “Landfill demand and allocation for municipal solid waste disposal in Dhaka city—an assessment in a GIS environment”. *Journal of Civil Engineering (IEB)*, 37 (2) (2009) 133-149.
- [13] New York State Department of Environmental Conservation (2010). What is Solid Waste. Available at: <http://www.dec.ny.gov/chemical/8732.html>
- [14] Nwambuonwo, O. Jude & Mughele, E S. (2012). Using Geographic Information System to Select Suitable Landfill Sites for Megacities (Case Study of Lagos, Nigeria). *Computing, Information Systems & Development Informatics* Vol. 3 No. 4, September, 2012.
- [15] Oyekan, J. A. (1988), “Benthic Macrofauna Communities of Lagos Lagoon, Nigeria, *Nigerian Journal of Science*, No. 21, 45-51.
- [16] Rugiramanzi Fidele (2013). Landfill sites selection for municipal solid waste using multi criteria evaluation techniques. Case of Rusizi town, Rwanda. National university of Rwanda- Post Graduate Diploma in Applied Geo-Information Science 2013.
- [17] Saaty, T. L. (1980). *The Analytic Hierarchy Process*. New York: McGraw-Hill Inc.
- [18] Siddiqui, M.Z., Everett, J.W. & Vieux, B.E. 1996. Landfill siting using geographic information systems: a demonstration. *Journal of Environmental Engineering*, 122(6): 515-523.
- [19] Tchobanoglous, G., & Kreith, F. (2002). *Handbook of Solid Waste Management*. New York: McGraw-Hill.
- [20] The Council of Scientific & Industrial Research- CSIR (saved 2014). “Solid waste management: Chapter 11”. *GUIDELINES FOR HUMAN SETTLEMENT PLANNING AND DESIGN* by CSIR. Available at: http://www.csir.co.za/Built_environment/RedBook/Vol_II/Chapter_011/Chapter_011_Vol_II.pdf; downloaded: 07/02/2014.
- [21] Transparent Accountable Local Governance- TALG (2008). “Solid Waste Collection and Transport Service Delivery Training Module 1 of 4”, Transparent Accountable Local Governance (TALG) Program by The Asia Foundation (TAF) funded by USAID.
- [22] Yesilnacar, M. and Cetin, H. 2005. Site selection for hazardous wastes: A case study from the GAP area, Turkey, *Engineering Geology*, 81, 371-388.

A Combined Approach for Intrusion Detection System Based on the Data Mining Techniques.

Pragya Diwan¹, Dr. R.C Jain²

¹Research Scholar, Department of Information Technology, SATI Vidisha (M.P.),

²Director, SATI Vidisha (M.P.)

Abstract:

All most all existing intrusion detection systems focus on low-level attacks, and only generate isolated alerts. They can't find logical relations among alerts. In addition, IDS's accuracy is low; a lot of alerts are false alerts. To reduce this problem we propose a hybrid approach which is the combination of K-Medoids clustering and Naïve-Bayes classification. The proposed approach will be clustering all data into the corresponding group before applying a classifier for classification purpose. The proposed work will explore Naïve-Bayes Classification and K-medoid methods for intrusion detection and how it will be useful for IDS. The reasons for introducing Naïve Bayes Classification are the involvement of many features where there is no division between normal operations and anomalies. Thus Naïve Bayes Classification can be mined to find the abstract correlation among different security features. In this, we will present implementation results on existing intrusion detection system and K-medoid cluster technique with Naïve Bayes classification for intrusion detection system. An experiment is carried out to evaluate the performance of the proposed approach using our own created dataset. Result show that the proposed approach performed better in term of accuracy, detection rate with reasonable false alarm rate.

Keywords: Association analysis, Database Protocol, Database, Data preprocessing, Data mining, Internet, Intrusion detection.

I. INTRODUCTION

Information security technology is an essential component for protecting public and private computing infrastructures. With the widespread utilization of information technology applications, organizations are becoming more aware of the security threats to their resources. No matter how strict the security policies and mechanisms are, more organizations are becoming susceptible to a wide range of security breaches against their electronic resources. Network-intrusion detection is an essential defense mechanism against security threats, which have been increasing in rate lately. It is defined as a special form of cyber threat analysis to identify malicious actions that could affect the integrity, confidentiality, and availability of information resources. Data mining-based intrusion-detection mechanisms are extremely useful in discovering security breaches.

II. INTRUSION DETECTION SYSTEM

An intrusion detection system (IDS) is a component of the computer and information security framework. Its main goal is to differentiate between normal activities of the system and behavior that can be classified as suspicious or intrusive [1]. IDS's are needed because of the large number of incidents reported increases every year and the attack techniques are always improving. IDS approaches can be divided into two main categories: misuse or anomaly detection [1]. The misuse detection approach assumes that an intrusion can be detected by matching the current activity with a set of intrusive patterns. Examples of misuse detection include expert systems, keystroke monitoring, and state transition analysis. Anomaly detection systems assume that an intrusion should deviate the system behaviour from its normal pattern. This approach can be implemented using statistical methods, neural networks, predictive pattern generation and association rules among others techniques. In this research using naïve byes classification with clustering data mining techniques to extract patterns that represent normal behavior for intrusion detection. This research is describing a variety of modifications that will have made to the data mining algorithms in order to improve accuracy and efficiency. Using sets of naïve byes classification rules that are mined from network audit data as models of "normal behavior." To detect anomalous behavior, it will generate Naïve Byes classification probability with clustering followed from new audit data and compute the similarity with sets mined from "normal" data. If the similarity values are below a threshold value it will show abnormality or normality.

2.1 Types of Intrusion Detection System

2.1.1 Network intrusion detection systems (NIDS):

Monitors packets on the network wire and attempts to discover an intruder by matching the attack pattern to a database of known attack patterns. A typical example is looking for a large number of TCP connection requests (SYN) to many different ports on a target machine, thus discovering if someone is attempting a TCP port scan. A network intrusion detection system sniffs network traffic, by promiscuously watching all network traffic.

2.1.2 Host based intrusion detection system (HIDS):

A host based intrusion detection system does not monitor the network traffic; rather it monitors what's happening on the actual target machines. It does this by monitoring security event logs or checking for changes to the system, for example changes to critical system files or to the systems registry. Host based intrusion detection systems can be split up into:

- **System integrity checkers:** Monitors system files & system registry for changes made by intruders (thereby leaving behind a backdoor). There are a number of File/System integrity checkers, such as "Tripwire" or "LAN guard File Integrity Checker".
- **Log file monitors:** Monitor log files generated by computer systems. Windows NT/2000 & XP systems generate security events about critical security issues happening on the machine. (for example a user acquires root/administrator level privileges) By retrieving & analyzing these security events one can detect intruders .

2.2 Types of attack on IDS

- **Information gathering:**
 1. Network mapping - ping sweeps.
 2. DNS zone transfers.
 3. E-mail recons.
 4. TCP or UDP port scans - Enumeration of services indexing of public web servers to find web server and CGI holes.
 5. OS fingerprinting.
- **Exploits:**

Attackers make use of vulnerabilities in target servers or misconfiguration on the system/network.
- **Denial-of-service (DoS) attacks:**

An attempt to break the system and make it inaccessible to other users. Intruders will attempt to crash a service or machine, overload network or hardware resources, such as overload the links, the CPU, or fill up the disk.

III. DATA MINING

Data mining (DM), also called Knowledge-Discovery and Data Mining, is one of the hot topic in the field of knowledge extraction from database. Data mining is used to automatically learn patterns from large quantities of data. Mining can efficiently discover useful and interesting rules from large collection of data. It is a fairly recent topic in computer science but utilizes many older computational techniques from statistics, information retrieval, machine learning and pattern recognition. Data mining is disciplines works to finds the major relations between collections of data and enables to discover a new and anomalies behavior. Data mining based intrusion detection techniques generally fall into one of two categories; misuse detection and anomaly detection. In misuse detection, each instance in a data set is labeled as 'normal' or 'intrusion' and a learning algorithm is trained over the labeled data. These techniques are able to automatically retrain intrusion detection models on different input data that include new types of attacks, as long as they have been labeled appropriately. Data mining are used in different field such as marketing, financial affairs and business organizations in general and proof it is success. The main approaches of data mining that are used including classification which maps a data item into one of several predefined categories. This approach normally output "classifiers" has ability to classify new data in the future, for example, in the form of decision trees or rules. An ideal application in intrusion detection will be together sufficient "normal" and "abnormal" audit data for a user or a program. The second important approach is clustering which maps data items into groups according to similarity or distance between them. Anomaly detection techniques thus identify new types of intrusions as deviations from normal usage. In statistics based outlier detection techniques the data points are modeled using a stochastic distribution and points are determined to be outliers depending upon their relationship with this model. However, with increasing dimensionality, it becomes increasingly difficult and in-accurate to estimate the multidimensional distributions of the data points [1]. However, recent outlier detection algorithms that we utilize in this study are based on computing the full dimensional distances of the points from one another as well as on computing the densities of local neighborhoods [6].

IV. PROPOSED CONCEPT

Data mining techniques have been successfully applied in many different fields including marketing, manufacturing, process control, fraud detection, and network management. Over the past five years, a growing number of research techniques have applied data mining to various problems in intrusion detection. In this will apply to data mining for anomaly detection field of intrusion detection. Presently, it is unfeasible for several computer systems to affirm security to network intrusions with computers increasingly getting connected to public accessible networks (e.g., the Internet). In view of the fact that there is no ideal solution to avoid intrusions from event, it is very significant to detect them at the initial moment of happening and take necessary actions for reducing the likely damage. One approach to handle suspicious behaviors inside a network is an intrusion detection system (IDS). For intrusion detection, a wide variety of techniques have been applied specifically, data mining techniques, artificial intelligence technique and soft computing techniques. Most of the data mining techniques like association rule mining, clustering and classification have been applied on intrusion detection, where classification and pattern mining is an important technique. Similar way, AI techniques such as decision trees, neural networks and fuzzy logic are applied for detecting suspicious activities in a network, in which fuzzy based system provides significant advantages over other AI techniques. This system is anomaly-based intrusion detection makes use of effective rules identified in accordance with the designed strategy, which is obtained by mining the data effectively.

The proposed concept is using data mining techniques. Data mining techniques have been successfully applied in many different fields including marketing, manufacturing, process control, fraud detection, and network management. Over the past five years, a growing number of research techniques have applied data mining to various problems in intrusion detection. In this K-medoids data mining technique has applied for anomaly detection field of intrusion detection.

Whole proposed IDS divided into following module:

1. Database Creation (Suggested Technique)
 - Selecting and generating the data source
 - Data scope transformation and pre-processing
2. Data mining Techniques
 - K-Means Cluster Technique
 - K-Medoids Cluster Technique
3. Naïve Bayes Classification
 - Naïve Bayes Classification with K-Means Cluster Technique
 - Naïve Bayes Classification with K-Medoids Cluster Technique
4. Performance
 - Time Analysis
 - Memory Analysis
 - CUP Analysis
 - Cluster Analysis
 - Probability Analysis of Normality and Abnormality

Database Creation (Suggested Technique):

Selecting and generating the data source:

First the acquisition of data will do. In the case of this research, Sample datasets from DATA- BASE will use. The DATABASE contained high volume network traffic data, and a subset of data ranging a period of 2 – 5 days will be select.

Data scope transformation and pre-processing: For the purpose of the research, the scope of the data was limited to TCP/IP packets. Only six intrinsic features were extracted from each packet within the dataset. These were timestamp, Source IP, Source Port, Destination IP, Destination Port, and Service. The table 4.1 below shows the scope of the input dataset.

Flags	Source	Destination
TCP Port Number	Source TCP Port	Destination Port Number
IP Address	Source IP Address	Destination IP Address
Timestamp		
Services		

Table 4.1: TCP packet frame format

For the purpose of reporting for this research the data was extracted from the DATABASE set using any data base tools. Because there are several data extraction tools are available in Public Domain. This extracted the necessary features and saved the data within the dataset. Once the data was loaded into the pre-processor, it was prepared for use by the Data Mining approach.

Data Mining Technique

Anomaly learning approaches are able to detect attacks with high accuracy and to achieve high detection rates. However, the rate of false alarm using anomaly approach is equally high. In order to maintain the high accuracy and detection rate while at the same time to lower down the false alarm rate, the proposed a combination of two learning techniques. For the first stage in the proposed technique, this grouped similar data instances based on their behaviors by utilizing a K-Mediod clustering as a pre-classification component. Next, using Naïve Bayes classifier this classified the resulting clusters into attack classes as a final classification task. This found that data that has been misclassified during the earlier stage may be correctly classified in the subsequent classification stage.

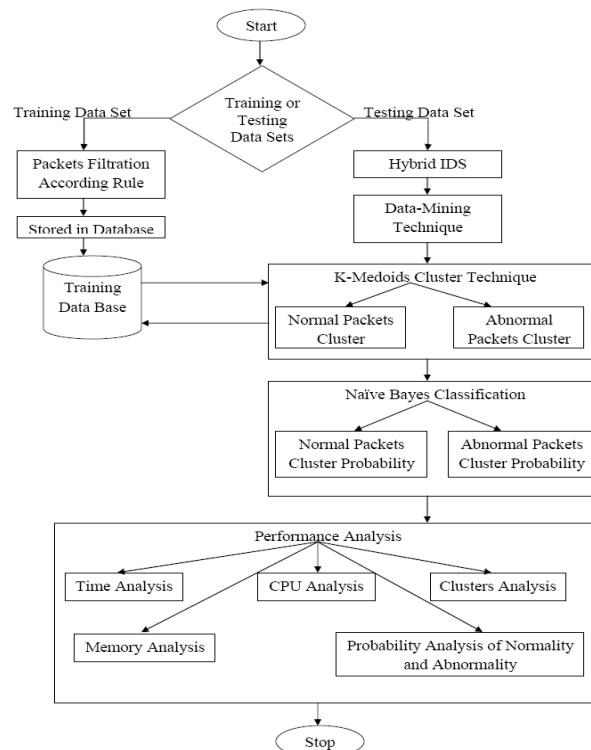


Figure 4.1. Flow Chart of the Proposed IDS

K-Medoids Cluster Technique: Network intrusion class labels are divided into four main classes, which are DoS, Probe, U2R, and R2L [1-2]. The main goal to utilize K-Mediod clustering approach is to split and to group data into normal and abnormal. K-medoids clustering are sometimes used, where representative objects called medoids are considered instead of centroids. Because it uses the most centrally located object in a cluster, it is less sensitive to outliers compared with the K-means clustering. Suppose that we have n objects having p variables that will be classified into k ($k < n$) clusters (Assume that is given). Let us define j^{th} variable of object i as X_{ij} ($i = 1 \dots n, j = 1 \dots p$). The proposed algorithm is composed of the following three steps:

The K-mediods algorithm is composed of the following three steps.

Step 1 : (Select initial medoids)

1.1. Using Euclidean distance as a dissimilarity measure, compute the distance between every pair of

$$d_{ij} = \sqrt{\sum_{a=1}^p (X_{ia} - X_{ja})^2} \quad i = 1, \dots, n; j = 1, \dots, n \tag{1}$$

1.2. Calculate P_{ij} to make an initial guess at the centers of the clusters.

$$P_{ij} = \frac{d_{ij}}{\sum_{l=1}^n d_{il}} \quad i = 1, \dots, n; j = 1, \dots, n \tag{2}$$

- 1.3 Calculate $\sum_{i=1}^n p_{ij}$ ($j = 1, \dots, n$) at each objects and sort them in ascending order. Selected objects having the minimum value as initial group medoids.
- 1.4. Assign each object to the nearest medoid.
- 1.5. Calculate the current optimal value, the sum of distance from all objects to their medoids.

Step 2: (Find new medoids)

Replace the current medoid in each cluster by the object which minimizes the total distance to other objects in its cluster.

Step 3: (New assignment)

- 3.1. Assign each object to the nearest new medoid.
- 3.2. Calculate new optimal value, the sum of distance from all objects to their new medoids. If the optimal value is equal to the previous one, then stop the algorithm. Otherwise, go back to the Step 2.
- The above algorithm runs just like K-means clustering and so this will be called as 'K-means-like' algorithm. The performance of the algorithm may vary according to the method of selecting the initial medoids.

V. CONCLUSION & FUTURE WORK

The proposed research have improved detecting speed and accuracy which is the prime concern of the proposed work, and presents more efficient associate and cluster rules mining method to abnormal detecting experiment based on network. Presented Approach is a hybrid approach which is the combination of K-Mediod clustering and Naïve Bayes classifier. The proposed approach was compared and evaluated using own prepared dataset. Considering the dependent relations between alerts, it proposed an improved cluster Algorithm with naive bayes classification; this hybrid approach can find more accurate probability of normal and abnormal packets. It is applied to find the probability of an attack. Compared with other method, proposed method can find the probability from the training data as well as testing data with high efficiency. Usually when an attack performed, it is very possible that there exist attack cluster transitions. Based on this it use the cluster sequences to filter false alarms generated by IDS, experimental results proved this method is effective and feasible. We have discussed some observations in a critical manner, which has led us to the following recommendations for further research:

Future research should pay closer attention to the data mining process. Either more work should address the (semi-automatic) generation of high-quality labeled training data, or the existence of such data should no longer be assumed. Future research should explore novel applications of data mining that do not fall into the categories feature selection and anomaly detection. To deal with some of the general challenges in data mining, it might be best to develop special-purpose solutions that are tailored to intrusion detection.

References

- [1] Wang Pu and Wang Jun-qing "Intrusion Detection System with the Data Mining Technologies" IEEE 2011.
- [2] Z. Muda, W. Yassin, M.N. Sulaiman and N.I. Udzir "Intrusion Detection based on K-Means Clustering and Naïve Bayes Classification" 7th IEEE International Conference on IT in Asia (CITA) 2011.
- [3] Ma Yanchun "The Intrusion Detection System Based on Fuzzy Association Rules Mining" IEEE Conferences 2010.
- [4] Lei Li, De-Zhang Yang, Fang-Cheng Shen "A Novel Rule-based Intrusion Detection System Using Data Mining" IEEE Conferences 2010.
- [5] Chunyu Miao and Wei Chen "A Study of Intrusion Detection System Based on Data Mining" IEEE Conferences 2010.
- [6] Ye Changguo, Wei Nianzhong, Wang Tailei, Zhang Qin and Zhu Xiaorong "The Research on the Application of Association Rules Mining Algorithm in Network Intrusion Detection" IEEE Conferences 2009.
- [7] Changxin Song, Ke Ma "Design of Intrusion Detection System Based on Data Mining Algorithm" 2009 IEEE International Conference on Signal Processing Systems.

Modelling and Prediction of Water Level for a Coastal Zone Using Artificial Neural Networks

Badejo, Olusegun Temitope¹, Udoudo, Daniel¹
Department of Surveying and Geoinformatics, University of Lagos, Nigeria

ABSTRACT

Research on Modern Coastal Water level modeling and prediction techniques has attracted growing concern in recent years. The reason for this is not far-fetched, as water continues to be the major contributor to disposal and movement of sediments, tracers and pollutants. This research work presents one of the most potent methods of coastal water level prediction using Artificial Neural Networks (ANNs). The ANNs model provides the prediction by learning the characteristic pattern of the historical event or in our case historical data. Back Propagation (BP) is the most popular supervised learning technique of ANNs. In back-propagation networks, the weights of the connections are adjusted to minimize the measure of the difference between the actual output vector of the network and the desired output vector. The BP technique with feed forward architecture and optimized training algorithm known as Levenberg-Marquardt was used in this work to develop a Neural Network Water Level Prediction model-(NNWLM) in a MatLab programming environment. The model was tested with data from five coastal water level gauge stations. The result revealed great performance with model prediction accuracy ranging from 0.012 to 0.045 in terms of Mean Square Error (MSE) and 0.82 to 0.97 in terms of correlation coefficient (R-value). With this high performance, the NNWLM developed in this work can be deemed as a veritable tool for a wide variety of coastal engineering and development, covering sediment management program: dredging, sand bypassing, breach-contingency plans, and protection of beaches vulnerable to storm erosion and monitoring and prediction of long-term water level variations in the coastal inlets.

Keywords: Modelling, Prediction, Tide, Coastal Zone, Neural Networks, Analysis, Sigmoid function

I. INTRODUCTION

The coast can be thought of as an area of interaction between the land and the ocean. It is the band of dry land and adjacent ocean space (water and submerged land) in which terrestrial processes and land uses directly affect oceanic processes and uses, and vice versa. Coastal zones are defined by the extent of territorial waters up to the high water mark. Generally the world's coastal zones are long narrow features of mainland, islands and seas. Coastal zones include the entire continental shelf and occupy about 18% of the surface of the globe, supplying about 90% of global fish catch and accounts for some 25% of global primary productivity while at the same time being some of the most endangered regions on the planet.

1.1 Importance of the Coastal Zone

The coastal zone is of great importance historically for human populations. Two-thirds of the world's cities occur on the coast. Valuable resources such as fish and minerals are considered to be common property and are in high demand for coastal dwellers for subsistence use, recreation and economic development.

Integrated coastal zone management protects habitats, i.e. wetlands, coral reefs and their water quality and also prevents the loss of life, while for others it provides a means of public access to coastal areas (which sometimes causes conflicts with private bodies)

The significance of monitoring and managing the coast has far reaching significance in many areas of human endeavour, some of which include:

- Protection of Coastal and low lying regions' residents.
- Monitoring and prediction of changes in complex marine ecosystems, harvest estimation for the fishery
- Planning and constructing of coastal and offshore structures,
- Development and implementation of ocean-based alternative energy technologies.

1.2 Water Level Observations

Water level observation started in Lagos during the colonial rule and was done primarily for water navigation especially for commercial shipping activities. The need for water level monitoring has increased over the years. Water level monitoring is among other things useful for oil and gas exploration and exploitation activities, and construction of ports and harbour works. Water level observations are carried out with the aid of tide gauges. Water level observations can be made with either automatic or manual tide gauges. An automatic tide gauge records the water level, mechanically or digitally, in a continuous manner without the need for a human observer to physically monitor the water level. These types of tide gauges are more expensive but produce more reliable results. There are now water level recorders, which use the time of flight of a pulse of radar, rather than sound, to measure level. Water level measurements are made to meet the needs of mariners, engineers, resource managers, researchers, and the general public. Some of the most important purposes for which they are measured are for the mariners to estimate draft under keel while in transit, data and datum reference for storm surge monitoring, data for production of tide and tidal current predictions, data for estuarine studies and numerical hydrodynamic models, for determination of mean sea level, for dredging and sand mining operations, for laying of underwater oil and gas pipelines and communication cables, for determination of tidal datum and for surveying and engineering purposes. Information on the variation of the coastal water levels in maintenance and capital dredging which are required in long-term regional sediment management program. It is apparent that continuous collection, analysis of tidal data is important for the integrated management of the Nigeria Coastal areas. Water level components are generally important for numerical model calibration (Wegde, 2006) and as such data recovery and prediction for extending measurement data is absolutely necessary. Due to the need for a period of 18.6 years measurement for an ideal water level prediction Forrester (1983) and Ghosh (1998) saw the need for alternative methods of water level prediction to save time, labour and cost. One of such methods is the subject matter of this paper.

1.3 Tidal Harmonic Analysis

The traditional method of water level prediction involves tidal harmonic analysis of tidal data covering a period of time ranging from 29 days to 18.6 years. Many authors have made significant contributions to tidal analysis and predictions, and several algorithms of tidal harmonic analysis have been proposed by Munk and Cartwright (1966), Doodson (1941), Godin (1972), Zetler and Cartwright (1979) and Schwiderski (1980), Greenberg, (1977), Stravisi (1983).

The traditional method is accurate but has the following disadvantages:

- i. More than 18.6 years of data are needed to resolve the modulation of the lunar tides.
- ii. Amplitude accuracy of 10^{-3} of the largest term requires that at least 39 frequencies be determined. Several researches that not less than 400 frequencies are needed for an amplitude accuracy of 10^{-4} of the largest term.
- iii. Non-tidal variability introduces large errors into the calculated amplitudes and phases of the weaker tidal constituents. The weaker tides have amplitudes smaller than variability at the same frequency due to other processes such as wind set up and currents near the tide gauge.
- iv. At many ports, the tide is non-linear, and many more tidal constituents are needed. For some ports, the number of frequencies is unmanageable. When tides propagate into very shallow water, especially river estuaries, they steepened and become non-linear. This generates harmonics of the original frequencies.

II. ARTIFICIAL NEURAL NETWORKS

This paper presents a veritable approach to water levels prediction using Artificial Neural Networks (ANNs). ANNs have been widely used in multivariate nonlinear time series modelling in many research areas such as electronics, aerospace, and manufacturing engineering.

Some of the merits of the ANN include:

- i. Capability of directly correlating the time series of multiple input variables to the output variables through the interconnected nodes using trainable weights and bias signal Hagan (1995).
- ii. Ability to achieving non-parametric (or semi-parametric) regression. They share the advantage of the curve-fitting approach: once their internal parameters have been set to appropriate values, they are able to interpolate (and in some cases extrapolate) to values that were not used in setting their parameters.

However, unlike the curve-fitting approach, ANNs are not limited by the choice of any particular mathematical function. A single ANN may therefore be used as a generic prediction tool across a wide range of Coastal data with varied sea-conditions.

ANNs are used to identify unknown multivariate functions from samples of data. This work is particularly concerned with the difference between local transfer functions that only have significant outputs across a small volume of input space and more diffuse transfer functions. Apart from the method used to train artificial neural networks (ANNs), ANNs may be differentiated in many ways.

The following perspectives give alternative ways of classifying ANNs, although the different perspectives are intertwined in complex ways:

- Choice of transfer function
- Selection of assessment function Maier and Dandy (2000).
- Choice of network architecture Maier and Dandy (2000).

2.1 Classifications of ANNs

ANNs can be classified into three main classes: pattern association, pattern recognition and function approximation.

2.1.1 Pattern Association

A neural network may be trained to act as an 'associative memory'. The process of training stores a set of patterns (vectors), which may be retrieved from the network.

2.1.2 Pattern Recognition

During pattern recognition, an ANN is required to identify the class to which an input pattern belongs. This model is analogous to processes within the human brain, such as the process by which we identify familiar objects despite variation in viewing angle, lighting conditions and other distortions to our visual inputs (Ullman, 1996). There are two ways in which the classification may be performed, i.e. unsupervised learning and the supervised learning.

2.1.3 Function Approximation

Within function approximation, tasks may be divided into modeling and forecasting. In the latter, time series data is available and the aim is to predict future data from past data. The main application investigated within this thesis, water level modeling and prediction, comes into the category of modeling and forecasting.

2.2 Initial Research in ANNs

Hebb (1949) noted that the strength of a synaptic connection is increased if the neurons on either side of the connection are activated synchronously. Later authors Sejnowski (1977) added the converse rule that the connection strength is decreased if the neurons on either side of the synapse fire asynchronously. Widrow and Hoff (1960) introduced a new training rule, i.e. 'least squares rule', and used it to train an ANN they called an adaptive linear element, or 'ADALINE'. The Hopfield network introduced in 1982 is a recurrent network. It contains a single layer of neurons and the output of each neuron is fed back into the ANN as an input to all of the other neurons. Rumelhart and McClelland (1986) presented a training algorithm that would allow the use of one or more hidden layers of neurons and a variety of transfer functions. The only condition was that the transfer function was differentiable, i.e. one could calculate a gradient for the function at all points. This rule out stepwise functions and led to the use of more sophisticated transfer functions. Hybrid neural networks, containing both sigmoidal and radial basis transfer functions in the same layer, have been suggested by Poggio and Girosi (1989).

2.3 Network Design

A number of authors have considered design issues in the context of ANN use for freshwater studies. Some of these authors are Maier et al. (2000). The network design issues fall into the following categories:

- Performance criteria
- Data pre-processing
- Choice of inputs
- Determination of network architecture
- Choice of training algorithm
- Stopping and validation criteria

2.4 Mathematical Approaches in Neural Networks

The mathematical approaches in ANNs include:

- i. Transfer of functions commonly used by neural networks.
- ii. Identification of algorithms and equations used to perform gradient descent optimisation, including back-propagation (BP) and several improvements to the basic BP.

2.5 Coastal Applications of ANNs

Maseet *al* (1995) predicted the stability of rubble-mound breakwaters using structural parameters, such as a permeability parameter, as well as sea-state information including water depth and wave steepness. Deo and Sridhar Naidu (1999) used previous wave heights to predict their future values. Overall, research on coastal applications has been more varied than that on freshwater applications. There have been more attempts to predict dependent variables from independent variables, rather than using time-series data, authors have been more adventurous in their choice of network architecture. Due to the paucity of research in this area however, a consensus has yet to appear on the most effective architectures and training algorithms.

III. METHODOLOGY

A Neural Networks for Coastal Water Level Modelling and Prediction was developed in this work. The modelling work covers creation of a sizeable Neural Networks Architecture with the aid of sensitivity test on number of neuron that would be devoid of outrageous result. A feed- forward method with a back-propagation algorithm and associated network training optimization technique known as Levenberg-Marquart optimization technique was deployed. The application was limited to some select water gauge stations for testing and validation of the model. Nonetheless, the model is built for regional application.

The following were carried out in the development of the Neural Networks for Coastal Water Level Modelling and Prediction

- Selection of Neural Networks Architecture
- Creation of the of the Neural Networks Model Using a chosen algorithm
- Preparation of data for training
- Training of the networks model
- Validation of the model
- Testing of the model
- Determination of the performance of the model in terms of preferred accuracy check (in terms of Mean Square Error(MSE) and Correlation Coefficient (R)
- Development of a Graphical User Interface (GUI) for ease of data entry and subsequent application of the model

3.1 Data Collection Preparation

The water level data that were used in this work were collected basically from two sources:

- Water level data acquired in 2008 by University of Lagos (UNILAG)
- Water level data from two Project sites at IkotAbasi, AkwaIbom, Nigeria, and obtained from Professor O. C. Ojinaka of the University of Nigeria. The observation was done on May, 2008.

Data preparation for this thesis covered visual inspection and selection of data from the array of sample of data available.

Issues involved in the data collection are:

- Difficulty in identifying an underlying function in the presence of very high variability.
- Partitioning of the data into their functional parts and perspectives due to some of the data being acquired during hourly and half an hour interval.

The geographic coordinates of the water level gauges used for this study are in Table 1.

I ã

Water Level Gauge Station	Latitude	Longitude	Relative Distance Apart
Harbour (Opobo)	4 ⁰ 33'N	7 ⁰ 32'E	
Lagos Harbour	4 ⁰ 28'N	7 ⁰ 35'E	Harbour –Lagos Harbour -12.376km
Oreta Lagoon (Lagos)	6 ⁰ 30N	3 ⁰ 30'E	
Unilag Lagoon	6 ⁰ 30'N	3 ⁰ 24'E	Oreta –Unilag -12.344km
Porto-Novo	6 ⁰ 24'N	3 ⁰ 20'E	Oreta-Porto-Novo-23.650km

Other data processing stages were handled during the Script- coding phase. They included

- Processing of unknown input
- Representing the unknown target

Every data presented to the network passes through a set processing rules

```
[tn,ts] = mapminmax(t);
net = train(net,pn,tn);
```

The original network inputs and targets are given in the matrices p and t. The normalized inputs and targets pn and tn that are returned will all fall in the interval [-1,1]. The structures ps and ts contain the settings, in this case the minimum and maximum values of the original inputs and targets.

3.1.1 Processing Unknown Inputs

Input data with unknown values in the network are represented with NaN values. Where this becomes too much in the data cluster, the program would not run rather error report with attention directed to NaN and rank of the matrices would be generated.

3.1.2 Representing Unknown Targets

The Unknown targets were also represented with NaN values. A method of representing unknown targets would be used to represent those unknown targets with NaN values. All the performance functions used in the programming were set to ignore those unknown targets for purposes of calculating performance and derivatives of performance. A typical example of this is observed when an input/target with location description on the top of the column is read in for training. The description names are ignored as they will pose challenge to the training process.

3.2 Network Building

Network building phase in ANNs modeling involves specification of the following:

- Number of hidden layers
- neurons in each layer,
- Transfer function in each layer
- Training function, weight/bias learning function, and performance function.

Through this sensitivity study, a standard feed forward back propagation network with a nonlinear differentiable log-sigmoid transfer function in the hidden layer was adopted for this work.

3.3 Mathematical Explanation of the ANN Model

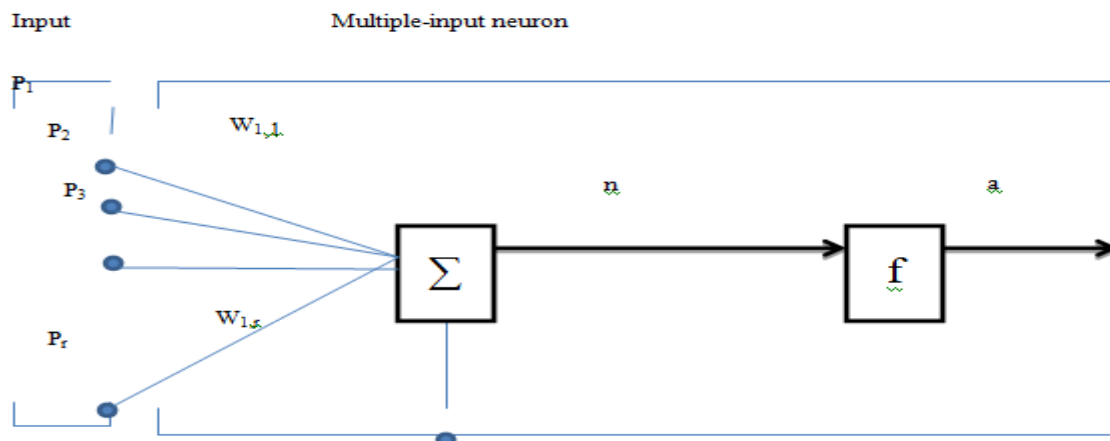


Figure 1:

From figure 1,

$$a = \text{output}, a = f(w_p+b)$$

f = Transfer function (activation/transfer function),

W = weight, b = bias,

P = inputs and n = neuron

The neuron has a bias b, which is summed with the weighted inputs to form the net- input n

$$n = W_{11} P_1 + W_{12} P_2 + \dots + W_{1r} P_r + b \tag{3.1}$$

The expression in (3.1) can be written in matrix form:

$$n = Wp + b, \tag{3.2}$$

where the matrix **W** for the single neuron case has only one row.

Now the neuron output can be written as: $a = f(Wp + b)$ (3.3)

3.4 The Concept of Transfer Function

With respect to the Artificial Neural Network sense, the transfer function is a mathematical function that takes a number of inputs and transforms them into a single output. Each transfer function has a number of adjustable parameters that correspond to the input weights of the neuron. Special attention was paid to the Log Sigmoid and linear transfer functions. These two functions are the transfer function used in this work.

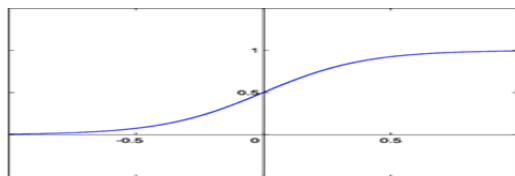
3.4.1 Log Sigmoid Function

When a detailed description is lacking, a **sigmoid function** is often used. A log-sigmoid function, also known as a logistic function is one of the members of sigmoid function, it is given by the relationship:

$$S(t) = \frac{1}{1 + e^{-t}} \tag{3.4}$$

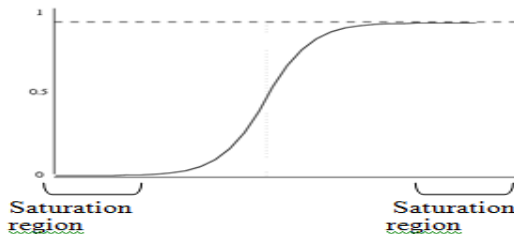
In general, a sigmoid is real-valued and differentiable function, having either a non-negative or non-positive first derivative which is bellshaped. There are also a pair of horizontal asymptotes as $t \rightarrow \pm\infty$. The logistic functions are sigmoidal and are characterized as the solutions of the differential equation.

The sigmoid shape of this function also explains its usefulness



18

$$\left. \begin{aligned} S(x) &= \frac{1}{1 + e^{-x}} \\ S'(x) &= -\frac{1}{(1 + e^{-x})^2} \cdot (1 + e^{-x})' \\ &= -\frac{1}{(1 + e^{-x})^2} \cdot (-e^{-x}) \\ &= \frac{1}{1 + e^{-x}} \cdot \frac{e^{-x}}{1 + e^{-x}} \\ &= S(x)(1 - S(x)) \end{aligned} \right\} \tag{3.5}$$



18

The sigmoid shape of this function also explains its usefulness. During the calculation of the weight updates in training algorithm, sufficiently large network is moved into one of the two saturation regions as shown in the figure above. By this illustration, a sigmoid function behaves like a threshold or ramp function.

3.5 Mathematical Explanation of Levenberg-Marquardt (LM) Optimization Method

Levenberg-Marquardt(m) was used as training optimization function in the Back Propagation algorithm in this work.

$$F(x) = \frac{1}{2} \sum_{i=1}^m [f_i(x)]^2 \tag{3.6}$$

Let the Jacobian of $f_{i(x)}$ be denoted by $j_i(x)$, then the Levenberg-Marquardt method searches in the direction given by the solution p to the equation (3.5)

$$(J_k^T J_k + \lambda_k I) p_k = -J_k^T f_k, \tag{3.7}$$

Where α_k are nonnegative scalars and I is the identity matrix (Gill *et al*, 1981).

The application of LM method artificial neural network is explained by (Fitch, et al., 1991; Hagan 1995) thus: the iteration process during the training of a neural network takes the following steps,

1. Initialize weight vector, w , by using uniform random numbers from the interval (-1, 1).
Calculate error gradient, g , at this point. Select initial search direction
 $d_0 = -g$ (3.8)
2. For each iteration k , determine constant α_k , which minimizes the error function $f(w + \alpha_k d_k)$ by line search where d_k is the search direction at iteration k . Update the weight vector w_{k+1} using: $w_{k+1} = w_k + \alpha_k d_k$ (2)
3. If error at this iteration, $k+1$, is acceptable, or if specified number of computations of the function and gradients is reached, terminate the algorithm.
4. Otherwise obtain new direction vector, d_{k+1} : $d_{k+1} = -g_{k+1}$ (3.9)
If $k+1$ is an integral multiple of N , where N is the dimension of w . Otherwise,
 $d_{k+1} = -g_{k+1} + \beta_k d_k$ (3.10)

If the algorithm is not converged, continue from step (2) for next iteration

3.6 Relating ANN Model to the Phenomenon Under Investigation

From Equation (3.3), $a = f(Wp + b)$

a = output (the water level to be predicted)

f = transfer /activation function: where Log-Sigmoid and linear transfer functions were chosen for hidden and output layers respectively. The logsigmoid function is differentiable

W = weight defined by the chosen training rule (Levenberg-Marquardt Method as applied in Backpropagation algorithm)

P = Input \equiv (the water level data used as output)

b = Bias usually given a constant value as one (1). The bias is an optional factor as the model can still give a reasonable result without the bias.

The generalized form of the ANN Model Equation can be represented as:

$$\text{Output } a(t) = f [w_1 * P_1(t), w_2 * P(t) \dots w_n * P_n(t)] \quad (3.11)$$

where w_i ($i= 1, \dots, n$) are the weights of the ANN network, p_i ($i= 1, \dots, n$) are water level input signals, and a is the water level output signal (Huanget al, 2003).

3.7 Network Modeling Steps

3.7.1 Step one: Network Creation

A callback function was developed to call a function which created a feed forward Backpropagation network in a Matlab environment.

3.7.2 Data division for Training, Validation and Testing

The water level dataset presented to the model was randomly divided into 3 sets in the ratio of '60:20:20', for training, Validation, and testing respectively.

3.7.3 Step 2: Network Training

The training process requires a set of examples of proper network behavior--network inputs p (water level data designated as input) and target outputs t (water level input designated as input). During training the weights and biases of the network are iteratively adjusted to minimize the network performance function and this was done using the Lavernberg-Marquardt training process. The training subroutine for reading the water level data into training module via the created network was developed. This subroutine reads prepared water level data from microsoft excel into the model for training.

3.7.4 Step 3: Performance Evaluation of the Trained Network

This was achieved by using:

- Regression Analysis (R)
- Mean Square Error (MSE)

Regression Analysis: This gives the measure of how well the variation in the output is explained by the targets. The GUI designed in this work is done in such a way that the user is allowed to check for this error with great ease before adopting the network. The subroutine which handled the regression analysis is expressed as:

$$[m,b,r] = \text{postreg}(Y,T)$$

POSTREG postprocesses the network training set by performing a linear regression between one element of the network response and the corresponding target.

Mean square error function: Mean Square Error (MSE) function used in the model is mathematically expressed as:

$$F = 1/n = \sum_{i=1}^n (e_i)^2 \tag{3.12}$$

where F = performance function, n = the total number of samples, i = counter or iterative term, e = error (difference between the target and output).

For each training instant, the threshold values which give good predictions are 0.8 and 0.05 for Regression and MSE respectively.

3.7.5 Adoption of Training Instant Using Regression and Mean Square Margin

The GUI developed during this study plots the results of regression, and mean square error at the prompt of performance button.

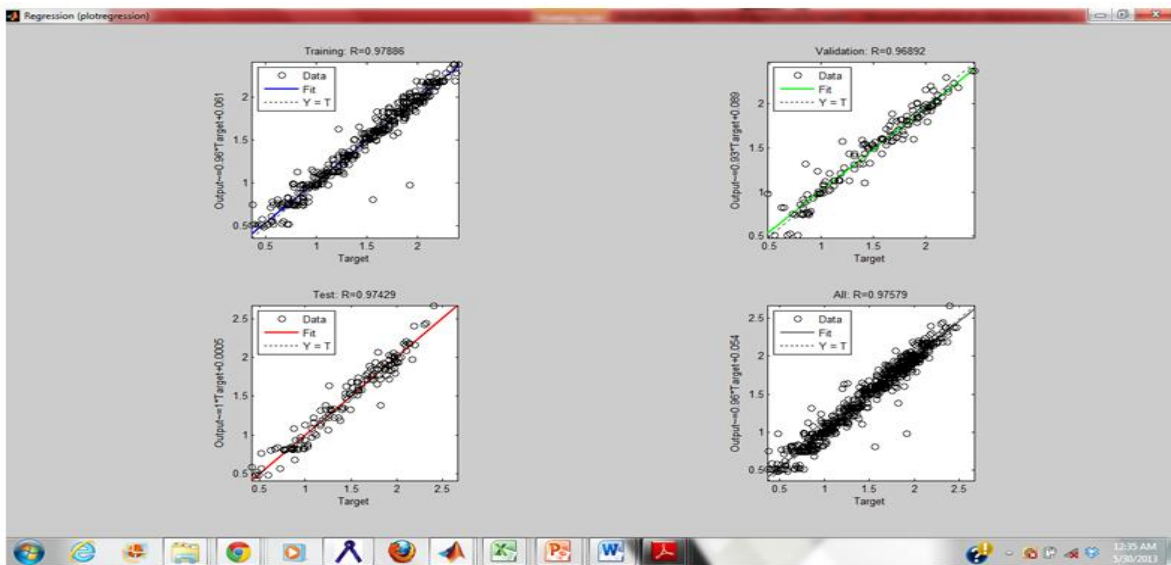


Figure 3: GUI showing the Results of the Regression

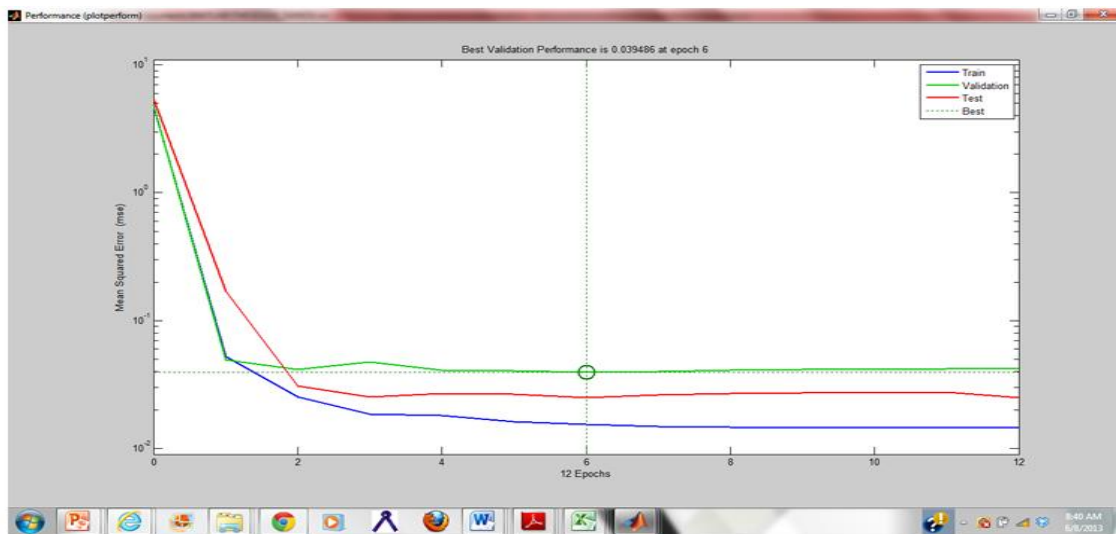


Figure 4: GUI showing the Mean Square Error

3.7.6 Step 4: Simulation and Prediction

Once the error analysis with the mean square error and regression analysis are satisfactory, the trained network is engaged for simulation by means of a call_back function via the GUI. This procedure enables a model simulation function known as ‘sim’ to be used for simulating the train datasets. All these steps (1-4) were developed and compiled into application with a functional user interface.

3.8 Development of the Model Graphical User Interface

For ease of data entry into the model, a GUI was developed. The GUI was mentally abstracted to cover the various components needed to interface the user and the model.

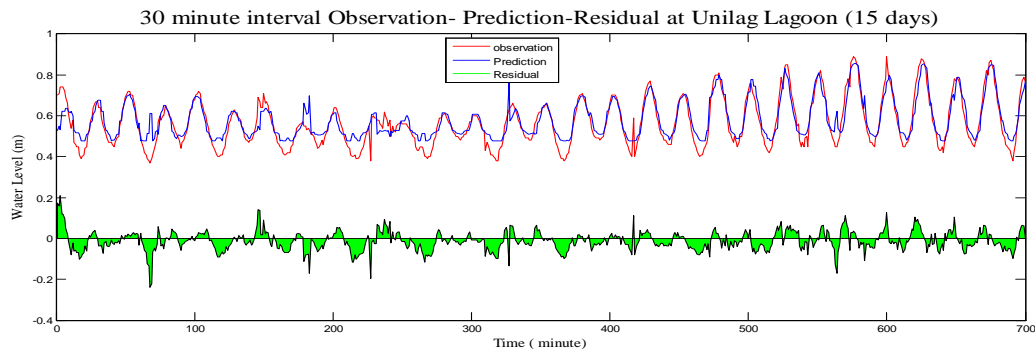
IV. RESULTS AND ANALYSIS OF RESULTS

This section focuses on the results of predictions done using the model. Each prediction result is reported with the associated statistical analysis. The statistical analysis is an integral part of the model. It was directly linked to the model Graphical User Interface(GUI) during the programming of the model. The prediction results are reported in two parts. The first part is termed by many as the ‘Regional Neural Network Prediction’ in which the water level of two stations are used for training and thereafter , one station data (designated as the ‘input’) is used to predict for the other (designated as the ‘target’). While the second part is a prediction where water level data for one station is used to train ANN model and afterward a prediction is made to cover time or days beyond the observation period. The result for these two types of prediction are shown below.

4.1 Water Level Prediction Using Two Stations (Regional Case)

4.1.1 Prediction for University of Lagos (Unilag) Lagoon using Oreta Lagoon Water Level

Thirty days water level data observed on August ,2008 for Unilag and Oreta Lagoons were divided into two parts for each of the tidal stations. The first 15 days data for both tidal stations were used for training (that is 15 days tidal data of Oreta lagoon wereused as inputs and 15 days of Unilag lagoon tidal data were used as target. The remaining 15 days water level data of Oreta Lagoon were used to predict water level data covering 15 days at Unilag lagoon.

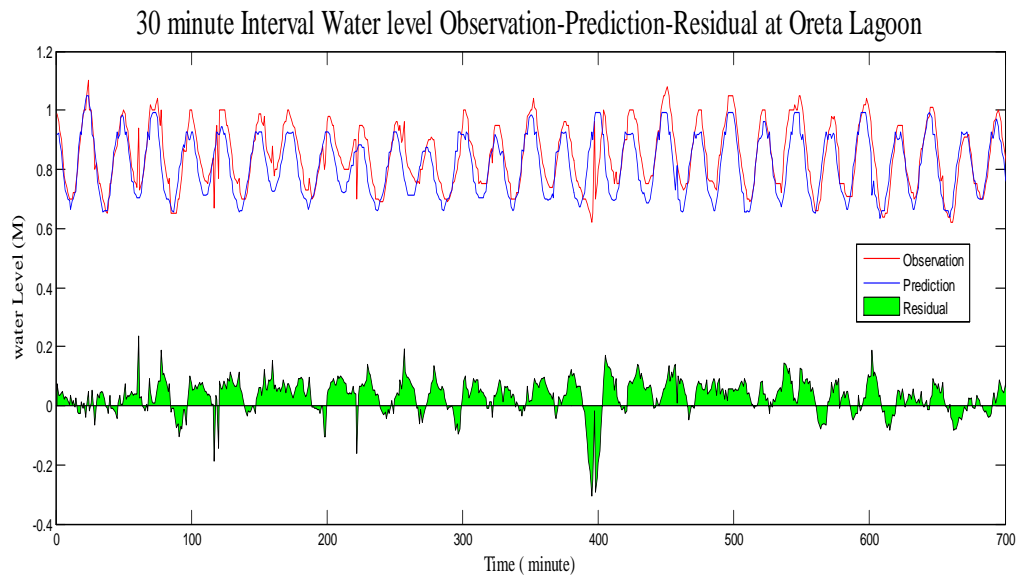


1ē

EPOCH (No of iteration)	TIME (secs)	PERFORMANCE (MSE)	GRADIENT	VALIDATION CHECK
20	2	0.00375	0.000353	6
REGRESSION				
Training		Validation		Test
0.834		0.869		0.868

4.1.2 Prediction of Water level at Oreta Lagoon using Porto-Novo Creek

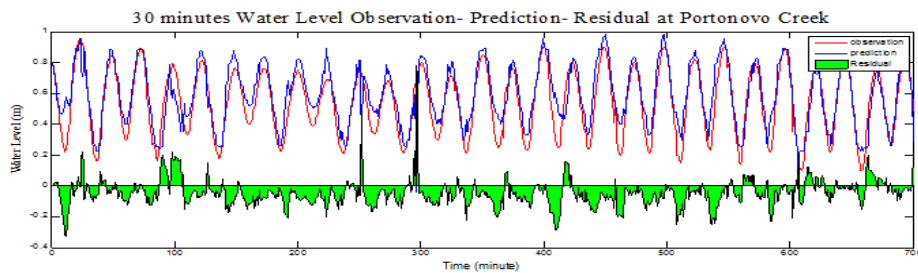
30 days water Level data for Porto-Novo creek and Oreta Lagoon were used in a similar case as discussed in one (4.1.1) above and the result is as shown below.



EPOCH (No of iteration)	TIME (secs)	PERFORMANCE (mse)	GRADIENT	VALIDATION CHECK
20	11	0.0012	0.000509	6
REGRESSION				
Training		Validation		Test
0.9337		0.91283		0.9087

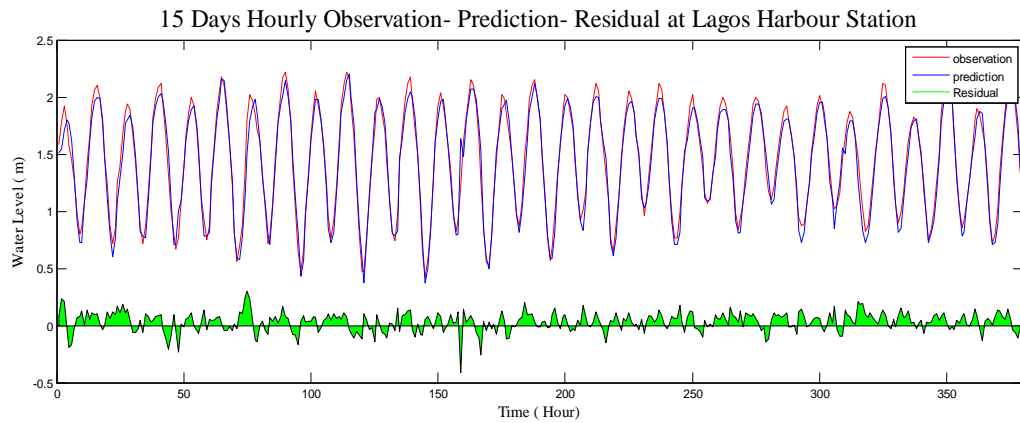
4.1.3 Prediction of Water Level for Porto-Novo Creek

Thirty days water level for Unilag lagoon and Porto-Novo creek were subjected to the same procedure as discussed in (4.1.1.) above, prediction was made for Porto-Novo creek covering a period of 15 days. The result of the prediction is as shown below.



œœ

EPOCH (No of iteration)	TIME (secs)	PERFORMANCE (MSE)	GRADIENT	VALIDATION CHECK
11	11	0.007	0.000509	6
REGRESSION				
Training		Validation		Test
0.9337		0.91283		0.9487



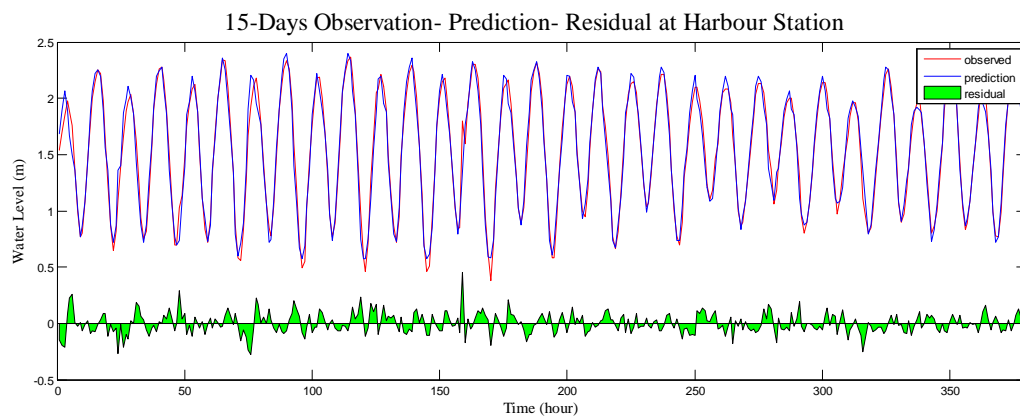
œ

œ

œ

œ

EPOCH (No of iteration)	TIME (secs)	PERFORMANCE (mse)	GRADIENT	VALIDATION CHECK
7	5	0.018	0.00065	6
REGRESSION				
Training		Validation		Test
0.9666		0.9631		0.9668



œ

œ

ë

EPOCH (No of iteration)	TIME (secs)	PERFORMANCE (mse)	GRADIENT	VALIDATION CHECK
12	3	0.0285	0.00065	6
REGRESSION				
Training		Validation		Test
0.8646		0.9238		0.9014

4.3 Statistical Test Analysis Between the Observed and the Predicted Water Level At Opobo Harbour Station

The objective of the statistical test is to compare the two populations of observed tide and predicted tides (Keller and Warrack, 2003). The parameter is the difference between the two means/standard deviations, \bar{x}_1/s_1 and \bar{x}_2/s_2 in all the water level gauge locations (where \bar{x}_1/s_1 = mean/standard deviation of observed water level and \bar{x}_2/s_2 = mean/standard deviation of the predicted water level).

Two hypotheses, the null (H_0) and the alternative (H_a) hypotheses were investigated using the t-distribution and the F-distribution . t- distribution is used to compare difference in mean between population and the F-distribution compares the variance between the population. In either case, the null Hypothesis is rejected when the calculated value is greater than the tabulated value.

The Hypothesis questions are:

- Null Hypothesis: Is the difference between the mean/variance of water level observation and water level prediction equals zero
- Alternative Hypothesis: Is the difference between the mean/variance of water level observation and water level prediction greater than zero

$H_0: (\bar{x} - \bar{x}) = 0$

$H_a: (\bar{x} - \bar{x}) > 0$ for mean

$H_0: (s_1 - s_2) = 0$

$H_a: (s_1 - s_2) > 0$ for variance

t-test distribution is given by t the expression,

$$t = \frac{\bar{x}_1 - \bar{x}_2}{\sqrt{\frac{s_1^2}{n_1} + \frac{s_2^2}{n_2}}} \tag{4.1}$$

Where S_1 = standard deviation for population 1
 S_2 = standard deviation for population 2
 n_1 = population 1 size
 n_2 = population 2 size
 $v = n_1 + n_2 - 2$ (degree of freedom)
 Standard Deviation is expressed as

$$s = \sqrt{\frac{1}{N - 1} \sum_{i=1}^N (x_i - \bar{x})^2}, \tag{4.2}$$

Equation (4.1) , (4.2) were used for computing t- test value for all the tidal gauge stations tested with the model. The analysis for one of the stations – OpoboHarbour Station is shown below

\bar{x}_1 = 1.54231771 (Observed) mean of observed data
 \bar{x}_2 = 1.497030556 (Predicted) mean of predicted data
 s_1 = 0.517422089 (Observed) standard deviation of observed data
 s_2 = 0.5141760 (Predicted) standard deviation of predicted data

$n_1 = 384$
 $n_2 = 384$
 $v = n_1 + n_2 - 2 = 702 + 702 - 2 = 1402$

$$t = \frac{\bar{x}_1 - \bar{x}_2}{\sqrt{\frac{s_1^2}{n_1} + \frac{s_2^2}{n_2}}}$$

$t = \{(0.045287154) \sqrt{0.000697202 + 0.0006884816}\}$
 $t = 1.2165$

The rejection region for a 5% significance level is $t > t_{\alpha,y} = t_{0.05,383} = -1.646$

The rejection region for a 95% significance level is $t < t_{\alpha,y} = t_{0.95,383} = 1.646$

Since $t < t_{\alpha,y}$ we therefore accept the null hypothesis that mean of the observed tide is equal to the mean of the predicted tide.

F –test for Opofo Harbor Location:

Since $s_1 > s_2$, $F_{calc} = s_1^2/s_2^2 = 0.517422089^2/0.5141760^2 = 1.011878727$. The tabulated value for $v = 383$ in each case, and a 95% confidence level is $F_{383,383} = 1.1887$. In this case, $F_{calc} < F_{383,383}$, so we accept the null hypothesis that the two standard deviations are equal. and we are 95% confident that any difference in the sample standard deviations is due to random error

The t-test and the F-test were conducted for all the stations used in this work and we are 95% confident that any difference in predicted and observed water level mean and standard deviations is due to random error incurred during observations

Station	S ₁	S ₂	x ₁	x ₂
Unilag Lagoon	0.116484012	0.093932638	0.56845934	0.582483452
Porto-Novocreek	0.107412287	0.196791059	0.54265335	0.59114693
Oreta Lagoon	0.107412287	0.1010110005	0.84510699	0.813130243
Lagos Harbour	0.456608894	0.458318126	1.452838542	1.421460677
Opofo Harbour	0.5141760	0.517422089	1.54231771	1.497030556

V. CONCLUSION AND RECOMMENDATION

5.1 Conclusion

A Neural Network for Water Level modeling and prediction has been successfully developed in this study for water level predictions at coastal zone. The Neural Networks Water Level Model (NNWLM) employs three-layer feed-forward, back propagation structure with optimized training method using Levenberg-Marquardt algorithm. The model requires the input of time series water level data with corresponding time series water level data of a coastal area whose water level is to be predicted. The two sets of data, the input and target are subjected to training with varying network parameters until a satisfactory model with some desired measure of accuracy is achieved.

The model was successfully tested in case studies using data from different coastal locations ranging from Lagos Harbour, Opofo Harbour, Porto-Novocreek, Oreta Lagoon, Unilag Lagoon. Field data indicate that water levels change substantially in both amplitude and phase over the coastal zone due to the complex coastal and estuarine topography and shallow water effects. Using short-term data sets (one month), the model was trained, validated and tested using a ratio of 6: 2: 2 for training, validation and testing respectively.

The result of the model predictions indicates great performance. The predicted tidal signals matched well with observations with performance index ranging from 0.008 -0.012 in terms of Mean Square Error(MSE) and 0.83- 0.97 in terms of correlation coefficient (R-value). Given this plausible performance, The Neural Networks Water Level Model (NNWLM) developed in this study is a practical tool for coastal engineers in coastal zone management. Thus researchers can predict long-term historic water level data at a station of interest or remote station using the regional approach.

5.2 Recommendation

We make the following recommendations based on this study:

- i. More research should be done in other areas of coastal zone management using ANN.
- ii. Recent innovations on combination of neural network and harmonic analysis for improved water level analysis and prediction should be explored to assess the validity of the innovation and further contribute to the body of knowledge on coastal study.
- iii. There should be collaboration between governmental agencies, non governmental agencies and the academia to enhance coastal zone management in the country.
- iv. More resources should be channeled to acquire more tidal data. Data sharing should also be encouraged among all the stakeholders in coastal zone management.

REFERENCES

- [1] J. Austin *The design and application of associative memories for scene analysis*. Ph.D. thesis, Brunel University 1986. <http://www.cs.york.uk/arch/NeuralNetworks/references.htm>
- [2] R. Abrahart. Single-Model-Bootstrap applied to neural network rainfall-runoff Forecasting. In *Geocomputation*, volume 6. September 24–26, 2001
- [3] R. Abrahart, L. See and Kneale, P. Using network pruning and model breeding algorithms to optimise neural net architectures and forecasting inputs in a rainfall-runoff model. *Journal of Hydroinformatics*, 1(2), pp. 103–114, 1999.
- [4] R. Abrahart., L. See, and Kneale, P. New tools for neurohydrologists: using ‘network pruning’ and ‘model breeding’ algorithms to discover optimum inputs and architectures. In *Geocomputation*, volume 3. September 17–19, 1998.
- [5] J. Andersen. An introduction to neural networks. MIT Press, Cambridge, MA, USA, 1995.
- [6] R. Andrews, J. Diederich and A. Tickle. Survey and critique of techniques for extracting rules from trained artificial neural networks. *Knowledge Based Systems*, 8(6), pp. 373–389, 1998.
- [7] K. Balakrishnan, and V. Honavar. Evolutionary design of neural architectures - a preliminary taxonomy and guide to literature. Technical Report CS-TR 95-01, Artificial Intelligence Research Group, Iowa State University, Iowa, USA, 1995
- [8] R. Belew, J. McInerney, & N. Schraudolph. Evolving networks: using the genetic algorithm with connectionist learning. Technical Report CS90-174, Cognitive Computer Science Research Group, University of California at San Diego, CA, USA, 1990
- [9] R. Belew. *Adaptive information retrieval: Machine learning in associative networks*. Ph.D. thesis, University of Michigan, Michigan, 1986
- [10] R. Brause, Medical analysis and diagnosis by neural networks. In J. Crespo, V. Maojo and F. Martin (editors), *2nd International Symposium on Medical Data Analysis*, pp. 1–13. Madrid, Spain, October 8–9, 2001. URL citeseer.ist.psu.edu/brause01medical.html. 2001
- [11] A. Broumandnia, & M. Fathy. Application of pattern recognition for Farsi license plate recognition. In *ICGST International Conference on Graphics, Vision and Image Processing*. Cairo, Egypt, 2005
- [12] C. Dawson, & R. Wilby. Hydrological modelling using artificial neural networks. *Progress in Physical Geography*, 25(1), pp. 80–108. 2001
- [13] M. Deo, & S. Jagdale. Prediction of breaking waves with neural networks. *Ocean Engineering*, 30, pp. 1163–1178, 2003. USA
- [14] M. Deo, A. Jha, Chaphekar & K. Ravikant. Neural networks for wave forecasting. *Ocean Engineering*, 28, pp. 889–898 USA, 2001
- [16] M. Deo, & N. K. Kumar. Interpolation of wave heights. *Ocean Engineering*, 27, pp. 907–919 USA, 2000
- [16] M. C. Deo and C. Sridhar Naidu: Real time wave forecasting using neural networks, *Ocean Engineering*, Elsevier, U.K., 26, 191–203. 1999
- [17] Y. Dibike, A. Minns, & M. Abbott. Applications of artificial neural networks to the generation of wave equations from hydraulic data. *Journal of Hydraulic Research*, 37(1), pp. 81–97. 1999
- [18] A. T. Doodson, & H. D. Warburg. Admiralty Manual of Tides. The Hydrographic Department, Admiralty, London. A. T. Doodson., The Harmonic Development of the Tide-generating Potential. Proc. Roy. Soc., London, pp 305–329. 1941, 1922
- [19] B. Efron, & R. Tibshirani. *An introduction to the bootstrap*. Monographs on statistics and applied probability. Chapman and Hall, London, UK, 1993
- [20] A. El-Shazly. The efficiency of neural networks to model and predict monthly mean sea level from short spans applied to alexandria tide gauge. In *FIG Working Week 2005: From Pharaohs to Geoinformatics*. 2005
- [21] S. Fahlman, & C. Lebiere. The cascade-correlation learning architecture. In *Advances in Neural Information Processing Systems*, volume 2, pp. 524–532. Morgan Kaufmann, San Mateo, CA, USA, 1990
- [22] A. Fernando, & A. Jayawardena. Runoff forecasting using RBF networks with OLS algorithm. *Journal of Hydrologic Engineering*, ASCE, 3(3), pp. 203–209. USA, 1998
- [23] G. Flake. Square unit augmented, radially extended, multilayer perceptrons. In *Neural Networks: Tricks of the Trade*, pp. 145–163. Springer-Verlag, 1998
- [24] D. Furundzic. Application example of neural networks for time series analysis: Rainfall-runoff modeling. *Signal Processing*, 64, pp. 383–396. 1998
- [25] D. A. Greenberg. Mathematical studies of tidal behaviour in the bay of fundy. Ph. D. Thesis, University of Liverpool. 1977

- [26] S. T. Grant. Simplified Tidal Analysis and Prediction. Lighthouse: Journal of the Canadian Hydrographers's Association, Edition No. 37, Spring, 1988
- [27] M.Hagan, & M.Menhaj. Training feedforward networks with the Marquardt algorithm. *IEEE Transactions on Neural Networks*, 5, pp. 989–993, 1994
- [28] M.Hagiwara. Theoretical derivation of momentum term in back-propagation. In *International Joint Conference on Neural Networks*, volume 1, pp. 682–686. Baltimore, MD, USA, June 7–11, 1992
- [29] M.Handzic, F. Tjandrawibawa & J.Yeo. How neural networks can help loan officers to make better informed application decisions. In E. Cohen (editor), *Informing Science and Information Technology Education*, pp.
- [30] B.Hassibi & D. Stork. Second Order Derivatives for Network Pruning: Optimal Brain Surgeon. *Advances in Neural Information Processing Systems*, pp. 164–171, 1992
- [31] M.Hassoun, *Fundamentals of artificial neural networks*. MIT Press, Cambridge, MA, USA, 1995
- [32] S.Haykin *Neural Networks: A Comprehensive Foundation*. Prentice Hall, Upper Saddle River, NJ, USA, second edition. 1999
- [33] J. Holland. *Adaptation in natural and artificial systems*. University of Michigan Press, London, 1975
- [34] J. Hopfield. Neural networks and physical systems with emergent collective computational abilities. *Proceedings of the National Academy of Sciences USA*, 79, pp. 2554–2558, 1982
- [35] W. Hsieh & B.Tang. Applying neural network models to Prediction and Data Analysis in Meteorology and Oceanography. *Bulletin of the American Meteorological Society*, 79(9), pp. 1855–1870, 1998.
- [36] K. Hsu, U. Gupta & S. Sorooshian,. Artificial neural network modeling of the rainfall-runoff process. *Water Resources Research*, 31(10), pp. 2517–2530, 1995
- [37] W. Huang & C.Murray. Application of an artificial neural network to predict tidal currents in an Inlet. Technical Report CHETN-IV-58, US Army Corps of Engineers, URL cirp.wes.army.mil/cirp/cetns/chetn-iv58, 2003
- [38] G. W. Irwin, K. Warwick & K. J Hunt. (Editors). *Neural network applications in control*, volume 53 of *IEE control engineering series*. Institution of Electrical Engineers, London, UK, 1995
- [39] A. Jayawardena & A. Fernando. Use of radial basis type artificial neural networks for runoff simulation. *Computer-Aided Civil and Infrastructure Engineering*, 13, pp. 91–99, 37(2), pp. 147–161, 1999
- [40] N.Jiang, Z.Zhao & L. Ren. Design of structural modular neural networks with genetic algorithm. *Advances in Software Engineering*, 34, pp. 17–24. 2003
- [41] M.Jordan & T.Petsche. (editors), *Advances in Neural Information Processing Systems*, volume 8, pp. 176–182. MIT Press, Cambridge, MA, USA, 1996
- [42] M. Jordan & R.Jacobs. Hierarchical mixtures of experts and the EM Algorithm. *Neural Computation*, 6, pp. 181–214. 1994
- [43] N.Karunanithi, W.Grenney, D.Whitley & K.Bovee. Neural Networks for River Flow Prediction. *Journal of Computing in Civil Engineering*, 8(2), pp 201–220. 1994
- [44] M.Kearns. A bound on the error of cross validation using the approximation and estimation rates, with consequences for the training-test split. In *Advances in Neural Information Processing Systems*, volume 8, pp. 524–532. MIT Press, Cambridge, MA, USA, 1996
- [45] P. Kershaw & P. Rossini. Using Neural Networks to Estimate Constant Quality House Price Indices. In *Fifth Annual Pacific-Rim Real Estate Society Conference*.
- [46] A. Krogh & J. Hertz. A Simple weight decay can improve generalization. In J. Moody, S. Hanson and R. Lippmann (editors), *Advances in Neural Information Processing Systems*, volume 4, pp. 950–957. Morgan Kaufmann, San Mateo, CA, USA, 1995
- [47] T.-L Lee. Back-propagation neural network for long-term tidal predictions. *Ocean Engineering*, 31, pp. 225–238, 2004
- [48] T.-L Lee. & D. Jeng. Application of artificial neural networks in tide forecasting. *Ocean Engineering*, 29, pp. 1003–1022, 2002.
- [49] H. Maier & G. Dandy. Neural networks for the prediction and forecasting of water resources variables: a review of the modelling issues and applications. *Environmental Modelling and Software*, 15, pp. 101–124, 2000
- [50] H.Maier & G.Dandy. The effect of internal parameters and geometry on the performance of back-propagation neural networks: an empirical study. *Environmental Modelling and Software*, 13, pp. 193–209. 1998
- [51] O.Makarynsky. Improving wave predictions with artificial neural networks. *Ocean Engineering*, 31, pp. 709–724. 2004
- [52] M.Markas, J.Salas & H.-K Shin. Predicting streamflow based on neural networks. In *Proceedings of the 1st International Conference on Water Resource Engineering*, pp. 1641–1646. ASCE, New York, USA, 2004
- [53] H.Mase, M. Sakamoto & T. Sakai. Neural network for stability analysis of rubble-mound breakwaters. *Journal of Waterway, Port, Coastal and Ocean Engineering*, 121(6), pp. 294–299. 1995
- [54] T.Masters. *Advanced Algorithms for neural networks: C++ Sourcebook*. John Wiley, Frankfurt, Germany, 1995
- [55] J. Medina, J. Gonzales-Escriva, J.Garrido, & R.ouck, J. de (2003). Overtopping analysis using neural networks. In N. Allsop (editor), *JCCE 2002*, volume 28. Thomas Telford.
- [56] P. Melchior. *The tides of the planet earth*. Pergamon Press, Great Britain, 1983
- [57] W.McCulloch. & W.Pitts. A logical calculus of the ideas immanent in nervous activity. *Bulletin of Mathematical Biophysics*, 5, pp. 115–133, 1943
- [58] W.Miller, R.Sutton & P.Werbos. (editors). *Neural Networks for Control*. MIT Press, Cambridge, MA, USA, 1990
- [59] M.Minsky, & S.Papert *Perceptrons*. MIT Press, Cambridge, MA, USA, 1969.
- [60] W.H.Münk, and D.E. Cartwright. *Tidal spectroscopy and prediction*. Philosophical Transactions of the 18 Royal Society of London, London, Ser. A, 259, pp. 533–581, 1966
- [61] R.Muttiah, R.Srinivasan, & P.Allen. Prediction of two-year peak stream discharges using neural networks. *Journal of the American Water Resources Association*, 33(3), pp. 625–630, 1997
- [62] U.Naftaly, N.Intrator & D. Horn. Optimal ensemble averaging of neural networks. *Network*, 8, pp. 283–296, 1997
- [63] M.Orr, K.Takezawa, A.Murray, S.Ninomiya, M.Oide & T. Leonard. Combining regression trees and radial basis function networks. *International Journal of Neural Systems*, 10(6), pp. 453–465, *Applications*, 5, pp. 113–120. 2002
- [64] M.Orr, Regularisation in the Selection of Radial Basis Function Centres. *Neural Computation*, 7, pp. 606–623, 1995
- [65] M.Perrone. *Improving regression estimation: Averaging methods for variance reduction with extensions, to general convex measure optimization*. Ph.D. thesis, Brown University, Rhode Island, 1993
- [66] M. Powell. Radial Basis Functions for Multivariable Interpolation: A Review. In J. Mason and M. Cox (editors), *Algorithms for Approximation*, pp. 143–167. Oxford University Press, Oxford, UK, 1985

- [67] Poff, N.Tokar, S. & Johnson, P.(1996) Stream hydrological and ecological responses to climate change assessed with an artificial neural network. *Limnology and Oceanography*, 41(5), pp. 857–863..
- [68] T.Poggio, &F.Girosi. A theory of networks for approximation and learning. A.I. Memo 1140, Massachusetts Institute of Technology, Artificial Intelligence Laboratory,1989
- [69] B.Pozueta, M.van Gent & van den Boogaard. Neural network modelling of wave overtopping at coastal structures. In J.M. Smith (editor), *The Proceedings of the 29th International Conference on Coastal Engineering*, volume 4.Lisbon, Portugal, September 19–24, 2004
- [70] J.D.Rosati, M.B.Gravens, and W.G Smith. Regional Sediment Budget for Fire Island to Montauk Point, New York, USA. Proc. Coastal Sediments '99, ASCE, Reston, VA, 802–817.1999
- [71] J.de.Rouck Second Detailed Interim Report. Technical Report CLA127/296, CLASH, Ghent University, Belgium.2004
- [72] D. E.Rumelhart, J. L.McClelland & the PDP research group.*Parallel distributed processing: Explorations in the microstructure cognition. Volume I*. Cambridge, MA: MIT Press. 1986
- [73] F.Stravisi. The IT Method for the Harmonic Tidal Prediction. Bollrino Di Oceanologia Ed Applicata. Vol 1 N.3 Luglio. pp 193-204. 1983
- [74] Y.Tamura.A harmonic development of tide-generating potential. Marees Terrestres, Bulletin d' Information, No.99, pp.6813-6855. 1987
- [75] B.Zetler, and D. Cartwright and et alSome comparisonsof responseandharmonic tidePredictions. International Hydrographic Review, Monaco, LVI (2),pp.105-115. 1979
- [76] B.Zhang, &R.Govindaraju. Prediction of watershed runoff using Bayesian concepts and modular neural networks. *Water Resources Research*, 36(3), pp.753–762.
www.mathworld.wolfram.com/LevenbergMarquardtMethod.html
www.mathworld.wolfram.com/LevenbergMarquardtMethod.html

Challenges and Design Issues in Search Engine and Web Crawler

Rahul Mahajan¹, Dr. S.K. Gupta², Mr. Rajeev Bedi³

¹M.Tech Student, Beant College of Engineering & Technology, Gurdaspur, Punjab, India

²HOD & Associate Professor (Computer Science & Engineering Department), Beant College of Engineering and Technology, Gurdaspur, Punjab, India

³Assistant Professor (Computer Science & Engineering Department), Beant College of Engineering and Technology, Gurdaspur, Punjab, India.

Abstract

With the drastic development of number of Internet users and the number of accessible Web pages, it is becoming increasingly difficult for users to find documents that are relevant to their particular needs. To make searching much easier for users, web search engines came into existence. Web Search engines are used to find specific information on the World Wide Web. Without search engines, it would be almost impossible to locate anything on the Web unless or until a specific URL address is known. Hence it is better to know how these search engines actually work and how they present information to the user initiating a search. Web crawling is the process used by search engines to collect pages from the Web. Web crawlers are one of the most crucial components in search engines and their optimization would have a great effect on improving the searching efficiency. This paper discusses the issues and challenges involved in the design of the various types of crawlers and search engine.

Keywords: Challenges, Design Issues, Web Crawler, Search Engine, Duplicate, Web Search Engine, Spam

I. INTRODUCTION

With the exponential growth of information on the World Wide Web, there is a great demand for developing efficient and effective methods to organize and retrieve the information available. All the search engines have powerful crawlers that visit the internet time to time for extracting the useful information over the internet. A web-crawler [4] is a program/software or automated script which browses the World Wide Web in a methodical, automated manner. Web crawlers are the programs or software that uses the graphical structure of the Web to move from page to page. Web crawlers are designed to retrieve Web pages and add them or their representations to local repository/databases. Web crawlers are mainly used to create a copy of all the visited pages for later processing by a search engine that will index the downloaded pages that will help in fast searches. Web search engines work by storing information about many web pages, which they retrieve from the WWW itself. These pages are retrieved by a Web crawler (sometimes also known as a spider), which is an automated Web browser that follows every link it sees. Search engines [1], [2], [3] operate as a link between web users and web documents. Without search engines, this vast source of information in web pages remain veiled for us. A search engine [6] is a searchable database which collects information from web pages on the Internet, indexes the information and then stores the result in a huge database where from it can be searched quickly.

II. RELATED WORK

Matthew Gray [5] wrote the first Crawler, the World Wide Web Wanderer, which was used from 1993 to 1996. In 1998, Google introduced its first distributed crawler, which had distinct centralized processes for each task and each central node was a bottleneck. After some time, AltaVista search engine introduced a crawling module named as Mercator [16], which was scalable, for searching the entire Web and extensible. UbiCrawler [14] a distributed crawler by P. Boldi, with multiple crawling agents, each of which run on a different computer. IPMicra [13] by Odysseus a location-aware distributed crawling method, which utilized an IP address hierarchy, crawl links in a near optimal location aware manner. Hammer and Fiddler [7], [8] has

critically examined the traditional crawling techniques. They purposed web crawling approach based on mobile crawlers powered by mobile agents. The mobile crawlers are able to move to the resources that need to be accessed in order to take advantage of local data access. After accessing a resource, mobile crawlers move on to the next server or to their home machine, carrying the crawling results in their memory.

The following sections describe the various issues and challenges in implementing these different categories of crawlers.

III. CHALLENGES IN SEARCH ENGINE

Web Search Engines are faced with number of difficult problems in maintaining and enhancing the quality of performance. The problems are either unique to particular domain. The various problems are [10],[11],[12]:

- Spam
- Content Quality
- Duplicate Hosts

3.1 Spam

The increasing importance of search engines to commercial web sites has given rise to a phenomenon we call “web spam”, that is, web pages that exist only to mislead search engines into mis-leading users to certain web sites. Web spam is a nuisance to users as well as search engines: users have a harder time finding the information they need, and search engines have to cope with an inflated corpus, which in turn causes their cost per query to increase. Therefore, search engines have a strong incentive to weed out spam web pages from their index.

3.2 Content Quality

The web is full of noisy, low quality, unreliable and contradictory content. While there has been a great deal of research on determining the relevance of documents, the issue of document quality or accuracy has not been received much attention in web search or information retrieval. The web is so huge, so techniques for judging document quality are essential for generating good search results. The most successful approach to determining the quality on the web is based on link analysis, for instance Page Rank[16,17] and HITS[9].

3.3 Duplicate Hosts

Web Search Engines try to avoid crawling and indexing duplicate and near-duplicate pages as they do not add new information to the search results and clutter up the results. The problem of finding duplicate or near-duplicate pages in set of crawled pages is well studied [7]. Duplicate hosts are the single largest source of duplicate pages on the web, so solving the duplicate hosts problem can result in a significantly improved web crawler. Standard check summing techniques can facilitate the easy recognition of documents that are duplicates of each other (as a result of mirroring and plagiarism). Web search engines face considerable problems due to duplicate and near duplicate web pages[15]. These pages enlarge the space required to store the index, either decelerate or amplify the cost of serving results and so exasperate users. The identification of similar or near-duplicate pairs in a large collection is a significant problem with wide-spread applications. In general, predicting whether a page is a duplicate of an already crawled page is very chancy work and lot of work is being done in this field but still it is not able to completely overcome this problem.

IV. WEB CRAWLER DESIGN ISSUES

The web is growing at a very fast rate and moreover the existing pages are changing rapidly in view of these reasons several design issues need to be considered for an efficient web crawler design. Here, some major design issues and corresponding solution are discussed below:-

How should the crawler get relevant pages to query? With the increase in web size, the number of applications for processing data also increases. The goal is to take advantage of the valuable information contain in these pages to perform applications such as querying, searching, data extraction, data mining and feature analysis. For some of these applications, notably for searching, the criteria to determine when a page is to be present in a collection are related to the page contents, e.g., words, phrases, etc.

What pages should the crawler download? In most cases, the crawler cannot download all pages on the Web. Even the most comprehensive search engine currently indexes a small fraction of the entire Web. Given this fact, it is important for the crawler to carefully select the pages and to visit "important" pages first by prioritizing the URLs in the queue properly, so that the fraction of the Web that is visited (and kept up-to-date) is more meaningful.

How should the crawler refresh pages? Once the crawler has downloaded a significant number of pages, it has to start revisiting the downloaded pages in order to detect changes and refresh the downloaded collection. Because Web pages are changing at very different rates, the crawler needs to carefully decide what page to revisit and what page to skip, because this decision may significantly impact the "freshness" of the downloaded collection. For example, if a certain page rarely changes, the crawler may want to revisit the page less often, in order to visit more frequently changing ones

How should the crawling process be parallelized? Due to the enormous size of the Web, crawlers often run on multiple machines and download pages in parallel. This parallelization is often necessary in order to download a large number of pages in a reasonable amount of time. Clearly these parallel crawlers should be coordinated properly, so that different crawlers do not visit the same Web site multiple times, and the adopted crawling policy should be strictly enforced. The coordination can incur significant communication overhead, limiting the number of simultaneous crawlers.

How should crawler get time sensitive information? Time Sensitive Searching is an issue that needs to be addressed to get the time sensitive information from the web. Usually Search engines crawl the web and take vast snapshots of site content. As previous crawls are not archived so search results pertain only to a single, recent instant in time. As a result when users request some pages which require past data then search engines are unable to provide because it is not possible to search files that represents snapshot of the web over time.

V. CONCLUSION

In this paper, I have discussed various issues and challenges faced in the development of the search engine and crawler architectures. I have found the many of the issues and challenges in these architectures are common i.e. reducing the network bandwidth consumption, maintaining the freshness of the database and maintaining the quality of pages etc.

References:

- [1] Arvind Arasu, Junghoo Cho, "Searching the Web", ACM Transactions on Internet Technology, August 2001.
- [2] Brian E. Brewington, George Cybenko, "How dynamic is the web.", In Proceedings of the Ninth International World-Wide Web Conference, Amsterdam, Netherlands, May 2000.
- [3] Dirk Lewandowski, "Web searching, search engines and Information Retrieval, Information Services & Use", pp: 137-147, IOS Press, May 2005.
- [4] Franklin, Curt, "How Internet Search Engines Work", 2002, www.howstuffworks.com.
- [5] Gray M., "Internet Growth and Statistics: Credits and background", http:www.mit.edu
- [6] Heydon A., Najork M., "Mercator: A scalable, extensible Web crawler.", WWW, vol. 2, no. 4, pp. 219-229, 1999.
- [7] J. Fiedler and J. Hammer, "Using the Web Efficiently: Mobile Crawling", In Proc. Of the 7th Int'l Conf. of the Association of Management (AoM/IAoM) on Computer Science, San Diego, CA, pp. 324-329, August 1999.
- [8] J. Fiedler and J. Hammer, "Using Mobile Crawlers to Search the Web efficiently", International Journal of Computer and Information Science, vol.1, no.1, pp.36-58, 2000.
- [9] J. Kleinberg, "Authoritative sources in hyperlinked environment", In Proceedings of the 9th Annual ACM-SIAM Symposium on Discrete Algorithms, pp:668-677, 1998.
- [9]. Mark Najork, Allan Heydon, "High- Performance Web Crawling", September 2001.
- [10]. Mike, Burner, "Crawling towards Eternity : Building an archive of the World Wide Web", Web Techniques Magazine, vol 2 ,no 5, May 1997.
- [11]. Niraj Singhal, Ashutosh Dixit, "Retrieving Information from the Web and Search Engine Application", In Proceedings of National Conference on "Emerging Trends in Software and Network Techniques- ETSNT'09", Amity University, Noida, India, Apr 2009 .
- [12] Odysseas Papapetrou and George Samaras, "Distributed Location Aware Web Crawling", 2004, ACM, New York, USA.
- [13] P. Boldi, B. Codenotti, M. Santini and S. Vigna, "UbiCrawler: A Scalable Fully Distributed Web Crawler, Software, Practice and Experience", Vol. 34, No. 8, pp. 711-726, 2004,
- [14] D. Gomes and M.J. Silva, *The Viuva Negra Crawler*, Software, Practice and Experience, , Volume 38, No. 2, 2008
- [15] Rahul Mahajan, Dr. S.K. Gupta, Mr. Rajeev Bedi, "A Survey of Duplicate And Near Duplicate Techniques, International Journal of Scientific & Engineering Research, Volume 5, Issue 2, February-2014
- [16]. Sergey Brin, Lawrence Page, "The anatomy of a large - scale hyper textual Web search engine", Proceedings of the Seventh International World Wide Web Conference, pages 107-117, April 1998.
- [17] S.Brin , L. Page , R. Motwani , T. Winograd , " What can you do with a Web in your Pocket?", Bulletin of the Technical Committee on Data Engineering, pp: 37-47 , 1998

Time Frequency Based Evaluation of Surface Electromyogram Signal Using Non Invasive Technique

Tanu Sharma*¹, Deepak Agarwal²

¹M.tech Student , Computer Science Department, BBSBEC, Fathegarh Sahib, Punjab, India

²Assistant Professor, Computer Science Department, BBSBEC, Fathegarh Sahib, Punjab, India

Abstract

It is well known that Surface Electromyography is activity generated due to a muscle activity and these signals can be easily acquired from surface of skin of the body using non-invasively technique and research with various algorithms for control of upper arm prostheses have been reported. In this investigation the Surface Electromyogram signal's study for upper arm muscles with different operation of arms were presented. Myoelectric signals from said muscles were extracted using Labview based soft scope simulated code. Acquiring Surface Electromyogram data from selected locations were interpreted for various feature extractions using various time and frequency domain parameters for computation of data in a way to analyze the effectiveness of recorded signal.

Keywords: Electromyogram signal, Simulation, RMS, Median frequency, interpretation, signal processing, arm motions.

I. INTRODUCTION

Electromyogram signal is a measure of electrical currents generated in muscle for measuring its responses. The nervous system controls the muscle activity i.e. contraction or relaxation of muscle. Because of its random nature, signal is controlled by the nervous system and is dependent on the anatomical and physiological properties of muscles. Surface Electromyogram sensor at the surface of the skin collects signals from different motor units at a time generated due to interaction of different action potential signals. Due to the complexity of Surface Electromyogram signal, powerful and advance methodologies of analysis are becoming a very important requirement in biomedical engineering [1-2].

Electromyography provides easy access to physiological processes that cause the muscle to generate force, produce movement and accomplish the countless functions to interact with the world around us. It provides many important signals which are still to be understood to extract important information. Signal acquisition using non invasive technique with its processing has been a challenging labor preferred as it does not require any medical qualification [3]. The membrane potential in the muscle is about -90 mV with the range of measured Surface Electromyogram potential lying between 0 to 10mV (peak to peak) with frequency range of 2 to 10 kHz having the most relevant information below 500 Hz [4-5].

The effect of force contraction at different levels on median frequency of Surface Electromyogram has been reported in various studies. Researchers have shown that under isometric conditions there exists linear relationship between median frequencies of Surface Electromyogram and force contraction [6]. The formal scheme of this paper is organized in following manner: the basic theory behind Surface Electromyogram signal production from muscles and its acquisition using LABVIEW, subsequent signal conditioning and processing, then the feature extractions and finally results and conclusion.

II. THE FORMAL SCHEME

A. Surface Electromyogram signal Acquisition

Surface Electromyogram signals were collected using non invasive electrodes at skin surface from the above elbow arm which have further been used for upper limb prosthetic control. A good acquisition of the Electromyogram signal is a prerequisite for good signal processing. The placement of electrodes of proper location is an important issue as Surface Electromyogram signal amplitude is influenced by electrode location.

Two positions, namely Biceps Brachii and Triceps Brachii were identified for signal acquisition in this experiment.

B. Signal Processing

The raw signal extracted using non invasive electrode consists of various kind of noise, so signal conditioning and processing is required in order to reduce artifacts and getting important information for data analysis. Signal processing is implemented using LABVIEW as this platform provides many mathematical tools for analyzing signal characteristics. Signal is amplified and passed from band-pass filter with high CMRR and gain in order to reduce motion artifacts (HPF) and noise (LPF) [4], [7].

C. Feature Extraction and Analysis

Different parameters are calculated for Surface Electromyogram signal acquired from all the subjects. The calculation of parameters that extracted is as follows:

a. Root mean square: The root mean square is a statistical measure of the magnitude of a varying quantity. It is especially useful when variants are positive and negative. RMS value is a quantity used to quantify ac quantities. Hence signals with higher energy have higher RMS values. It is defined as:

$$V_{\text{rms}} = \sqrt{\frac{(x_1^2 + x_2^2 + x_3^2 + \dots + x_n^2)}{n}}$$

b. Median Frequency [8]: Median frequency (MDF) is described as the frequency which divides the power contained in the signal into two equal halves. The unit of measurement is Hz.

c. Standard Deviation: It is the measurement of variability or diversity used in statistics and probability theory. It shows variation or dispersion from the average (mean, or expected value). A low standard deviation indicates that the data points tend to be very close to the mean whereas high standard deviation indicates that the data are spread out over a large range of values. It is given by the equation:

$$SD = \sqrt{\frac{\sum (x_i - u)^2}{n - 1}}$$

d. Energy: It is also defined as simple square integral (SSI). It is the summation of square values of the amplitude of sEMG signal samples and is given by the equation:

$$E = \sum_{n=1}^N |x(n)|^2$$

e. Power Spectrum: For a given signal, the power spectrum gives a plot of the portion of a signal's power (energy per unit time) falling within given frequency limits. Power spectrum of signal gives peaks at the fundamental harmonics. Quasi periodic signals give peaks at linear combinations of two or more irrationally related frequencies (often giving the appearance of a main sequence and sidebands) and chaotic dynamics gives broad band components to the spectrum.

III. METHODOLOGY

Activities Performed: Subjects were seated on a chair. Each subject was asked to perform four different movements for different muscles activation. These four different movements are as follows:

- ✓ P1- Arm was in rest with downward position parallel to body.
- ✓ P2- Hand was moved upside. This position is called flexion elbow.
- ✓ P3- Arm was rotated in clockwise direction.
- ✓ P4- Arm was rotated in anticlockwise direction.

Experiment: Five healthy male volunteers, age 22-28 year, weight 55-90 Kg's and height of 170 to 180 cm participated in the complete part of this study. They were not informed of what the experiment was about. The Surface Electromyogram signal was acquired from two upper-arm muscles, the biceps and triceps brachii as shown in Fig. 1 through non invasive electrodes placed on the midline of muscle belly using NI DAQ card and LABVIEW based soft scope code.



Figure 1 SEMG Sensor placement for biceps and triceps positions for AE [9]

The samples were saved with specific name in the workspace. LABVIEW has large number of functions for numerical analysis and design and visualization of data. It is a graphical development environment with built in functionality for data acquisition, instrument control, measurement analysis, and data presentation.

About 1024 samples were recorded for the time window of 3000ms of the soft scope in the workspace. A program was made to filter the signal in the frequency band 70 to 280 Hz in order to minimize movement artifacts and aliasing effect. The different parameters were then calculated. The general schematic of proposed system is illustrated in Fig. 2. In order to understand Surface Electromyogram signal's behavior, the experiment was carried out in two phases. In first phase, the arm is at "rest" without moving hand (No Surface Electromyogram) and in second phase, it is with different movements (with Surface Electromyogram).

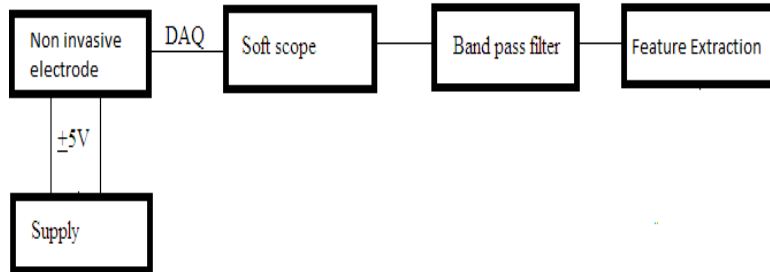


Figure 2 Block diagram of the system

IV. RESULT

The observations were taken from different subjects from two different points with different movements and are tabulated in figure 3 & 4. It is clear that there value of Root mean square amplitude are more than in rest position from both muscles. From figure 3 and 4, it is evident that there is change in V_{rms} value for flexion elbow (P2) movement for both biceps and triceps muscles as compared to rest (P1) position. Figure 5 and 6 shows that V_{rms} for clock wise (P3) movements is higher than anti-clock wise (P4) movements with biceps muscle and for triceps muscle anti-clock (P4) has higher value compare to clk (P3) movement respectively.

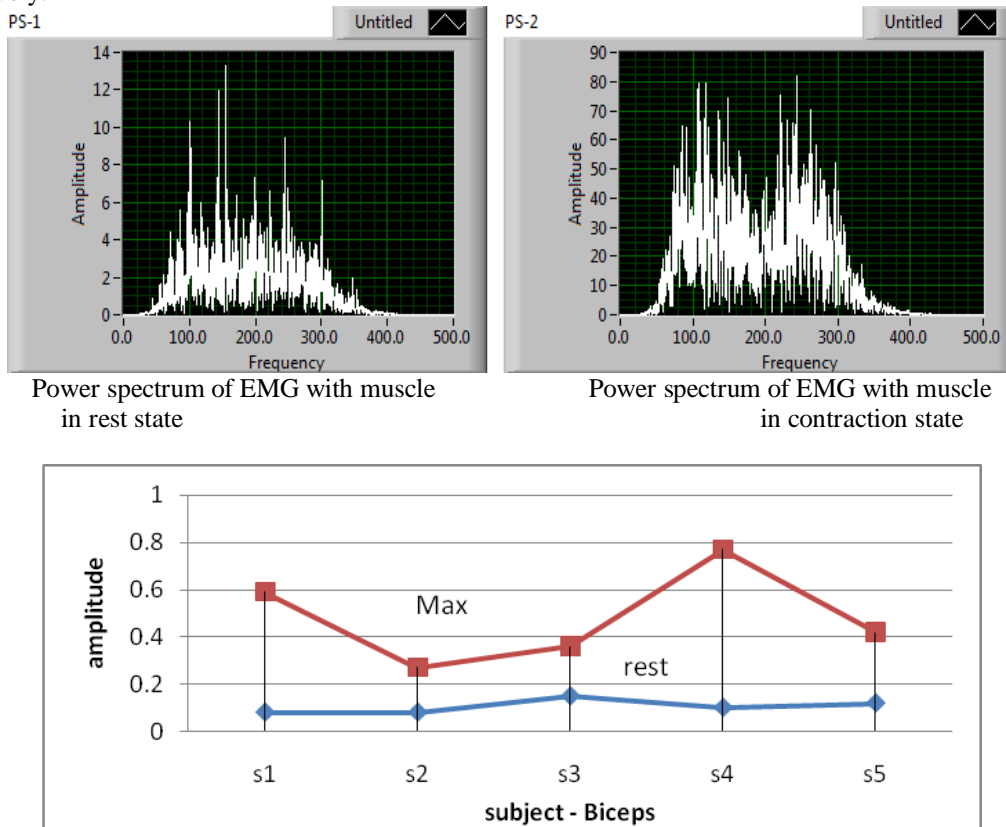


Figure 3 Results for activity P1 and P2 for biceps muscles

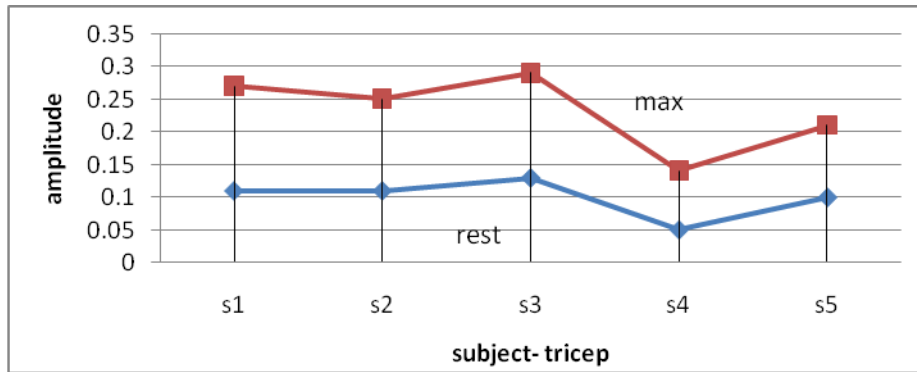


Figure 4 Results for activity P1 and P2 for triceps muscles

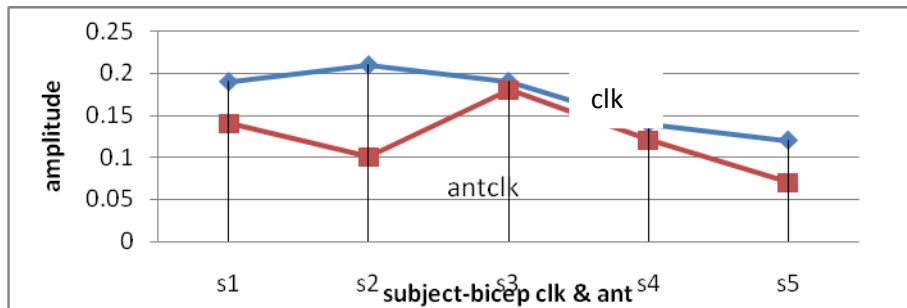


Figure 5 Results for activity P3 and P4 for biceps muscles

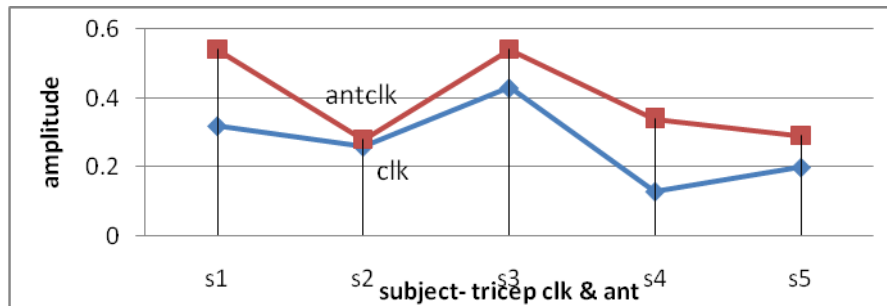


Figure 6 Results for activity P3 and P4 for triceps muscles

Table 1. Comparison of Parameters

Parameters	No Surface Electromyogram	With Surface Electromyogram
V_{rms}	0.08	0.59
SD	0.0627	0.5882
Median Freq. (*1000)	0.1305	0.2429
Energy (*1000)	0.0118	1.0363

V. CONCLUSION

Surface Electromyogram signal is random in nature and some-how the complete study of these signals is complex. The work done on these signals at different locations with different movements will act as helping tool for future work to control artificial arm for above elbow. It can be concluded that biceps muscle is dominant for P-2 (elbow flexion) movements whereas triceps muscle is dominant for P-4 (anti clockwise) movements, whereas for P-3 movement both has moderate values. Figure 7 shows different calculated features with no Surface Electromyogram and with Surface Electromyogram giving relationship between median frequency and force of contraction. The result also shows that content of the signal are highly dependent upon the proper location of placement of electrodes. In future studies more advanced signal processing and evaluation techniques will be implemented for the interpretation of effectiveness of recorded signal.

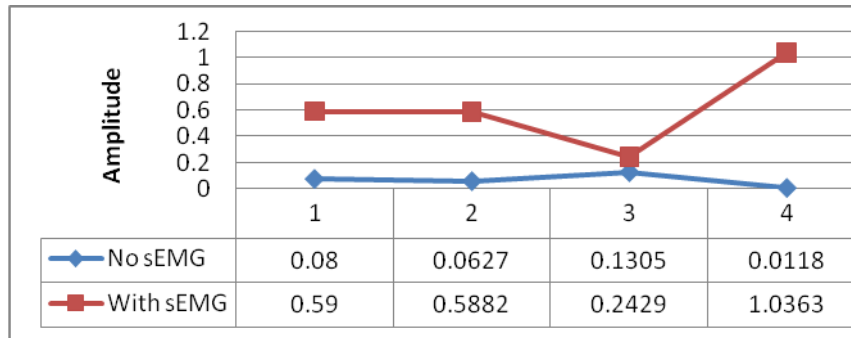


Figure 7 Comparisons of Parameter

REFERENCES

- [1]. Reaz MBI, Hussain MS and Mohd-Yasin F. Techniques of EMG Signal Analysis: detection processing, classification and applications. *IEEE Transactions on Biomedical Engineering*, 10:11-35, 2006.
- [2]. <http://www.ncbi.nlm.nih.gov/pmc/articles/PMC1455479>.
- [3]. DeLuca CJ. The use of surface electromyography in biomechanics. *Journal of Applied Biomechanics*, 13: 135-163, 1997.
- [4]. Jung Kyung and Kim Joo Woong. EMG Pattern Classification using Spectral Estimation and Neural network, *SICE Annual Conference, Kagawa University, Japan*, pages 1108-1111. 2007.
- [5]. Micera Silvestro. Control of hand prostheses using peripheral information. *IEEE reviews in BME*, 3: 48-68, 2010.
- [6]. K A Wheeler, H Shimada, D K Kumar and S P Arjunan. A sEMG Model with Experimentally Based Simulation Parameters, *32nd Annual International Conference of the IEEE Engineering in Medicine and Biology Society, Argentina*, pages 4258-4261, 2010
- [7]. Zecca M and Micera S. Control of Multifunctional Prosthetic Hands by Processing the Electromyographic Signal. *Critical Reviews in Biomedical Engineering*, 30: 59-485, 2002.
- [8]. DeLuca CJ and Roy Serge H. Median frequency of the myoelectric signal, effect of hand dominance. *Eur. Journal of Appl. Physiology*, 55: 457-464, 1986.
- [9]. Cram R J, Kasman S G, and Holtz J. *Introduction to surface electromyography*, Aspen Publishers, 1998.

Design of Wireless to Wired Audio Conversation System

Digambar P. Patil¹, Prof. B. T. Salokhe²

¹, PG Student, ², (Associate. Professor) Electronics Dept., TKIET Warananagar, Maharashtra, India

ABSTRACT

We have design of the wired system as Audio transmitter and receiver with Microcontroller, LCD, Keypad, Audio amplifier, Speaker, Mike and Interfacing Circuitry is a wired communication system so there is no radiation effect on human body that's why we made wireless to wired audio conversation system. The design of this audio conversation system mainly consists of GSM Modem, Interfacing Circuitry and Microcontroller. The GSM Modem as wireless unit has antenna to receive and transmit the signal, and also it has SIM slot to keep the SIM card in that slot. It has Serial communication port for interfacing with other peripherals. We have used the Microcontroller as a central processing unit to perform different operations. We have used GSM Modem for transmission and reception of audio information from wired system through a SIM card which is placed in GSM Modem. At wired system there is hardware same like a telephone Receiver system. We made the connection between wireless system and wired system by using cables or wires. So as the distance increases away from cell phone handset of human body, the effect of cell phone radiation on it goes on decreasing, similarly it happens in this design.

Keywords - GSM Modem, Microcontroller, Serial Connection, I/O devices, Power Supply

1. INTRODUCTION

PIC microcontroller PIC18F4520 is used in this System. Digital data comes from GSM Modem port and passes it to the microcontroller for incoming call. GSM Modem continuously sends data from the distant site. This system is interfaced with a GSM modem. This GSM Modem senses the conditions continuously and sent signal to the wired unit for incoming call. Incoming call indicated by Buzzer and the received data is displayed on the LCD. 16X 2 LCD is provided for user interface. After receiving the signal by the microcontroller it processes the data and sends the read data using keypad to mobile number through GSM modem. The GSM modem is connected to microcontroller using RS232 interface. Whenever user wants to make outgoing call, it send signal from wired unit using keypad and LCD to the GSM modem, the GSM modem receives the data and sends to another subscriber.

2. Block Diagram

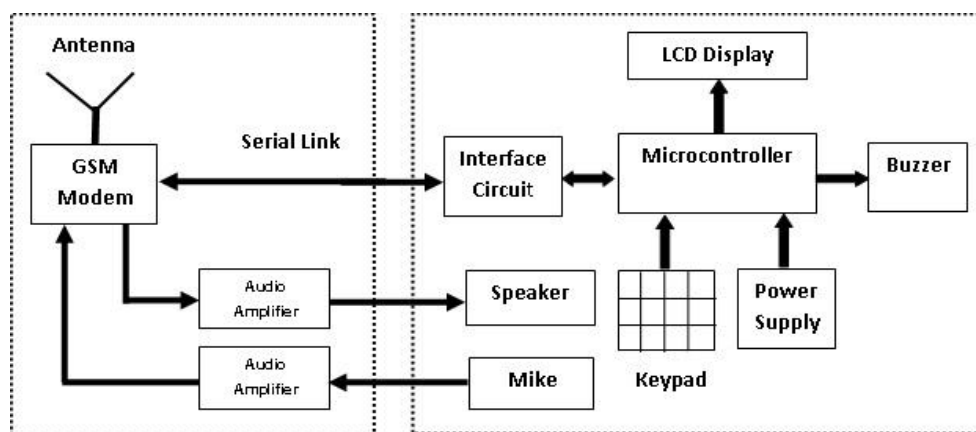


Figure 1 Design of Wireless to Wired Audio Conversation System

2.1 Working

- This system uses PIC microcontroller PIC18F4520. This system is interfaced with a GSM modem.
- RS-232 serial interface is used to transmit and receive the signal from Microcontroller unit and from GSM Modem.
- Since RS232 is not compatible with microcontrollers we need a voltage converter to convert the RS232's signals to TTL voltage levels. The MAX 232 converts the RS232 voltage levels to TTL voltage levels and vice versa.
These are acceptable to the microcontroller's TxD and RxD pins.
- This transceiver data is sensed by the microcontroller and the system continuously monitors the data condition.
- The system monitors the conditions continuously and sends signal to and from SIM to the Microcontroller unit.
- This data is displayed on LCD every time.
- for incoming call to the system SIM or user, the GSM modem gets signal through antenna and transmits it to the Microcontroller via RS-232 serial interface then that signal is displayed on LCD and also buzzer provides beep indications by Microcontroller. Using ATA Command we can receive this call. This ATA Command is assigned with "R" button on Keypad. When we push "R" button on keypad the call may get connected. To disconnect the call we can use ATH Command. For this we can use "H" button on Keypad.
- for outgoing call Microcontroller sends data using RS-232 serial interface to the GSM modem using keypad. Using keypad we can dial a number, it is shown on LCD. After typing a number we can press "C" button on keypad for calling to other subscriber.

3. GSM Modem

This GSM Modem can accept any GSM network operator SIM card and act just like a mobile phone with its own unique phone number. Advantage of using this modem will be that you can use its RS232 port to communicate and develop embedded applications. Applications like SMS Control, data transfer, remote control and logging can be developed easily. The modem can either be connected to PC serial port directly or to any microcontroller. It can be used to send and receive SMS or make/receive voice calls. It can also be used in GPRS mode to connect to internet and do many applications for data logging and control. The Modem is designed with RS232 Level converter circuitry, which allows you to directly interface PC Serial port. The baud rate can be configurable from 9600-115200 through AT command. Initially Modem is in Autobaud mode. This GSM/GPRS RS232 Modem is having internal TCP/IP stack to enable you to connect with internet via GPRS. It is suitable for SMS as well as DATA transfer application in M2M interface. The modem needed only 3 wires (Tx, Rx, GND) except Power supply to interface with microcontroller.

3.1 Features of SIM300 GSM Module

Uses the extremely popular SIM300 GSM module

- provides the industry standard serial RS232 interface for easy connection to computers and other devices
- provides serial TTL interface for easy and direct interface to microcontrollers
- Power, RING and Network LEDs for easy debugging
- can be controlled through standard AT commands
- Module's operation mode can be controlled through the PWR Switch connected to the PWR pin
- The SIM300 allows an adjustable serial baud rate from 1200 to 115200 bps
- Operating Voltage: 7– 15V AC or DC (board has onboard rectifier), Designed for global market, SIM300 is a Tri-band GSM engine.
- Works on frequencies EGSM 900 MHz, DCS 1800 MHz and PCS 1900 MHz
- SIM300 can fit almost all the space requirements in your applications, such as smart phone, PDA phone and other mobile devices.
- Supports features like Voice, Data/Fax, SMS, GPRS and integrated TCP/IP stack.

3.2 Interfaces

RS-232 through D-TYPE 9 pin connector,

- Serial port baud rate adjustable 1200 to 115200 bps (9600 default)
- BRK connector for MIC & SPK, SIM card holder
- Power supply through DC socket
- SMA antenna connector and Murata Antenna (optional)
- LED status of GSM / GPRS module

3.3 AT Commands

AT Commands are used to control a modem. AT means Attention. Every command line starts with "AT". These are of two types: Basic and Extended.

- ATE0 – Echo off
- ATE1- Echo on

Initiating outgoing call:

- ATD+mobile number; <enter key>

For disconnecting the active call:

- ATH<enter key>

For receiving incoming call:

- ATA<enter key>

4. Wired Hardware Unit

This unit has Microcontroller, Keypad, LCD, Speaker, and Microphone. This Microcontroller family offers the advantages of all PIC18 microcontrollers namely, high computational performance at an economical price, with the addition of high endurance, Enhanced Flash program memory. On top of these features, the PIC18F2420/2520/4420/4520 family introduces design enhancements that make these microcontrollers a logical choice for much high performance, power sensitive applications. The PICkit 2 Development Programmer/Debugger is a low-cost development programmer. It is capable of programming most of Microchip's Flash microcontrollers and serial EEPROM devices. The PICkit 2 unit hardware prevents it from being powered by the target through the ICSP connector VDD pin. The PIC 18F4520 has 5 usable ports or I/O registers. These ports are labeled A-E with Ports A-D having 8 bits each and Port E having 4 bits.

4.1 RS 232 Circuit

Since RS232 is not compatible with microcontrollers, we need a voltage converter to convert the RS232's signals to TTL voltage levels. These are acceptable to the microcontroller's TxD and RxD pins. The MAX 232 converts the RS232 voltage levels to TTL voltage levels and vice versa. The chip uses +5V power source which is the same as the power source for the microcontroller. It provides 2-channel RS232C port and requires external 10uF capacitors.

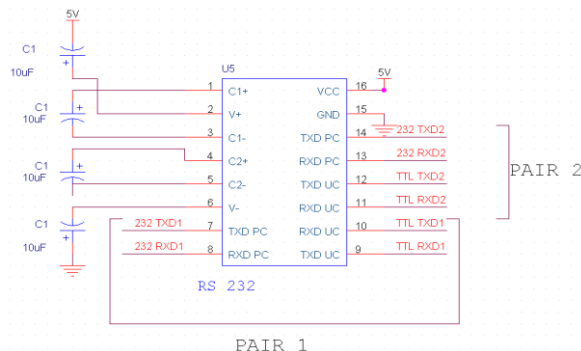


Figure 2: Interfacing of RS232

5. SOFTWARE TECHNOLOGIES

The software part will consist of: 1. mikroC PRO for PIC 2. Orcad. These two parameters are useful for programming and drawing the circuits respectively. The mikroC PRO software is used for Programming code which is to be transplanted into PIC microcontroller and Orcad is used for circuit simulation and layout design. The mikroC PRO for PIC is a powerful, feature-rich development tool for PIC microcontrollers. It is designed to provide the programmer with the easiest possible solution to developing applications for embedded systems, without compromising performance or control. PIC and C fit together well: PIC is the most popular 8-bit chip in the world, used in a wide variety of applications, and C, prized for its efficiency, is the natural choice for developing embedded systems. mikroC PRO for PIC provides a successful match featuring highly advanced IDE, ANSI compliant compiler, broad set of hardware libraries, comprehensive documentation, and plenty of ready-to-run examples. The fast growing market of embedded systems there is an increasing need to write application programs in a high-level language such as C. Basically there are two reasons for this trend: programs for embedded systems become more complex (and hence are difficult to maintain in assembly language), and processor models for embedded systems have a decreasing lifespan (more frequent re-adapting of applications to new instruction sets). The code re-usability achieved by C- programming is considered to be a major step forward in addressing these issues.

5.1 Flowchart of the System:

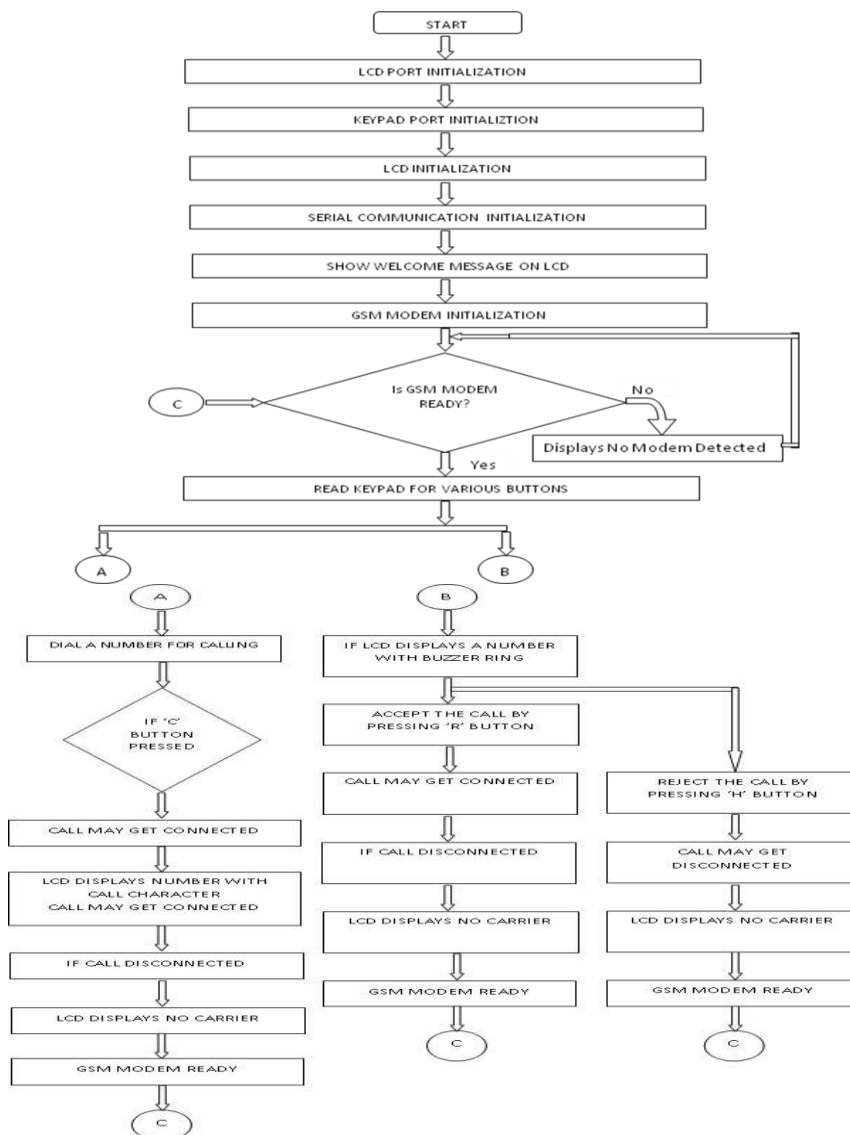


Figure 3: Flow Chart of System

6. RESULTS

Basically there are three conditions for this system. First, when there is no conversation using this system, system is Idle. Second, for incoming call to the system SIM or user, the GSM modem gets signal through antenna and transmits it to the Microcontroller via RS-232 serial cable then that signal is displayed on LCD and also buzzer provides beep indications by Microcontroller. Third, for outgoing call Microcontroller sends data using UART and RS-232 serial cable to the GSM modem using keypad to dial the number. In this way this design is used for audio conversation system.

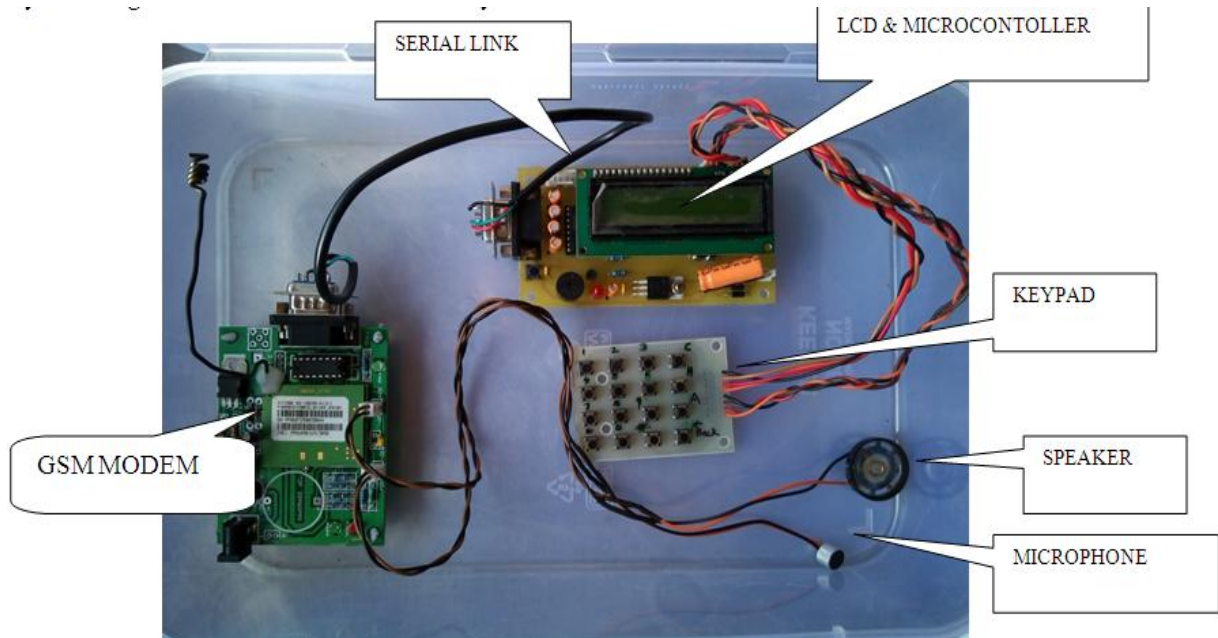


Figure 4: Descriptive Hardware diagram of the Design

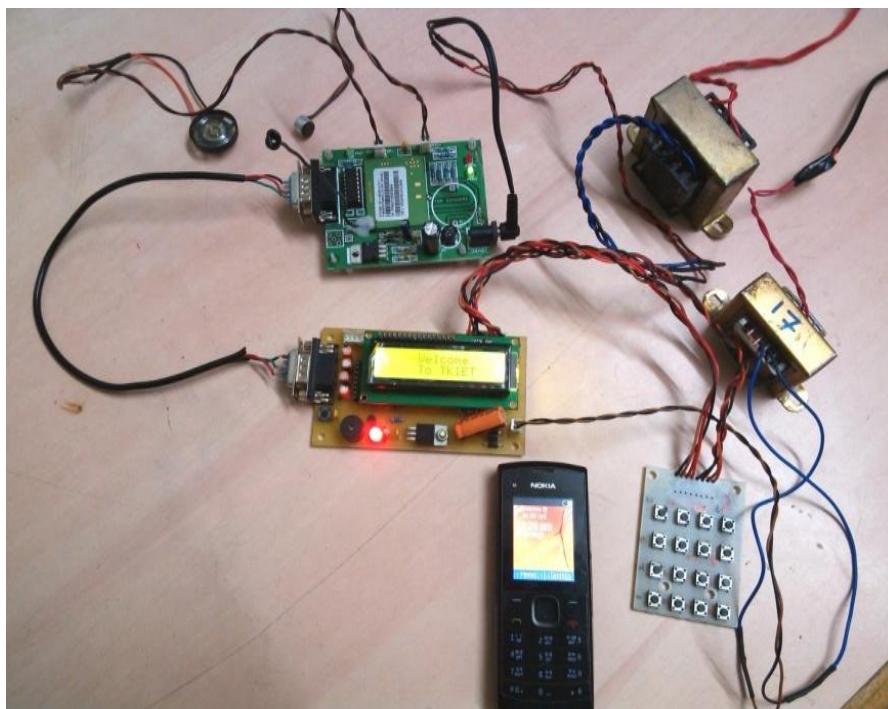


Figure 5: The experimental hardware unit.

Now we can see some results obtained during operation of this conversation system as follows:

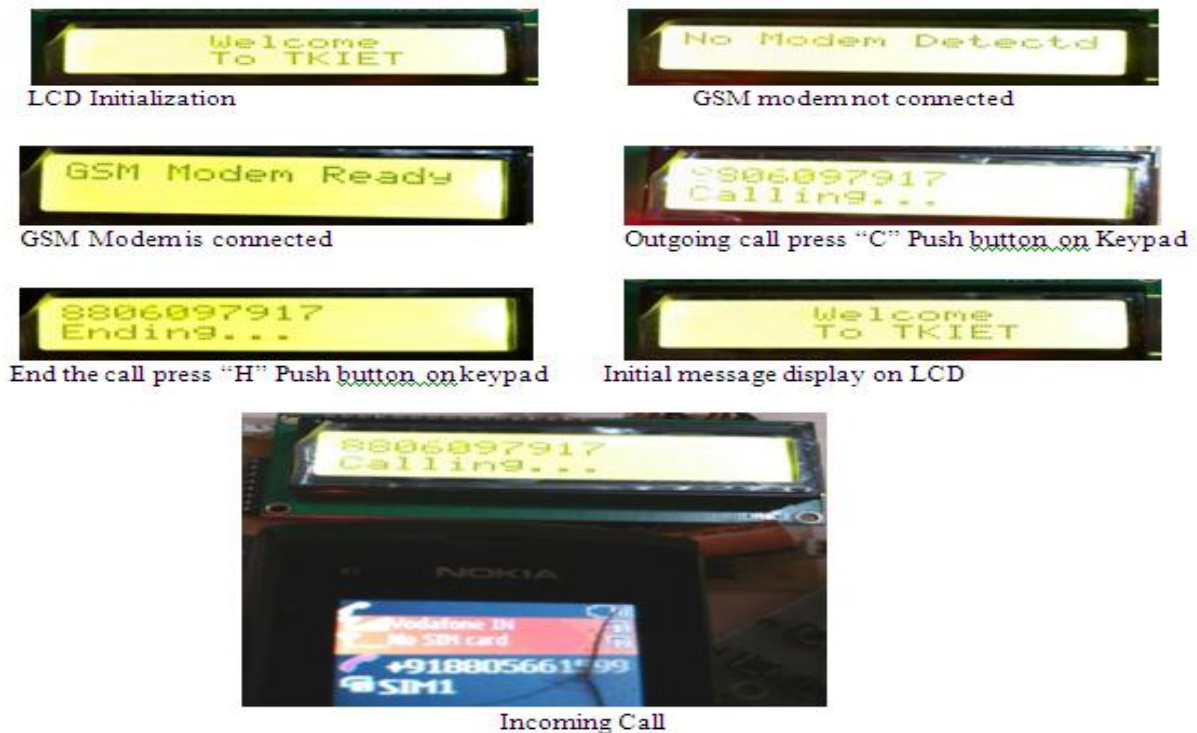


Figure 6: The experimental results

At first LCD displays Initial Message. If GSM Modem is not connected to MCU then it shows a message on LCD as No modem detected. If GSM Modem is connected to MCU then it shows a message as GSM Modem Ready on LCD. For Outgoing call, dial another subscriber number using keypad. For calling press “C” push button on Keypad. To end the call press “H” push button on keypad. After call disconnection, again it will display the initial message on LCD as Welcome to TKIET. For Incoming Call, When another subscriber calling to the SIM which is placed in our system i.e. to the user of this design then it displays a number of called party as shown above.

After call disconnection, it may be due to pressing “H” button by user of this system or by another subscriber in this conversation, LCD displays the same messages as shown in above figures. So these are the Results of this audio conversation system.

REFERENCES

- [1] Vandana Pandya and Deepali Shukla “ GSM Modem Based Data Acquisition System”, *International Journal Of Computational Engineering Research (ijceronline.com) Vol. 2 Issue.5, September 2012*
- [2] Smt.M.Baby, P.Harini, Y.Eleena Slessor, Y.Tejaswi, K.Ramajyothi, M.Sailaja, K.Annie Sumantha “SMS based Wireless E-notice board” *International Journal of Emerging Technology and Advanced Engineering, (ISSN 2250-2459, ISO 9001:2008 Certified Journal, Volume 3, Issue 3, March 2013)*
- [3] Mrs. M.S.Vanjale, Namrata Dokre, Harshad Manekar, Harshal Atwal, “ Gsm Based Water Billing Machine”, *International Journal For Technological Research In Engineering Volume 1, Issue 8, April-2014*
- [4] Dr.B.Ramamurthy S.Bhargavi Dr.R.ShashiKumar , “Development of a Low-Cost GSM SMS-Based Humidity Remote Monitoring and Control system for Industrial Applications”. (*IJACSA) International Journal of Advanced Computer Science and Applications, Vol. 1, No. 4, October 2010*
- [5] Pankaj Verma, J.S Bhatia, “ Design And Development Of Gps-Gsm based Tracking System With Googlemap Based Monitoring ” *International Journal of Computer Science, Engineering and Applications, Vol.3, No.3, June 2013*
- [6] SMS Tutorial –How to use Microsoft hyperterminal to send AT commands
- [7] Hardware description of GSM modem simcom300 reference manual

Embed Watermarking in High of Image Coarseness

Esraa Jaffar Baker¹, Sundos Abdul_ameer Hameed²
^{1,2} Al-Mustansiriyah University/ Iraq/Baghdad

Abstract:

Watermarking is a technique to hide data inside an image to show authenticity or proof of ownership. In this paper (research) the proposed system is an implementation of image watermarking techniques. The proposed watermarking scheme incorporates HVS models into watermark embedding and watermarking is performed in wavelet domain (the implementation of image watermarking scheme incorporates HVS models into watermark embedding and watermarking is performed in wavelet domain was proposed). in this algorithm (our main algorithm is divided into three algorithms). (First,) are (is a find coarseness), (second is to) chosen the high coarseness subband to hide watermarking in it by using coarseness algorithm a applied on many images, (third, is test a) similarity between original image and image watermarking. and the (This) method (was) robust against extracting watermarking on average(80-95%) (when it applied on many images), (the extracted method is implement)by using lowpass and highpass filters in data payload(256 bits).

Keyword: watermark, coarseness, wavelet transform, HVS

I. INTRODUCTION

The rapid growth of the Internet increased the access to multimedia data tremendously. The development of digital multimedia is demanding as an urgent need for protect multimedia data in internet. [1] Digital watermarking is nothing but the technology in which there is embedding of various information in digital content which have to protect from illegal copying. This embedded information to protect the data is embedded as watermark. Digital watermarks are of different types as robust, fragile, visible and invisible .Application is depending upon these watermarks classifications. There are some requirements of digital watermarks as integrity, robustness and complexity.[2] All watermarking methods share a watermark embedding system and a watermark extraction system. There are two main watermarking techniques available: spatial domain and frequency domain. [3] In spatial domain, the pixels of one or two randomly selected subsets of an image are modified based on perceptual analysis of the original image. However in the Frequency or transform domain, the values of certain frequencies are altered from their original image. [4], Various types of frequency transforms that have been used are Discrete Fourier Transform (DFT), Discrete Cosine Transform (DCT), and Discrete Wavelet Transform (DWT). Earlier watermarking schemes used DFT and DCT. [5] The watermarking problem is to achieve a better trade-off between robustness and perceptivity. Robustness can be achieved by increasing the strength of the embedded watermark, but the visible distortion would be increased as well. However, DWT is much preferred because it provides both a simultaneous spatial localization and a frequency spread of the watermark within the host image. The basic idea of discrete wavelet transform in image process is to multi differentiated decompose the image into sub-image of different spatial domain and independent frequencies.[2]

II. HUMAN VISUAL SYSTEM (HVS) IN WATERMARKING

The Human Visual System is found to be less sensitive to the highly textured area of the image. Moreover, in all colors the blue is least sensitive to the HVS (Human Visual System). While working on colored images when using the mathematical and biological models of HVS, the preferred color model must be HSV (Hue, Saturation and Value) color model rather than RGB color model because it most closely defines how the image is interpreted by HVS. The high visual transparency in the technique is achieved.[7] Digital watermarking of images can be performed by employing similar visual models. Robustness, perceptual transparency and capacity are the requirements of digital watermarking techniques.[3][6] This means watermark is made highly robust against different types of attacks by performing the watermark insertion in transformed domain and making use of the transformation functions such as DWT.[7]

III. THE SYSTEM

In this research , the proposed system is an implementation of image watermark techniques. Our system will be used for embedding a watermark string into an image, which is BMP file format image by using wavelet transform technique to embedding text.

3.1 Embedding Algorithm

The wavelet method is depending on the selecting the best sub bands to embedding text watermarking in it depending on high texture in it. The coarseness is the feature of texture used in this method. In our wavelet method, we must compare among three sub band(HH,HL and LH) to choice one of them and embedding in high value coarseness sub band , the technique can be described in algorithm:-

Step1: input original image and watermark text

Step2: convert images RGB channel to grey level (256)

Step3: convert the watermark into steam of bits (0 and 1)

Step4: decomposition image by using wavelet transform, then find all bands of wavelet transform

Step 5: calculate the value coarseness of three subbands(HH,HL and LH) by using coarseness algorithm.

Step 6: compare between three coarseness values and choice the high coarseness value to hide watermark in this subband for it.

Step 7: store two bits key contains of two bits (00, 01, 10) represent LH, HL, HH of subband ; there is benefits to select band of high coarseness, theses bits store in left top corner first two byte of corners from subband LL

Step 8: store data in subband that is high coarseness, the subband is represented by a two dimensional array of values. The present paper divides the subband into non overlapped window of a predefined size. The size of any window is 3 x 3 coefficients. Check the center of window if odd value then store data in first diagonal or if even value store in the first and second diagonal by using LSB.

Example:

In this example see array of subbands 6x6 is proposed:-

Figure (1) shown window 3x3 the center for this window is even number (10) therefore we hidden watermarking in corner coefficients (2,9,22, and 2).

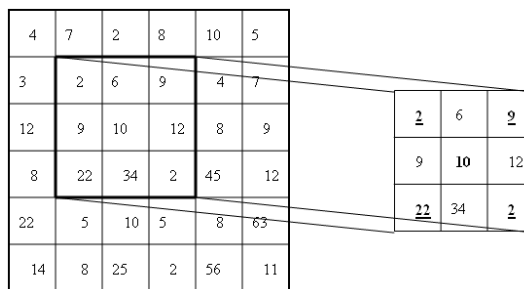


Figure (1) windows the center even and the corner coefficients selected

While in figure (2) see the center is odd number (3) therefore we hidden watermarking in middle coefficients (4,12,9, and 45)

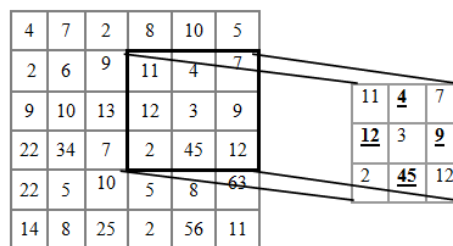


Figure (2) shown windows the center odd and the middle coefficients selected

Step9: saves watermarked color image as BMP (24-bit) file, then displays it.

3.2 Coarseness algorithm

Step1: Coarseness for subband or block can be defined as:-

$$C = 1 - \frac{1}{1 + SD} \dots\dots(3)$$

Step 2: SD is dispersion of the subband, is defined as: - $SD = \sum_{i=0}^{L-1} (i - Sm)^2 h[i] \dots\dots (4)$

h[i] means the histogram of the subband or block

Sm means the Mean of the histogram can be calculated by using equation:-

Step 3: $Sm = \frac{1}{N} \sum_{i=0}^N val [i] \dots\dots (5)$

Val[i] is pixel value

N is the dimension of subband (width X depth) [9]

3.3 Extraction algorithm

In Extracted method, we need to input the image watermarking and the output watermarking text then find two bits from LL corner band to limit the band that using storage on it.

Step1: input image watermarking

Step2: convert images RGB channel to grey level (256)

Step3: decomposition image by using wavelet transform, then find all bands of wavelet transform

Step4: check from key two bits in left top corner first two byte from LL subband to determine the subband that selected to store data watermark in it.

Step5: divide subband that selected into windows 3X3 and check the center of window to determined coefficients extraction text watermarking by using same method in the example.

IV. EXPERIMENTAL RESULTS

In this algorithms, many true color was implemented, Balloons image is a test true color for our *system or method*, Figure(3) was show : (a) origin image, (b) balloon image before hiding a text watermark, (c) balloon image after hiding a text watermark, (d) image watermark after high pass filter, and (e) image watermark after low pass filter.

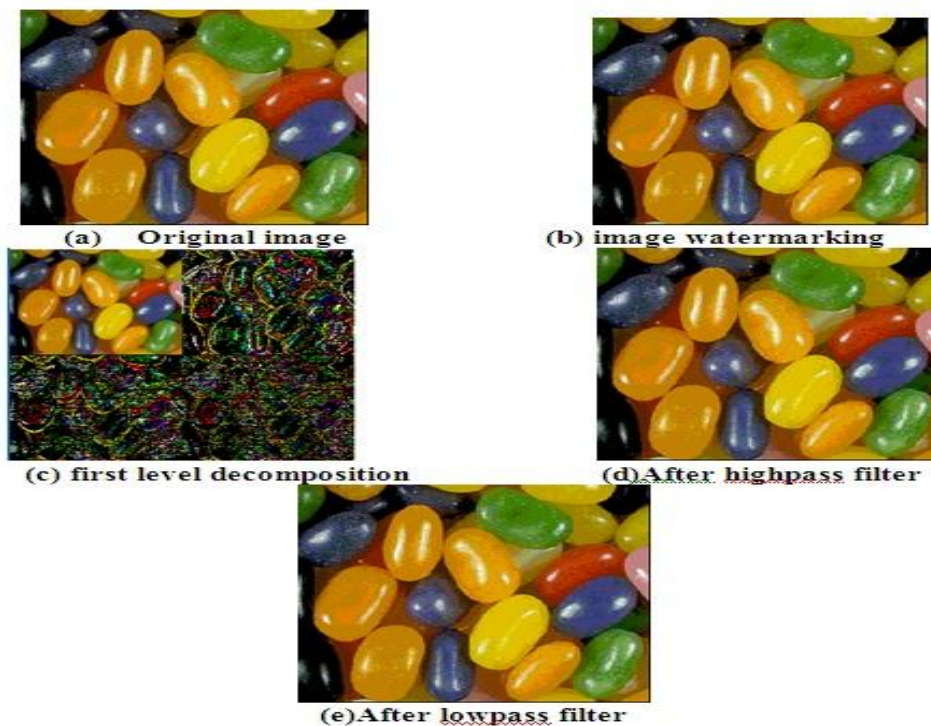


Figure (3) implementation of wavelet method for balloons image

For original image and image after embedded Watermark, an imperceptibility of watermarking is measured by the watermark image quality in term of Peak-Signal-to-Noise Ratio (PSNR) (in dB). Most common difference measure between tow images is the mean square error. The mean square error measure is popular because it correlates reasonably with subjective visual tests and it is mathematically tractable. The quality measure of PSNR is defined with,

$$PSNR = 10 \log_{10} \left(\frac{I_{\max}^2}{MSE} \right) \text{ dB} \dots\dots\dots(1)$$

Where max I is equal to 255 for 8 bit gray scale images.
The MSE is calculated by using the Eq. (2) given below:

$$MSE = \frac{1}{MN} \sum_{i=1}^M \sum_{j=1}^N (Y_{i,j} - S_{i,j})^2 \dots\dots\dots(2)$$

Were, M and N denote the total number of the pixels in the horizontal and the vertical dimensions of the image, Si,j, represent the pixels in the original image, and Yi,j, represent the pixels of the steg-image, the results shows in table(1) and its shown Simulations on the images.

The simulations table, is contains some images was tested through our *system or method*, the coarseness value in each of subbands(LH,HL and HH), PSNR measure for image after: watermark hiding, lowpass and highpass filters, and MSE measure for image after watermark hiding.

Table (1) : Simulations of Test Images

images	subband	Coarseness values	PSNR			MSE After hiding watermarking
			After hiding watermarking	After lowpass filter	After highpass filter	
Balloons	LH	0.156030	61.010457	28.892155	28.795898	0.051527
	HL	0.167565				
	HH	0.114692				
Car	LH	0.460789	38.574837	27.536013	25.826790	9.028105
	HL	0.139319				
	HH	0.381036				
Lion	LH	0.312850	35.772292	29.233935	25.532085	17.212785
	HL	0.329154				
	HH	0.239908				
Sky	LH	0.139608	61.332747	23.095036	23.091272	0.047842
	HL	0.13				
	HH	0.188458				

In **Simulations of Test Images**, the bits embedding in one of three subbands (LH, HL and HH) depending on high value of coarseness and the three values different in each image, the data payload used (256 bit), therefore see in each image choice subband different.

Figure (4), shown the relation between PSNR after hiding watermark in image and after low and high pass filters in four test images(Sky, Lion, Car, and Balloons).

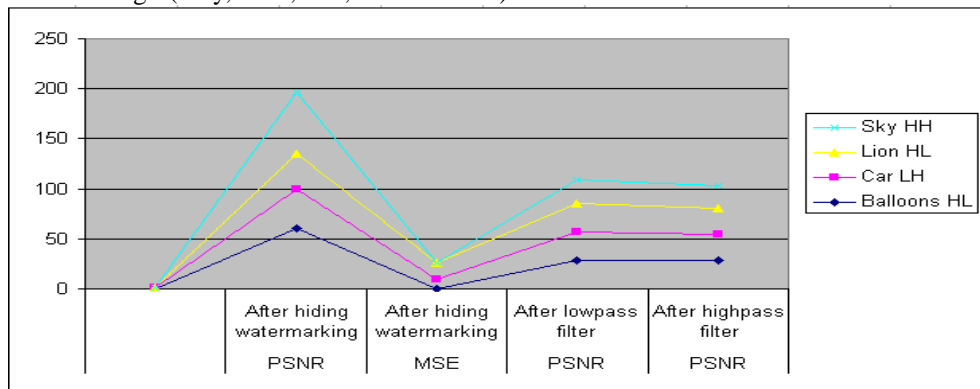


Figure (4) relation between PSNR measure in tested images

V. CONCLUSION

There are number of conclusions were noticed from:-

1. The proposed system gives us the random location of watermark text in different test images.
2. The criteria of accuracy of watermark image acceptable because the PSNR values are high and MSE is low values, it means low distortion and Resistant to low and high pass filter is acceptable.
3. In our method bits of watermarking hiding in different subband(LH,HL and HH) depending on high value of coarseness this increase secure and choice the best subband from HVS system to hide watermarking.

REFERENCES

- [1] G.RoslineNesaKumari, B. VijayaKumar, L.Sumalatha, and Dr V.V.Krishna, "Secure and Robust Digital Watermarking on Grey Level Images", International Journal of Advanced Science and Technology, Vol. 11, October, 2009.
- [2] Pravin M. Pithiya and H.L.Desai, " DCT Based Digital Image Watermarking, De-watermarking & Authentication ", International Journal of Latest Trends in Engineering and Technology (IJLTET), ISSN: 2278-621X, Vol. 2 Issue 3 May 2013.
- [3] Evelyn Brannock , Michael Weeks, and Robert Harrison, " Watermarking with Wavelets: Simplicity Leads to Robustness ", *Computer Science Department Georgia State University Atlanta, Georgia, USA 30303* , 2008 IEEE.
- [4] O P Singh, Satish Kumar, G R Mishra, Charu Pandey, and Vartika Singh " Study of Watermarking Techniques Used in Digital Image", Deptt. of Electronics & Electrical Engineering (ASET), Amity University, Uttar Pradesh, Lucknow_mishra, International Journal of Scientific and Research Publications, Volume 2, Issue 10, October 2012 ISSN 2250-3153.
- [5] C. Patvardhan , A. K. Verma and C. Vasantha Lakshmi," A Robust Wavelet Packet based Blind Digital Image Watermarking using HVS characteristics", International Journal of Computer Applications (0975 – 8887), Volume 36– No.9, December 2011.
- [6] V. Padmanabha Reddy and Dr. S. Varadarajan, "Human Visual System Sentient Imperceptible and Efficient Wavelet-Based Watermarking Scheme for Copyright Protection of Digital Images", IJCSNS International Journal of Computer Science and Network Security, VOL.9 No.4, April 2009.
- [7] Piyush Kapoor, , Krishna Kumar Sharma, S.S. Bedi and , Ashwani Kumar, " Colored Image Watermarking Technique Based on HVS using HSV Color Model", ACEEE Int. J. on Network Security , Vol. 02, No. 03, July 2011.
- [8] Gonzalez R. C. and Woods R. E., "Digital Image Processing", University of Tennessee, Addison-Wesley Publishing Company, Internet Report, 2000 .

Block Based Discrete Wavelet Transform for Image Compression

K. Bhanu Rekha¹, S. Ramachandran²

¹ Sir MVIT, Bangalore

² SJBIT, Bangalore

ABSTRACT

The main challenge in 2-D DWT structure is the amount of internal memory required to produce wavelet coefficients to suit hardware implementation. The previous structures reported need fixed memory size depending on input frame size, but in the proposed technique, memory size is parametric and trades off with the number of output memory accesses. In this method, we divide an image into non-overlapping macro-blocks (16x16 pixels) and to each macro-block 2D-DWT coefficients using lifting scheme are computed. The coefficients obtained from each macro block are Quantized and reconstructed using Inverse Discrete Wavelet Transform. As the image is divided into non-overlapping macro-blocks, it offers a convenient approach for optimum compression using entropy coding where an image has to be divided into code blocks. The proposed Block Based method compares favourably with other methods such as Line Based and Direct methods.

KEYWORDS – Block Based, Discrete Wavelet Transform, PSNR, MSE

I. INTRODUCTION

The two-dimensional Discrete Wavelet Transform (2D-DWT) is nowadays established as a key operation in image processing. In the area of image compression, the 2D DWT has clearly prevailed against its predecessor, the 2D Discrete Cosine Transform. This is mainly because it achieves higher compression ratios owing to the sub-band decomposition, while it eliminates the 'blocking' artefacts that deprive the reconstructed image of the desired smoothness and continuity. The high algorithmic performance of the 2D DWT in image compression justifies its use as the kernel of the JPEG-2000 still image compression standard. The disadvantage of DWT is that it requires more processing power. DCT overcomes this disadvantage since it needs less processing power, but it gives less compression ratio for the same quality. DCT based standard JPEG uses blocks of image, but there is still some correlation existing across blocks [1-4].

For the execution of the multilevel 2D DWT, several computation schedules based on various input traversal patterns have been proposed. Among these, the most commonly used in practical designs are: the Direct and the line-based methods [5, 6].

In this paper, a new non-overlapping block based technique is proposed which ensures faster processing when compared to the Direct and the Line Based methods without compromising on the quality of the reconstructed image. Test images of varying sizes ranging from 150x250 pixels to 600x912 pixels are divided into various sizes from 8x8 pixel blocks to 64x64 pixel macro-blocks in order to arrive at the optimum block size in terms of processing speed and quality. 2D-DWT is applied to each block, Quantized and Reconstructed. Simulation results show the impact of this structure in terms of image quality metrics.

The rest of the paper is organized as follows. Section II briefly reviews the lifting scheme. Section III describes the Direct and the Line Based 2D-DWT Structures followed by a description of the Proposed Technique in Section IV. The next section presents the experimental results and the conclusion is presented in the last section.

II. LIFTING SCHEME

Wim Sweldens developed a lifting scheme for the construction of bi-orthogonal wavelets. The main feature of the lifting scheme is that all constructions are derived in the spatial domain [7-9]. Lifting scheme is a simple and an efficient algorithm to calculate wavelet transforms as a sequence of lifting steps. Constructing wavelets using lifting scheme comprises three steps:

1. *Split step*: The original signal, $X(n)$, is split into odd and even samples.
2. *Lifting step*: This step is executed as N sub steps depending on the type of the filter, where the odd and even samples are filtered by the prediction and update filters, $p(z)$ and $u(z)$.
3. *Normalization or Scaling step*: After N lifting steps, scaling coefficients K and $1/K$ are applied respectively to the odd and even samples in order to obtain the low pass sub band $Y_L(i)$ and the high-pass sub band $Y_H(i)$.

Fig.1 shows the lifting scheme of wavelet filter computing one dimension signal. The inverse transform could easily be found by exchanging the sign of the predict step and the update step and applying all operations in reverse order as shown in Fig. 2. Lifting based

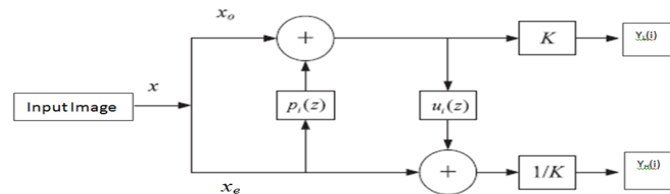


Figure1 Block Diagram of Forward Lifting Scheme

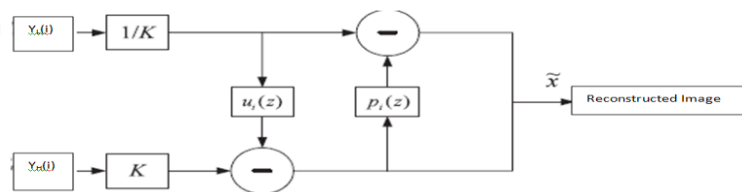


Figure2 Block Diagram of Backward Lifting Scheme

inverse transform (IDWT) is simple and involves the reversal of the order of operations in DWT. Therefore the same resources can be reused to define a general programmable architecture for forward and inverse DWT [10-15].

Lifting scheme implements a filter bank as a multiplication of upper and lower triangular matrices, where each matrix constitutes a lifting step. For the 9/7 wavelet, four lifting steps and one scaling can be used; its poly-phase analysis filter banks $P(z)$ can be written as

$$P(z) = \prod_{i=1}^2 \begin{pmatrix} 1 & s^i(z) \\ 0 & 1 \end{pmatrix} \begin{pmatrix} 1 & 0 \\ t^i(z) & 1 \end{pmatrix} \begin{pmatrix} K & 0 \\ 0 & 1/K \end{pmatrix} \quad (1)$$

where $s^1(z) = \alpha(1+z^{-1})$, $s^2(z) = \gamma(1+z^{-1})$, $t^1(z) = \beta(1+z^{-1})$ and $t^2(z) = \delta(1+z^{-1})$. The parameters α, γ, β and δ are symmetric coefficients while K and $1/K$ are scaling factors.

The lifting steps lead to the following equations:

$$\begin{aligned} \text{Predict P1: } d_i^1 &= \alpha(x_{2i} + x_{2i+2}) + x_{2i+1} \\ \text{Update U1: } a_i^1 &= \beta(d_i^1 + d_{i-1}^1) + x_{2i} \\ \text{Predict P2: } d_i^2 &= \gamma(a_i^1 + a_{i+1}^1) + d_i^1 \\ \text{Update U2: } a_i^2 &= \delta(d_i^2 + d_{i-1}^2) + a_i^1 \\ \text{Scale G1: } a_i &= K a_i^2 \\ \text{Scale G2: } d_i &= d_i^2 / K \end{aligned} \quad (2)$$

The original data to be filtered is denoted by x_i , and the outputs are the approximation coefficients a_i and detail coefficients d_i . The superscripts on intermediate values show the lifting step number.

III. D DWT STRUCTURES

In this section, we will review 2 different structures for 2-D DWT, the direct method and the line based method.

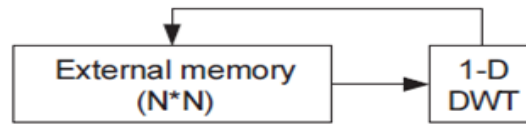


Figure 3 Direct Method

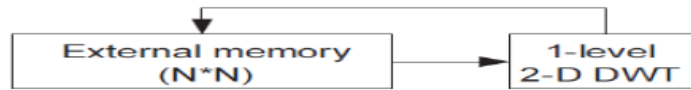


Figure 4 Line Based Method

Direct Method

In this method, the input image is stored in an external memory; scanned row by row and 1-D DWT is applied. The primary outputs are wavelet coefficients computed row-wise and are stored in the external memory. Thereafter, they are input to the 1-D DWT block column-wise. The outputs of the 1-D DWT block are the desired 2-D DWT coefficients of the input image and are stored back in the external memory as shown in Fig. 3. If the computation of coefficients for one more decomposition level is needed, this procedure must be repeated for the LL part of the previous level, whose size is a quarter of the input image size. This routine will be repeated for higher levels. Although the method is simple, the resulting latency and the number of external memory accesses are unduly large [16-19].

Line-based method

The line-based method can be implemented by a 2-D DWT block. In this method, only internal memory is used to compute one level DWT for both the row and column directions. Therefore, there is no external memory access during the computation of one level 2-D DWT. The required internal memory is the sum of the data memory and the temporal memory for each line [20-22]. Once the DWT coefficients are computed, they are stored in the external memory. This line based structure is shown in Fig. 4.

IV. PROPOSED BLOCK BASED METHOD

The block diagram of the proposed structure is presented in Fig. 5. An image is transformed from RGB to Gray component. Then, the component is partitioned into non-overlapping 16x16 pixel Macro Blocks to form an array of "Macro-components". In turn, every Macro-component is wavelet transformed into 4 sub-bands for every level of the wavelet transformation. Then, each Macro Block is Quantized and transformed back using

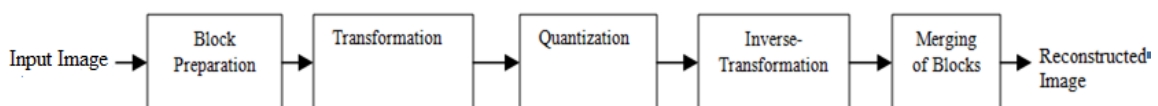


Figure 5 Block Diagram of the Block Based Scheme

Inverse Wavelet transform. The Image is reconstructed by merging all the Macro Blocks to form the Reconstructed Image.

The idea of Macro Block serves the same purpose as the partition of 8x8 blocks in the JPEG standard. All Macro Blocks are handled independently. Therefore, it reduces memory requirements as the entire bit-stream is not needed to process a portion of the image. Macro Block also makes extraction of a region of the image for editing easier by specifying the indexes of the corresponding Macro Block. All Macro Blocks are square and have same dimensions.

Each Macro Block is wavelet transformed into N_L decomposition level. Thereafter, N_L+1 numbers of different resolutions are provided for this macro block. We denote the resolutions by an index r , ranging from 0 to N_L . The lowest resolution is $r = 0$, which is represented by the N_L numbers of LL sub-band coefficients while $r = N_L$ is the highest resolution, which is reconstructed from the 1LL, 1HL, 1LH and 1HH sub-bands. For a specific resolution, r not equal to 0, it is reconstructed from nLL , nHL , nLH , and nHH sub-bands, where n is equal to $N_L - r + 1$.

For a 5-tap or 3-tap wavelet transformation, no quantization is used to reduce the precision of the coefficients. That means the quantization step is one and the coefficients have integer values. On the other hand, for the 9-tap/7-tap wavelet transformation, each sub-band from a Macro Block can have its own quantization step value. The quantization step, Δ_b , for subband b is specified by the following equation:

$$\Delta_b = 2^{R_b - \epsilon_b} \left(1 + \frac{\mu_b}{2^{11}} \right) \tag{3}$$

where R_b is the nominal dynamic range for sub-band b. It is the sum of the number of bits that are used to represent the original source image Macro Block. The exponent, mantissa pairs (ϵ_b, μ_b) are either applied for all sub-bands or for the LL sub-band only. In the latter case, the exponent/mantissa pairs (ϵ_b, μ_b) are determined from the exponent/mantissa pair (ϵ_0, μ_0) corresponding to the LL sub-band, according to the following equation:

$$(\epsilon_b, \mu_b) = (\epsilon_0 + nsd_b - nsd_0, \mu_0) \tag{4}$$

where nsd_b denotes the number of sub-band decomposition levels from the original image Macro block to the sub-band b. Therefore, ϵ_b for the lower frequency sub-bands tend to be larger and render the quantization steps for these sub-bands to be smaller. Therefore, less distortion results from the quantization error. Each of the wavelet transformed coefficients, $a_b(u,v)$ of the sub-band b is quantized into $q_b(u,v)$ according to the following equation:

$$q_b(u,v) = \text{sign}(a_b(u,v)) \times \left\lfloor \frac{|a_b(u,v)|}{\Delta_b} \right\rfloor \tag{5}$$

The decoding procedures perform only the inverse functions of the Wavelet Transform. The Macro Blocks are merged to reconstruct the image.

V. EXPERIMENTAL RESULTS

The quality of the reconstructed image is computed using a Mean Square Error. This requires the original and the reconstructed image of the same size to evaluate the error between them. The quality measure PSNR is expressed in decibel scale (dB). High value of PSNR indicates a high quality of image [23, 24]. It is defined using Mean Square Error (MSE). Lower value of MSE results in higher value of PSNR. The PSNR is expressed as:

$$PSNR = 10 \cdot \log_{10} \left(\frac{255^2}{MSE} \right) \tag{6}$$

where

$$MSE = \frac{1}{m \cdot n} \sum_{i=0}^{m-1} \sum_{j=0}^{n-1} [I(i,j) - K(i,j)]^2 \tag{7}$$

$I(i,j)$: Original Image
 $K(i,j)$: Reconstructed Image and
 $m \times n$: Total number of Pixels in the Original image.

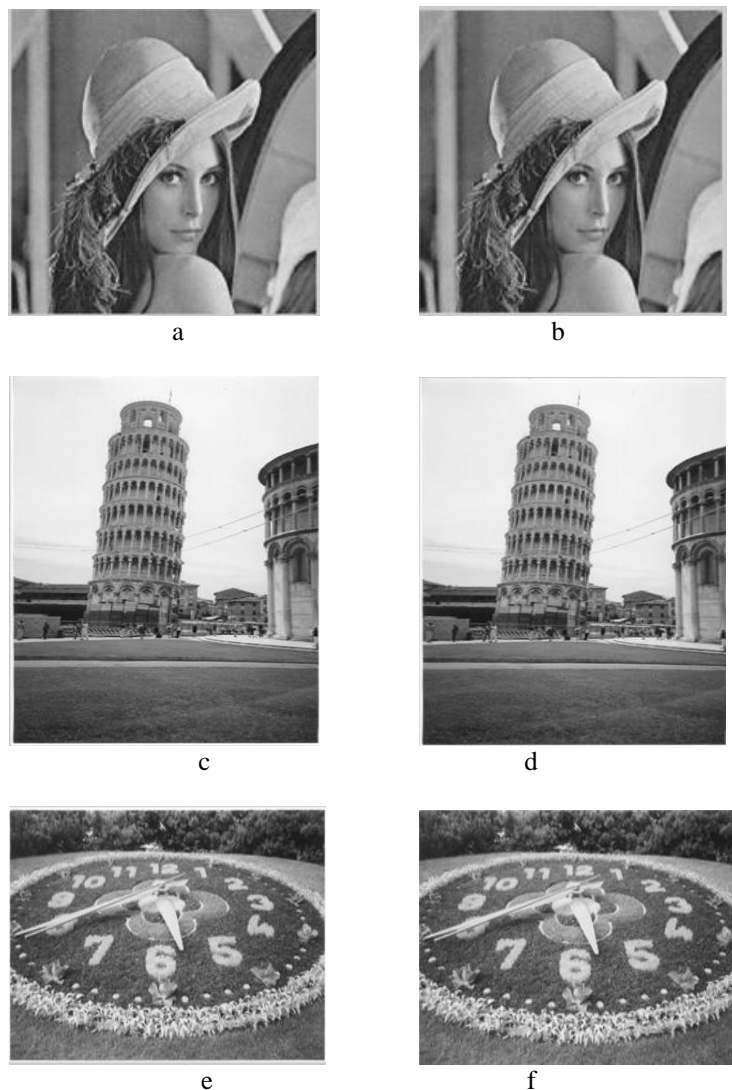
The Block based scheme was implemented in Matlab. As examples, four “standard” test images were chosen for the experiment. All these test images have different dimensions. As per the requirements of JPEG2000 standard, one can select blocks of size 4x4 pixels or more. Smaller the block size, smaller will be the computation time required for processing transforms DWT and IDWT. However, if transformed coefficients are quantized, artefacts are likely to manifest along the edges since there is no correlation between two adjacent blocks transformed. Therefore, a higher sized block would be optimum in terms of computation time as well as minimizing artefacts. For these reasons, macro block of size 16x16 pixels are chosen in the present work.

Table 1 Comparison of Quality of Reconstructed Images Using Different Methods and the Proposed Method

Level of Decomposition: 2D-DWT

Input Image	PSNR for Direct DWT in dB[22]	MSE for Direct DWT	PSNR for Line based DWT in dB	MSE for Line based DWT[23]	PSNR for Block Based DCT in dB	MSE for Block Based DCT in dB	PSNR Proposed Method 16x16 pixels in dB	MSE Proposed Method 16x16 pixels
Lena1.tiff	53.0	0.2	53.0	0.2	34.9	20.9	51.9	0.27
Pisa1.tiff	52.3	0.3	52.3	0.3	36.9	13.0	52.1	0.26
clkgeneva1.tiff	51.8	0.4	51.8	0.4	33.5	28.4	51.7	0.28
titanic51.tiff	53.0	0.3	53.0	0.3	41.9	4.1	52.3	0.25

Table 1 presents the quality measure of the reconstructed images obtained by the proposed method as well as that for other methods. It may be seen that the reconstructed image quality got by the proposed method is comparable with other methods such as the Direct and the Line based methods. The proposed block processing scheme improves the on-chip memory and frame buffer utilization to suit hardware implementation of 2-D DWT/IDWT structure. The reconstructed images by the block based method are presented for various test images in Fig. 7. It may be observed that there are no blocking artefacts.



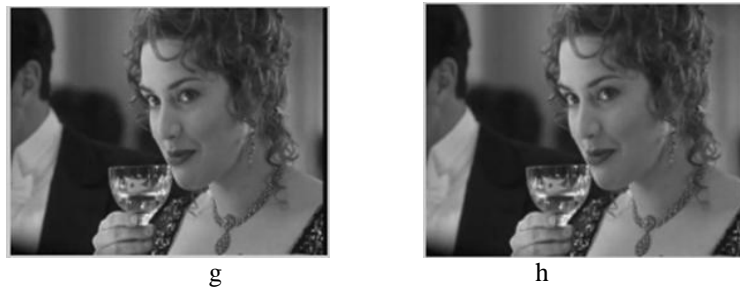


Figure 7 Original and Reconstructed Images Using the Proposed Method

- | | |
|---------------------------------|--|
| (a) Original Lena Image | (b) Reconstructed Lena image, PSNR = 51.9 dB |
| (c) Original Pisa Image | (d) Reconstructed Pisa image, PSNR = 52.1 dB |
| (e) Original Clock Geneva Image | (f) Reconstructed Clock Geneva image, PSNR = 51.7 dB |
| (g) Original Titanic Image | (h) Reconstructed Titanic image, PSNR= 52.3 dB |

VI. CONCLUSION

A block based 2D-DWT/IDWT has been implemented in Matlab by applying the transforms on macro block basis in order to minimize artefacts as well as to speed up hardware implementation. This method also helps in the reduction of on-chip memory requirements of the implementation. The original image is divided into non-overlapping macro-blocks, and as a result it offers a convenient approach for compression using entropy coding where an image has to be divided into code blocks. The proposed Block Based method is more favourable in terms of less computation time and less memory utilization when compared to other methods such as the Line Based and Direct methods. The quality of the reconstructed images obtained by the proposed method is comparable with other methods. Currently, RTL Verilog coding is in progress for the block based DWT/IDWT.

REFERENCE

- [1] Liu Chien-Chih, Hang Hsueh-Ming, "Acceleration and Implementation of JPEG 2000 Encoder on TI DSP platform", *IEEE International Conference on Image Processing*, Vol. 3, pp. III-329-339, 2005.
- [2] Sonja Grgic, Mislav Grgic, "Performance Analysis of Image Compression Using Wavelets", *IEEE Transactions on Industrial Electronics*, Vol. 48, No. 3, pp. 682-694, June 2001.
- [3] Keshika Jangde, Rohit Raja, "Image Compression Based on Discrete Wavelet and Lifting Wavelet Transform Technique", *International Journal of Science, Engineering and Technology Research*, Vol. 3, Issue 3, March 2014.
- [4] Taizo Suzuk, "Integer DCT Based on Direct-Lifting of DCT-IDCT for Lossless-to-Lossy Image Coding", *IEEE Transactions on Image Processing*, Vol. 19, No. 11, pp 2958-2965, November 2010.
- [5] Charilaos Christopoulos, Athanassios Skodras, Touradj Ebrahimi, "The JPEG2000 Still Image Coding System: An Overview", *IEEE Transactions on Consumer Electronics*, Vol. 46, No. 4, pp. 1103-1127, November 2000.
- [6] V. Subramanyam, Sabu Emmanuel, "Robust Watermarking of Compressed and Encrypted JPEG2000 Images", *IEEE Transactions on Multimedia*, Vol. 14, No. 3, pp. 703-715, June 2012.
- [7] Cohen, I. Daubechies, J. Feauveau, "Bi-orthogonal bases of compactly supported wavelets", *Communication on Pure Applied Mathematics*, Vol. 45, pp. 485-560, 1992.
- [8] W. Sweldens, "The Lifting Scheme: A Custom-Design Construction of Bi-orthogonal Wavelets", *Applied and Computational Harmonic Analysis*, Vol. 3, No. 15, pp. 186-200, 1996.
- [9] Usha Bhanu N., A. Chilambuchelvan, "A Detailed Survey on VLSI Architectures for Lifting based DWT for efficient hardware implementation", *International Journal of VLSI design and Communication Systems*, Vol.3, No.2, April 2012.
- [10] Srikanth S., M. Jagadeeswari, "High Speed VLSI Architecture for Multilevel Lifting 2-D DWT Using MIMO" *International Journal of Soft Computing and Engineering*, ISSN: 2231-2307, Vol. 2, No. 2, May 2012.
- [11] S. Nagaraja Rao, M. N. Giriprasad, "The Effective Utilization of Lifting Schemes for Constructing Second Generation Wavelets: A Survey on Current State-of-the Art", *International Journal of Signal Processing, Image Processing and Pattern Recognition*, Vol. 4, No. 4, December 2011.
- [12] B. Eswara Reddy, K. Venkata Narayana, "A Lossless Image Compression using Traditional and Lifting Based Wavelet", *An International Journal on Signal and Image Processing*, Vol.3, No.2, April 2012.
- [13] Vrankic M, Sersic D, Sucic V, "Adaptive 2-D Wavelet Transform Based on the Lifting Scheme With Preserved Vanishing Moments", *IEEE Transactions on Image Processing*, Vol. 19, No. 8, pp. 1987 – 2004, August 2010.
- [14] NST Sai, R. C. Patil, "Image Retrieval using 2D Dual-Tree Discrete Wavelet Transform", *International Journal of Computer Applications*, Vol. 14, No.6, pp. 1-7, February 2011.
- [15] A. F. Mulla, N. N. Mane, R. C. Wagavekar, R. S. Patil, "High Speed DWT Processor Implementation in FPGA" *International Journal of Emerging Technology and Advanced Engineering*, Vol. 2, No. 4, April 2012.
- [16] Maria E. Angelopoulou, Peter Y. K., "Implementation and Comparison of the 5/3 Lifting 2D Discrete Wavelet Transform Computation Schedules on FPGAs", *International Journal on Signal Processing Systems*, Vol. 51, pp. 3–21, 2008.
- [17] Mohanty B. K., Meher P. K., "Memory-Efficient High-Speed Convolution-Based Generic Structure for Multilevel 2-D DWT", *IEEE Transactions on Circuits and Systems for Video Technology*, Vol. 23, No. 2, pp. 353-363, February 2013.

- [18] Mansouri, A. Ahaitouf, and F. Abdi “An Efficient VLSI Architecture and FPGA Implementation of High-Speed and Low Power 2-D DWT for (9, 7) Wavelet Filter”, *International Journal of Computer Science and Network Security*, Vol. 9, No. 3, pp. 50-60, March 2009.
- [19] Marino F, “Two fast architectures for the direct 2-D discrete wavelet transform”, *IEEE Transactions on Signal Processing*, Vol. 49, No. 6, pp. 1248-1259, June 2001.
- [20] Tze-Yun Sung, “A High-Efficient Line-Based Architecture for 2-D Lifting-Based DWT Using 9/7 Wavelet Filters”, *Journal of Colloid and Interface Science*, pp. 8-11, October 2006.
- [21] Mohanty B. K., Mahajan A, Meher P. K., “Area and Power-Efficient Architecture for High-Throughput Implementation of Lifting 2-D DWT”, *IEEE Transactions on Circuits and Systems II*, Vol. 59, No. 7, pp. 434-438, July 2012.
- [22] Usha Bhanu N., A. Chilambuchelvan, “A Detailed Survey on VLSI Architectures for Lifting based DWT for efficient hardware implementation”, *International Journal of VLSI design and Communication Systems*, Vol. 3, No. 2, April 2012.
- [23] W H. Chang, Y. S. Lee, W. S. Peng, C. Y. Lee, “A line-based, memory efficient and programmable architecture for 2D DWT using lifting scheme”, *IEEE International Symposium on Circuits and Systems*, Vol. 4, pp. 330–333, 2001.
- [24] Kim-Han Thung, Raveendran P, “A survey of image quality measures”, *International Conference on Technical Postgraduates*, pp. 1-4, December 2009.
- [25] Jain A., Bhateja V, “A full-reference image quality metric for objective evaluation in spatial domain”, *International Conference on Communication and Industrial Application*, pp. 1-5, December 2011.

Input Image	PSNR for Direct DWT in dB[22]	MSE for Direct DWT	PSNR for Line based DWT in dB	MSE for Line based DWT[23]	PSNR for Block Based DCT in dB	MSE for Block Based DCT in dB	PSNR Proposed Method 16x16 pixels in dB	MSE Proposed Method 16x16 pixels
Lena1.tiff	53.0	0.2	53.0	0.2	34.9	20.9	51.9	0.27
Pisa1.tiff	52.3	0.3	52.3	0.3	36.9	13.0	52.1	0.26
clkgeneval.tiff	51.8	0.4	51.8	0.4	33.5	28.4	51.7	0.28
titanic51.tiff	53.0	0.3	53.0	0.3	41.9	4.1	52.3	0.25

Software as a Service (SaaS): Security issues and Solutions

Navneet Singh Patel¹, Prof. Rekha B.S.²

¹ Dept. of ISE, R.V. College of Engineering, Bangalore, India

² Assistant Professor, Dept. of ISE, R.V. College of Engineering, Bangalore, India

ABSTRACT:

Cloud computing is becoming increasingly popular in distributed computing environment. Data storage and processing using cloud environments is becoming a trend worldwide. Software as a Service (SaaS) one of major models of cloud which may be offered in a public, private or hybrid network. If we look at the impact SaaS has on numerous business applications as well as in our day to day life, we can easily say that this disruptive technology is here to stay. Cloud computing can be seen as Internet-based computing, in which software, shared resources, and information are made available to devices on demand. But using a cloud computing paradigm can have positive as well as negative effects on the security of service consumer's data. Many of the important features that make cloud computing very attractive, have not just challenged the existing security system, but have also exposed new security risks. In this paper we are going to showcase some major security issues of current cloud computing environments.

KEYWORDS: Cloud Computing, Software as a Service, Security Challenges, Privacy, Multi-tenant Architecture, Data Confidentiality, Service-level Agreements

I. INTRODUCTION

A lot of studies and research has been done about Cloud Computing genre, by IT experts, business leaders and industry. While some believe it is a disruptive trend representing the next stage in the evolution of Internet, some believe it is just hype, as it uses earlier established computing technologies. According to Gartner [1], cloud computing can be defined as “a style of computing, where massively scalable IT- enabled capabilities are delivered ‘as a service’ to external customers using Internet technologies”. According to the Seccombe [2] and National Institute of Standards & Technology [3], guidelines for cloud computing, it has four different deployment models namely private, community, public and hybrid as well as three different delivery models that are utilized within a particular deployment model. These delivery models are the SaaS (Software as a Service), PaaS (Platform as a Service) and IaaS (Infrastructure as a Service). Adopting SaaS applications allow companies to save their information technology cost. The Cloud (or SaaS) model has no physical need for indirect distribution since it is not distributed physically and is deployed almost instantaneously. The customers do not take ownership of the software product, but instead they rent a total solution that is delivered remotely. The large majority of SaaS solutions are based on multi-tenant architecture. In this model, a single version of the application, with a unique single configuration (i.e. hardware, network, operating system), is used for every customers ("tenants"). But with its all attractive features there are a lot of issues that need to be identified and treated. Organization of this paper is as follows: Section 2 describes the related work and trends of Software as a Service (SaaS) delivery model. Section 3 lists some of misconception and reality about the SaaS. Section 4 describes the security issues that are posed by the SaaS. Section 5 lists some of the current solutions. Section 6 derives conclusion of the study done.

II. RELATED WORK AND TRENDS

According to a Gartner Group estimate, SaaS sales in 2010 reached \$10 billion, and were projected to increase to \$12.1bn in 2011, up 20.7% from 2010. Customer relationship management (CRM) continues to be the largest market for SaaS [4].

In an IEEE paper “A Privacy Preserving Repository for Securing Data across the Cloud” authors presented a privacy preserving repository for acceptance of integration requirements from clients to share data in the cloud and maintain their privacy, collect and integrate the appropriate data from data sharing services, and return the integration results to users [5].

A common approach to supply the data subject with information and control over data privacy is the provision of privacy policies specific to the data shared [6]. SLA negotiation is the subject of previous research based in the Gird community [7] and now extending into the cloud [8,9]. Within the cloud the SLA negotiation process involves the creation of a SLA captured using the WS Agreement XML standard [10].

In the cloud the service provider negotiates SLA on behalf of the user with cloud infrastructure providers. The process of an assessment of privacy has spurred a separate area of research in the form of Privacy Impact Assessments (PIA) [11]. PIA have emerged from existing work on data access by organisations in the 1920's to more specific mentions of PIA in terms of technology in the 1970s, a wide ranging study can be seen in [12].

As a result of widespread fragmentation in the SaaS provider space, there is an emerging trend towards the development of SaaS Integration Platforms (SIP). These SIPs allow subscribers to access multiple SaaS applications through a common platform. They also offer new application developers an opportunity to quickly develop and deploy new applications.

According to a survey of 600 enterprises by Enterprise Strategy Group 2012 indicate that SaaS use is bound to continue rising. In this survey 46% currently use it, 17% do not use but planning to use, 21% no use or plan but were interested to use, 14% no use, plan or interest and 1% was not clear [13].

Security is one of the most important concerns of SaaS. In a survey 51% of the people thought security the biggest concern where as 40% said integration with other application, 34% lack of customization and 33% total cost of ownership [14].

Fortunately, downward pressure on enterprise cloud providers to expose data security tools and options is beginning to have an effect. Newer companies are raising the competitive bar, providing first-generation tools to help customers see and control aspects of data security. HP has developed a program to assist enterprises in finding SaaS application vendors who are already taking an early lead in addressing the security injunction. HP Cloud Connections is a select affiliation of SaaS providers who have demonstrated best-of-breed customer security features.

III. MISCONCEPTION AND REALITY

The flexibility of cloud to scale bandwidth up or down at will, and its affordability as a pay-as-you-go service, have resulted in an interconnected, intelligent approach to smarter computing. The benefits of cloud computing are well-recognized. In fact, cloud computing ranks among the most popular new IT initiatives. Yet the excitement about cloud is often tempered by concern that this external delivery of services could compromise security. Cloud may seem new technology, but the fact is companies have been outsourcing their services and technology for many years. Service providers already deliver hosted technology offerings which are located offsite with client access using the Internet. And just because companies may give up some control to these service providers when they upgrade to a cloud-based environment (just like they give up some of their control in any outsourced arrangement), it doesn't mean that they have to compromise on their security features.

Companies still weighing the advantages of cloud with the perceived security risk should begin by asking the right questions and examining the right considerations to help build a "trust and verify" relationship with the cloud provider that will support success. SaaS puts most of the responsibility for security management with the cloud provider and is commonly used for services such as customer relationship management and accounting. This popular option cloud is considered low-risk technology because it primarily deals only with only software and not with hardware or storage.

IV. SECURITY ISSUES

In Software as a Service (SaaS) model, the client needs to be dependent on the service provider for proper security measures of the system. The service provider must ensure that their multiple users don't get to see each other's private data. So, it becomes important to the user to ensure that right security measures are in place and also difficult to get an assurance that the application will be available when needed [15]. Cloud computing providers need to provide some solution to solve the common security challenges that traditional communication systems face. At the same time, they also have to deal with other issues inherently introduced by the cloud computing paradigm itself.

A. Authentication and authorization

The authorization and authentication applications used in enterprise environments need to be changed, so that they can work with a safe cloud environment. Forensics tasks will become much more difficult since it will be very hard or maybe not possible for investigators may to access the system hardware physically.

B. Data confidentiality

Confidentiality may refer to the prevention of unintentional or intentional unauthorized disclosure or distribution of secured private information. Confidentiality is closely related to the areas of encryption, intellectual property rights, traffic analysis, covert channels, and inference in cloud system. Whenever a business, an individual, a government agency, or any other entity wants to shares information over cloud, confidentiality or privacy is a questions may need to be asked

C. Availability

The availability ensures the reliable and timely access to cloud data or cloud computing resources by the appropriate personnel. The availability is one of the big concerns of cloud service providers, since if the cloud service is disrupted or compromised in any way; it affects large no. of customers than in the traditional model.

D. Information Security

In the SaaS model, the data of enterprise is stored outside of the enterprise boundary, which is at the SaaS vendor premises. Consequently, these SaaS vendor needs to adopt additional security features to ensure data security and prevent breaches due to security vulnerabilities in the application or by malicious employees. This will need the use of very strong encryption techniques for data security and highly competent authorization to control access private data.

E. Data Access

Data access issue is mainly related to security policies provided to the users while accessing the data. Organizations have their own security policies based on which each employee can have access to a particular set of data. These security policies must be adhered by the cloud to avoid intrusion of data by unauthorized users. The SaaS model must be flexible enough to incorporate the specific policies put forward by the organization.

F. Network Security

In a SaaS deployment model, highly sensitive information is obtained from the various enterprises, then processed by the SaaS application and stored at the SaaS vendor's premises. All data flow over the network has to be secured in order to prevent leakage of sensitive information.

G. Data breaches

Since data from various users and business organizations lie together in a cloud environment, breaching into this environment will potentially make the data of all the users vulnerable. Thus, the cloud becomes a high potential target.

H. Identity management and sign-on process

Identity management (IdM) or ID management is an area that deals with identifying individuals in a system and controlling the access to the resources in that system by placing restrictions on the established identities. Aria of IdM is considered as one of the biggest challenges in information security. When a SaaS provider want to know how to control who has access to what systems within the enterprise it becomes a lot more challenging task..

V. PROPOSED SOLUTIONS

There are several research works happening in the area of cloud security. Several organization and groups are now interested in developing security solutions and standards for the cloud. The Cloud Security Alliance (CSA) is gathering solution providers, non- profits and individuals to enter into discussion about the current and future best practices for information assurance in the cloud [16]. The Open Web Application Security Project (OWASP) maintains list of top vulnerabilities to cloud-based or SaaS models which is updated as the threat landscape changes. The Cloud Standards website collects and coordinates information about cloud-related standards under development by the groups. The Open Grid Forum publishes documents to containing security and infrastructural specifications and information for grid computing developers and researchers.

We will discuss a security checklist for SaaS which can be used. To assess the security threats or capabilities of third-party SaaS providers, all customers need to ask some right questions:

A. What metrics can be used for reporting?

Will the service providers be able to present reports which will satisfy the CIO, the board and auditors that enterprise data is secured and meets regulatory requirements?

B. What is the level of the access controls?

The most established mechanism for data breaches now a day is through malicious or unintentional misuse of user access credentials. Visibility of the activity of individual users, which also includes administrative changes, is essential for data protection.

C. Is provided data such that it can be easily adapted into internal monitoring tools, to preventing data silos?

To make reporting simple and foolproof, you'll need to monitor enterprise's internal applications alongside SaaS applications, from a centralized dashboard.

D. How important and critical the enterprise data is?

Each SaaS application, must know the business criticality of the data involved. Is the SaaS application managing confidential customer data properly or not? You can then perform an inventory of the applicable compliance issues.

VI. CONCLUSION

Cloud computing is a disruptive technology with profound implications not only for Internet services but also for the IT sector as a whole. Though there are numerous advantages in using a cloud-based system, there are still many practical issues which have to be solved particularly related to privacy and security, service-level agreements (SLA), and power efficiency. As described in this paper, currently security has lot of issues which scares away several potential users. Until a proper security module is not in place, potential users will not be able to leverage the true benefits of this technology. This security module should cater to all the issues arising from all directions of the cloud. In a cloud, where there are heterogeneous systems having a variation in their asset value, a single security system would be too costly for certain applications and if there is less security then the vulnerability factor of some applications like financial and military applications will shoot up. On the other side, if the cloud has a common security methodology in place, it will be a high value asset target for hackers because of the fact that hacking the security system will make the entire cloud vulnerable to attack.

REFERENCES

- [1]. Heiser J.(2009) What you need to know about cloud computing security and compliance, Gartner, Research, ID Number: G00168345.
- [2]. Seccombe A., Hutton A, Meisel A, Windel A, Mohammed A, Licciardi A, (2009).Security guidance for critical areas of focus in cloud computing, v2.1. Cloud Security Alliance, 25 p.
- [3]. Mell P, Grance T (2011) The NIST definition of Cloud Computing. NIST, Special Publication 800–145, Gaithersburg, MD
- [4]. McHall, Tom (7 July 2011). "Gartner Says Worldwide Software as a Service Revenue Is Forecast to Grow 21 Percent in 2011". Gartner.com. Gartner. Retrieved 28 July 2011.
- [5]. Ranjita Mishra, Sanjit Kumar Dash, Debi Prasad Mishra, Animesh Tripathy "A Privacy Preserving Repository for Securing Data across the Cloud," Proc. Electronics Computer Technology (ICECT), 2011 3rd International Conference , pp. 6-10, 2011
- [6]. J. Karat, C.-M. Karat, C. Brodie, and J. Feng. Privacy in information technology: Designing to enable privacy policy management in organizations. Int. Journal of Human-Computer Studies, 63(1-2):153–174 2005.
- [7]. Hasselmeyer P, Qu C, Schubert L, Koller B, Wieder P. Towards autonomous brokered SLA negotiation. Proceedings of the 2006 eChallenges Conference—Exploiting the Knowledge Economy—Issues, Applications, Case Studies, Cunningham P, Cunningham M (eds.), vol. 3. IOS Press: Amsterdam, 2006
- [8]. Rochwerger B, Galis A, Levy E, Caceres J, Breitgand D, Wolfsthal Y, IM Llorente MW, Montero R, Elmroth "E. RESERVOIR: Management technologies and requirements for next generation service oriented infrastructures." Proceedings of the 11th IFIP/IEEE International Symposium on Integrated Management, New York, U.S.A.,2009
- [9]. Contract based e-Business System Engineering for Robust, Verifiable Cross-organisational Business Applications (CONTRACT), 2009
- [10]. WS-Agreement-Negotiation v 1.0 2011 http://www.gridforum.org/Public_Comment_Docs/Documents/2011-03/WSAgreementNegotiation+v1.0.pdf
- [11]. R. Clarke, Privacy Impact Assessments February 1998, <http://www.anu.edu.au/people/Roger.Clarke/DV/PIA.html>
- [12]. R. Clarke. Privacy impact assessment: Its origins and development. Computer Law & Security Review, 25 (2009)
- [13]. Keep SaaS secure from the start, <http://h30458.www3.hp.com/us/us/discover-performance/security-leaders/2012/jun/enterprise-saas-security-issues--concerns--threats---risks---hp-.html>
- [14]. 5 problems with SaaS security, <http://www.networkworld.com/news/2010/092710-software-as-service-security.html>
- [15]. Choudhary V.(2007). Software as a service: implications for investment in software development. In: International conference on system sciences, 2007, p. 209.
- [16]. Cloud Security Alliance. Guidance for identity & access management V2.1,2010a
- [17]. <http://www.cloudsecurityalliance.org/guidance/csaguide-dom12-v2.10.pdf> [Accessed: July 2012].

High Frequency Performance of Dual Gated Large Area Graphene MOSFET

¹, Md. Tawabur Rahman, ², Muhammad Mainul Islam, ³, Md. Tajul Islam
^{1, 2, 3} Department of Electrical and Electronic Engineering, Khulna University of Engineering & Technology,
Khulna, Bangladesh.

ABSTRACT:

This paper presents a detailed study of the high frequency performance of dual gate large area graphene MOSFET. A quasi analytical modeling approach is presented here. To know the high frequency performance of a graphene MOSFET, the drain and output transconductances along with intrinsic gain are calculated here using small signal equivalent model. Finally the cut off frequency of Graphene MOSFET as an important figure of merit is also shown.

KEYWORDS: Cut-off frequency, Dual gate effects, GFET, Graphene MOSFET, Intrinsic gain, Large area graphene, Self-consistent quantum capacitance.

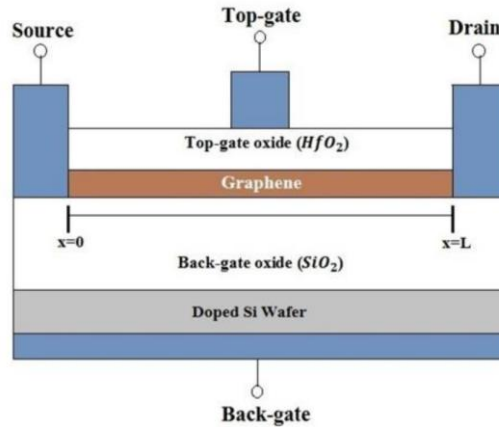
I. INTRODUCTION

Graphene is a single layer of sp²-bonded carbon atoms that are packed in a honeycomb lattice. It wasn't until the year 2004 that Andre Geim and Konstantin Novoselov managed to produce graphene flakes with a technique called mechanical exfoliation. Geim and Novoselov were awarded the Nobel Prize in Physics in 2010 for their discovery of graphene. It is, therefore, easy to claim that 2010 has been the year of graphene [1]. Graphene offers many of the advantages such as high carrier mobilities up to $2 \times 10^5 \text{ cm}^2 \text{ V}^{-1} \text{ s}^{-1}$ in substrate supported devices and high saturation velocity [2]–[6]. The novel electronic properties of graphene lead to intense research into possible applications of this material in nano scale devices. The presence of high mobility and high saturation velocity makes graphene very promising for high speed field effect devices as a channel material.

There have been studies on modeling and characterizing of graphene FETs and MOSFETs in different dimensions. However, the progress is at initial stage. In order to fabricate high performance G-MOSFETs, understanding of detailed device modeling and performance evaluations is urgently required. The recent works have been concentrated mostly on the current voltage characteristics of large area graphene MOSFETs using different approaches. However, there have no significant works on high frequency performance although graphene is predicted to highly attracted material for high speed nano-scale devices.

II. MODELING OF GRAPHENE MOSFET

This work is about the modeling of large-area graphene metal-oxide semiconductor field-effect transistors (Graphene MOSFETs). In every FET an electric field is used to change the conductivity of the channel. This electric field is generated by applying a gate voltage to the gate terminal. Thus the name gate can be understood literally. It controls how many electrons can pass the channel. There are two other terminals in all FETs which are essential. These are the source and the drain terminal. Their names refer also to their functions. If a positive drain-source voltage is applied to these terminals, electrons are injected from the source into the channel and collected by the drain. The resulting current is referred to as the drain current. The feature which distinguishes GFETs from other FETs is that the channel is made of graphene.



“Figure 1. The cross section of the modeled graphene MOSFET with top- and back-gate” [7].

A simple model of the GFET which is described in this paper is shown in “Figure1”. Here the channel is made of large-area single-layer graphene, which has a zero band gap. We have used channel length of 5µm and width of 1µm. It is located on a heavily doped oxidized silicon wafer. This acts as a second gate and is referred to as the back-gate. It is used to control whether the graphene is p- or n-conducting by applying a back-gate voltage. The source terminal is grounded and a drain-source voltage can be applied to the drain terminal. Both contacts between these terminals and the channel are considered to be ohmic. The top-gate is separated from the graphene channel by an insulator and is used to control the charge carrier density and therefore the conductivity in the channel.

2.1. Channel Charge Calculation

Besides modeling the DC behavior of GFETs the goal of this work is also to model the high-frequency characteristics of these devices. This will be done by calculating the elements of the small-signal equivalent circuit. Before we can deal with these elements we need to know how to calculate the channel charge, since this is essential in order to determine the gate-source and gate-drain capacitances. In general the channel charge Q_{ch} can be calculated by subtracting the amount of electrons from the amount of holes and multiplying the result by the elementary charge. This can be written as [2]

$$Q_{ch} = qW \int_0^L (p(x) - n(x)) dx \tag{1}$$

To obtain Q_{ch} , a simple numerical integration is performed using a trapezoidal approximation. For the model from section 6.1 the calculation of Q_{ch} is a little more tricky since we only know $p(V(x))$ and $n(V(x))$. The x dependence of the local hole and electron sheet densities can be translated into a dependence on the local voltage $V(x)$. By using this equation [2]

$$\frac{dx}{dV(x)} = \frac{qW \rho_{real}(V(x)) \mu}{I_d} + \frac{\mu}{v_{sat}(V(x))} \tag{2}$$

The overall net charge can be expressed using equation (1) and (2). Thus the necessary equation of Q_{ch} is

$$Q_{ch} = qW \int_0^{V_{ds-int}} [p(V(x)) - n(V(x))] \frac{dx}{dV(x)} dV(x) \tag{3}$$

$$Q_{ch} = \int_0^{V_{ds-int}} [\rho(V(x)) - nV(x)] \left(\frac{qW \rho_{real}(V(x)) \mu}{I_d} + \frac{\mu}{v_{sat}(V(x))} \right) dV(x) \tag{4}$$

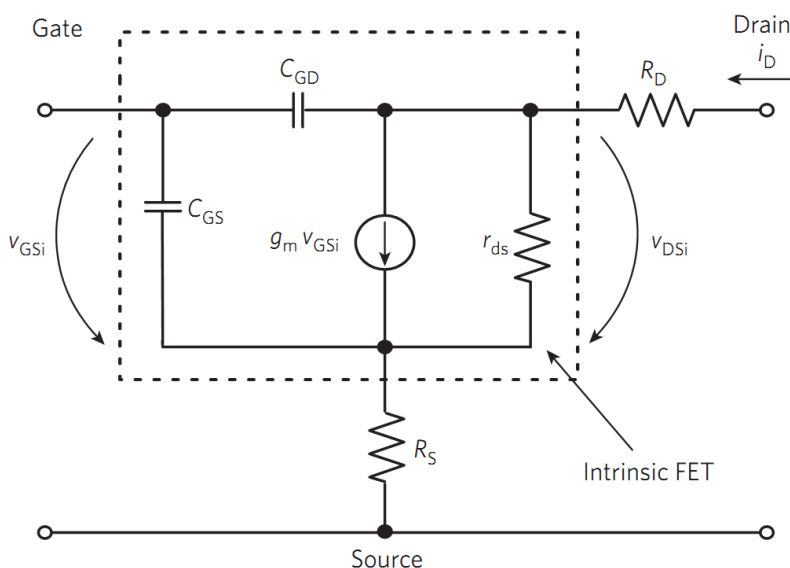
It is important to distinguish between p, n and ρ_{real} in the formula above. If we neglect the minority charge carriers, $p(V(x)) - n(V(x))$ is equal to ρ_{real} can be expressed as:

$$p(V(x)) - n(V(x)) \cong - (V_{gs-top} - V(x) - V_{gs-top,0}) \frac{\frac{1}{2} C_{ox-top} C_q}{C_{ox-top} + C_{ox-top} + \frac{1}{2} C_q} - (V_{gs-top} - V(x) - V_{gs-top,0}) \frac{\frac{1}{2} C_{ox-back} C_q}{C_{ox-top} + C_{ox-top} + \frac{1}{2} C_q} \quad (5)$$

The integral to determine Q_{ch} is solved numerically. The whole simulation is carried on MATLAB environment.

III. SMALL-SIGNAL EQUIVALENT CIRCUIT

The high-frequency behavior of the transistor can be modeled with a small-signal equivalent circuit [2] as shown in “Figure 2”. The intrinsic transistor is described by the transconductance g_m , the drain conductance g_{ds} , the gate-source capacitance C_{gs} , and the gate-drain capacitance C_{gd} . Thereby the whole behavior of the device is described by these four elements: g_m , g_{ds} , C_{gs} and C_{gd} . The reason why this is possible is the following. The high-frequency AC signal is thought to be superimposed onto a DC signal, which defines the DC operating point. If the amplitude of the AC signal is small, the nonlinear transistor characteristics can be linearized around the DC operating point. Thus, all elements of “Figure 2” are explained in the following as mentioned [2].



“Figure 2. The small-signal equivalent circuit of a graphene MOSFET”.

Here the intrinsic transconductance, g_m , is related to the internal small-signal gate source and drain–source voltages, V_{GSi} and V_{DSi} , whereas the terminal transconductance, $g_{m,t}$, is related to the applied gate–source and drain–source voltages, V_{GS} and V_{DS} [2].”

3.1. Transconductance Calculation

The transconductance calculation is very important to know the radio-frequency characteristics of a graphene MOSFET. They are of two types: intrinsic transconductance and drain transconductance.

3.2. Intrinsic Transconductance, g_m

Transconductance describes the change of the drain current I_d caused by small variations of the internal gate-source voltage $V_{gs-top-int}$ at a fixed drain source voltage $V_{ds-int-const}$ [2]. In other words, the transconductance is defined as the variation in the drain current I_d caused by a small variation in the top-gate voltage V_{gs-top} as:

$$g_{m-top} = \left. \frac{dI_d}{dV_{gs-top-int}} \right|_{V_{ds-int} = const} \quad (6)$$

$$g_{m-back} = \left. \frac{dI_d}{dV_{gs-back-int}} \right|_{V_{ds-int} = const} \quad (7)$$

The transconductance due to top-gate voltage (g_{m-top}) and the transconductance due to back-gate voltage (g_{m-back}) can be evaluated using equation (6) and equation (7) clearly. It describes how the output signal (drain current) reacts on changes of the input signal (gate- source-voltage).

3.3. Drain Transconductance of GFET, g_{ds}

The drain-source transconductance g_{ds} describes the resistance of the graphene channel, since it is the inverse of r_d . It is expressed by the variation of the drain current I_d caused by a change of the internal drain-source voltage V_{ds-int} at a fixed $V_{gs-top-int}$.

$$g_{ds-top} = \left. \frac{dI_d}{dV_{ds-int}} \right|_{V_{gs-top-int} = const} \quad (8)$$

$$g_{ds-back} = \left. \frac{dI_d}{dV_{ds-int}} \right|_{V_{gs-back-int} = const} \quad (9)$$

The drain conductance due to fixed value of top-gate voltage (g_{ds-top}) and the drain conductance due to fixed value of back-gate voltage ($g_{ds-back}$) can be evaluated using equation (8) and (9).

3.4. Intrinsic Capacitance Calculation

The intrinsic capacitance is very necessary to calculate the cut-off frequency and other radio-frequency behaviour of a graphene MOSFET. The mobile channel charge Q_{ch} depends on the top-gate voltage $V_{gs-top-int}$, the back-gate voltage $V_{gs-back-int}$ and drain-source voltage V_{ds-int} . This dependence is modeled by the gate-source capacitance C_{gs} & the gate-drain capacitance C_{gd} [2].

3.4.1. Gate-Source Capacitance, C_{gs}

The gate-source capacitance C_{gs} is defined as the variation in the channel charge Q_{ch} caused by a small variation in the top-gate voltage $V_{gs-top-int}$ with a fixed value of drain-source voltage V_{ds-int} .

$$C_{gs-top} = - \left. \frac{dQ_{ch}}{dV_{gs-top-int}} \right|_{V_{ds-int} = const} \quad (10)$$

$$C_{gs-back} = - \left. \frac{dQ_{ch}}{dV_{gs-back-int}} \right|_{V_{ds-int} = const} \quad (11)$$

The gate-source capacitance due to top-gate voltage (C_{gs-top}) and the gate-source capacitance due to back-gate voltage ($C_{gs-back}$) can be evaluated using equation (10) and equation (11) clearly.

3.4.2. Gate-Drain Capacitance, C_{gd}

The gate-drain conductance C_{gd} is defined as the variation in the channel charge Q_{ch} caused by a small variation in the drain-source voltage V_{ds-int} with a fixed value of top-gate voltage $V_{gs-top-int}$.

$$C_{gd-top} = - \left. \frac{dQ_{ch}}{dV_{ds-int}} \right|_{V_{gs-top-int} = const} \quad (12)$$

$$C_{gd-back} = - \left. \frac{dQ_{ch}}{dV_{ds-int}} \right|_{V_{gs-back-int} = const} \quad (13)$$

The gate-drain capacitance due to the fixed value of top-gate voltage (C_{gd-top}) and the gate-drain capacitance due to the fixed value of back-gate voltage ($C_{gd-back}$) can be evaluated using equation (12) and equation (13) also.

As described earlier, the total amount of charge carriers in the channel is changing with varying $V_{gs-top-int}$, $V_{gs-back-int}$ and V_{ds-int} . Its dependence is described by two capacitances: the gate-source capacitance C_{gs} and the gate-drain capacitance C_{gd} as described in the above sections (3.4.1 and 3.4.2).

3.5. Intrinsic Gain Calculation

Finally, we show an example of projection of the intrinsic gain as a figure of merit commonly used in RF/analog applications. In small signal amplifiers, for instance, the transistor is operated in the ON-state and small RF signals that are to be amplified are superimposed onto the DC gate-source voltage [8]. Instead, what is needed to push the limits of many analog/RF figures of merit, for instance the cut-off frequency or the intrinsic gain, is an operation region where high transconductance together with a small output conductance is accomplished. Next, we will give an example on how to use our current-voltage DC model to project an important figure-of-merit (FOM) used in RF applications, namely the intrinsic gain (G).

3.5.1. Intrinsic Top-Gate Gain, G_{top}

The intrinsic top-gate gain G_{top} , which is defined as the ratio of the transconductance (g_{m-top}) to the drain-conductance (g_{ds-top}) expressed as:

$$\text{Intrinsic top-gate gain, } G_{top} = \frac{g_{m-top}}{g_{ds-top}} \quad (14)$$

The top-gate gain (G_{top}) is very important in RF applications as well as cut-off frequency.

3.5.2. Intrinsic Back-Gate Gain, G_{back}

The intrinsic back-gate gain G_{back} , which is defined as the ratio of the transconductance (g_{m-back}) to the drain-conductance ($g_{ds-back}$) expressed as:

$$\text{Intrinsic back-gate gain, } G_{back} = \frac{g_{m-back}}{g_{ds-back}} \quad (15)$$

Both g_m and g_{ds} are small-signal quantities [8]. Here the internal quantities of voltages have to be considered. The intrinsic back-gate gain is more than the intrinsic top-gate gain, as found in our simulation.

3.6. Cut-off Frequency Calculation

Now all elements of the equivalent circuit are known and we are able to calculate the cut-off frequency f_T of the graphene MOSFET [2]. It is related to the short circuit current gain h_{21} , which is the ratio of the small-signal output current to the input current. This ratio is frequency dependent and decreases with increasing frequency. The frequency where this ratio becomes unity is defined at the cutoff frequency f_T , which can be approximated by:

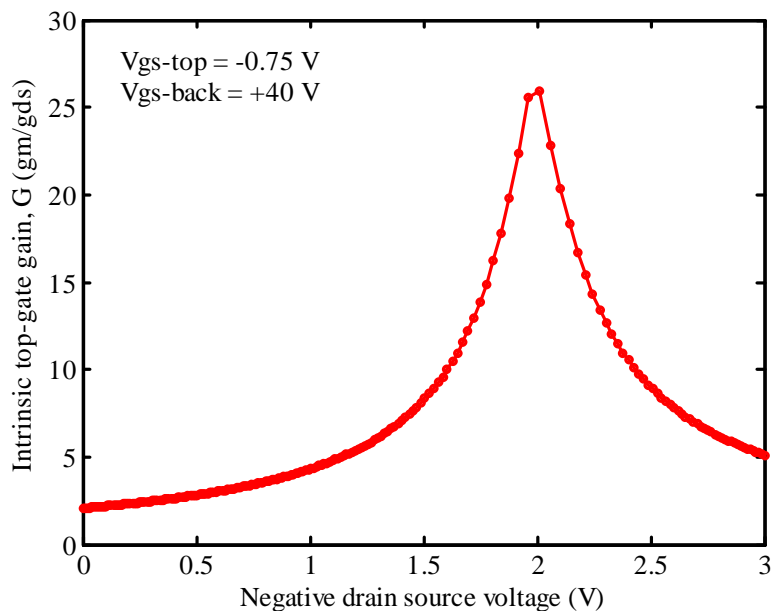
$$f_T = \frac{g_m}{2\pi [(C_{gs} + C_{gd})(1 + g_{ds}(R_s + R_d)) + C_{gs}g_m(R_s + R_d)]} \quad (16)$$

For large-area GFETs, the output characteristic shows a weak saturation that could be exploited for analog/RF applications. The cut-off frequencies in the THz range are envisioned [8].

IV. RESULTS

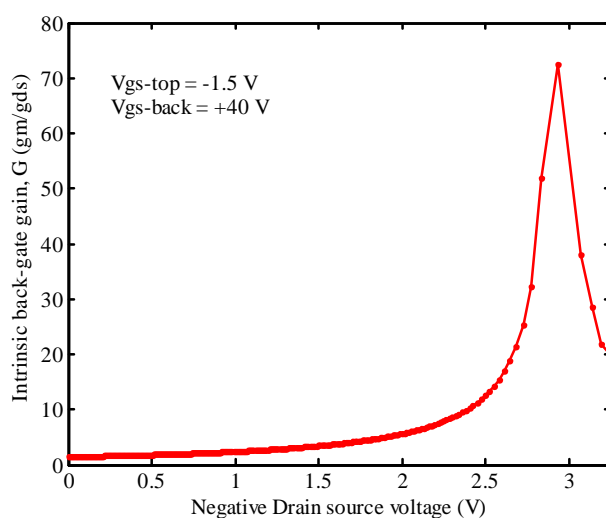
4.1. Intrinsic Top-Gate Gain, G_{top}

“Figure 3” shows that the variation of intrinsic top-gate gain as a function of drain source voltage. Here, the intrinsic peak top-gate gain (G_{top}) is found 25.93 for $V_{ds} = -2.01V$ at $V_{gs-top} = -0.75V$ and $V_{gs-back} = +40V$. We have found a wide peak at $V_{ds} = -2.01V$ when the intrinsic top-gate gain was plotted against the drain to source voltage.



“Figure 3. Intrinsic top-gate gain (G_{top}) as a function of drain source voltage V_{ds} at $V_{gs-top} = -0.75 V$ with $V_{gs-back} = +40V$ ”.

4.2. Intrinsic Back-Gate Gain, G_{back}



“Figure 4. Intrinsic back-gate gain (G_{back}) as a function of drain source voltage V_{ds} at $V_{gs-back} = +40V$ with $V_{gs-top} = -1.5V$ ”.

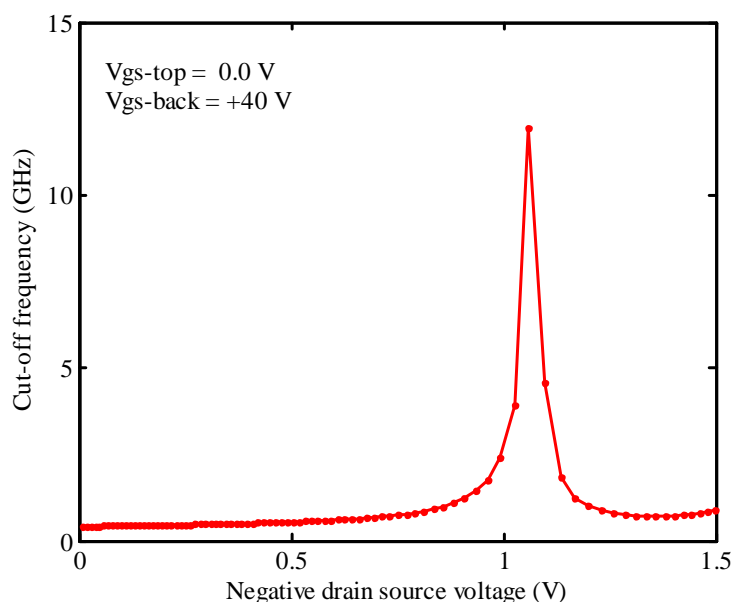
“Figure 4” shows the intrinsic peak back-gate gain (G_{back}) are found 72.38 as a function of drain source voltage ($V_{ds} = -2.934V$) at $V_{gs-top} = -1.5V$ and $V_{gs-back} = +40V$. We have found a narrow peak at $V_{ds} = -2.934V$ when the intrinsic top-gate gain was plotted against the drain to source voltage. The peak of Intrinsic back-gate gain was found at a higher negative drain-source voltage in comparison with Intrinsic top-gate gain.

4.3. High frequency Performance

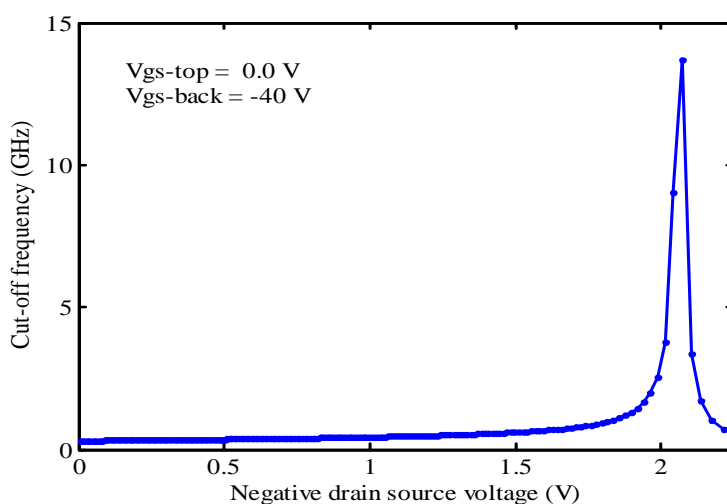
In radio frequency applications the high speed field effect device is desired. In this case of graphene MOSFET the cut-off frequency is also increased in GHz range. We have found a narrow peak of cut-off frequency plotted versus the drain-source voltage that coincides with the inflection point of the output characteristics.

Our simulated peak cut-off frequencies are found 11.96 GHz and 13.69 GHz for back-gate voltage $V_{gs-back} = +40V$ and $-40V$ with zero top-gate voltage i.e. $V_{gs-top} = 0.0V$ as shown in “Figure 5” and “Figure 6” respectively.

The result in high cut-off frequency is very much promising for RF application.



“Figure 5. The cut-off frequency f_T as a function of drain-source voltage V_{ds} with $V_{gs-top} = 0V$ and $V_{gs-back} = +40V$.”



“Figure 6. The cut-off frequency f_T as a function of drain-source voltage with $V_{gs-top} = 0V$ and $V_{gs-back} = -40V$.”

V. CONCLUSION

In this paper, the high frequency performance of large area of Graphene MOSFET is studied using quasi-analytical approach. The drain transconductance of the device is computed . The resulting high intrinsic top gate gain ~ 73 which is promising and important figure of merit for RF devices. In addition, high cut-off frequency of 14GHz is obtained at $V_{ds} = -2.07V$ which is very much promising for high speed nano devices.

REFERENCES

- [1]. A. K. Geim and K. Novoselov. The Rise of Graphene, 6:183-191, 2007.
- [2]. E. Schwierz. Graphene transistors, 5:487-496, 2010
- [3]. K. S. Novoselov, A. K. Geim. Two-dimensional gas of mass less Dirac fermions in graphene, 438:197-200, 2005.
- [4]. F. Schedin, A. K. Geim. Detection of individual gas molecules adsorbed on graphene, 6:652-655, 2007
- [5]. I. Meric, M. Y. Han, A. F. Young. Current saturation in zerobandgap, top-gated graphene field-effect transistors, 3:654-659, 2008.
- [6]. K. I. Bolotina, K. J. Sikes, Z. Jianga, M. Klimac, G. Fudenberg, J. Honec, P. Kima, H. L. Stormer. Ultrahigh electron mobility in suspended graphene, 146:351-355, 2008.
- [7]. Md. Tawabur Rahman*, Ashish Kumar Roy, Hossain Md. Abu Reza Bhuiyan, Md. Tajul Islam and Ashraf G. Bhuiyan, "DC Characteristics of Dual Gated Large Area Graphene MOSFET", 1st International Conference on Electrical Information and Communication Technology (EICT 2013), 13-15 February 2014, Khulna-9203, Bangladesh.
- [8]. D. Jimenez and O. Moldovan. Explicit drain-current model of graphene field-effect transistors targeting analog and radio-frequency applications, 58:4049-4052, 2011.

Automated systems for fall detection of individuals based on a network of overlapping cameras with Dempster-Shafer Theory (DST)

Seyed Hojjat Moghaddasi¹, Aliakbar Poyan², vahid ghasemi³

¹,moghadasi@shahroodut.ac.ir

²,apouyan@shahroodut.ac.ir

³, v.ghasemi@gmail.com

ABSTRACT:

With the increase in the elderly population (over 65 years) new challenges related to monitoring and caring these people are discussed. These challenges include the reduced number of people involved in monitoring these people or helping their independence. In this regard, building smart houses is one of the proposed solutions. Falling of the elderly or the disabled is one of the common events. Health smart homes that are equipped with the fall detection system are appropriate solutions for fall detection. Using overlapping cameras is the most economical method. In this paper, an automatic diagnosis system based on a network of overlapping cameras has been introduced and implemented. From any camera with a fuzzy vision, a percentage of falling, or non-occurrence of falling or uncertain events is obtained. Finally, there is a need to combine the theories extracted from the camera and achieve a unified theory. To combine the theories, the highest levels of data fusion or inference is used. In this article, Dempster-Shafer Theory is used for inference between cameras. Finally, our experiments show the superiority of this method compared to similar approaches.

KEYWORDS: fall detection, Health smart homes, data fusion (data combination), inference, Dempster-Shafer Theory

I. INTRODUCTION

According to the studies, the elderly population is increasing [1] the increase in population is more in developed countries (such as America where one person per five Americans, is aged over 65 years). [1, 2] The elderly tend to maintain their independence in their daily affairs. To achieve this goal and also reduce the number of people involved in monitoring these individuals, various ideas have been proposed such as monitoring with electronic equipment as smart.

The fall of the elderly and disabled is a common occurrence that causes damage to them. [3]. For smart monitoring of these individuals, there are three main strategies [3]: Equipment or portable gadgets, visual monitoring by cameras, and combinational methods. The first method which includes devices such as accelerometers and gyroscopes has very high detection accuracy [4-8]. The only problem with this method is its inefficiency in a real environment (permanent carrying, forgetting about the tools ...) [3]. The category includes the visual methods (using different cameras, from regular cameras to Kinect depth cameras) [9-14]. The accuracy of these methods are lower than the first category. Instead, low cost low cost, and applicability of these methods is their prominent feature. The third category has the advantages and disadvantages of both methods. (Such as audio-visual methods).

In this article we will try to provide an appropriate method of fall detection by visual method (second approach). One of the most controversial methods is using overlapping cameras in the desired space. For this purpose, we first present an appropriate analysis and introduction in the field of falling. In the next section we will introduce the used database. Finally, we will describe the pre-processing and feature extraction. So far, a theory is extracted from each event in each moment of (frame). In the next step we try to combine multiple theories of cameras using Dempster-Shafer Theory and extract a unique result. Fuzzy logic must be used to take the atmosphere of the problem to the Dempster-Shafer Theory. In general, the results show superior speed than the single-camera modes and similar methods.

II. REVIEW OF LITERATURE

In this section we review the fall of individuals from the visual perspective. We also present an overview of existing approaches in this regard.

2.1. What are the steps of falling on the ground from a visual perspective?

Falling usually occurs suddenly. During this event, the person moves towards the ground a lot faster than other routine activities (sitting, lying down, etc.). Falling in [9] is divided into four stages. Pre-falling phase, critical phase, post-falling phase, and the recovery phase (Fig. 1).

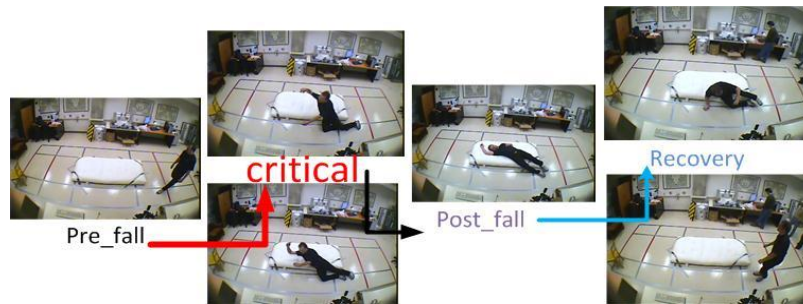


Figure 1 - The four stages of a person falling on the floor.

2.2. Fall detection

Fall detection means the design and implementation of a hardware and software system. The system should have the ability of fall detection. The topic discussed in this report is to visually detect the falling of individuals. Fall detection can be done in these methods with the installation of cameras at fixed locations of a home. These homes are considered on the topic of smart homes [15] and in the sub-set of Health smart homes [16]. Cameras installed in these houses constitute a visual sensor network [17] to identify a special event, such as falling of individuals. In [9] several methods have been listed for fall detection. Using the MHI and ghost's information, changes in the shape ghost with the help of OF, GMM, using three-dimensional data (such as the direction vector of the center of each one). However, in [13] two vertical cameras form an occupied three-dimensional environment s for each individual (The cubic form).

III. THE PROPOSED METHOD FOR FALL DETECTION IN INDIVIDUAL CAMERAS

3.1. Introduction of dataset

In this report, the database [18] that was developed at the University of Montreal is used. For this dataset in [18], two important features are listed. First, it covers the most common actions and behaviors of a person during the day. On the other hand, all the possible states of a person falling are also covered (Fig 2). Also in figure 3 the position of cameras can be seen.



Figure 2 – dataset that using.

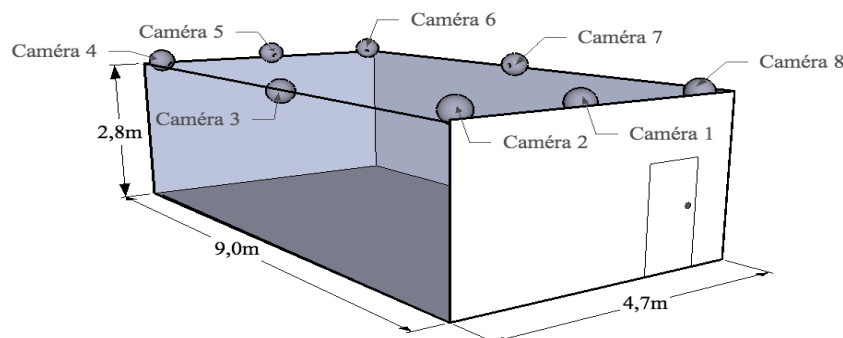


Figure 3 – position of cameras in testing room.

3.2. Pre-processing and feature extraction

In this report, two groups of features were used for the fall detection. The first category includes only a feature called constant motion C_{motion} and to achieve this feature we need a special type of image called MHI. MHI is a grayscale image that obtained for each frame. In MHI, the recent movements are displayed more clearly (image ...). To extract C_{motion} , MHI can be used as follows. In this equation, $H(x, y, t)_\tau$ is MHI that has been obtained in frame τ . blob represents the individual's ghost.

$$C_{motion} = \frac{\sum_{pixel(x,y) \in blob} H(x, y, t)_\tau}{\#pixels \in blob} \quad 1$$

The nature of C_{motion} with high values shows the occurrence of sharp and sudden movements in the environment. While C_{motion} with low values shows the occurrence of slow events in the environment. High C_{motion} includes sitting up suddenly on a chair or falling. Low C_{motion} includes slow activities such as walking, doing chores, etc. In figure 4, you can see the C_{motion} signal for camera number 3 from sample 7. The main pre-processing for a video sequence is to remove its background. To remove the background, MOG and GMM algorithms can be used. But the point of tested videos is the two challenging noises of shadow and light reflection. See a sample of these noises in figure 4. In this figure, applying the GMM algorithm and its unfavorable outcome can be seen. We have used an advanced and powerful algorithm called CB to deal with these two types of noises.

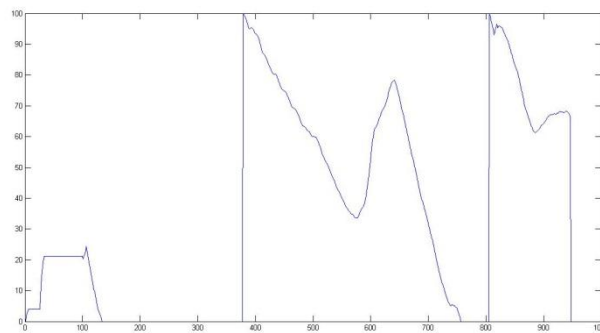


Figure 4– signal of C_{motion}

3.3. Fall detection

Fall detection is done with the help of a fuzzy inference system. The values of table 1 will be the input of this fuzzy system. In determining the rules of this fuzzy system such as table 1. The output of this fuzzy system can be seen below. Characteristics of this system can be seen in table 1. (Other outputs are defined like figure 5).




calculate	Description	parameter
	<p>Angle changes the center of the ellipse</p>	δ_{θ}
	<p>Larger diameter than the small diameter oval inscribed ellipse changes</p>	δb_{θ}
	<p>Inscribed ellipse center height changes</p>	δ_x

Table1– Fuzzy Inference System Inputs

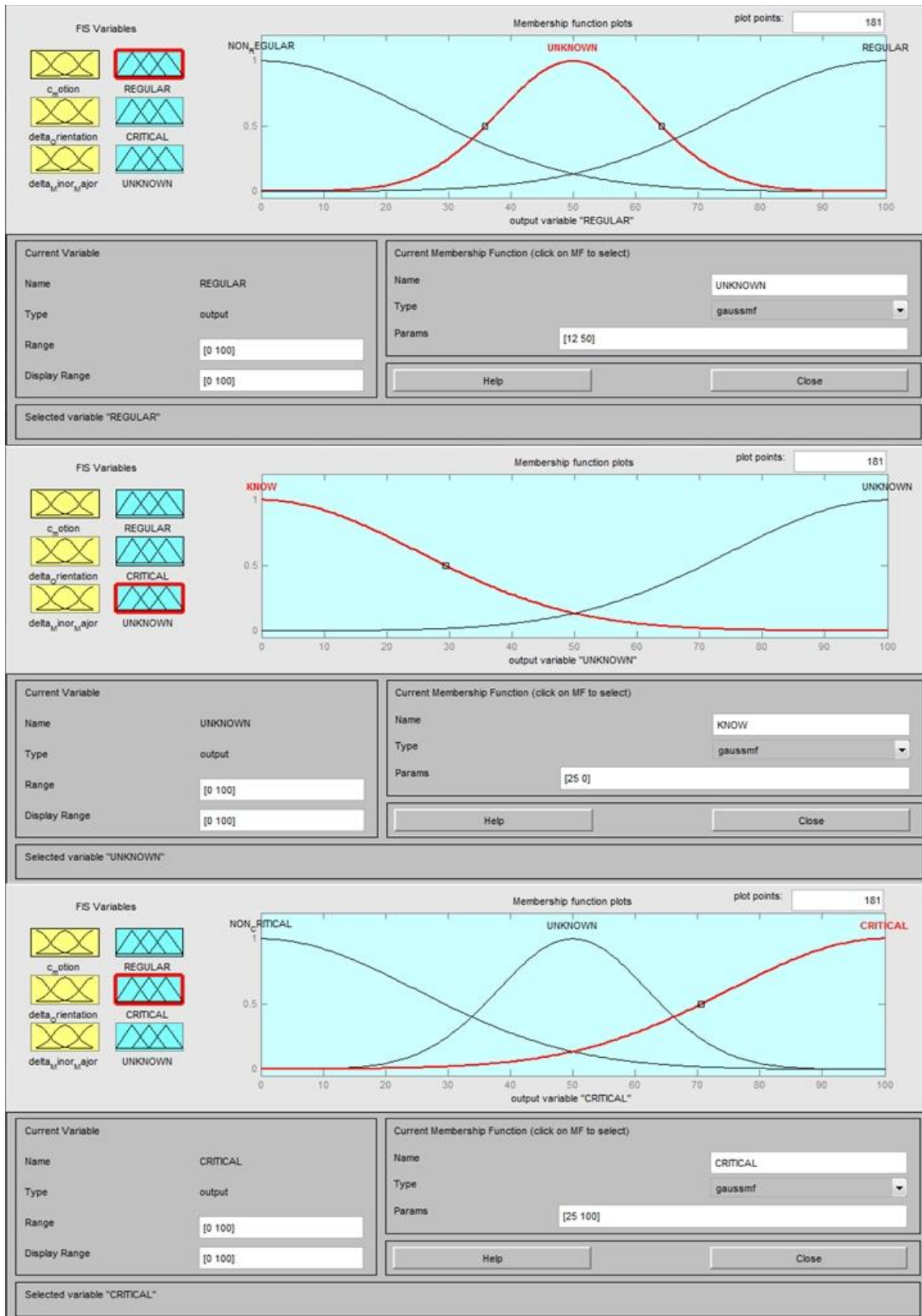


Figure 5– Fuzzy Inference Systems outputs

description	features
mamdani	FIS
Min	AND method
Max	OR method
bisector	Defuzzification method
Min	Implication method
Max	Aggregation method
$C_{motion}, \delta_a, \delta_B$	Inputs
{{regular},{critical},{regular, critical}}	outputs

Table 2 – Characteristics of this system

IV. INFERENCE IN OVERLAPPING CAMERAS WITH THE HELP OF DEMPSTER-SHAFER THEORY

Data fusion is a process in which a group of data are combined together to build new data (generated data are more desirable than the original data). [19]. inference is the highest degree of Data fusion. During the inference, the high-level data (from decision or classification results) are combined together [20].

4.1. Dempster-Shafer Theory

Dempster-Shafer Theory is an approach for inference. This theory is very close to BDT. In 2, The application of this theory in data fusion can be observed.

$$m(Z) = \frac{\sum_{A \cap B = Z \neq \emptyset} m(A) \times m(B)}{1 - \sum_{A \cap B = \emptyset} m(A) \times m(B)} = \frac{\sum_{A \cap B = Z \neq \emptyset} m(A) \times m(B)}{\sum_{A \cap B \neq \emptyset} m(A) \times m(B)} \quad 2$$

$A, B, Z \subseteq \Omega$

4.2. Definition of Mass function using fuzzy theory

The outputs that were introduced in Section 3.3 are the Mass functions of this DST.

4.3. Inference in overlapping cameras for fall detection using Dempster-Shafer Theory

In the proposed algorithm, FIS is used to estimate the mass function values. This is due to the fuzzy nature of human motion [21]. For example, we can not specify an exact boundary between sitting and standing position of a person. The start or end point of falling cannot be said exactly. FIS or fuzzy inference system is a rule-based system [22]. The rules make a mapping between input and output that are both fuzzy numbers [22]. Here it is necessary to recall the design of a fuzzy system. In a fuzzy system, firstly the membership functions of fuzzification stage are done. Then with the help of a number of predefined rules within the FIS (Figure 3-1), mapping from input to output is done. In the final stage, the fuzzy output numbers are transformed from fuzzification to defuzzification.

How to apply FIS for estimating mass function can be cited as follows:

1. fuzzification on inputs and transforming them to fuzzy values
2. applying fuzzy rules and achieving fuzzy outputs

Note that by using FIS to gain mass, defuzzification stage will not be needed any longer. In other words, due to the nature of Dempster-Shafer Theory when all the mass values were obtained for all sources, the ultimate goal which is the preparation of problem for the use of DST will be realized. These masses form our DST input. DST output will be the final answer to the posed question.

V. CONCLUSION

Inference is one of the operators which can improve the result of various decisions or classifiers. One of the main issues in this report is how inference is performed. Finally, our approach is compared to the similar

methods. Our method is two-dimensional, while methods 2 and 3 are three-dimensional. The first method is supervised while our method is non-supervised and does not need any training.

specificity	Sensitivity	Methods	Numbers
100%	95.8%	[13]	1
100%	80.6%	[23]	2
95.8%	95.4%	[24]	3
87.6%	83.33%	Proposed method	4

VI. FUTURE WORKS

Using the three-dimensional features can have an effective effect on the improvement of the quality. In future works, this method must be used. It is better to add the trust coefficient to the DST parameters in which case the algorithm quality will increase.

REFERENCES

- [1] Liu, C.-L., C.-H. Lee, and P.-M. Lin, *A fall detection system using k -nearest neighbor classifier*. Expert Systems with Applications, 2010. **37**(10): p. 7174-7181.
- [2] Bureau, U.C. *Population profile of the united states*. 2008; Available from: <http://www.census.gov/population/www/pop-profile/elderpop.html>.
- [3] Mubashir, M., L. Shao, and L. Seed, *A survey on fall detection: Principles and approaches*. Neurocomputing, 2013. **100**: p. 144-152.
- [4] Li, Q., et al. *Accurate, fast fall detection using gyroscopes and accelerometer-derived posture information*. in *Wearable and Implantable Body Sensor Networks, 2009. BSN 2009. Sixth International Workshop on*. 2009. IEEE.
- [5] Nyan, M., F.E. Tay, and M.Z. Mah, *Application of motion analysis system in pre-impact fall detection*. Journal of biomechanics, 2008. **41**(10): p. 2297-2304.
- [6] Grassi, M., et al., *A Multisensor System for High Reliability People Fall Detection in Home Environment*, in *Sensors and Microsystems*. 2010, Springer. p. 391-394.
- [7] Zhang, T., et al., *Fall detection by embedding an accelerometer in cellphone and using KFD algorithm*. International Journal of Computer Science and Network Security, 2006. **6**(10): p. 277-284.
- [8] Bourke, A.K. and G.M. Lyons, *A threshold-based fall-detection algorithm using a bi-axial gyroscope sensor*. Medical engineering & physics, 2008. **30**(1): p. 84-90.
- [9] Rougier, C., et al., *Video surveillance for fall detection*. 2009, Department of Computer Science and Operations Research, University of Montreal, Canada.
- [10] Zhang, Z., et al. *A viewpoint-independent statistical method for fall detection*. in *Pattern Recognition (ICPR), 2012 21st International Conference on*. 2012. IEEE.
- [11] Machajdik, J., S. Zambanini, and M. Kampel. *Fusion of data from multiple cameras for fall detection*. in *Workshop on Behaviour Monitoring and Interpretation, BMI*. 2010.
- [12] Spehr, J., et al. *Visual fall detection in home environments*. in *International Conference of the International Society for Gerontechnology*. 2008.
- [13] Hung, D.H. and H. Saito. *Fall detection with two cameras based on occupied areas*. in *Proc. of 18th Japan-Korea Joint Workshop on Frontier in Computer Vision*. 2012.
- [14] Debard, G., et al., *Camera-based fall detection on real world data*, in *Outdoor and Large-Scale Real-World Scene Analysis*. 2012, Springer. p. 356-375.
- [15] Chan, M., et al., *A review of smart homes—Present state and future challenges*. Computer methods and programs in biomedicine, 2008. **91**(1): p. 55-81.
- [16] Fleury, A., et al. *Data fusion in health smart home: Preliminary individual evaluation of two families of sensors*. in *Proceedings of the conference of the International Society of Gerontechnology (ISG 2008)*. 2008.
- [17] Soro, S. and W. Heinzelman, *A survey of visual sensor networks*. Advances in Multimedia, 2009. **2009**.
- [18] E. Auvinet, C.R., J.Meunier, A. St-Arnaud, J. Rousseau, *Multiple cameras fall dataset*. 2010, Université de Montréal.
- [19] Moya, D. *Data fusion*. 2013 3 March 2014 Available from: http://en.wikipedia.org/wiki/Data_fusion.
- [20] Koks, D. and S. Challa, *An introduction to Bayesian and Dempster-Shafer data fusion*. 2003.
- [21] Medjahed, H., et al., *A fuzzy logic system for home elderly people monitoring (EMUTEM)*. Fuzzy Systems, 2009.
- [22] Dernoncourt, F., *Introduction to fuzzy logic*. 2011.
- [23] Auvinet, E., et al., *Fall detection with multiple cameras: An occlusion-resistant method based on 3-d silhouette vertical distribution*. Information Technology in Biomedicine, IEEE Transactions on, 2011. **15**(2): p. 290-300.
- [24] Rougier, C., et al., *Robust video surveillance for fall detection based on human shape deformation*. Circuits and Systems for Video Technology, IEEE Transactions on, 2011. **21**(5): p. 611-622.